



Isolated γ production in pp, p-Pb & Pb-Pb collisions measured with ALICE

- Differential p_T cross section
 - * pp at $\sqrt{s} = 13$ TeV [arXiv:2407.01165](https://arxiv.org/abs/2407.01165)  accepted last week by EPJ C!
 - * pp at $\sqrt{s} = 8$ TeV & p-Pb at $\sqrt{s_{NN}} = 5.02, 8.16$ TeV preliminary
 - * pp & Pb-Pb at $\sqrt{s_{NN}} = 5.02$ TeV [arXiv:2409.12641](https://arxiv.org/abs/2409.12641), ALICE-PUBLIC-2024-003 
- Isolated γ -hadron correlation
 - * Pb-Pb at $\sqrt{s_{NN}} = 5.02$ TeV preliminary

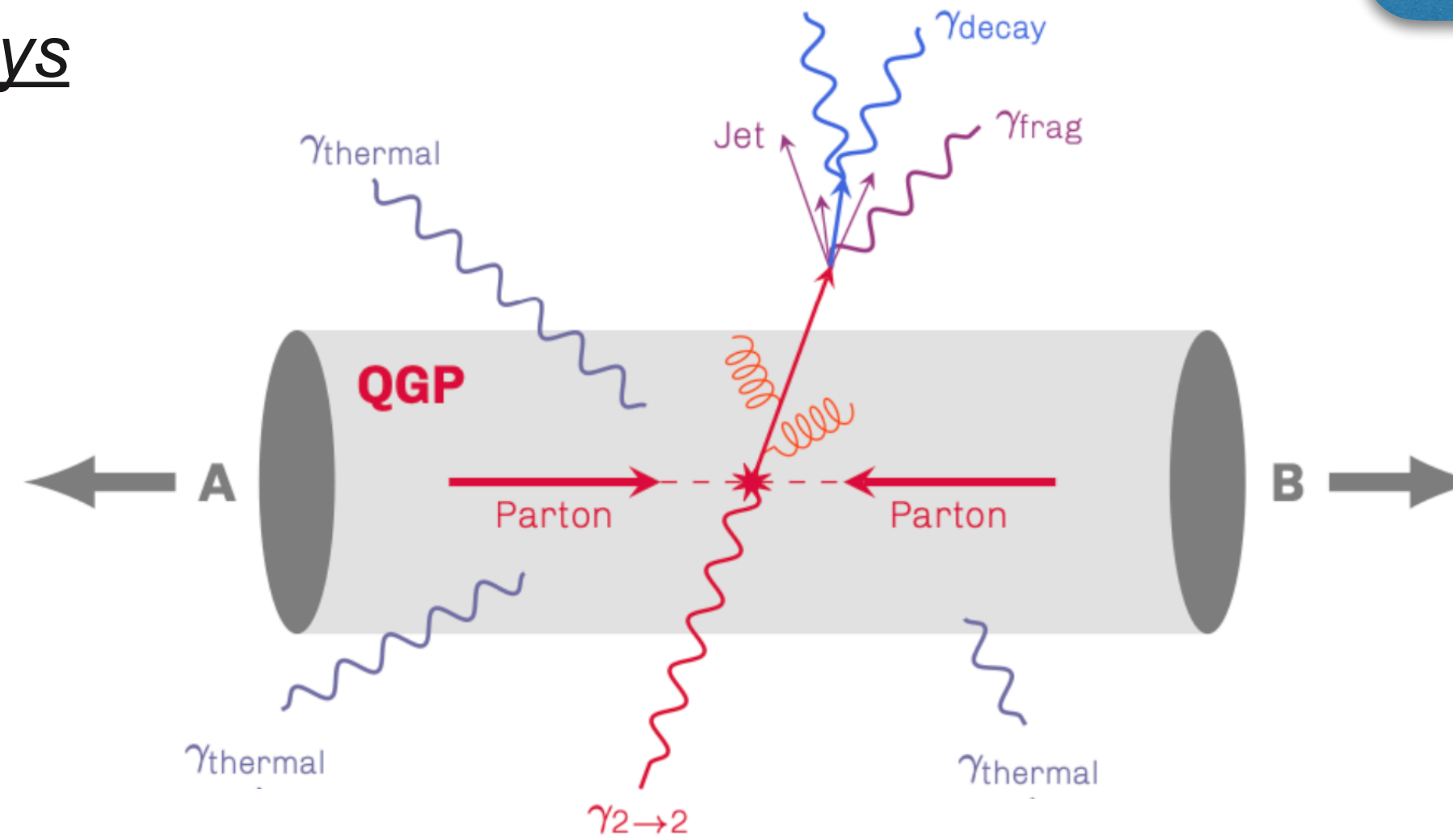
Gustavo CONESA BALBASTRE
LPSC Grenoble — IN2P3-CNRS-UGA
for the ALICE Collaboration



Motivation

- γ are **color neutral**: **not affected** by “*quark-gluon plasma*” (QGP) presence in heavy-ion collisions unlike **partons** that **lose energy**
- Direct γ , not originating from hadronic decays

$$R_{AA} = \frac{1}{\langle N_{\text{coll}} \rangle} \frac{d^2\sigma_{AA} / (dp_T d\eta)}{d^2\sigma_{pp} / (dp_T d\eta)}$$

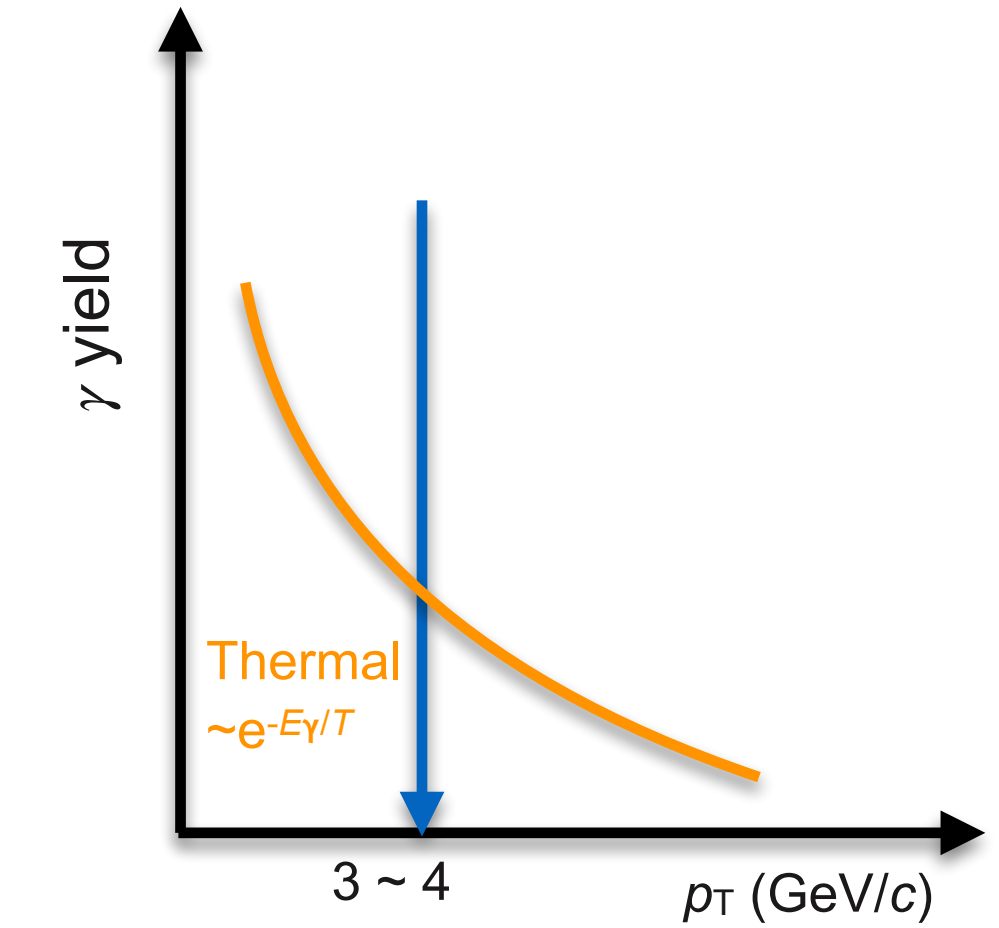
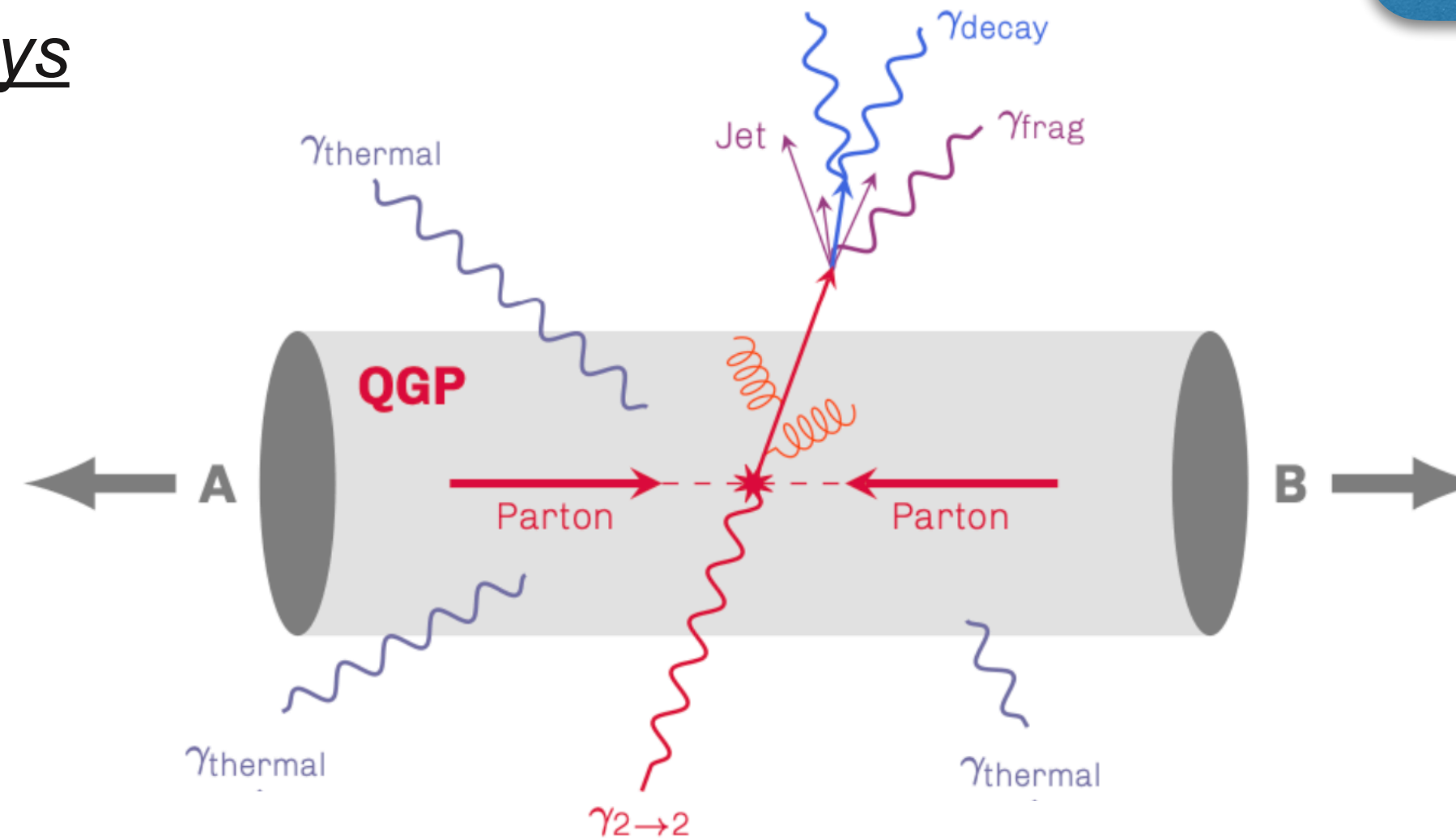


Motivation

- γ are **color neutral**: not affected by “quark-gluon plasma” (QGP) presence in heavy-ion collisions unlike **partons** that **lose energy**
- Direct γ , not originating from hadronic decays

- ➔ **Direct thermal γ : $R_{AA} \gg 1$**
 - QGP thermal radiation
 - Measure **T** & time/size evolution

$$R_{AA} = \frac{1}{\langle N_{\text{coll}} \rangle} \frac{d^2\sigma_{AA} / (dp_T d\eta)}{d^2\sigma_{pp} / (dp_T d\eta)}$$

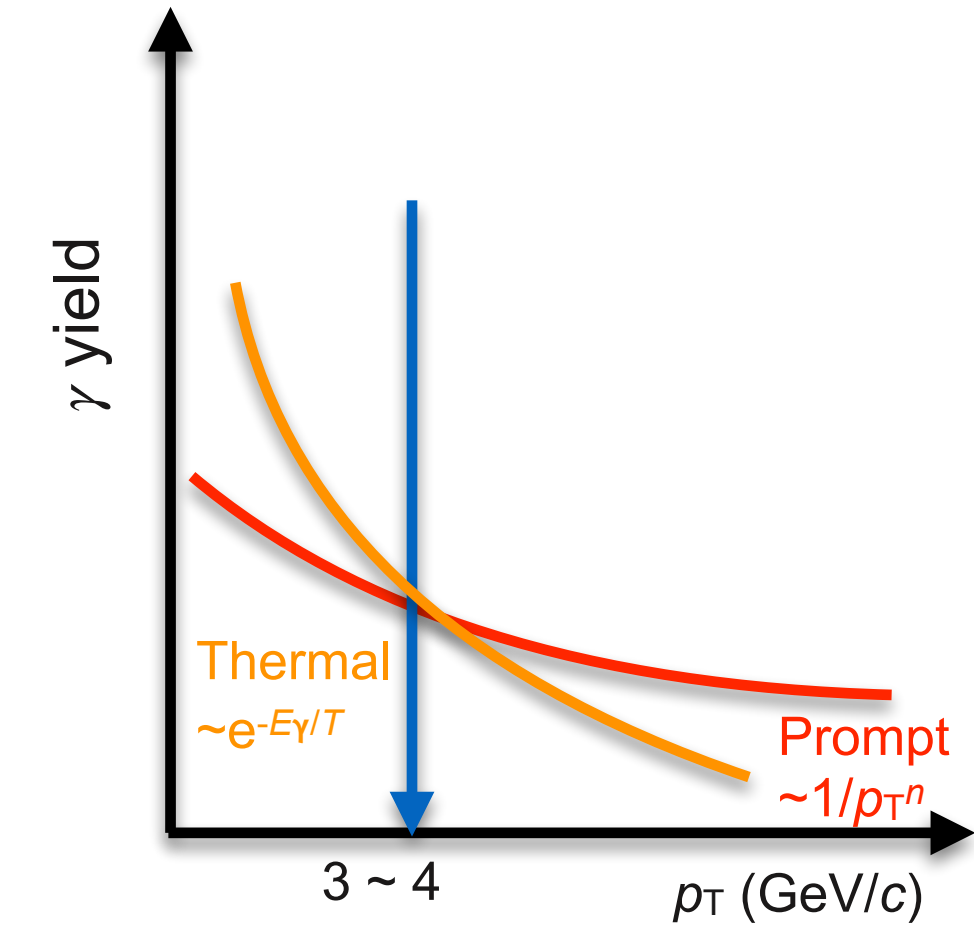
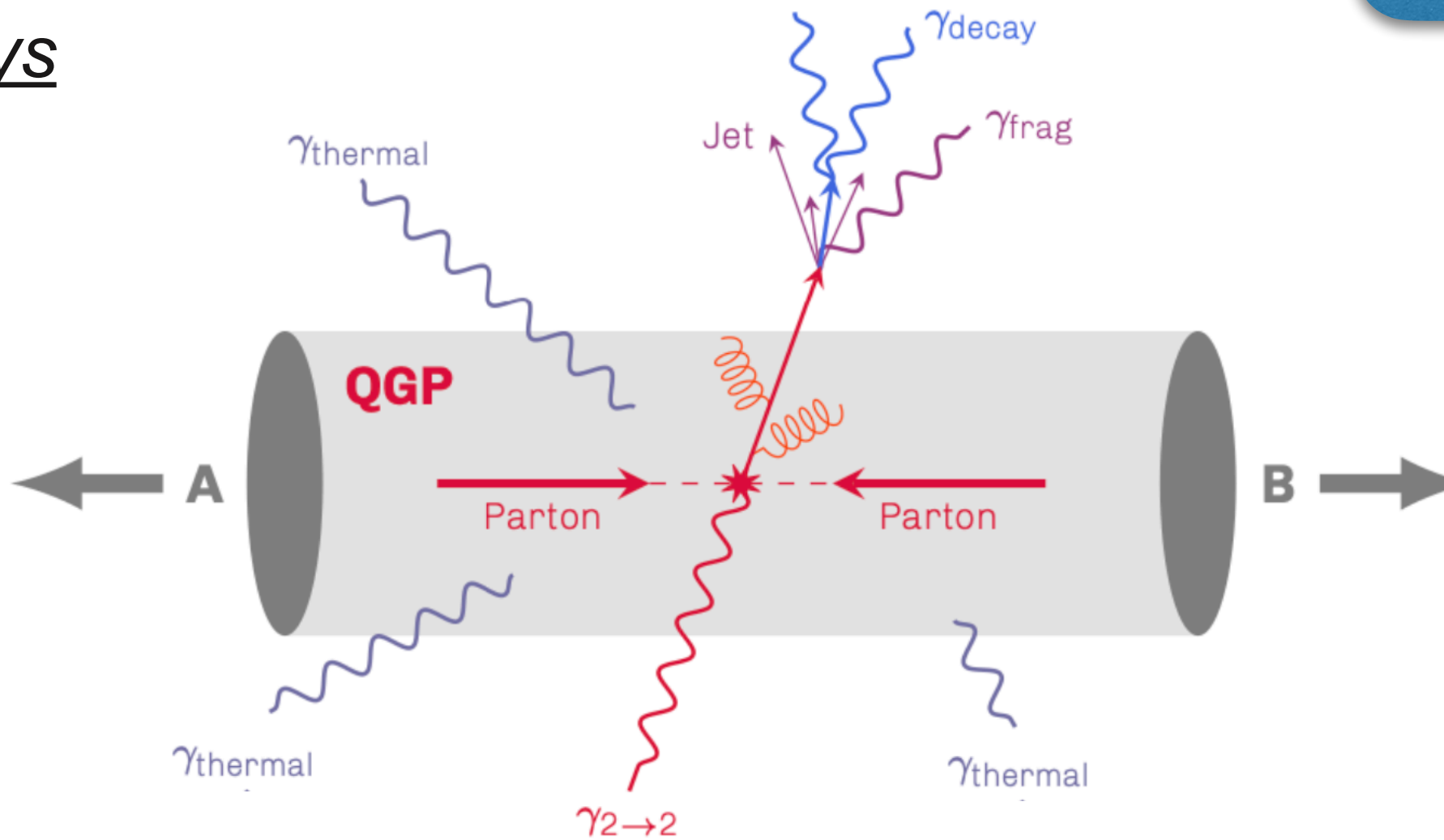
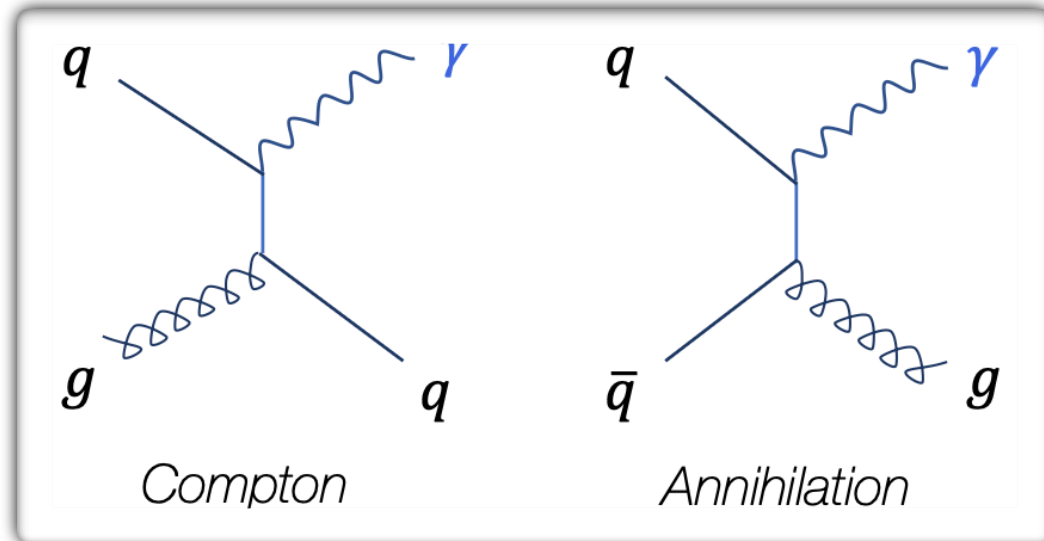


Motivation

- γ are **color neutral**: not affected by “quark-gluon plasma” (QGP) presence in heavy-ion collisions unlike **partons** that **lose energy**
- Direct γ , not originating from hadronic decays

$$R_{AA} = \frac{1}{\langle N_{coll} \rangle} \frac{d^2\sigma_{AA} / (dp_T d\eta)}{d^2\sigma_{pp} / (dp_T d\eta)}$$

- ➔ **Direct thermal γ** : $R_{AA} \gg 1$
 - QGP thermal radiation
 - Measure T & time/size evolution
- ➔ **Direct prompt γ** : $R_{AA} \approx 1$
 - Initial hard scattering, processes at LO:



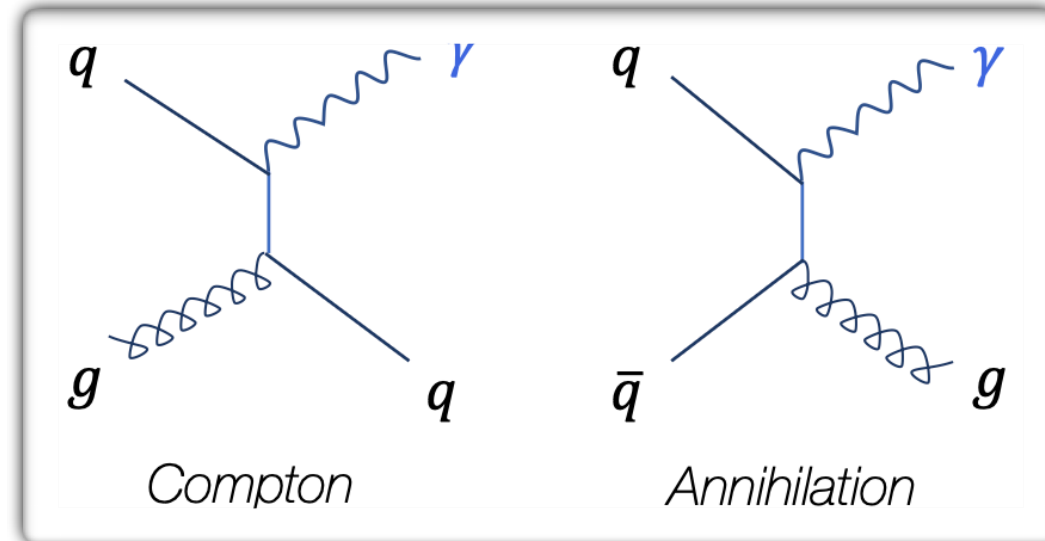
$$d\sigma_{AB \rightarrow h}^{hard} = \underbrace{f_{a/A}(x_1, Q^2)}_{PDFs} \otimes \underbrace{f_{b/B}(x_2, Q^2)}_{PDFs} \otimes \underbrace{d\sigma_{ab \rightarrow c}^{hard}(x_1, x_2, Q^2)}_{Hard\ scattering\ (pQCD)} \otimes \underbrace{D_{c \rightarrow h}(z, Q^2)}_{Fragmentation\ function\ (FF)}$$

- **Test pQCD predictions, constrain (n)PDFs & FF**
 - ▶ Cold nuclear matter (nPDF) effects can lead to $R_{AA} \neq 1$
- $p_T^\gamma \simeq p_T^{parton}$, before parton loses ΔE in QGP
- Measure **FF modifications**, where is the ΔE radiated?

Motivation

- γ are **color neutral**: **not affected** by “*quark-gluon plasma*” (QGP) presence in heavy-ion collisions unlike **partons** that **lose energy**
- Direct γ , not originating from hadronic decays

- ➔ **Direct thermal γ** : $R_{AA} \gg 1$
 - QGP thermal radiation
 - Measure T & time/size evolution
- ➔ **Direct prompt γ** : $R_{AA} \approx 1$
 - Initial hard scattering, processes at LO:

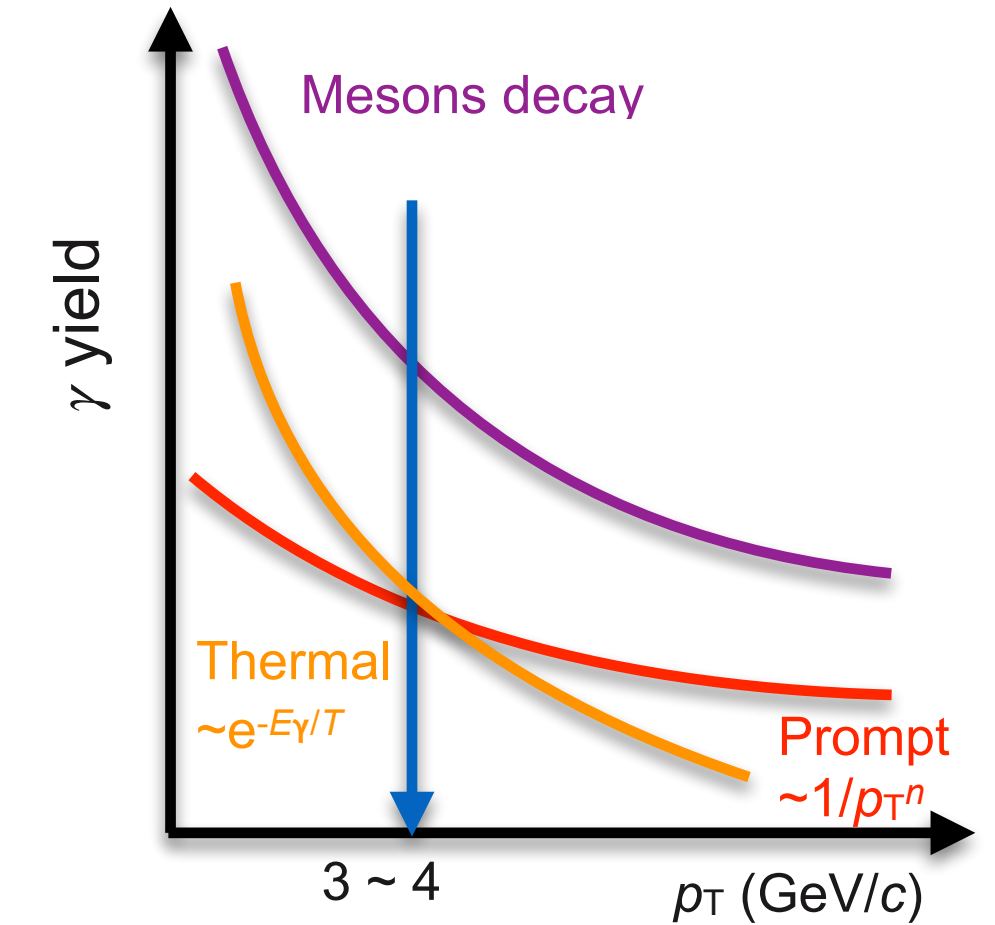
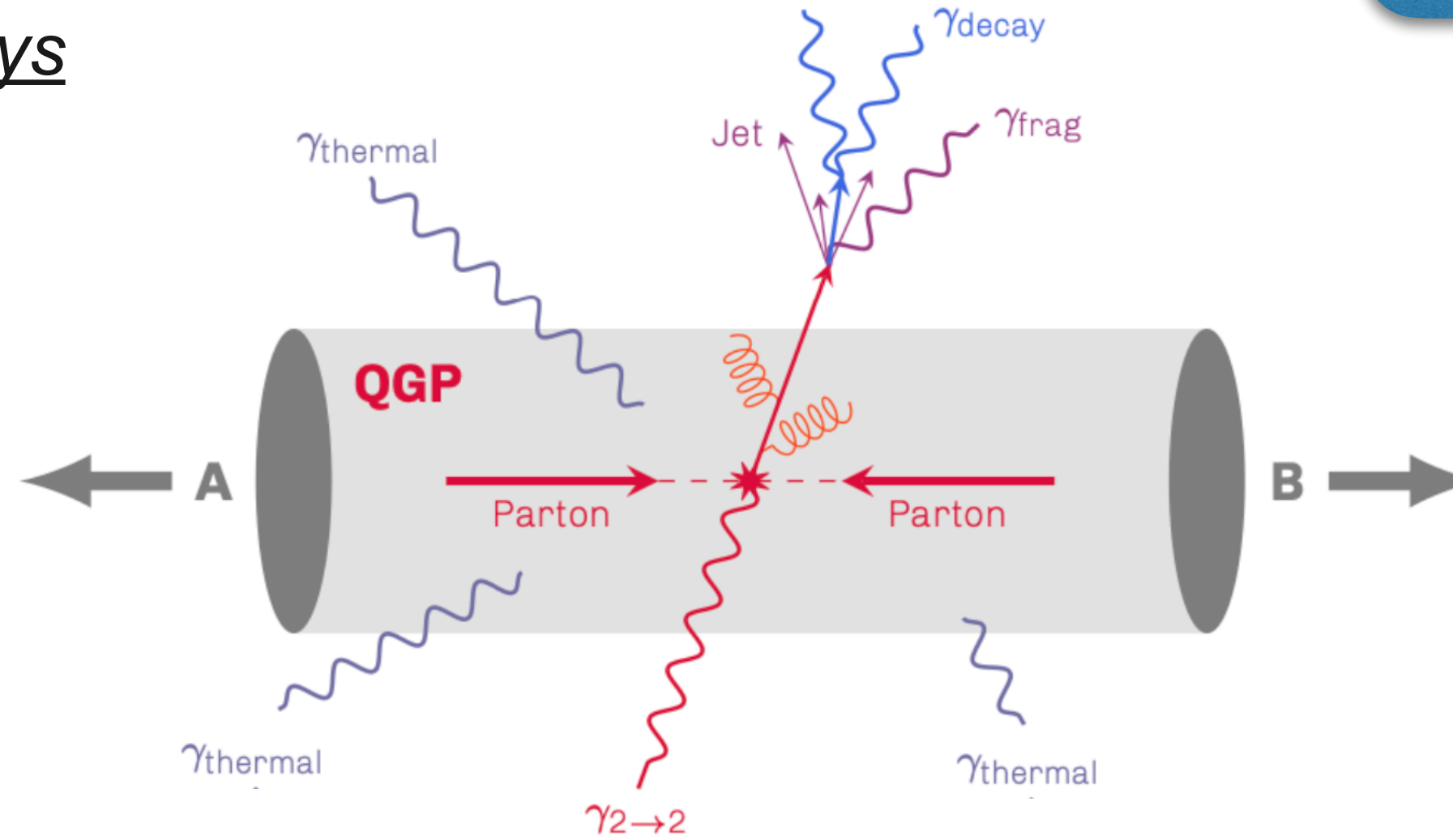


$$d\sigma_{AB \rightarrow h}^{hard} = \underbrace{f_{a/A}(x_1, Q^2)}_{PDFs} \otimes \underbrace{f_{b/B}(x_2, Q^2)}_{PDFs} \otimes \underbrace{d\sigma_{ab \rightarrow c}^{hard}(x_1, x_2, Q^2)}_{Hard\ scattering\ (pQCD)} \otimes \underbrace{D_{c \rightarrow h}(z, Q^2)}_{Fragmentation\ function\ (FF)}$$

- **Test pQCD predictions, constrain (n)PDFs & FF**
 - Cold nuclear matter (nPDF) effects can lead to $R_{AA} \neq 1$
- $p_T^\gamma \simeq p_T^{parton}$, before parton loses ΔE in QGP
- Measure **FF modifications**, where is the ΔE radiated?

- ➔ **Decay γ (π^0 & η)**: $R_{AA} \ll 1$
 - **Main background for direct γ measurements**

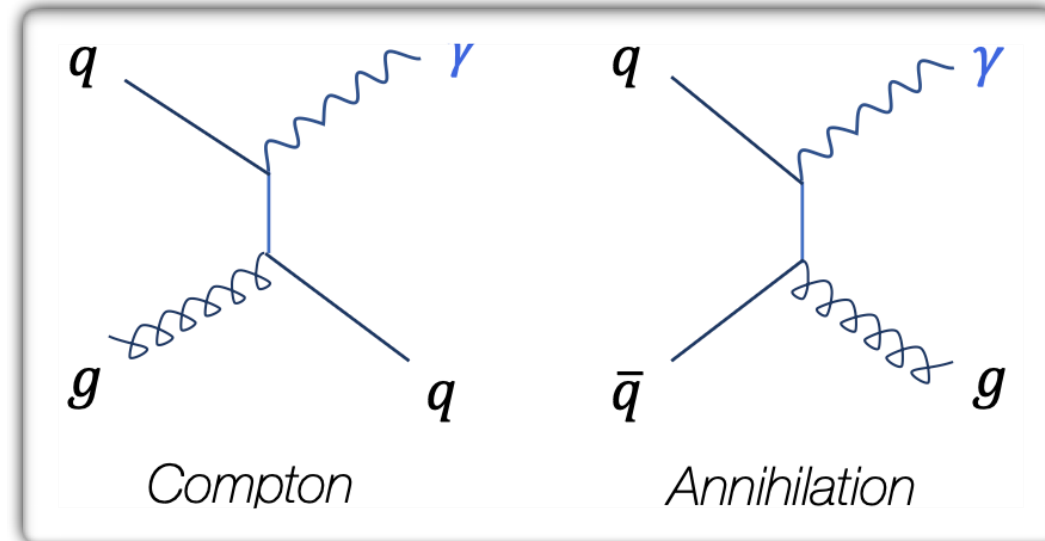
$$R_{AA} = \frac{1}{\langle N_{coll} \rangle} \frac{d^2\sigma_{AA} / (dp_T d\eta)}{d^2\sigma_{pp} / (dp_T d\eta)}$$



Motivation

- γ are **color neutral**: **not affected** by “quark-gluon plasma” (QGP) presence in heavy-ion collisions unlike **partons** that **lose energy**
- Direct γ , not originating from hadronic decays

- ➔ **Direct thermal γ** : $R_{AA} \gg 1$
 - QGP thermal radiation
 - Measure T & time/size evolution
- ➔ **Direct prompt γ** : $R_{AA} \approx 1$
 - Initial hard scattering, processes at LO:



$$d\sigma_{AB \rightarrow h}^{hard} = \underbrace{f_{a/A}(x_1, Q^2)}_{PDFs} \otimes \underbrace{f_{b/B}(x_2, Q^2)}_{PDFs} \otimes \underbrace{d\sigma_{ab \rightarrow c}^{hard}(x_1, x_2, Q^2)}_{Hard\ scattering\ (pQCD)} \otimes \underbrace{D_{c \rightarrow h}(z, Q^2)}_{Fragmentation\ function\ (FF)}$$

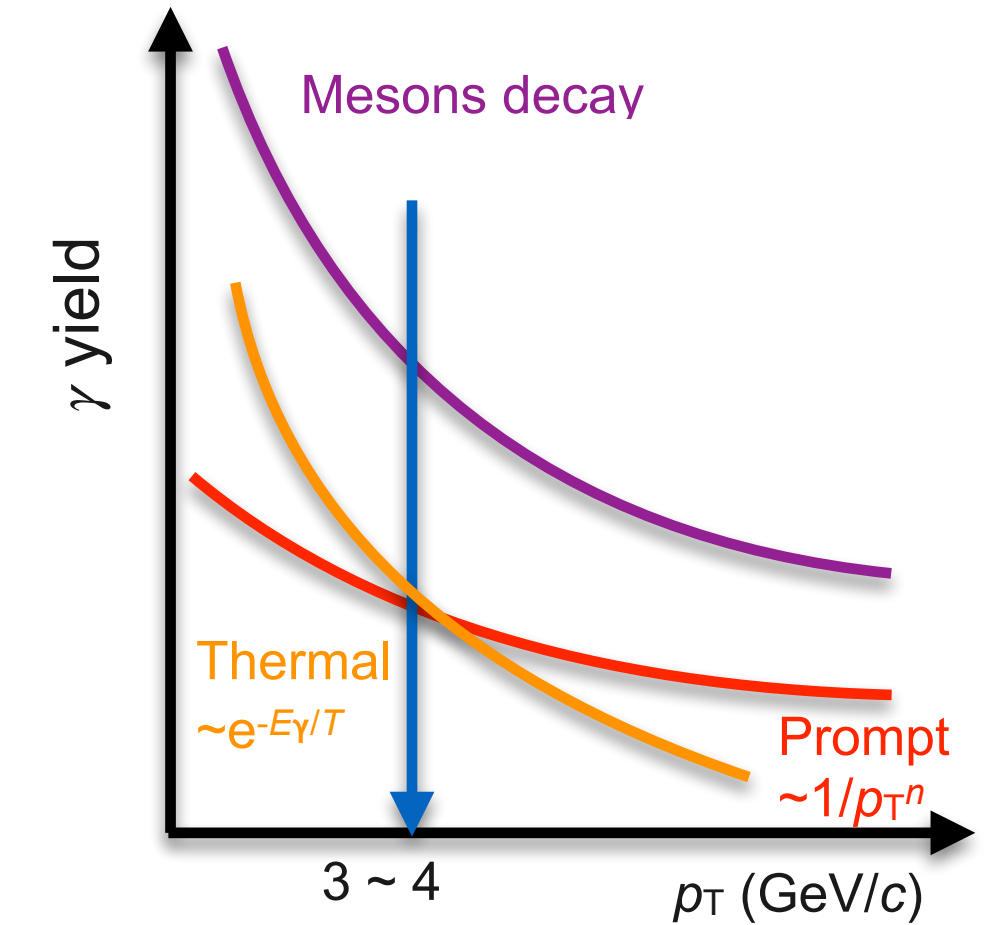
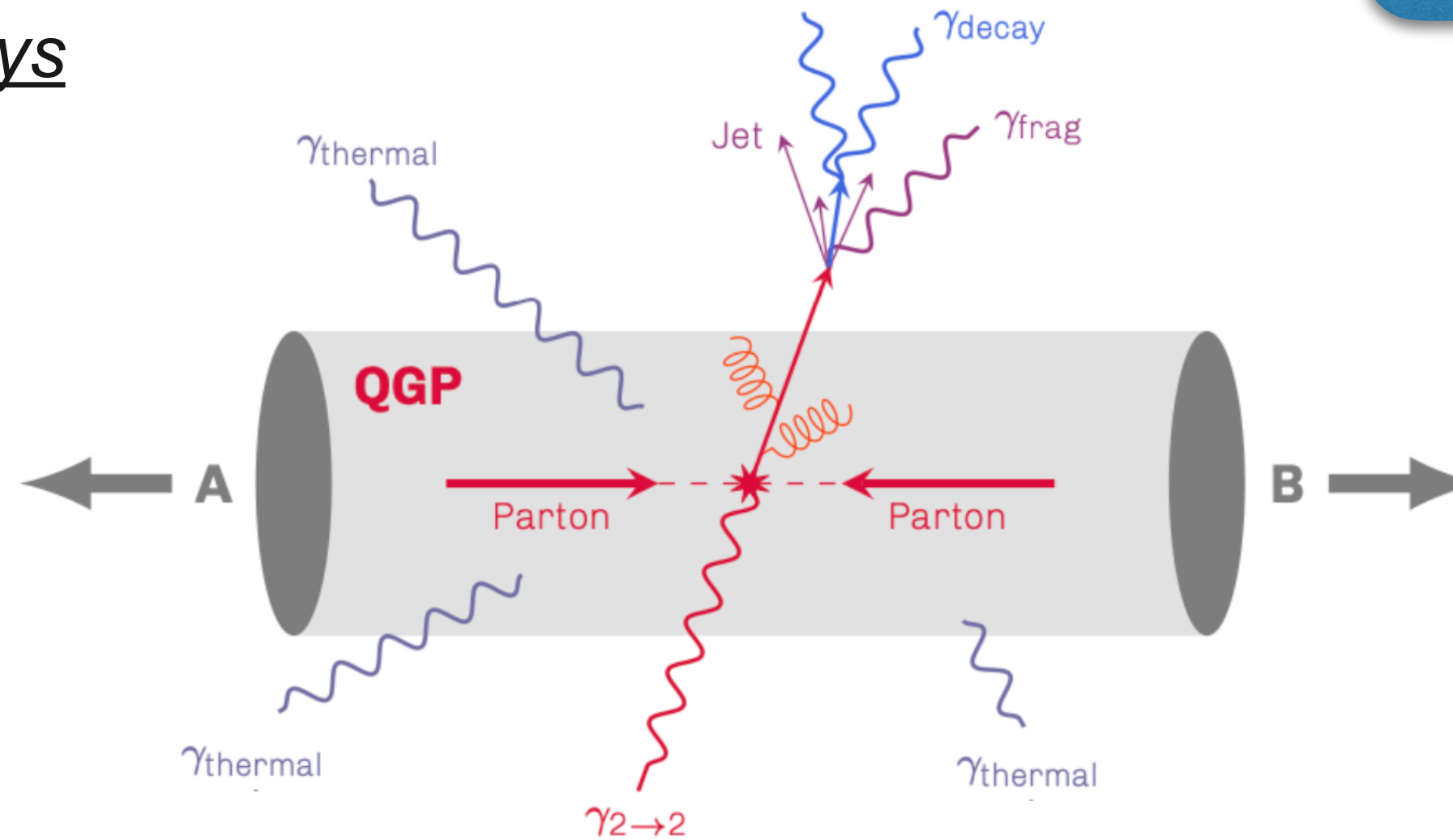
- **Test pQCD predictions, constrain (n)PDFs & FF**
 - Cold nuclear matter (nPDF) effects can lead to $R_{AA} \neq 1$
- $p_T^\gamma \simeq p_T^{parton}$, before parton loses ΔE in QGP
- Measure **FF modifications**, where is the ΔE radiated?

- ➔ **Decay γ (π^0 & η)**: $R_{AA} \ll 1$
 - **Main background for direct γ measurements**

➔ Other direct γ sources:

- Fragmentation γ : $R_{AA} < 1$ comparable yield to direct prompt γ
- QGP pre-equilibrium γ ? $R_{AA} \gg 1$ (glasma phase)
- Jet-QGP interaction γ ? $R_{AA} \gg 1$ (hard partons scattering)

$$R_{AA} = \frac{1}{\langle N_{coll} \rangle} \frac{d^2\sigma_{AA} / (dp_T d\eta)}{d^2\sigma_{pp} / (dp_T d\eta)}$$



Prompt γ identification in ALICE: EM shower spread shape & isolation with tracks

Prompt γ at LO $2 \rightarrow 2$: *isolated*

→ TPC+ITS charged tracks

* ITS only for pp col. at $\sqrt{s} = 5.02$ TeV

→ Select γ with low hadronic activity in R , small $p_T^{\text{iso, ch}}$

$$\sqrt{(\eta_{\text{track}} - \eta_\gamma)^2 + (\phi_{\text{track}} - \phi_\gamma)^2} < R = 0.4 \text{ (0.2)}$$

$$p_T^{\text{iso, ch}} = \sum p_T^{\text{tracks in cone}} - \rho_{\text{UE}} \cdot \pi \cdot R^2 < 1.5 \text{ GeV}/c$$

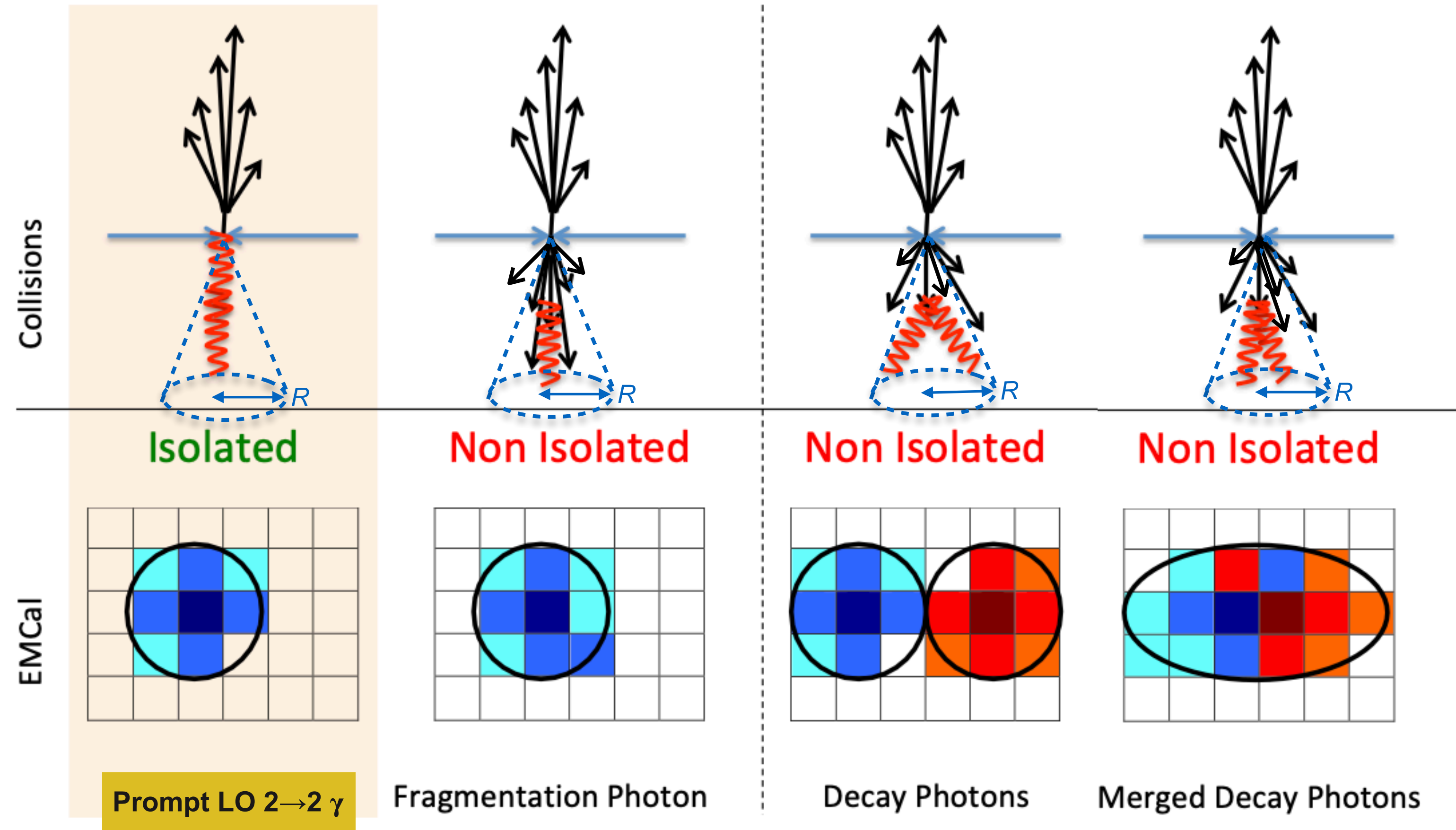
* Underlying event (UE) subtracted event-by-event, ρ_{UE} density estimation (back-up slide)

EM shower discrimination

→ EMCal

→ Shower elongation σ_{long}^2

* pp & Pb-Pb collisions at $\sqrt{s} = 5.02$ TeV: Calculated in 5×5 cells around the highest energy cell $\rightarrow \sigma_{\text{long}, 5 \times 5}^2$



→ **circular** “narrow” cluster

→ circular narrow clusters, potentially wider due to jet particles nearby merging

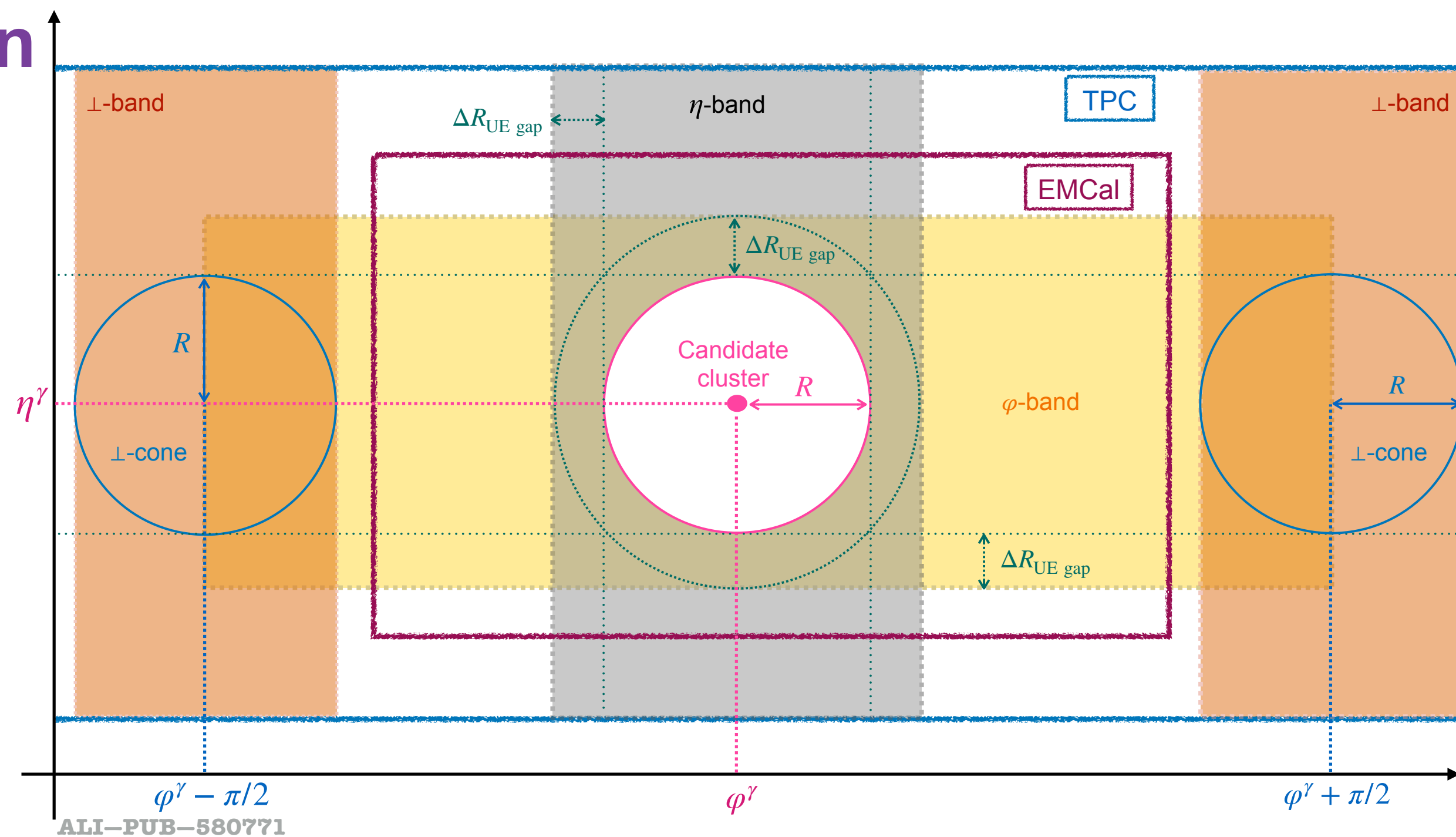
→ decay γ merge, $E_{\pi^0} > 6$ GeV **elliptical** “wide” cluster

Underlying event estimation

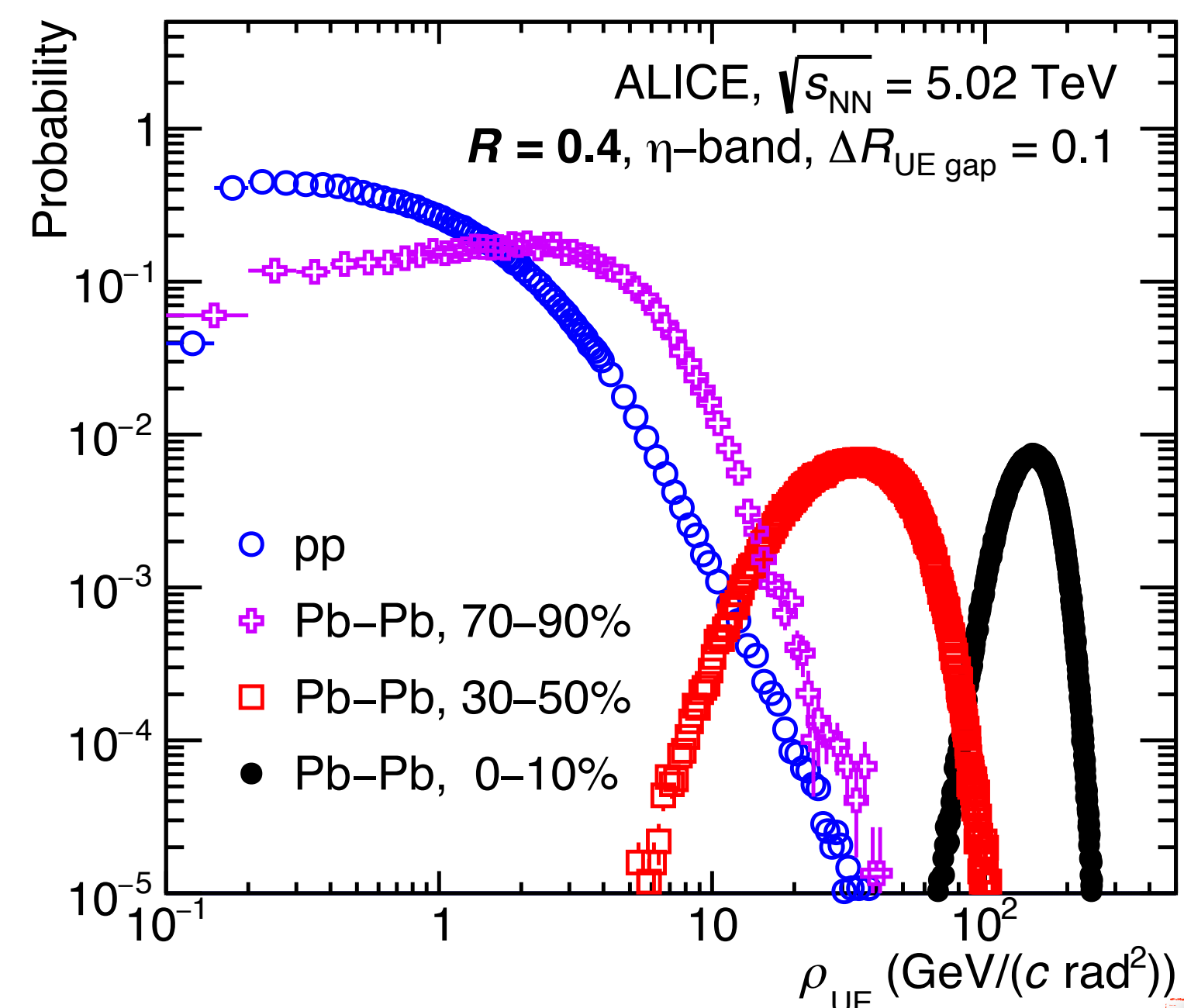
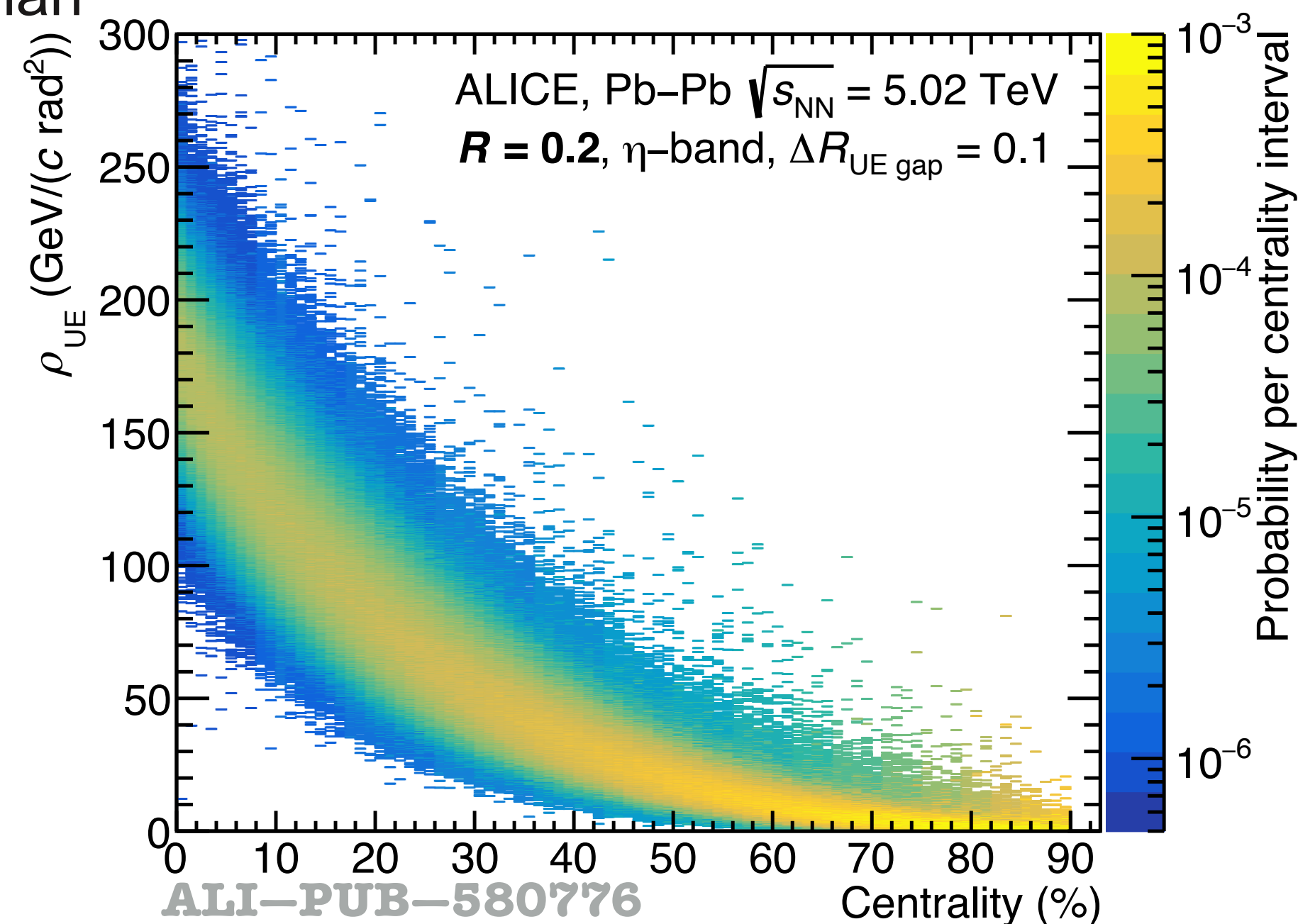


Track p_T UE density estimated on:

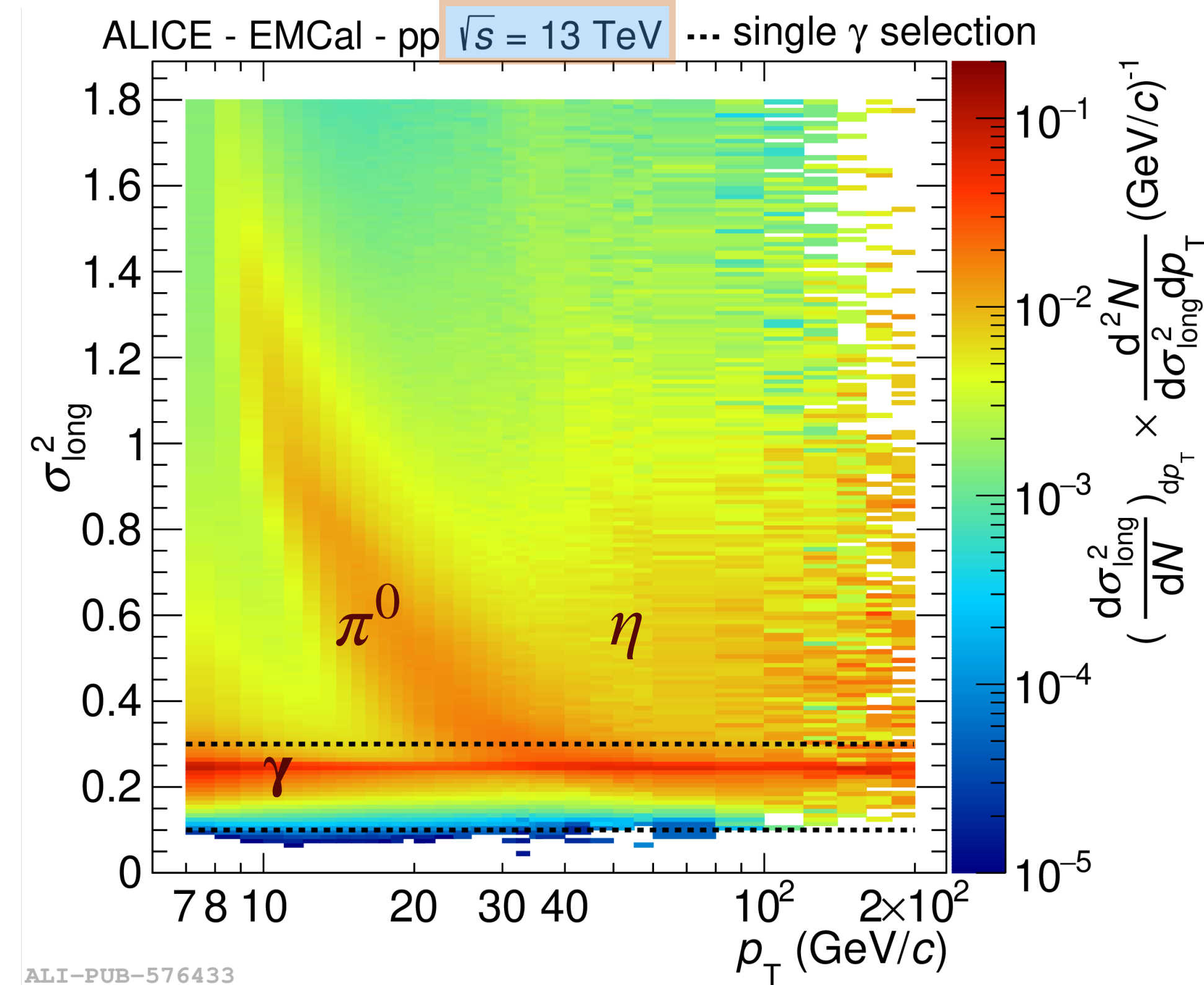
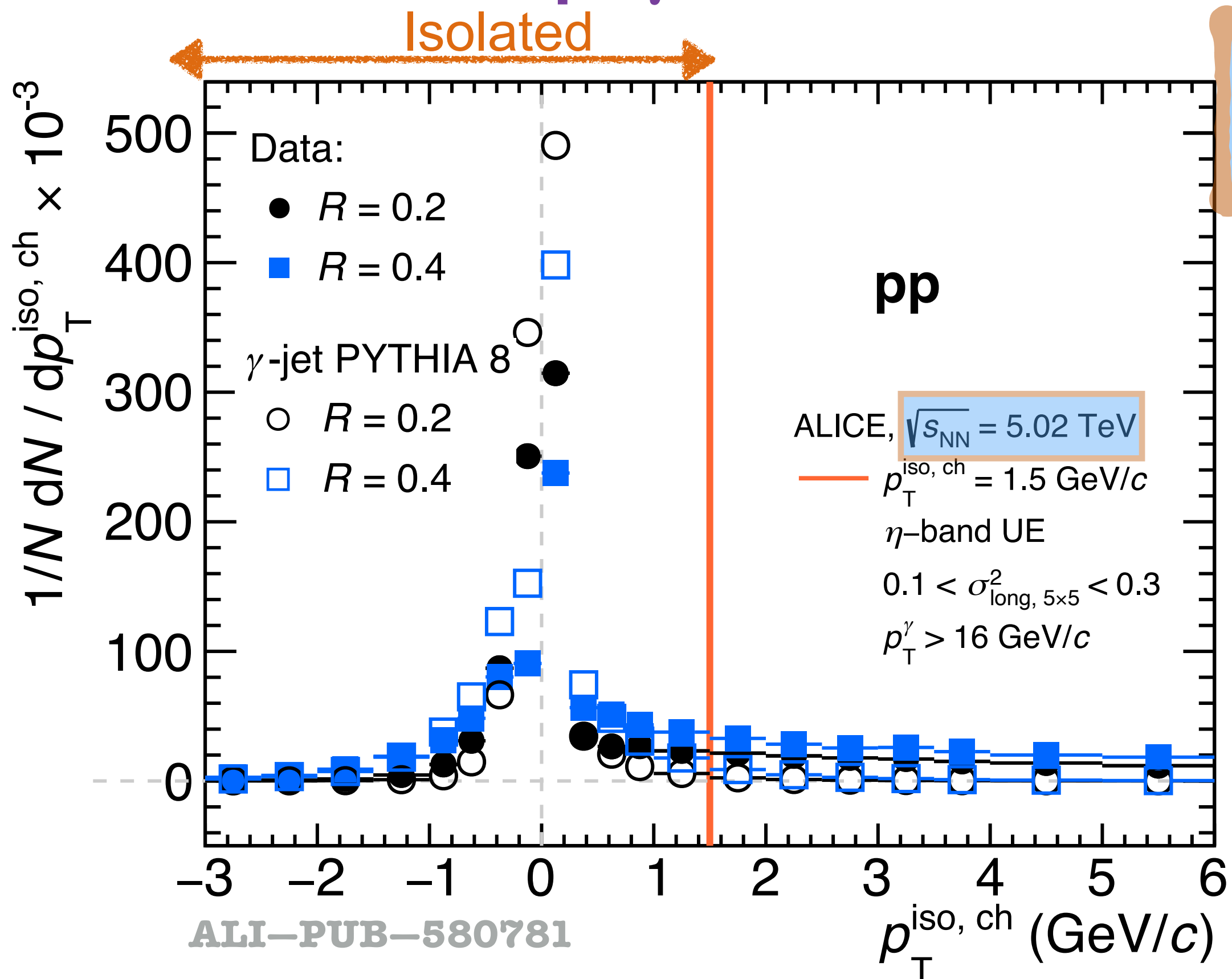
- Pb-Pb & pp at $\sqrt{s_{NN}} = 5.02$ TeV:
 - ➔ Sum of tracks p_T normalised by η -band area
→ Avoid flow effects
 - ➔ Gap between cone and band of $\Delta R_{UE\ gap} = 0.1$
→ Avoid jet remnants
- p-Pb $\sqrt{s_{NN}} = 5.02, 8.16$ TeV, pp $\sqrt{s} = 8$ TeV
 - ➔ Perpendicular cone & jet-median



Remark: UE was not subtracted in pp $\sqrt{s} = 7$ & 13 TeV measurements, UE small



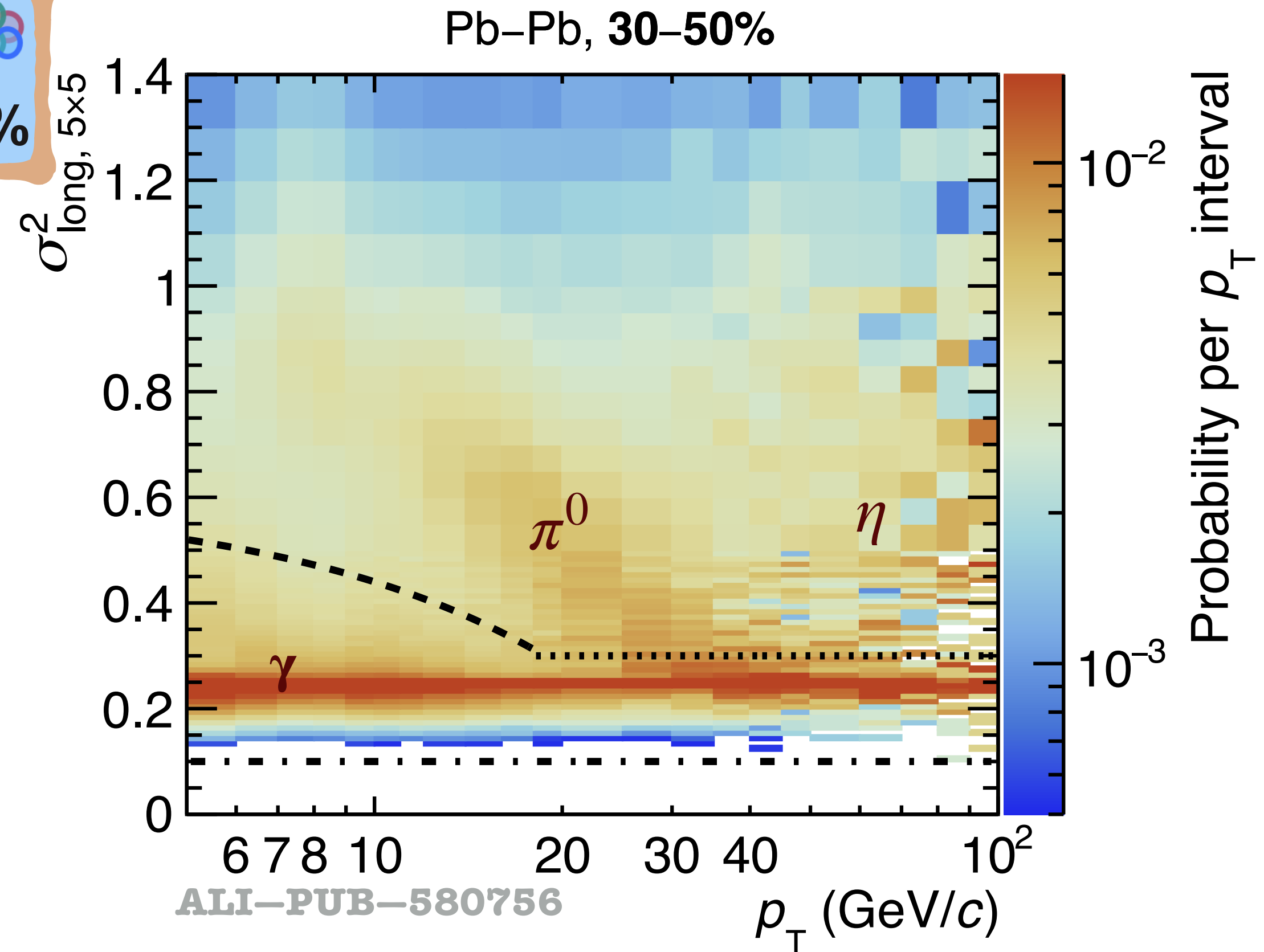
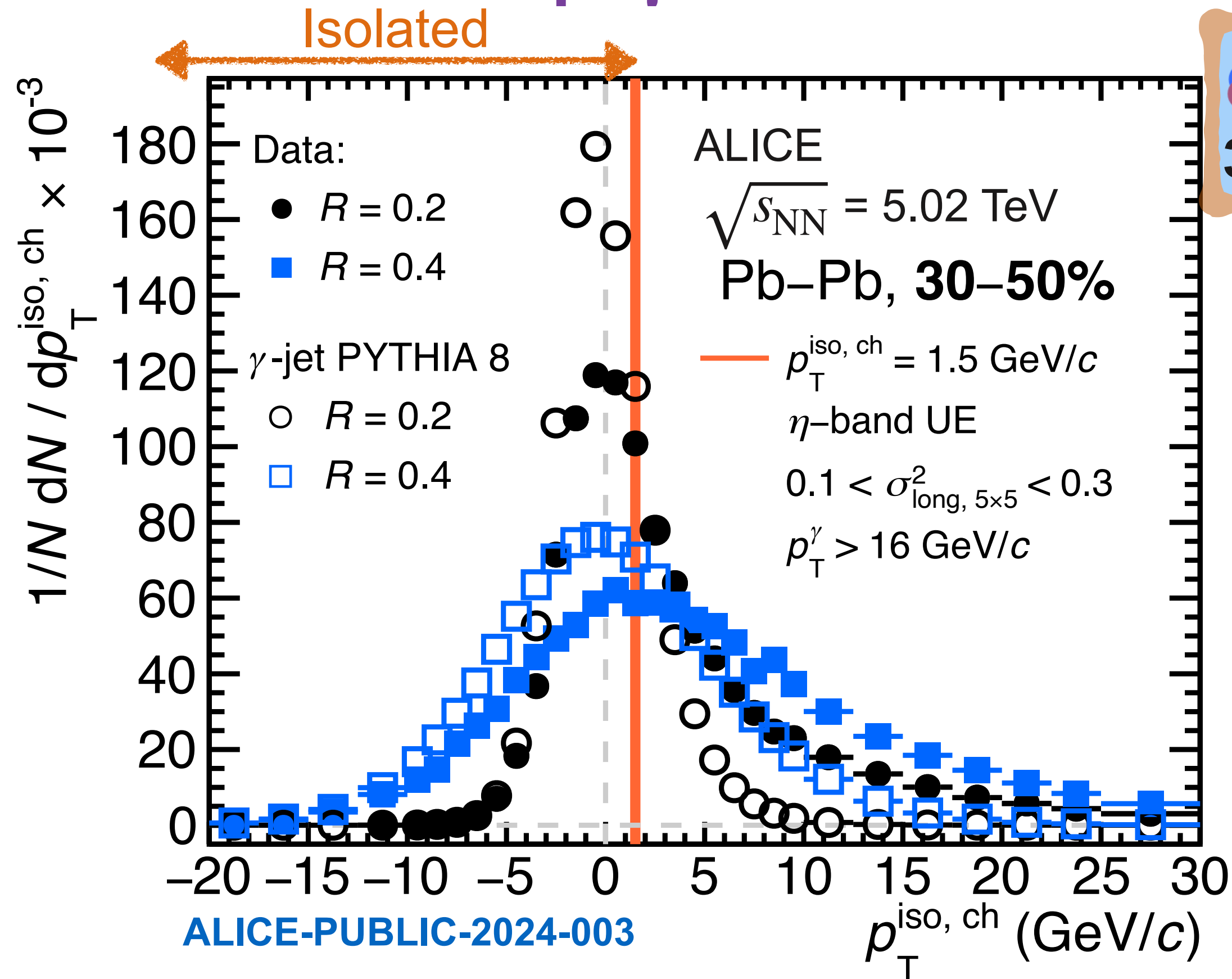
Prompt γ identification in ALICE: EM shape & isolation



- Isolated if $p_T^{\text{iso, ch}} < 1.5 \text{ GeV}/c$ with $R = 0.4$ or 0.2
- Symmetric in PYTHIA 8 γ -jet process simulation
- In data, more asymmetric and less peaked distribution due to jet contribution
- Wider for $R = 0.4$ due to UE fluctuations

- Visible bands for γ (narrow clusters) & π^0 (wide clusters)
- Select as γ clusters with $0.1 < \sigma_{\text{long, } 5 \times 5}^2 < 0.3$

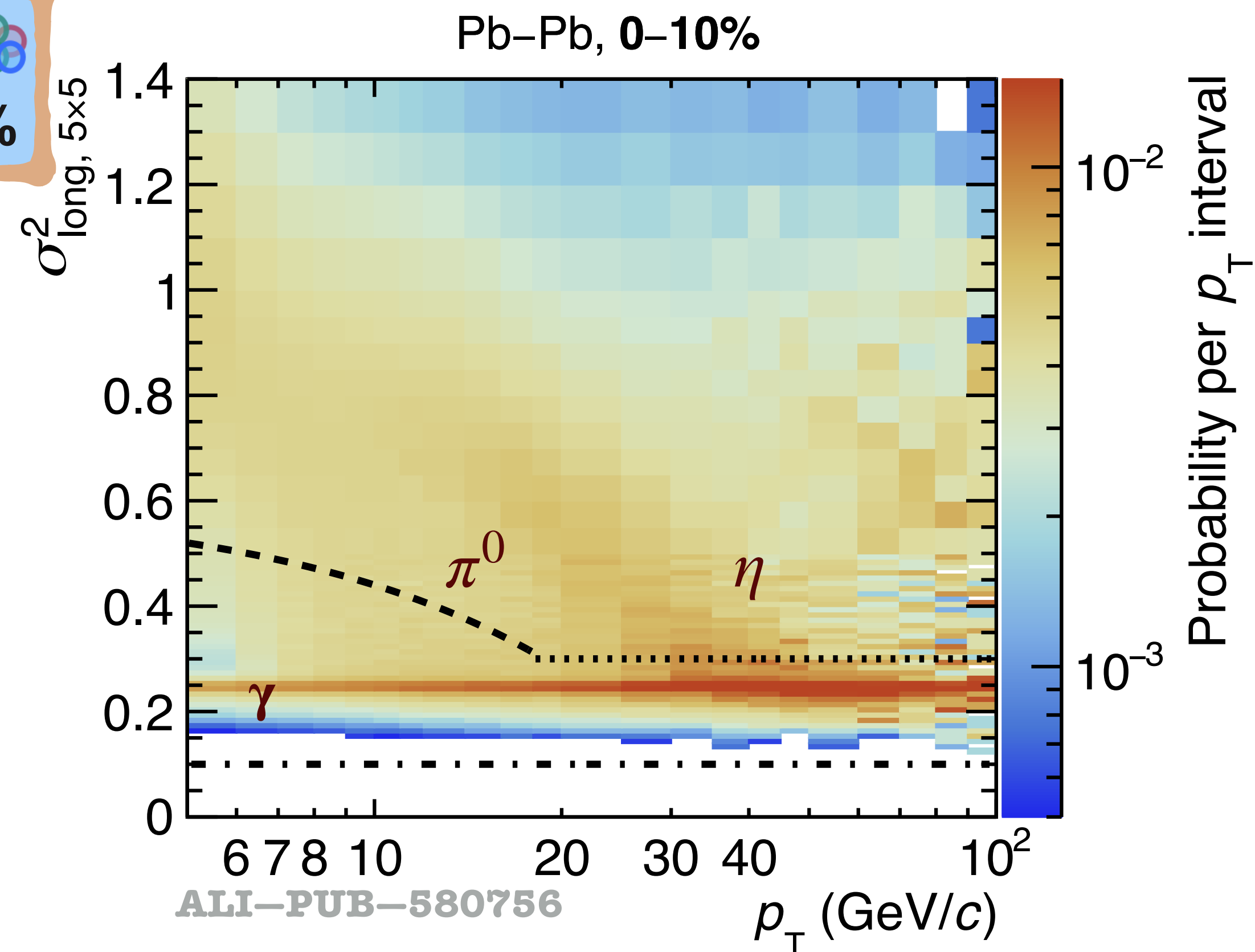
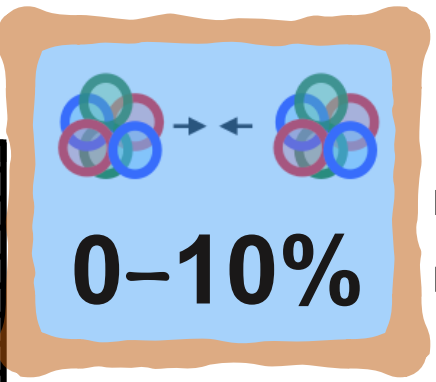
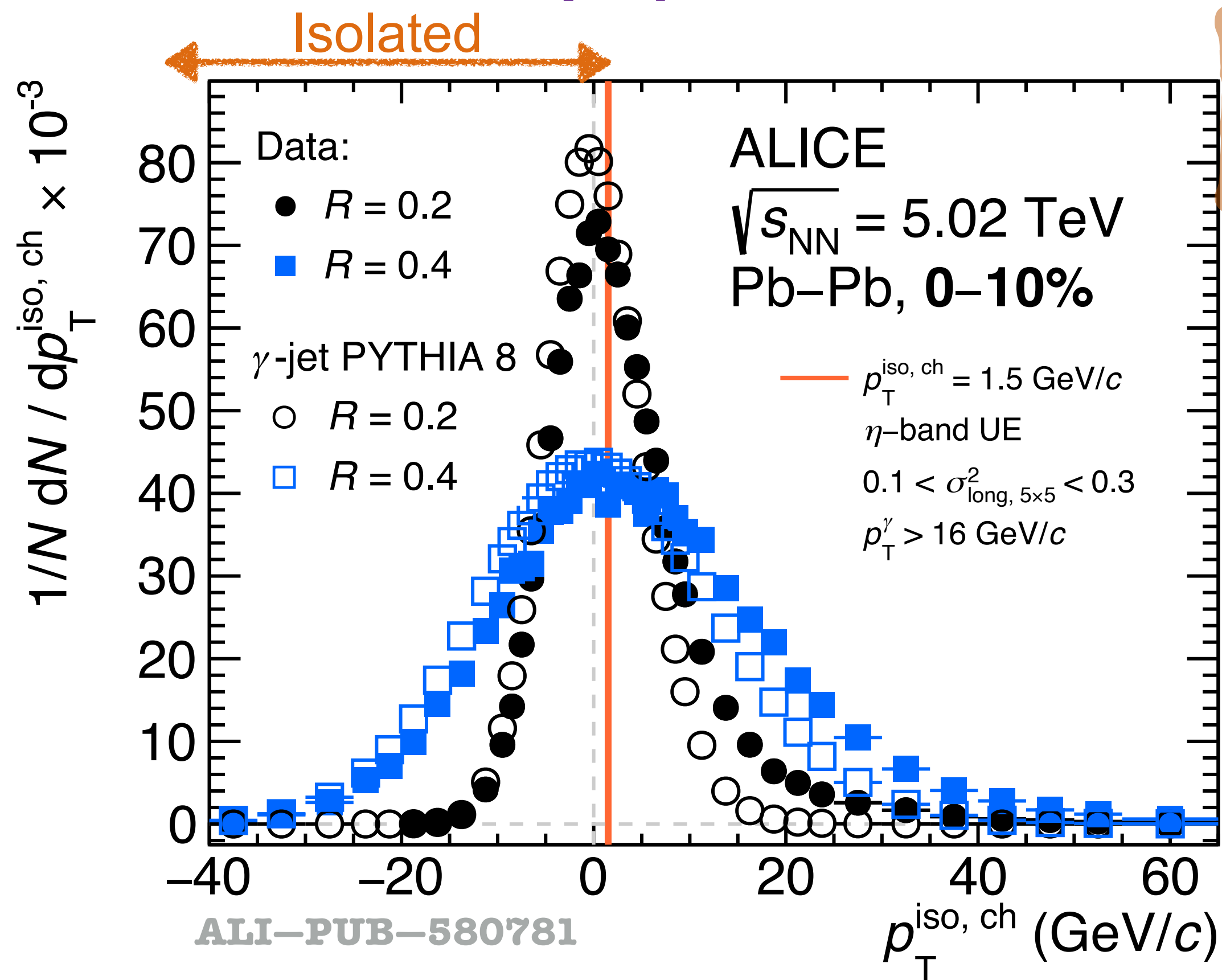
Prompt γ identification in ALICE: EM shape & isolation



- Isolated if $p_T^{\text{iso, ch}} < 1.5 \text{ GeV}/c$ with $R = 0.4$ or 0.2
- Embedded pp PYTHIA 8 simulation into MB data, symmetric distribution
- In data, more asymmetric distribution due to jet contribution
- Significantly wider distributions for $R = 0.4$ due to UE fluctuations

- Visible bands for γ (narrow clusters) & π^0 (wide clusters)
- Select as γ clusters with
 - ◆ Pb-Pb:
 - ➔ $p_T < 18 \text{ GeV}/c: 0.1 < \sigma_{\text{long, 5x5}}^2 < 0.6 - 0.016 \cdot p_T$
 - ➔ $p_T > 18 \text{ GeV}/c: 0.1 < \sigma_{\text{long, 5x5}}^2 < 0.3$
 - ◆ pp & p-Pb:
 - ➔ $0.1 < \sigma_{\text{long, 5x5}}^2 < 0.3$

Prompt γ identification in ALICE: EM shape & isolation



- Isolated if $p_T^{\text{iso, ch}} < 1.5 \text{ GeV}/c$ with $R = 0.4$ or 0.2
- Embedded pp PYTHIA 8 simulation into MB data, symmetric distribution
- In data, more asymmetric distribution due to jet contribution
- Significantly **much** wider distributions for $R = 0.4$ due to UE fluctuations

- Visible bands for γ (narrow clusters) & π^0 (wide clusters)
- Select as γ clusters with
 - ❖ Pb-Pb:
 - ➔ $p_T < 18 \text{ GeV}/c: 0.1 < \sigma_{\text{long, 5x5}}^2 < 0.6 - 0.016 \cdot p_T$
 - ➔ $p_T > 18 \text{ GeV}/c: 0.1 < \sigma_{\text{long, 5x5}}^2 < 0.3$
 - ❖ pp & p-Pb:
 - ➔ $0.1 < \sigma_{\text{long, 5x5}}^2 < 0.3$

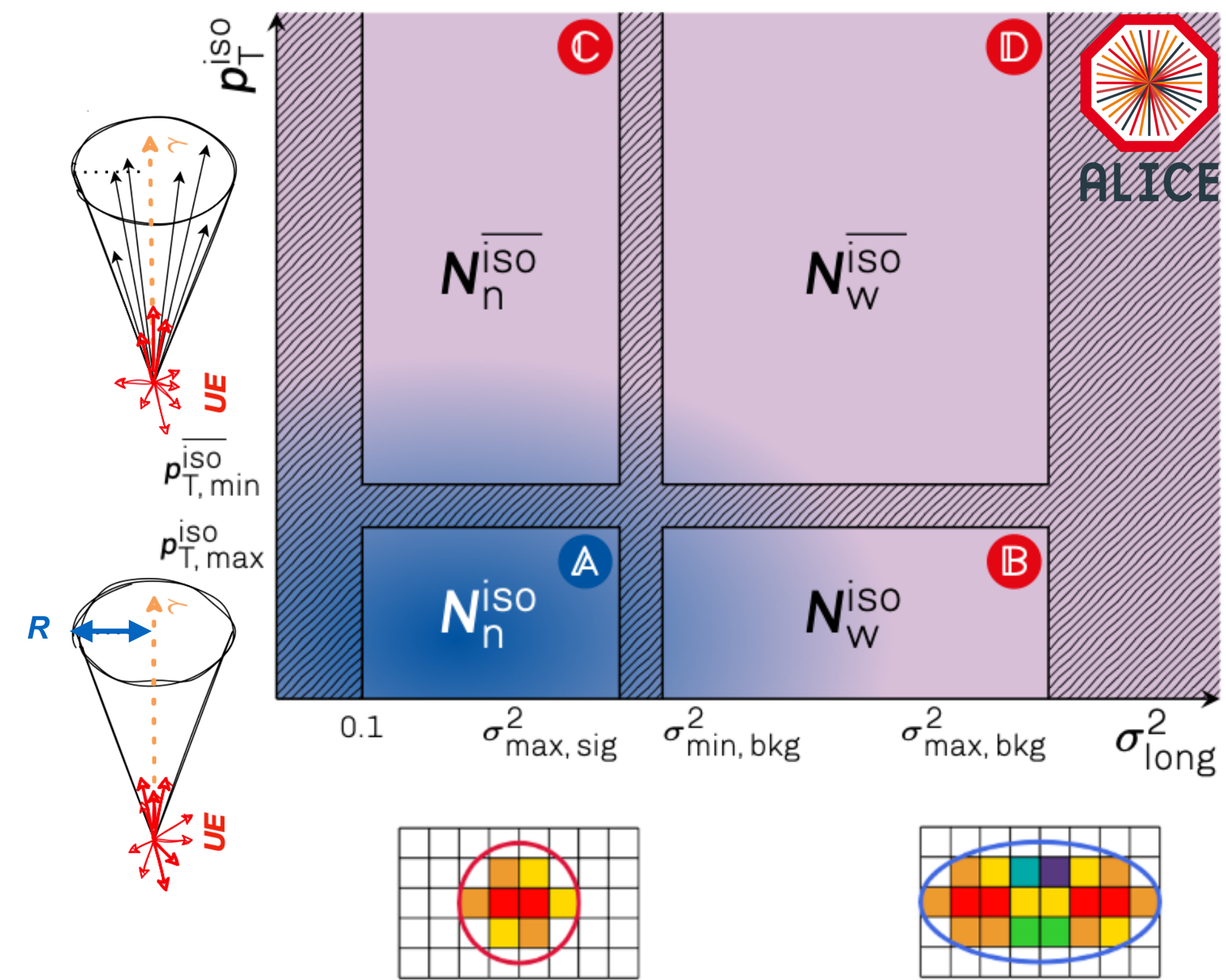
γ increase their $\sigma_{\text{long, 5x5}}^2$ due to the UE

Purity

- Purity, ABCD method: Phase space of calorimeter clusters divided in 4 regions: **A**, signal dominated & **B-C-D**, background dominated

$$P = 1 - \left(\frac{N_n^{\text{iso}} / N_n^{\text{iso}}}{N_w^{\text{iso}} / N_w^{\text{iso}}} \right)_{\text{data}} \times \left(\frac{B_n^{\text{iso}} / N_n^{\text{iso}}}{N_w^{\text{iso}} / N_w^{\text{iso}}} \right)_{\text{MC}} \quad N_{n,w}^{\text{iso,iso}} = \text{jet-jet} (B_{n,w}^{\text{iso,iso}}) + \gamma\text{-jet} (S_{n,w}^{\text{iso,iso}})$$

- ➔ Semi data-driven approach, simulation used to correct correlations between $p_T^{\text{iso, ch}}$ and σ_{long}^2



Purity, pp $\sqrt{s} = 13$ TeV

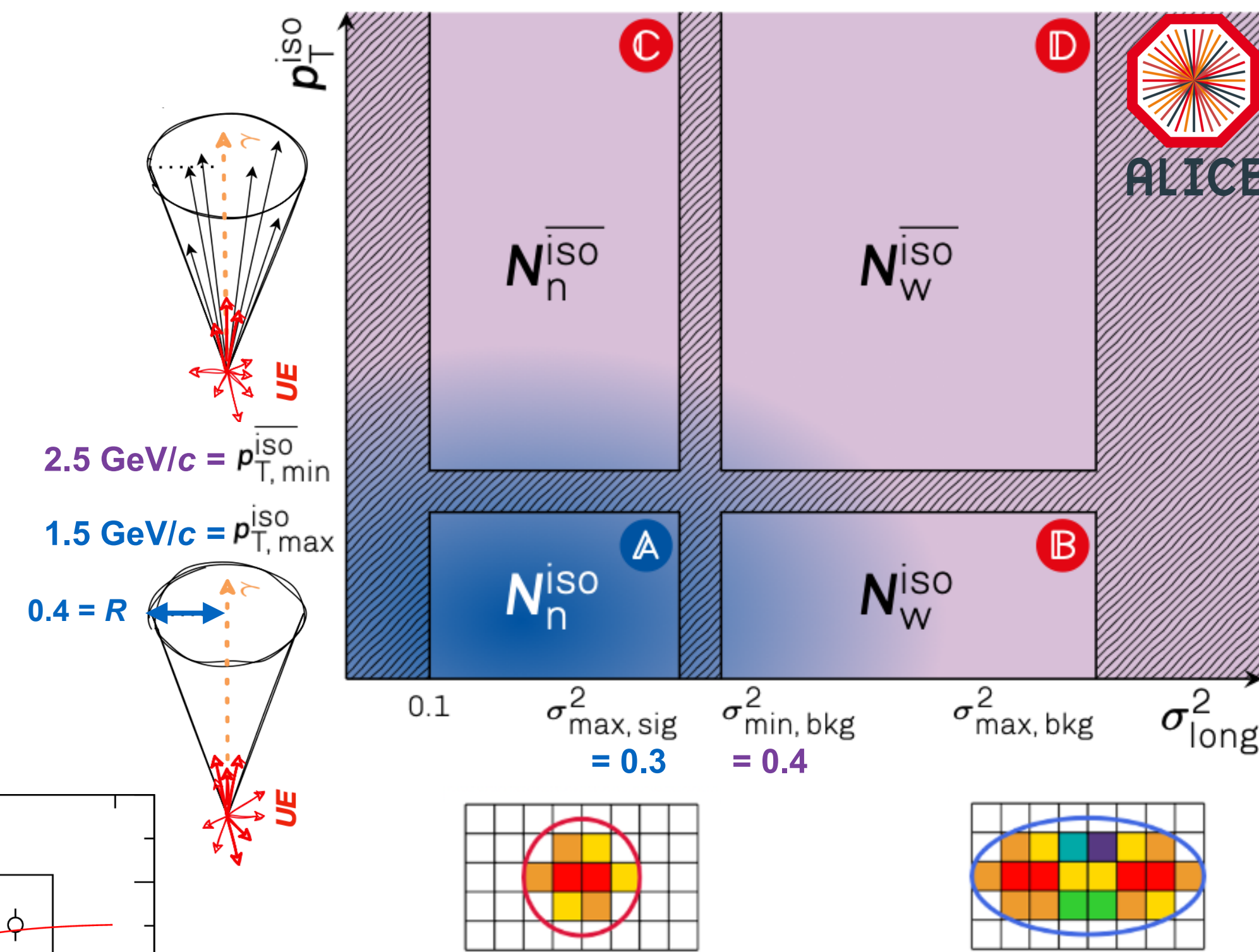
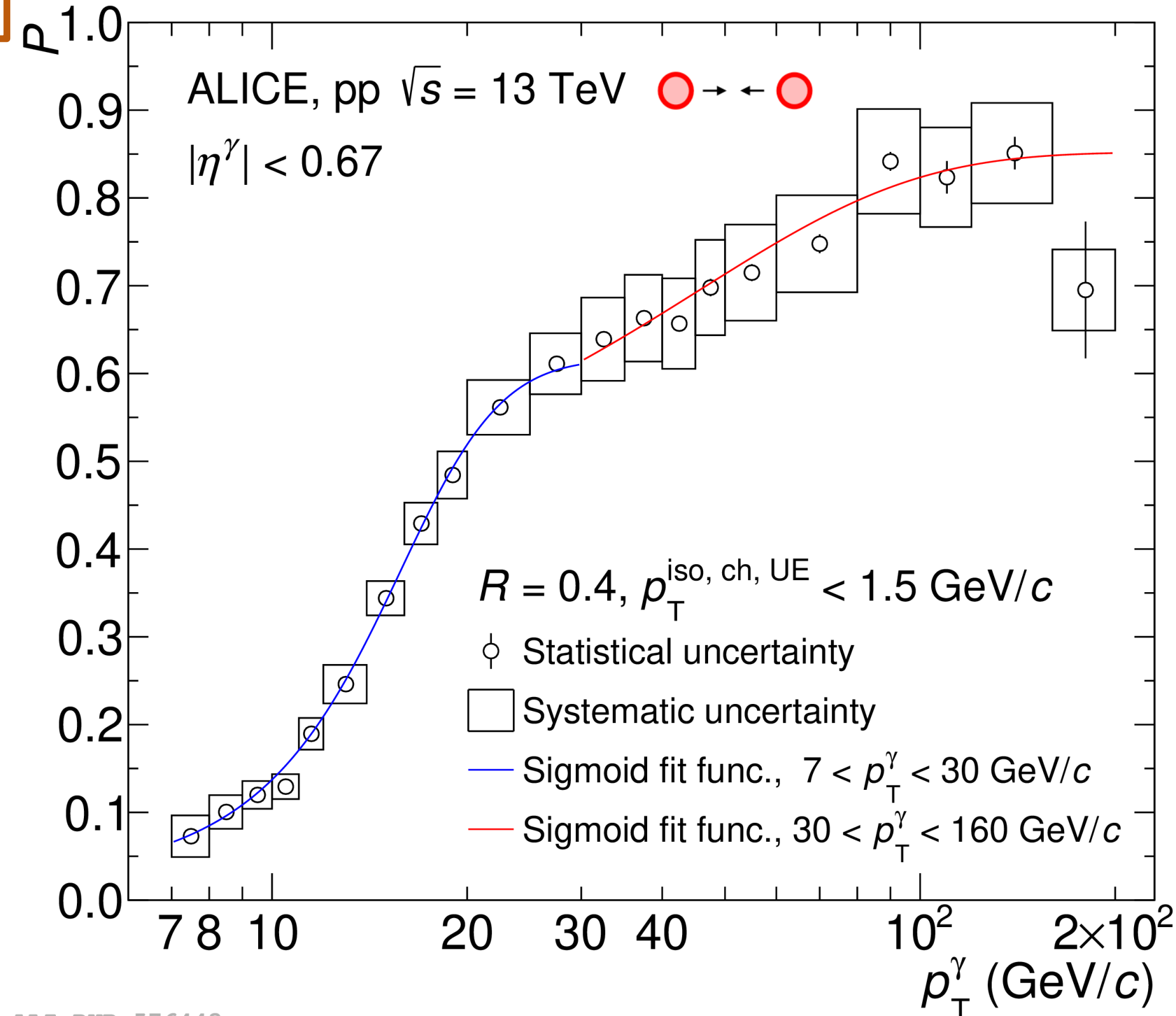
- Purity, ABCD method: Phase space of calorimeter clusters divided in 4 regions: **A**, signal dominated & **B-C-D**, background dominated

$$P = 1 - \left(\frac{N_n^{\text{iso}} / N_n^{\text{iso}}}{N_w^{\text{iso}} / N_w^{\text{iso}}} \right)_{\text{data}} \times \left(\frac{B_n^{\text{iso}} / N_n^{\text{iso}}}{N_w^{\text{iso}} / N_w^{\text{iso}}} \right)_{\text{MC}}$$

Data driven PYTHIA

$$N_{n,w}^{\text{iso,iso}} = \text{jet-jet} (B_{n,w}^{\text{iso,iso}}) + \gamma\text{-jet} (S_{n,w}^{\text{iso,iso}})$$

- ➔ Semi data-driven approach, simulation used to correct correlations between $p_T^{\text{iso, ch}}$ and σ_{long}^2



- Reduce the influence of statistical fluctuations with sigmoid function fits

Purity, Pb-Pb $\sqrt{s_{NN}} = 5.02$ TeV

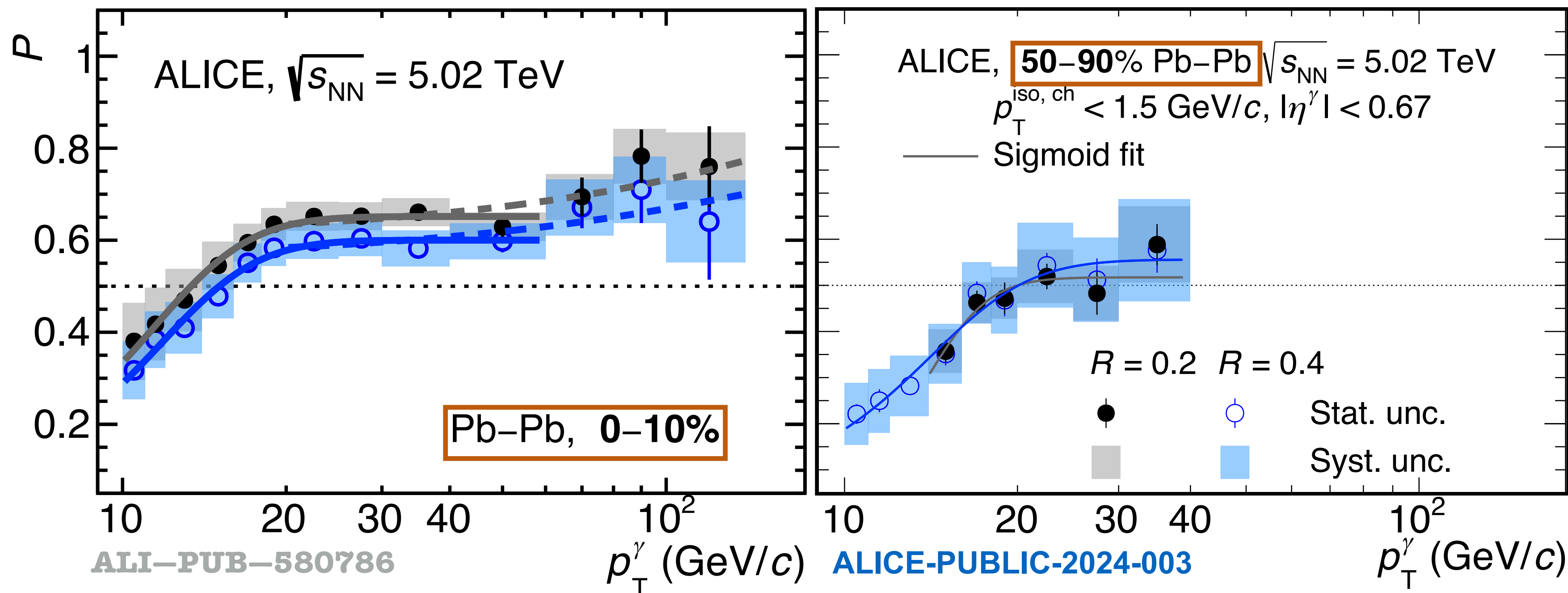
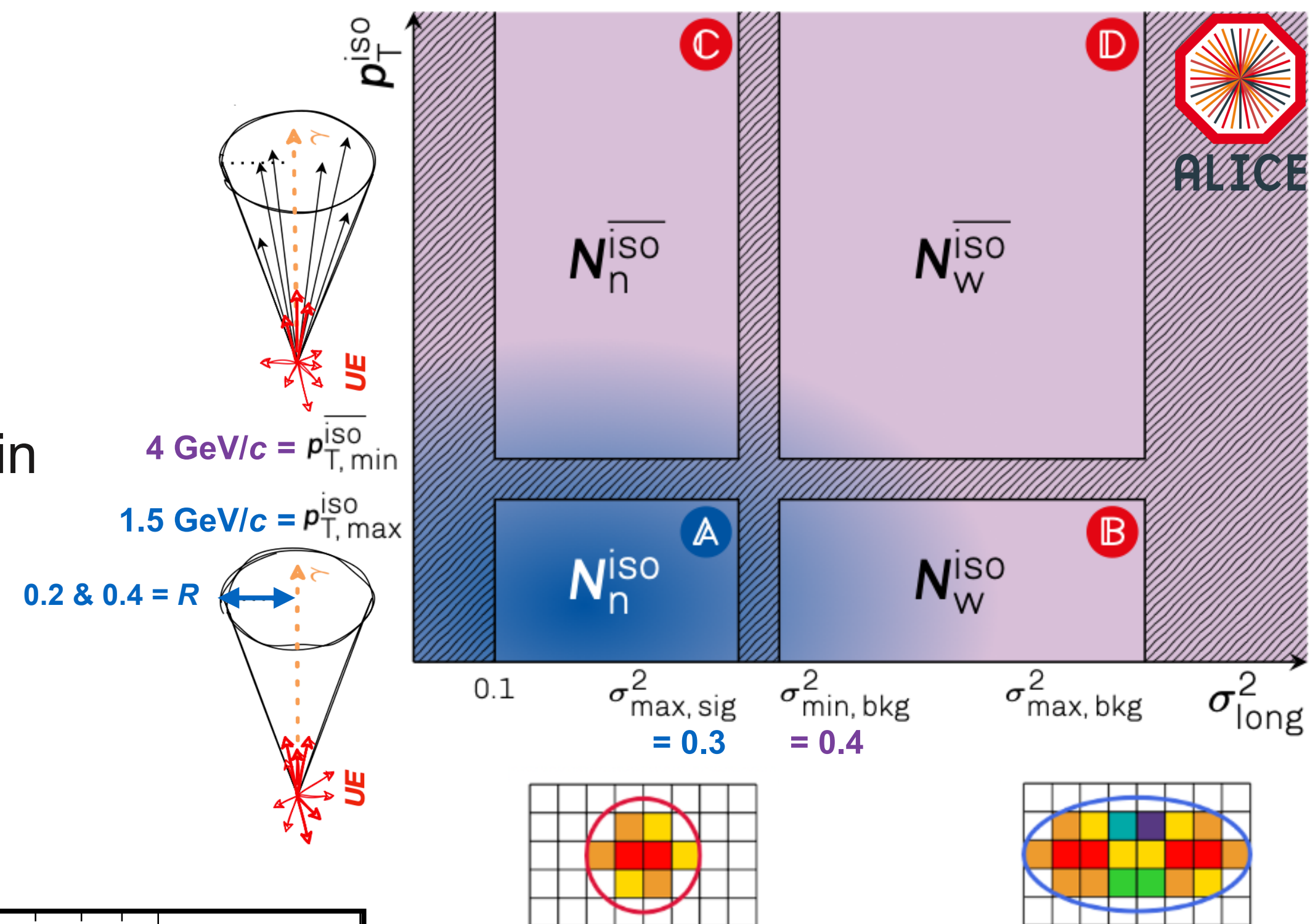
- Purity, ABCD method: Phase space of calorimeter clusters divided in 4 regions: **A**, signal dominated & **B-C-D**, background dominated

$$P = 1 - \left(\frac{N_n^{\text{iso}}/N_n^{\text{iso}}}{N_w^{\text{iso}}/N_w^{\text{iso}}} \right)_{\text{data}} \times \left(\frac{B_n^{\text{iso}}/N_n^{\text{iso}}}{N_w^{\text{iso}}/N_w^{\text{iso}}} \right)_{\text{MC}}$$

Data driven PYTHIA

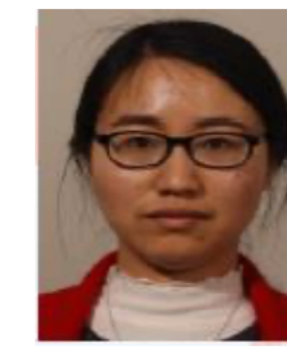
MC

$$N_{n,w}^{\text{iso,iso}} = \text{jet-jet} (B_{n,w}^{\text{iso,iso}}) + \gamma\text{-jet} (S_{n,w}^{\text{iso,iso}})$$

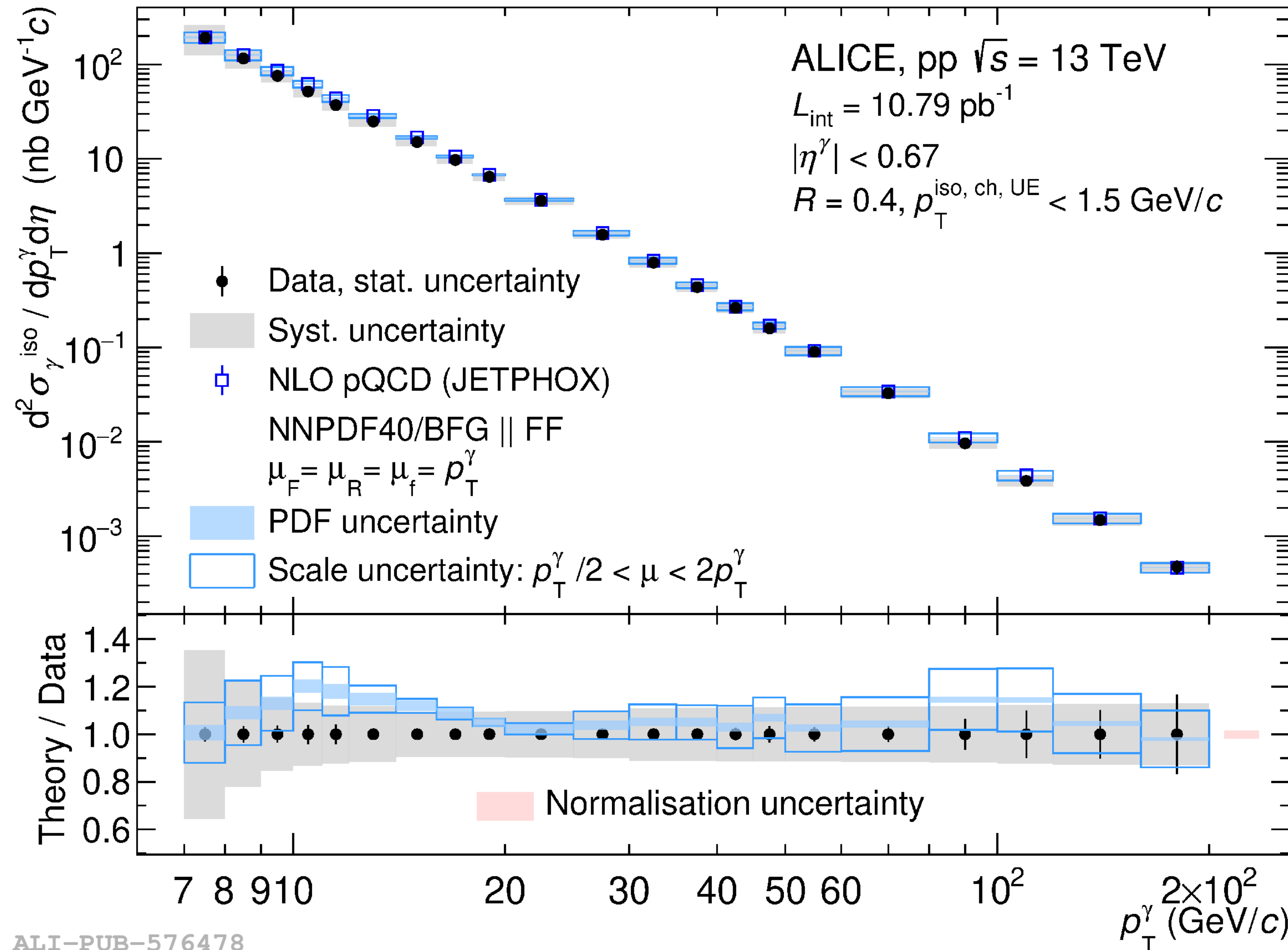


- Reduce the influence of statistical fluctuations with sigmoid function fits

Cross section, pp $\sqrt{s} = 13$ TeV



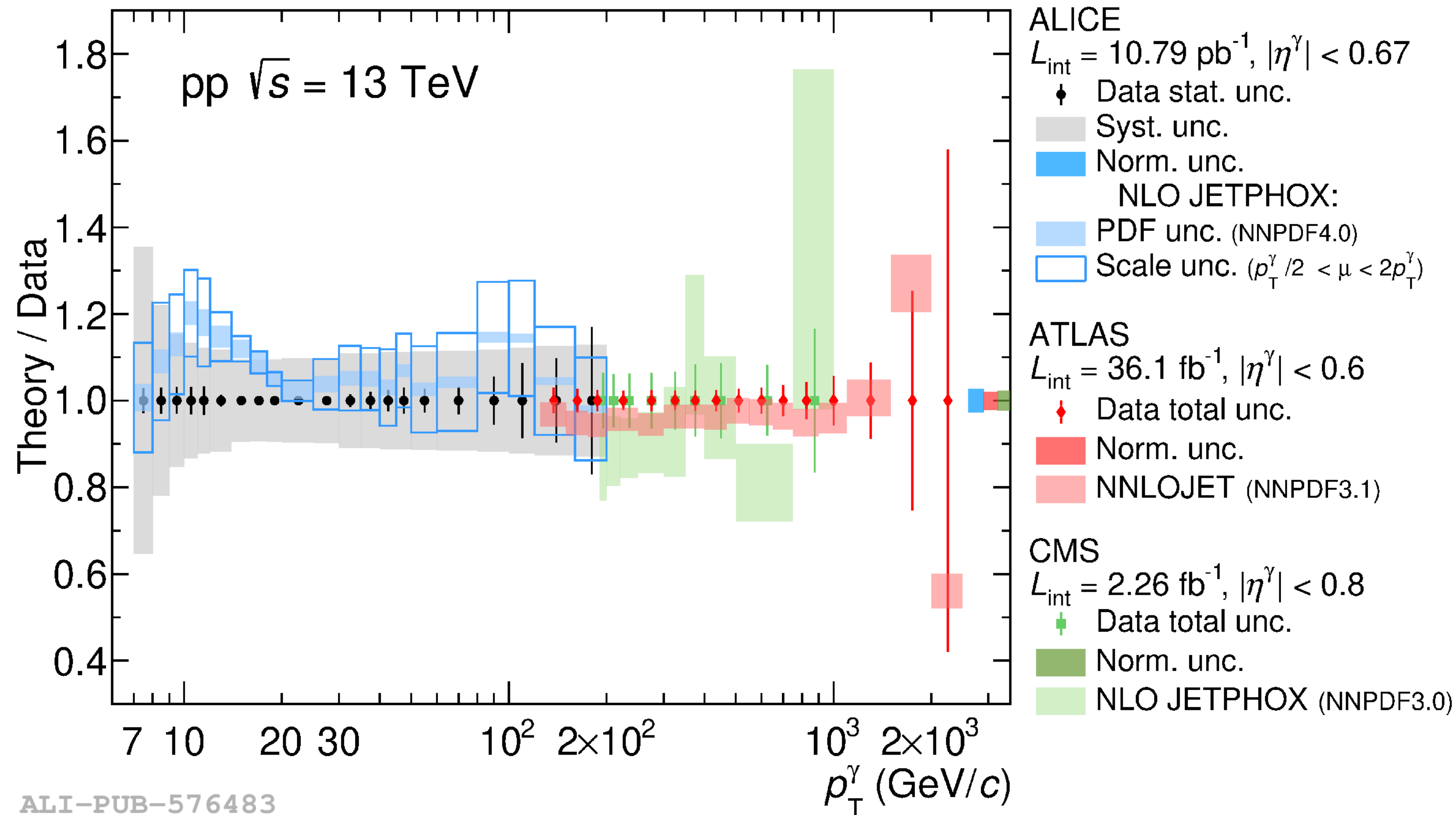
Ran Xu thesis
Publication
accepted by EPJ C



- ➔ NLO pQCD predictions (JETPHOX) and data agree
- ➔ Significantly lower p_T than CMS and ATLAS at $\sqrt{s} = 13$ TeV
- ➔ Lowest x_T at mid-rapidity

ALI-PUB-576478

Cross section, pp $\sqrt{s} = 13$ TeV



➔ NLO pQCD predictions (JETPHOX) and data agree

➔ Significantly lower p_T than CMS and ATLAS at $\sqrt{s} = 13$ TeV

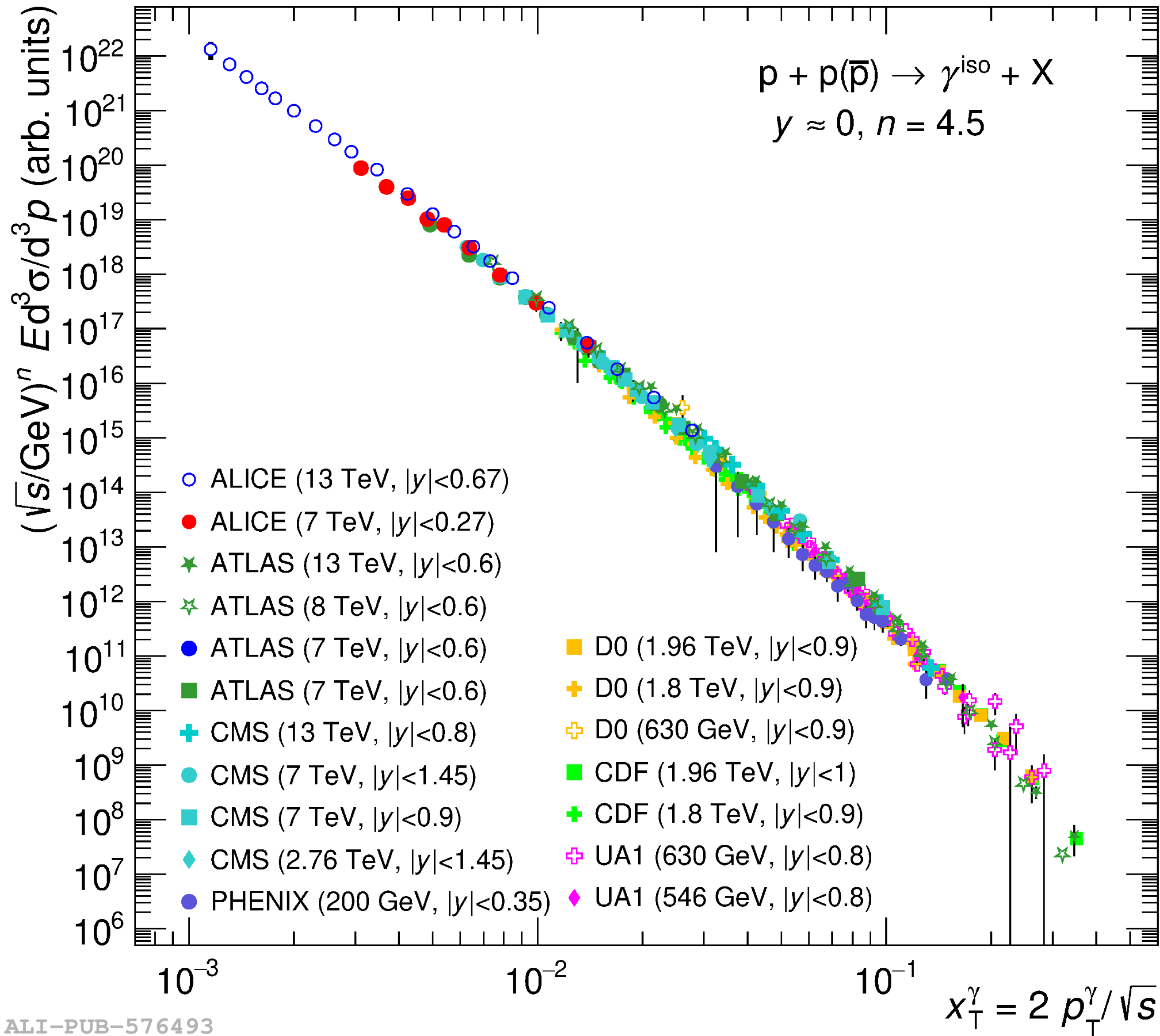
➔ Lowest x_T at mid-rapidity

ALI-PUB-576483

ATLAS JHEP 2019 (2019) 203
 arXiv:1908.02746 [hep-ex]

CMS Eur. Phys. J. C 79 (2019) 20
 arXiv:1807.00782 [hep-ex]

Cross section, pp $\sqrt{s} = 13$ TeV

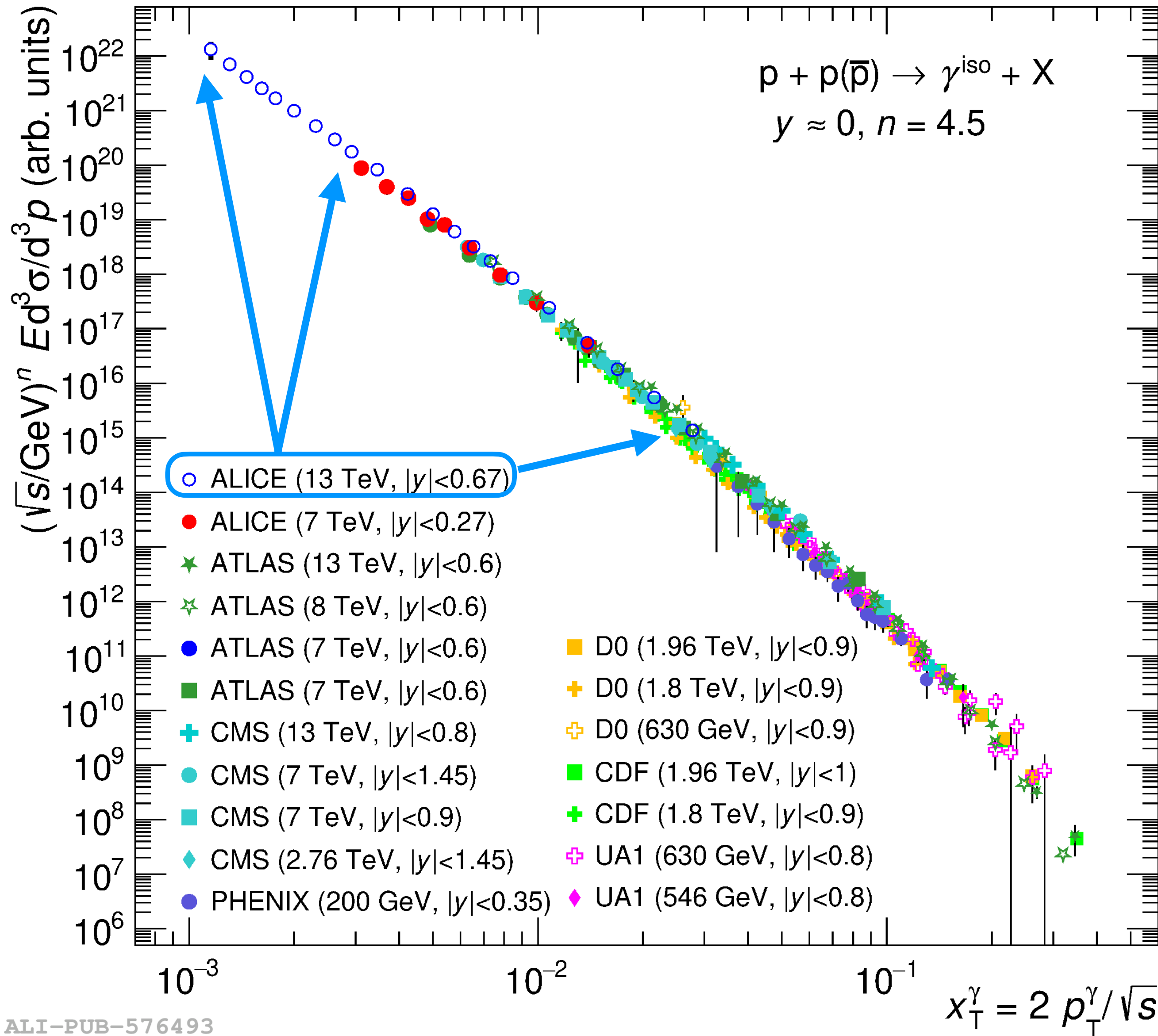


- ➔ NLO pQCD predictions (JETPHOX) and data agree
- ➔ Significantly lower p_T than CMS and ATLAS at $\sqrt{s} = 13$ TeV
- ➔ Lowest x_T at mid-rapidity

◆ $(\sqrt{s})^{4.5}$ scale from $x_T \sim 10^{-3}$ to 10^{-1}

Full list of older results compiled in [D. D'Enterria & J. Rojo Nucl. Phys. B 860 \(2012\), arXiv:1202.1762 \[hep-ph\]](#)

Cross section, pp $\sqrt{s} = 13$ TeV



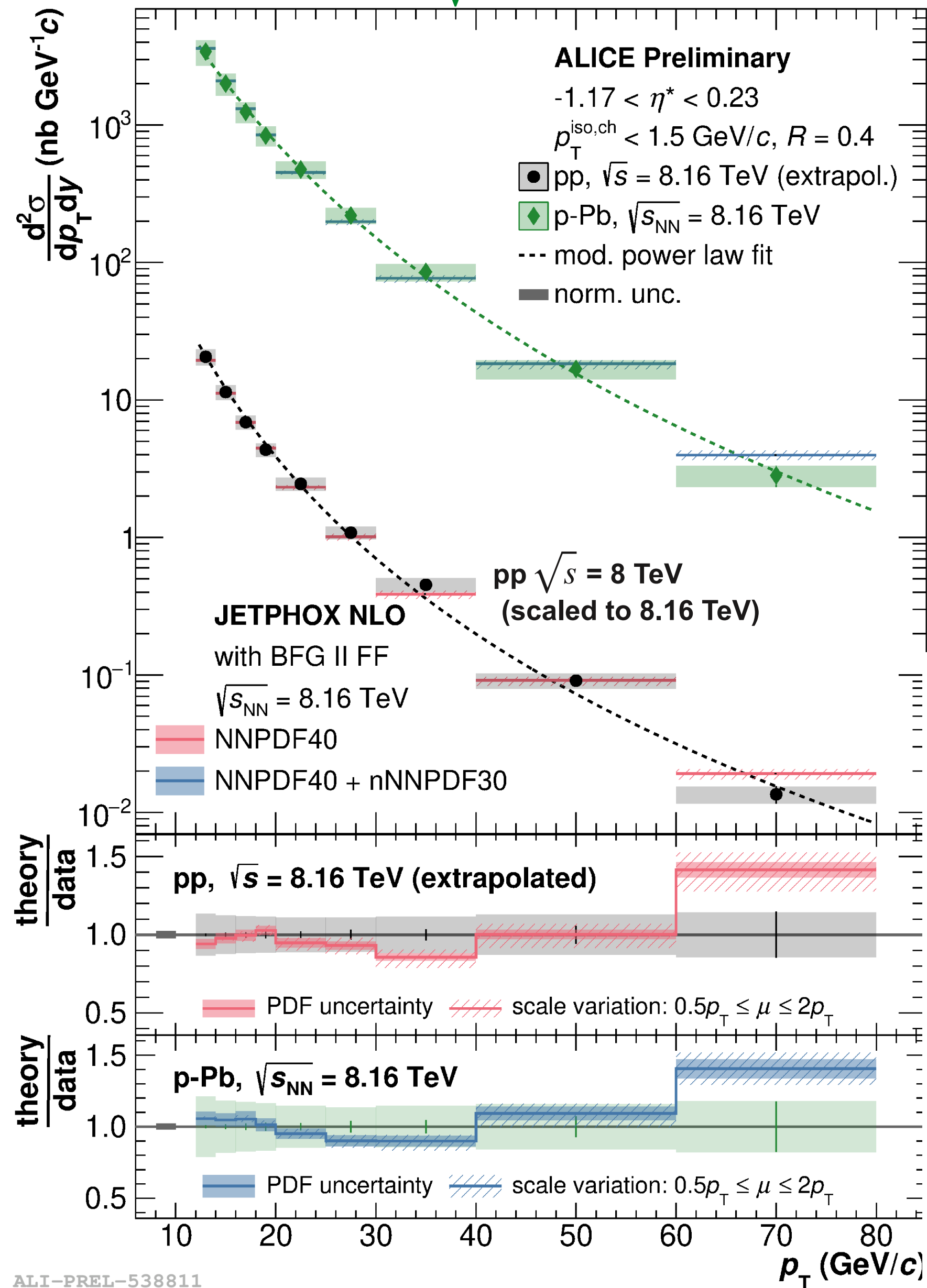
- ➔ NLO pQCD predictions (JETPHOX) and data agree
- ➔ Significantly lower p_T than CMS and ATLAS at $\sqrt{s} = 13$ TeV
- ➔ Lowest x_T at mid-rapidity

$(\sqrt{s})^{4.5}$ scale from $x_T \sim 10^{-3}$ to 10^{-1}

Full list of older results compiled in [D. D'Enterria & J. Rojo Nucl. Phys. B 860 \(2012\), arXiv:1202.1762 \[hep-ph\]](#)

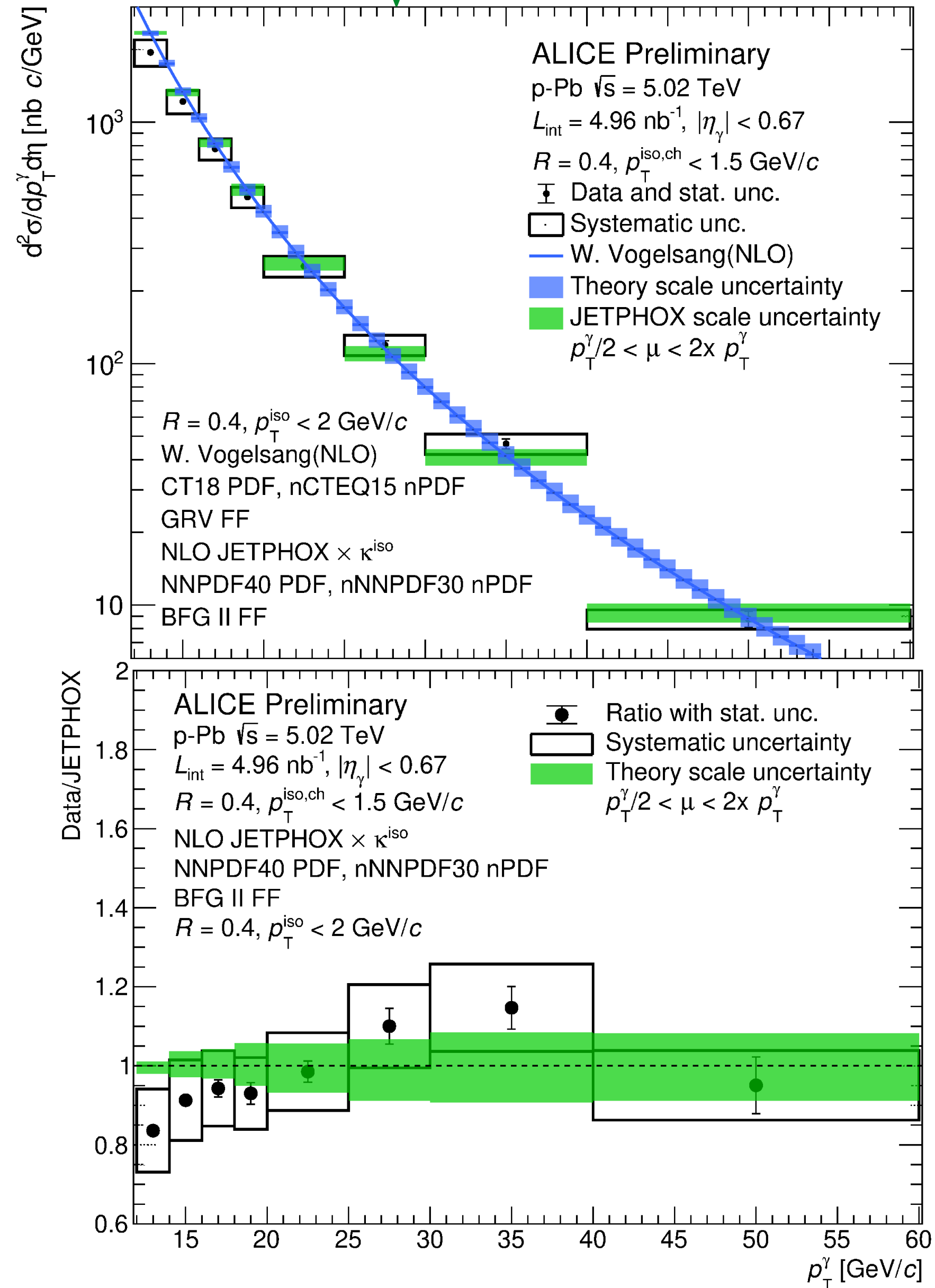
Cross section, p-Pb

pp, p-Pb, $\sqrt{s_{NN}} = 8.16$ TeV



ALI-PREL-538811

p-Pb, $\sqrt{s_{NN}} = 5.02$ TeV

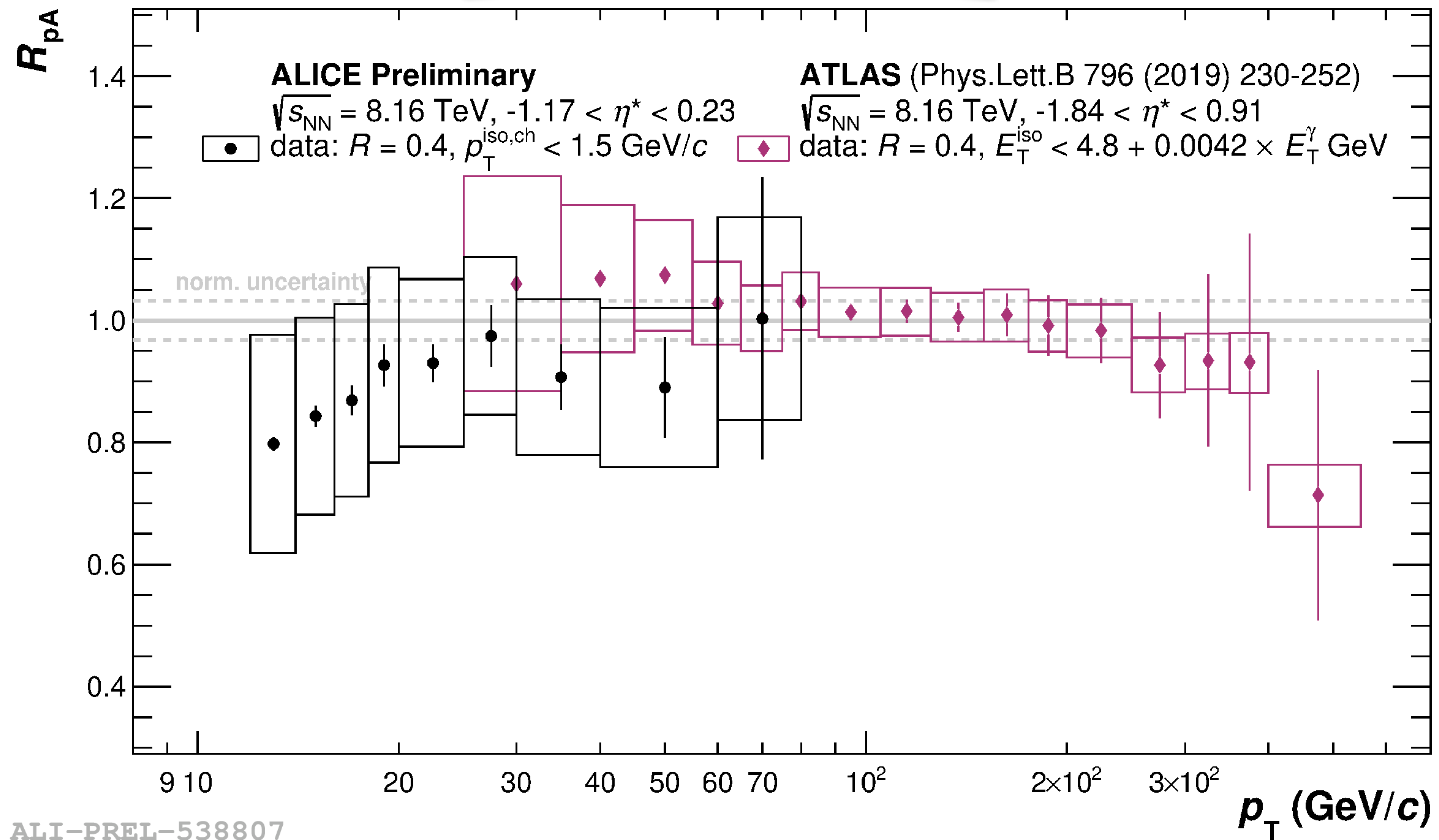


ALI-PREL-508690

➔ NLO pQCD predictions (JETPHOX) and data agree

Nuclear modification factor R_{pA}

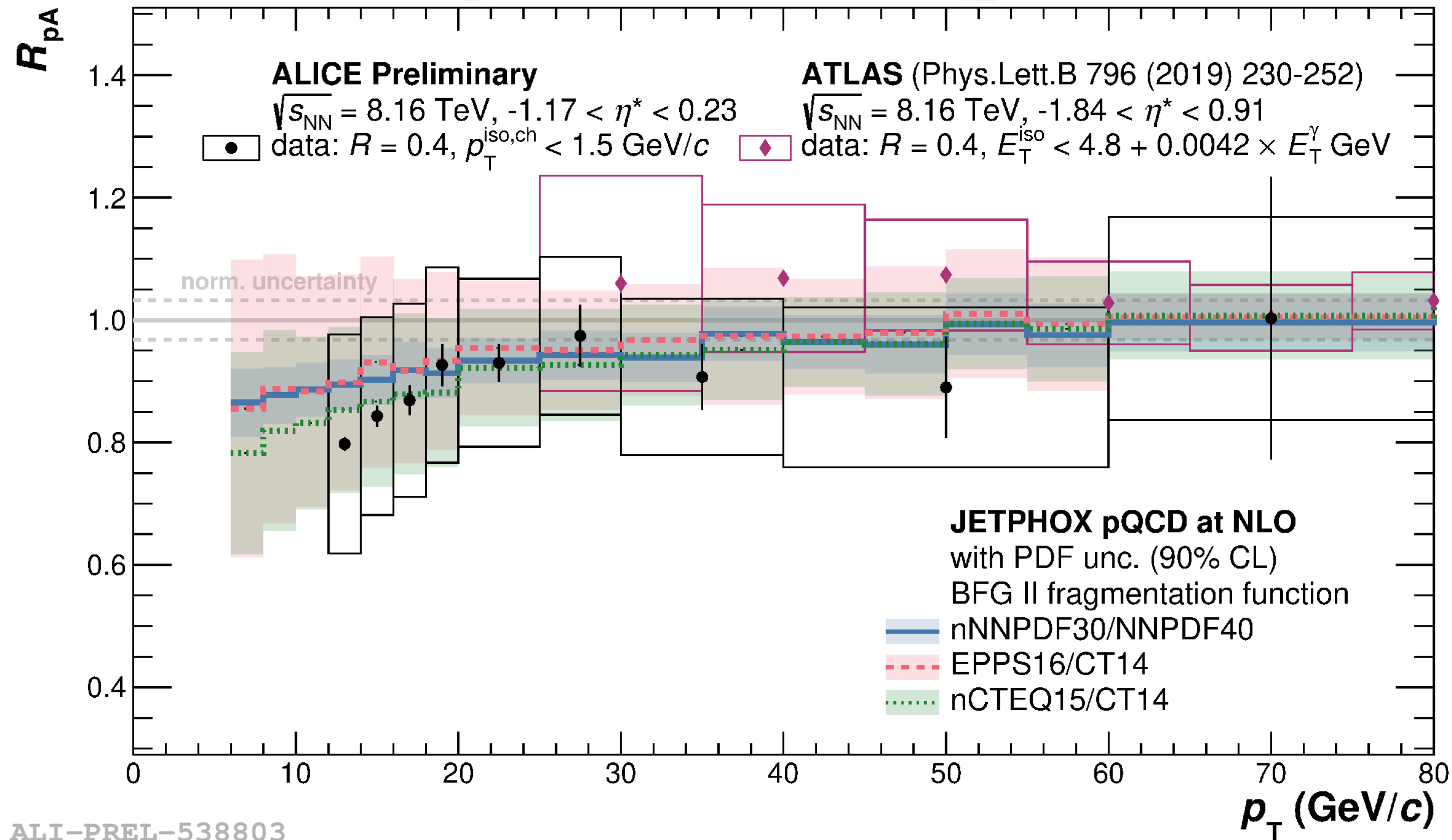
$$R_{pA} = \frac{d^2\sigma_{pA}^\gamma / dp_T dy^*}{A_{Pb} \times d^2\sigma_{pp}^\gamma / dp_T dy^*}$$



- R_{pA} in agreement with unity
 - No suppression at high p_T , agreement with ATLAS
 - Hints of lower than unity for $p_T < 20$ GeV/c, expected in theory, cold nuclear matter effects, shadowing

Nuclear modification factor R_{pA}

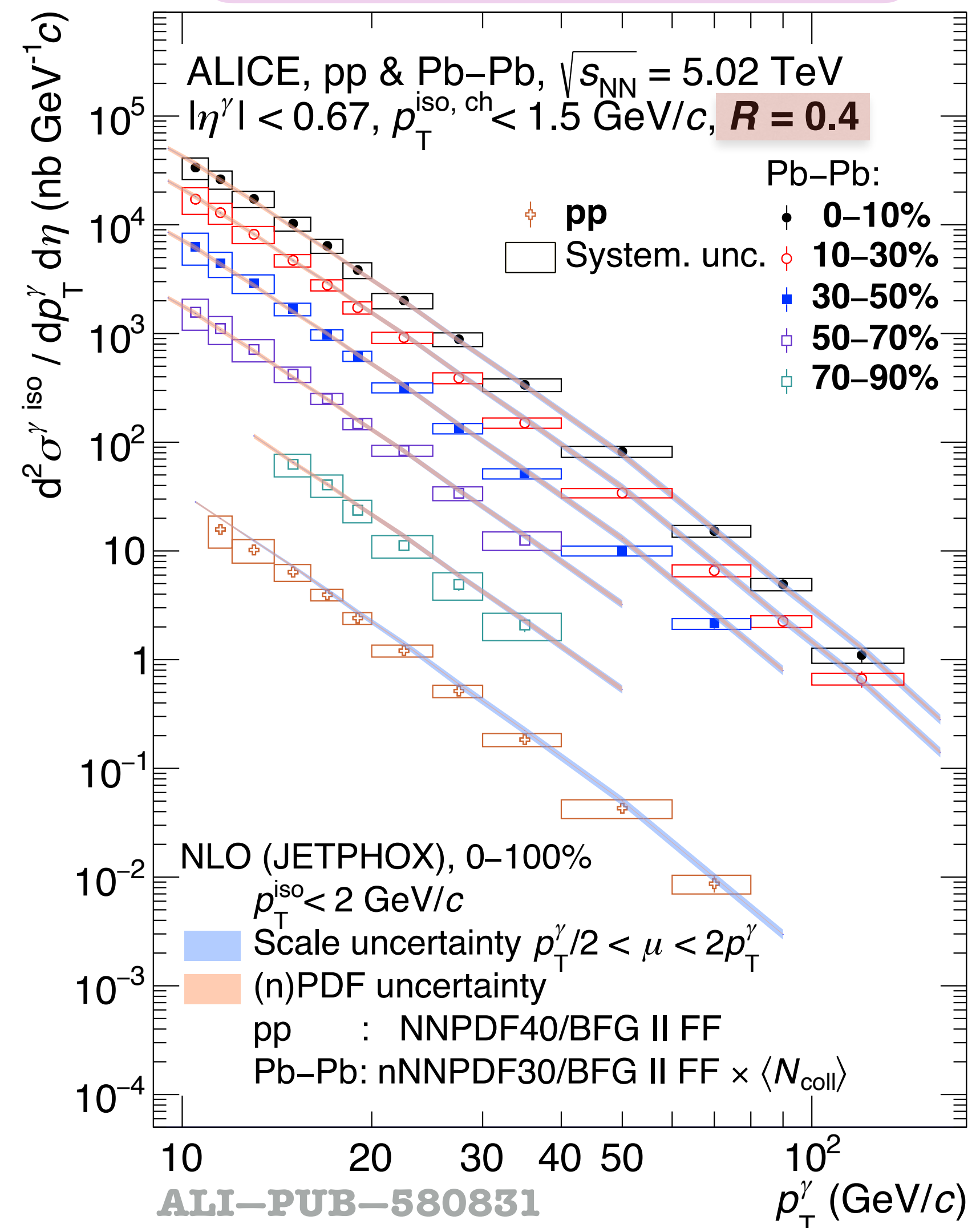
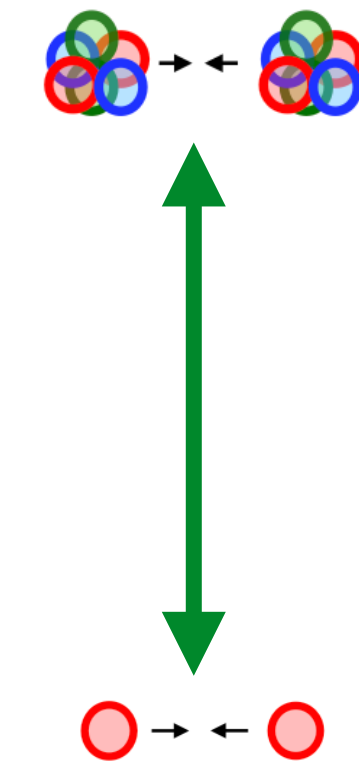
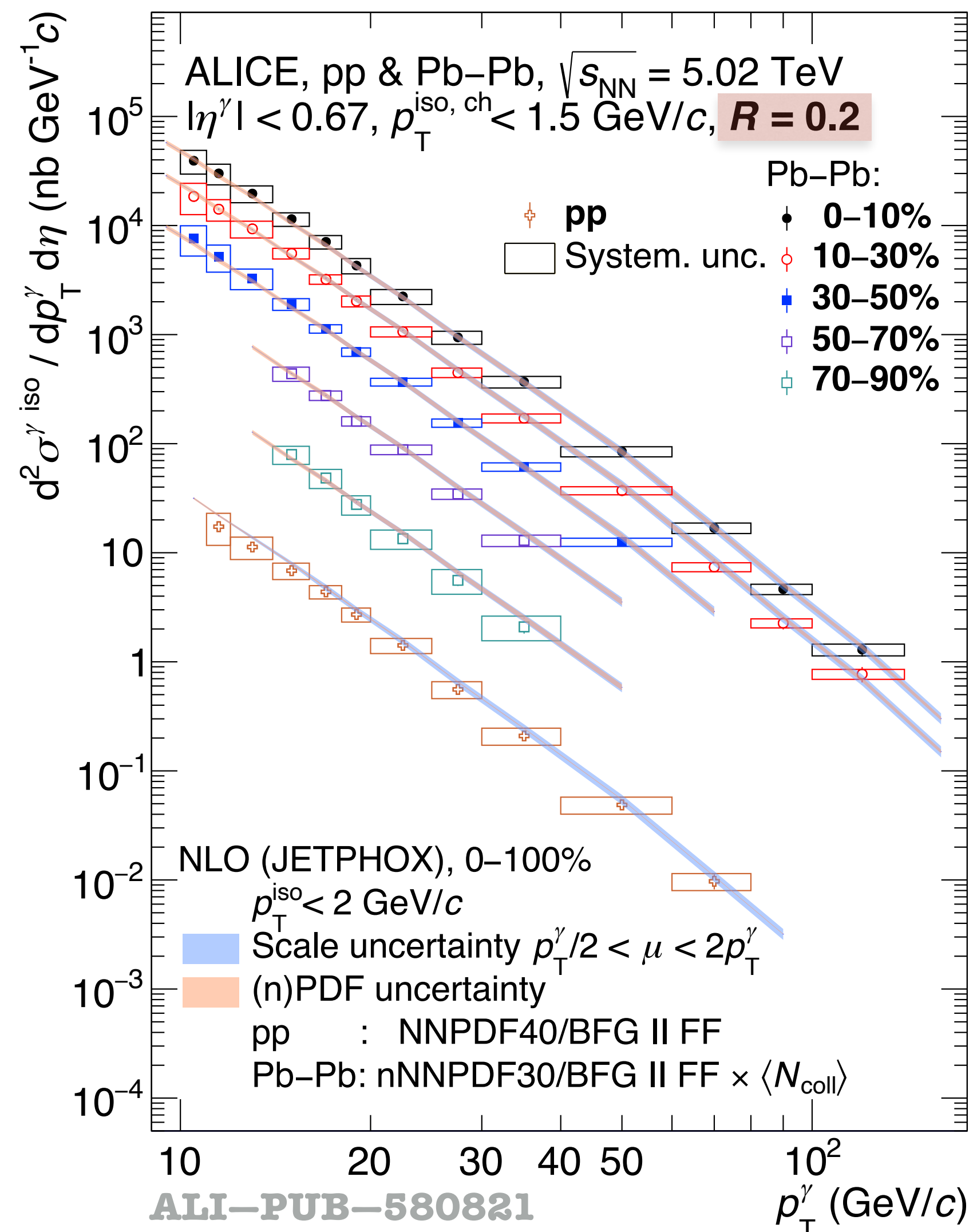
$$R_{pA} = \frac{d^2\sigma_{pA}^\gamma / dp_T dy^*}{A_{Pb} \times d^2\sigma_{pp}^\gamma / dp_T dy^*}$$



- R_{pA} in agreement with unity
 - No suppression at high p_T , agreement with ATLAS
 - Hints of lower than unity for $p_T < 20 \text{ GeV}/c$, expected in theory, cold nuclear matter effects, shadowing

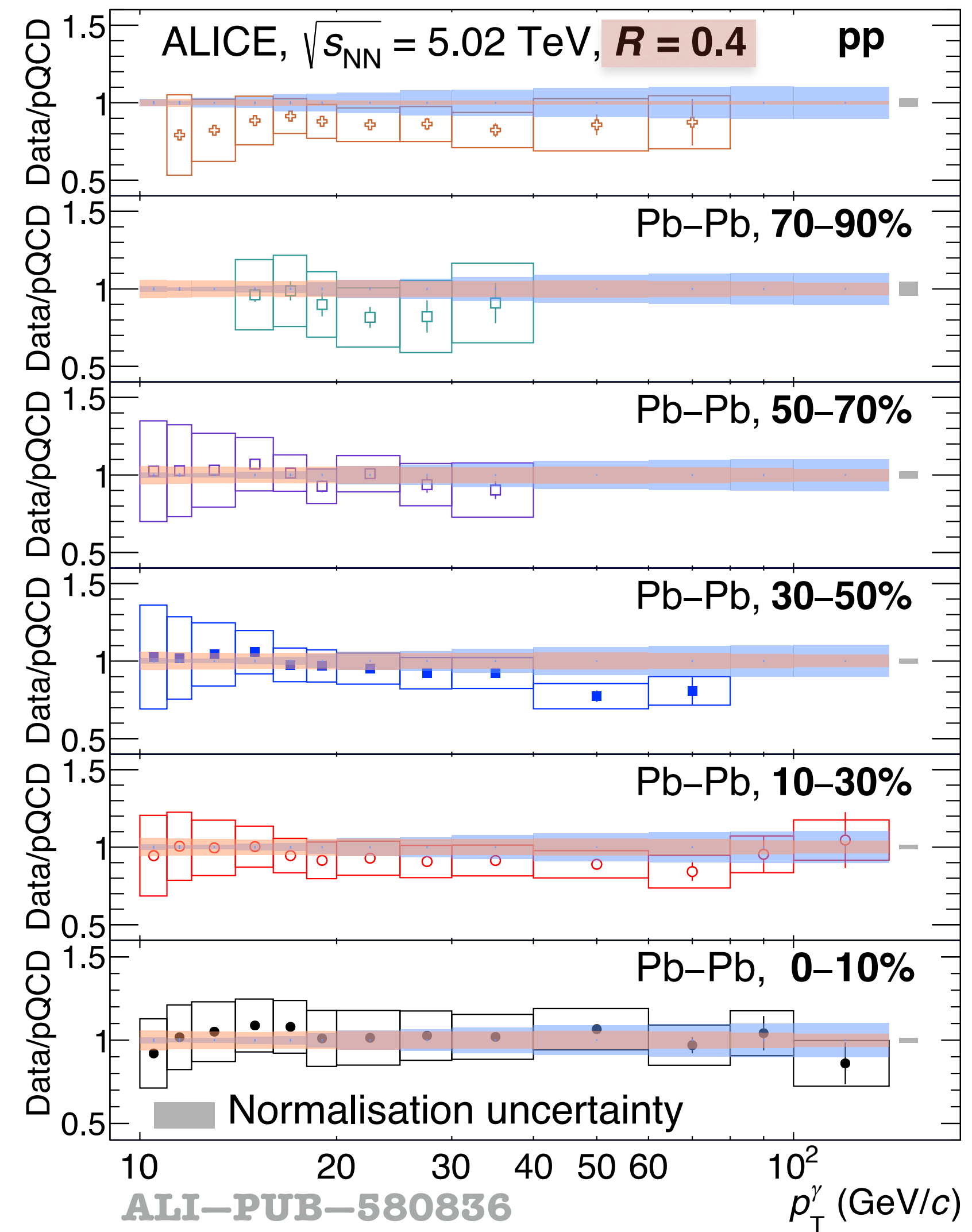
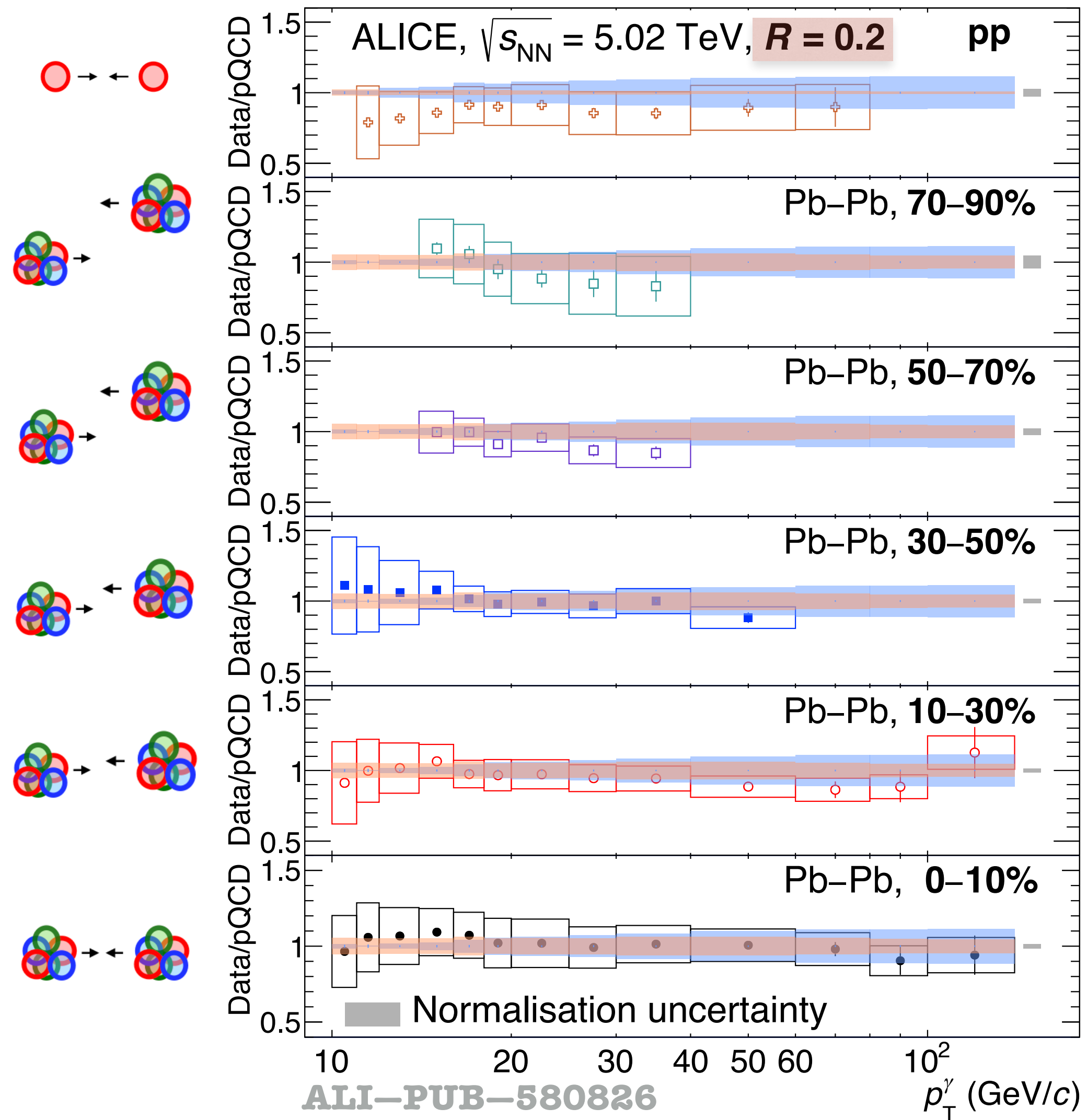
Cross section, pp & Pb-Pb at $\sqrt{s_{NN}} = 5.02$ TeV

$$\frac{d^2\sigma^{\gamma \text{ iso}}}{dp_T d\eta} = \frac{\sigma_{NN}^{\text{INEL}}}{N_{\text{events}} \times \text{RF}_{\text{trig}}} \times \frac{d^2N}{dp_T d\eta} \times \frac{P}{\text{Acc} \times \epsilon_{\gamma}^{\text{iso}} \times \epsilon_{\text{trig}}}$$



- Wide range: $10 < p_T < 140$ GeV/c in Pb-Pb 0-30% & $11 < p_T < 80$ GeV/c in pp
- NLO pQCD predictions (JETPHOX)
- ➔ Note: Theory calculated for 0-100%, PDF (pp) & nPDF $\times N_{\text{coll}}$ (Pb-Pb)

Cross section, pp & Pb–Pb at $\sqrt{s_{NN}} = 5.02$ TeV



- NLO pQCD predictions (JETPHOX)
- ➔ Note: Theory calculated for 0–100%, PDF (pp) & nPDF $\times N_{coll}$ (Pb–Pb)
- Theory & data agreement for both R and collision system

Cross section R ratio, pp & Pb–Pb at $\sqrt{s_{NN}} = 5.02$ TeV

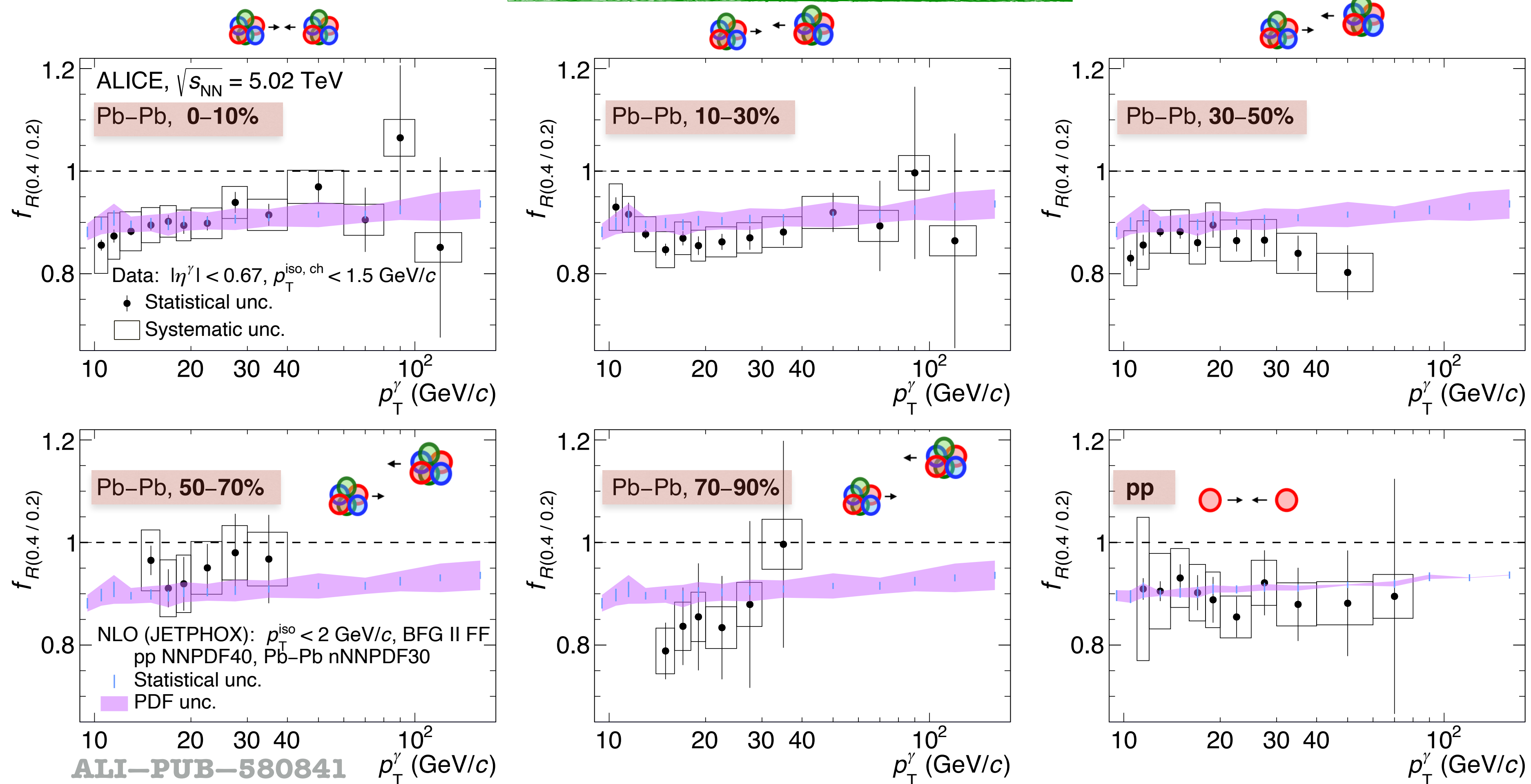
$$f_{R(0.4/0.2)} = \frac{d^2\sigma}{dp_T d\eta} \Big|_{(R=0.4)} / \frac{d^2\sigma}{dp_T d\eta} \Big|_{(R=0.2)}$$

- Sensitive to fraction of fragmentation γ surviving the isolation selection

➔ Interesting for theory models

- Agreement with theory and between collision systems

➔ Theory (NLO): controls the isolation mechanism, fragmentation γ & prompt γ production even in Pb–Pb

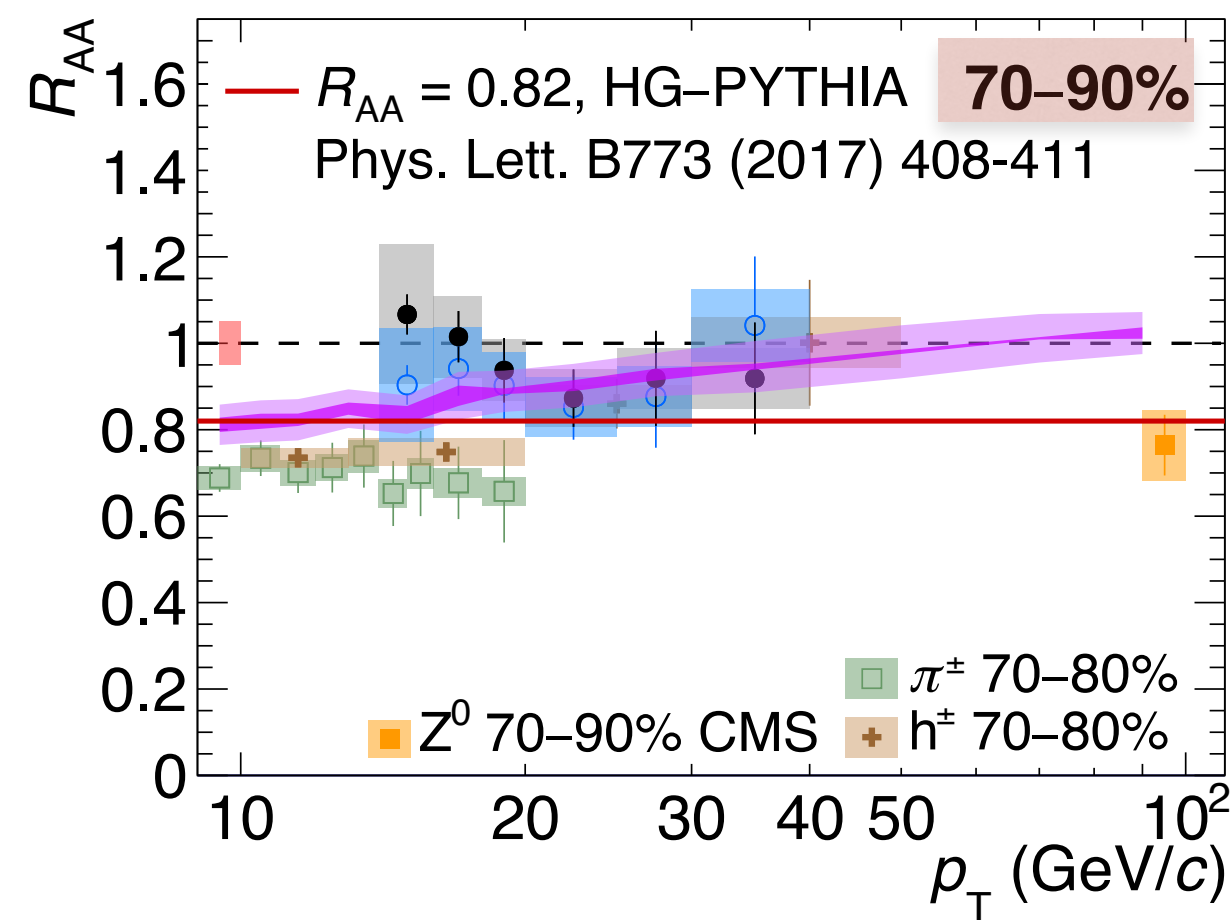
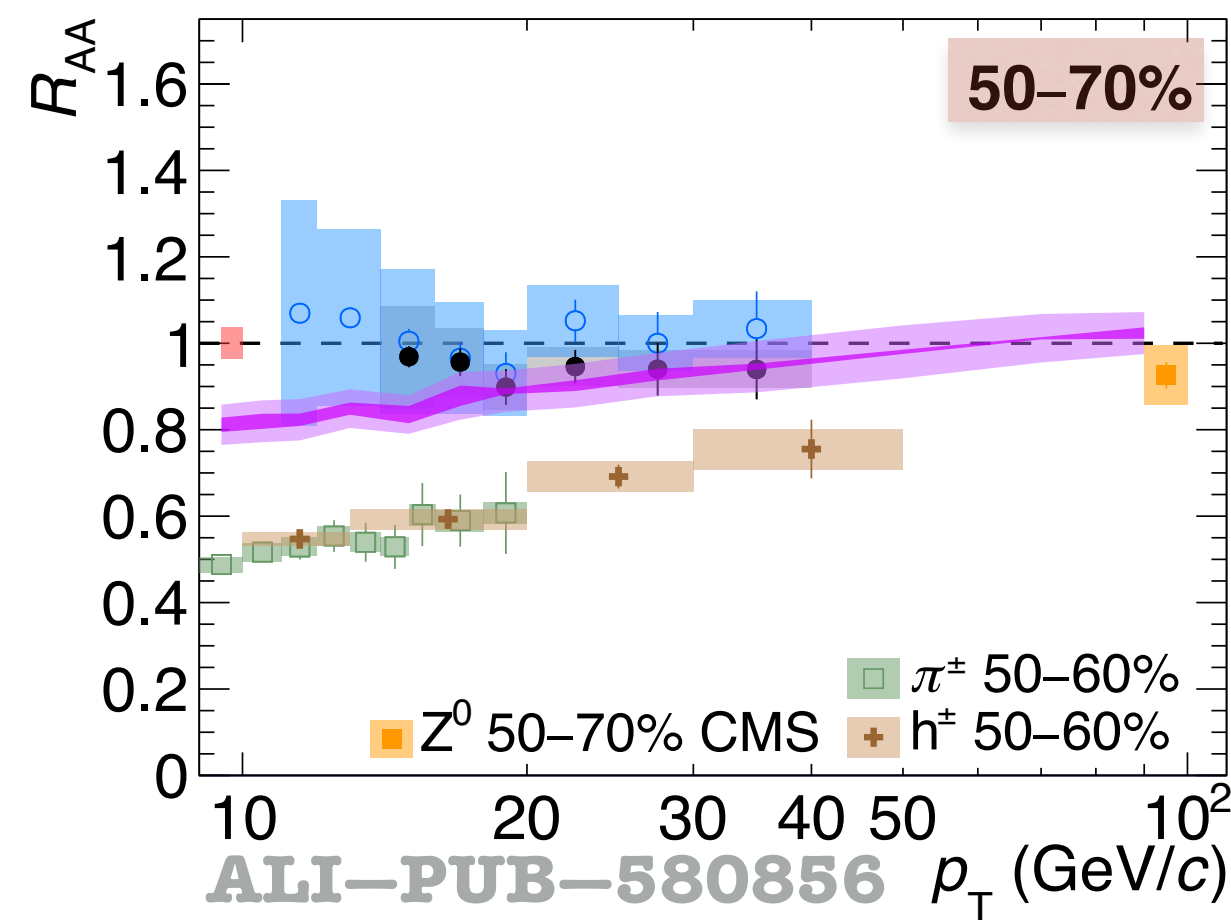
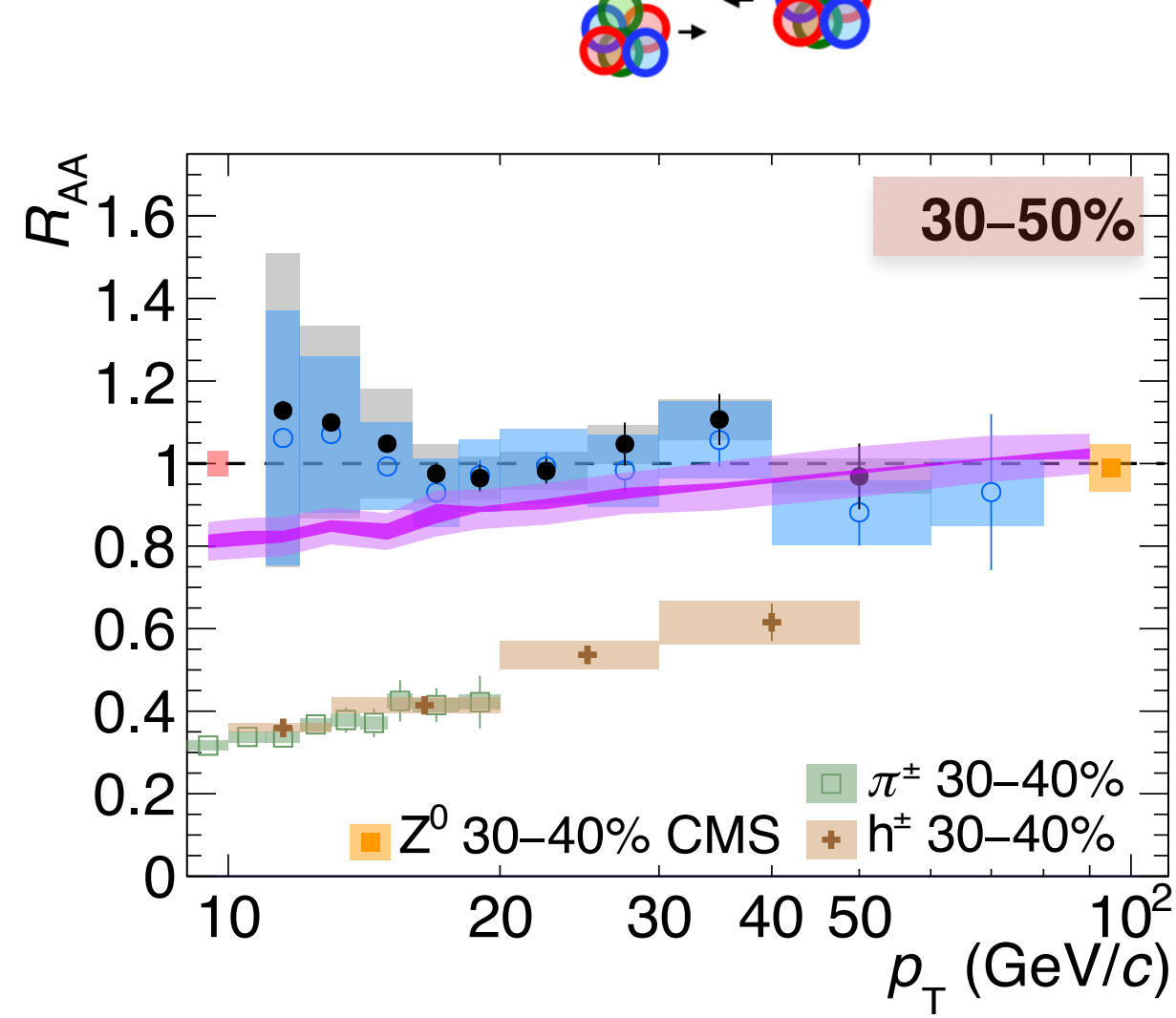
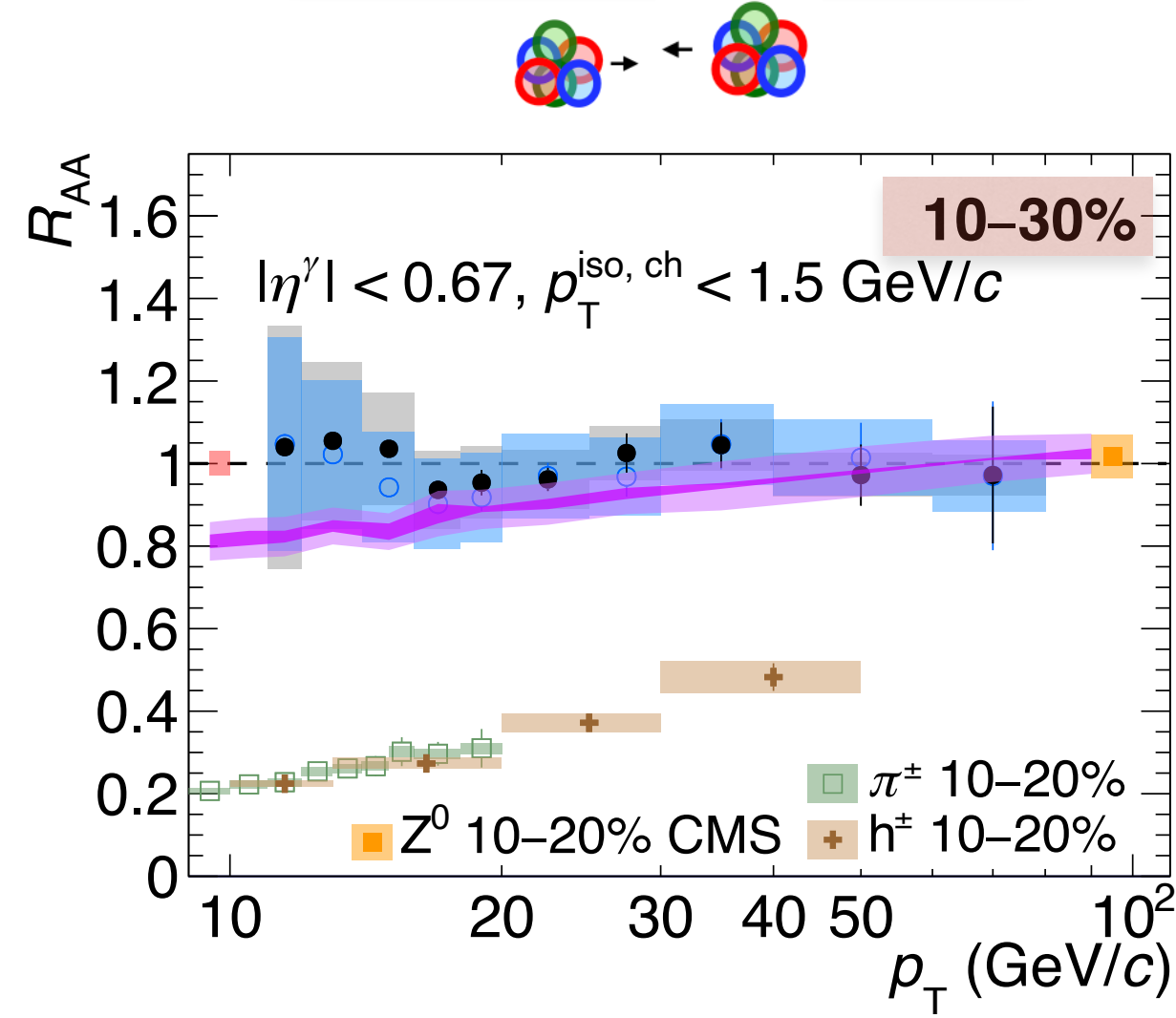
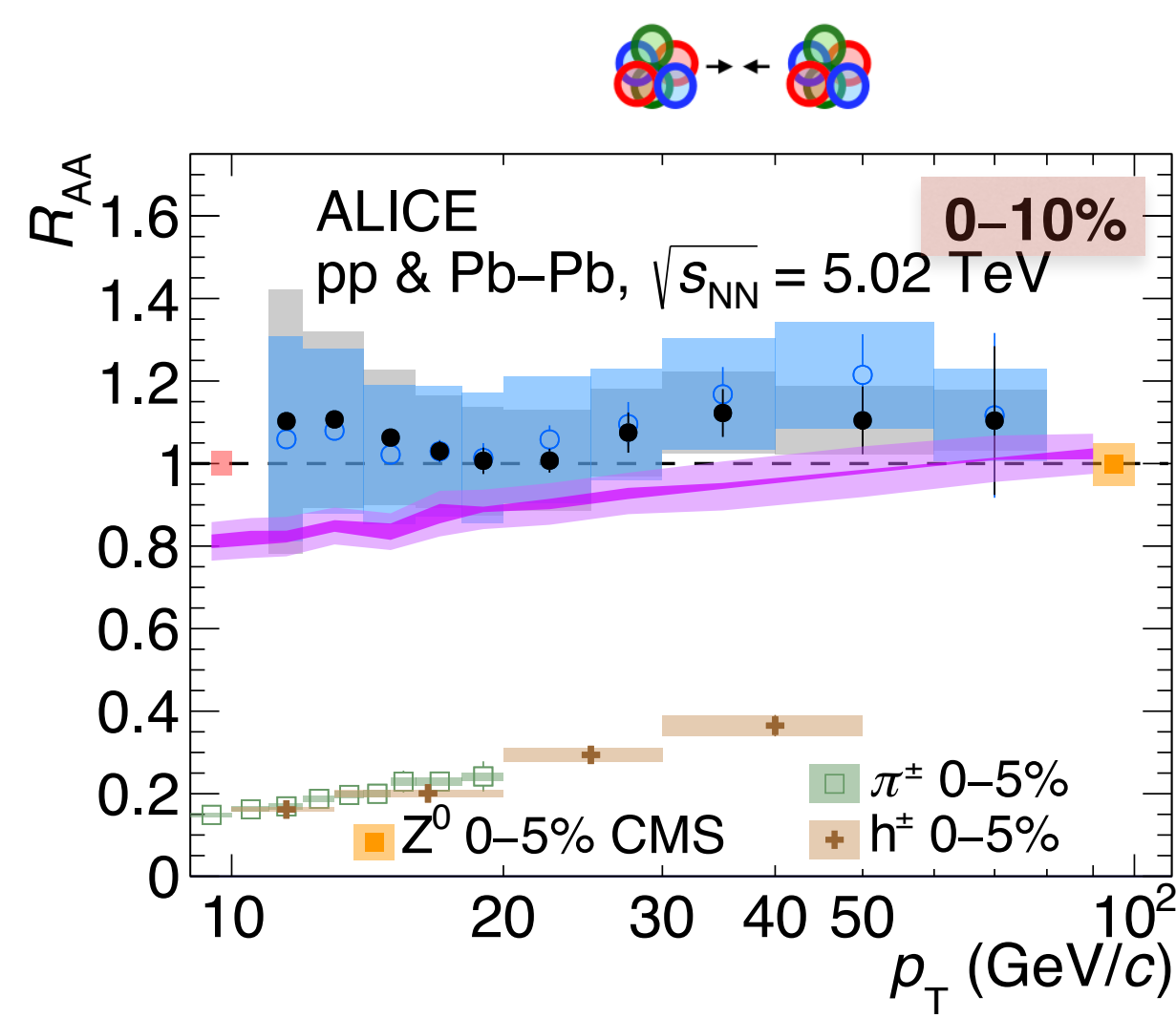


* Not shown (back-up): ATLAS pp $\sqrt{s} = 13$ TeV, for $p_T > 250$ GeV/c
JHEP 07 (2023) 86 arXiv:2302.00510

Nuclear modification factor R_{AA} , pp & Pb-Pb at $\sqrt{s_{NN}} = 5.02$ TeV

- 0-70%
 - Consistent with unity within the unc. for both R
 - No modification of the prompt γ yield due to the QGP as expected
 - Agreement with NLO pQCD incorporating cold matter nuclear effects: PDF vs nPDF

$$R_{AA} = \frac{1}{\langle N_{coll} \rangle} \frac{d^2\sigma_{AA} / (dp_T d\eta)}{d^2\sigma_{pp} / (dp_T d\eta)}$$



- $R = 0.2$ stat. unc. ◯ $R = 0.4$ stat. unc.
- $R = 0.2$ syst. unc. ■ $R = 0.4$ syst. unc.
- Normalisation unc.
- NLO (JETPHOX), 0-100%
 $p_T^{iso} < 2$ GeV/c, $R = 0.2$
pp : NNPFD40/BFG II FF
Pb-Pb: nNNPDF30/BFG II FF, 0-100%
- Scale unc. $p_T^\gamma/2 < \mu < 2p_T^\gamma$
- PDF unc.

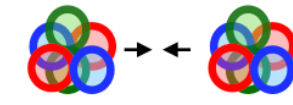
Nuclear modification factor R_{AA} , pp & Pb-Pb at $\sqrt{s_{NN}} = 5.02$ TeV

0-70%

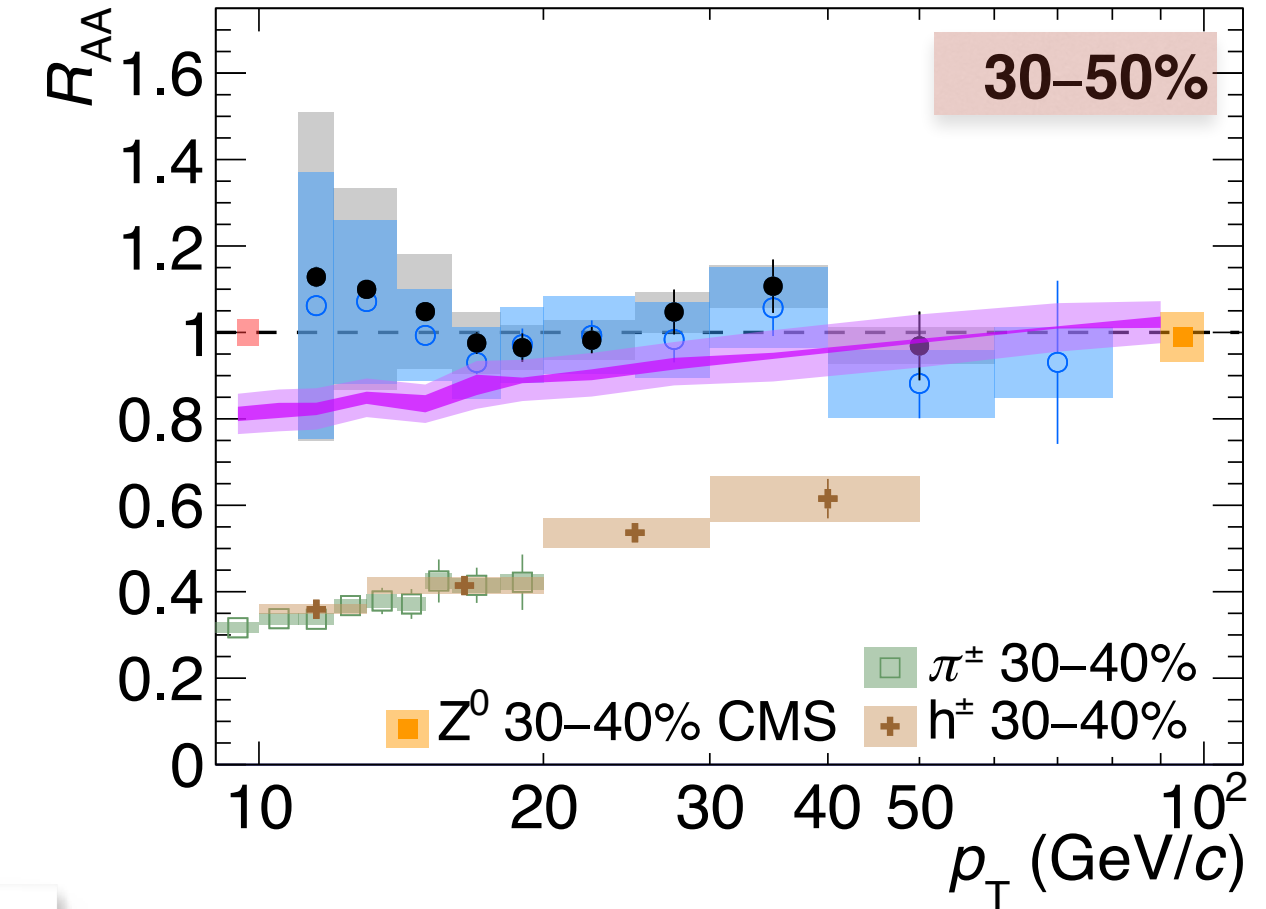
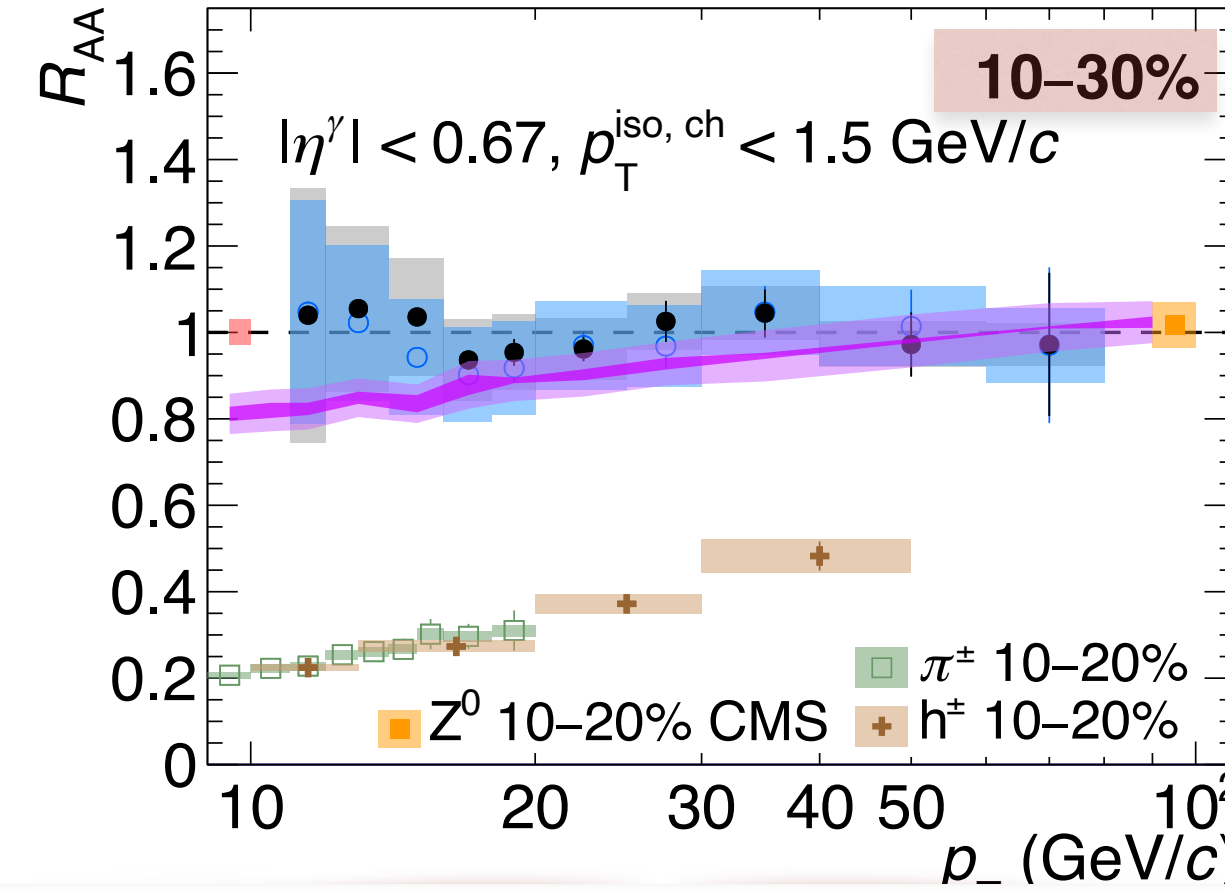
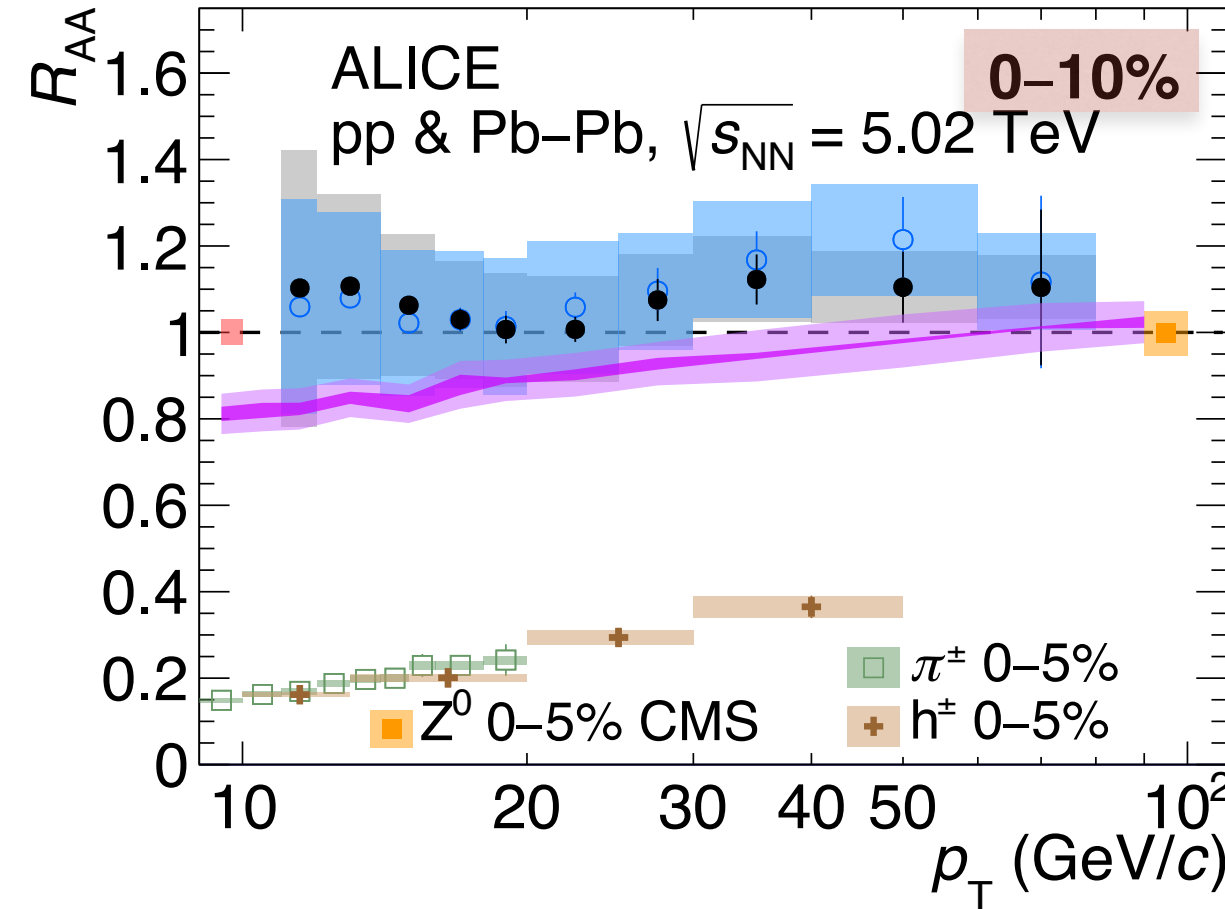
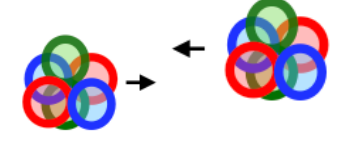
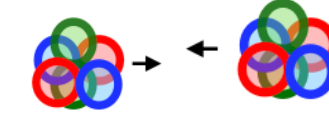
Consistent with unity within the unc. for both R

No modification of the prompt γ yield due to the QGP as expected

Agreement with NLO pQCD incorporating cold matter nuclear effects: PDF vs nPDF



$$R_{AA} = \frac{1}{\langle N_{coll} \rangle} \frac{d^2\sigma_{AA} / (dp_T d\eta)}{d^2\sigma_{pp} / (dp_T d\eta)}$$



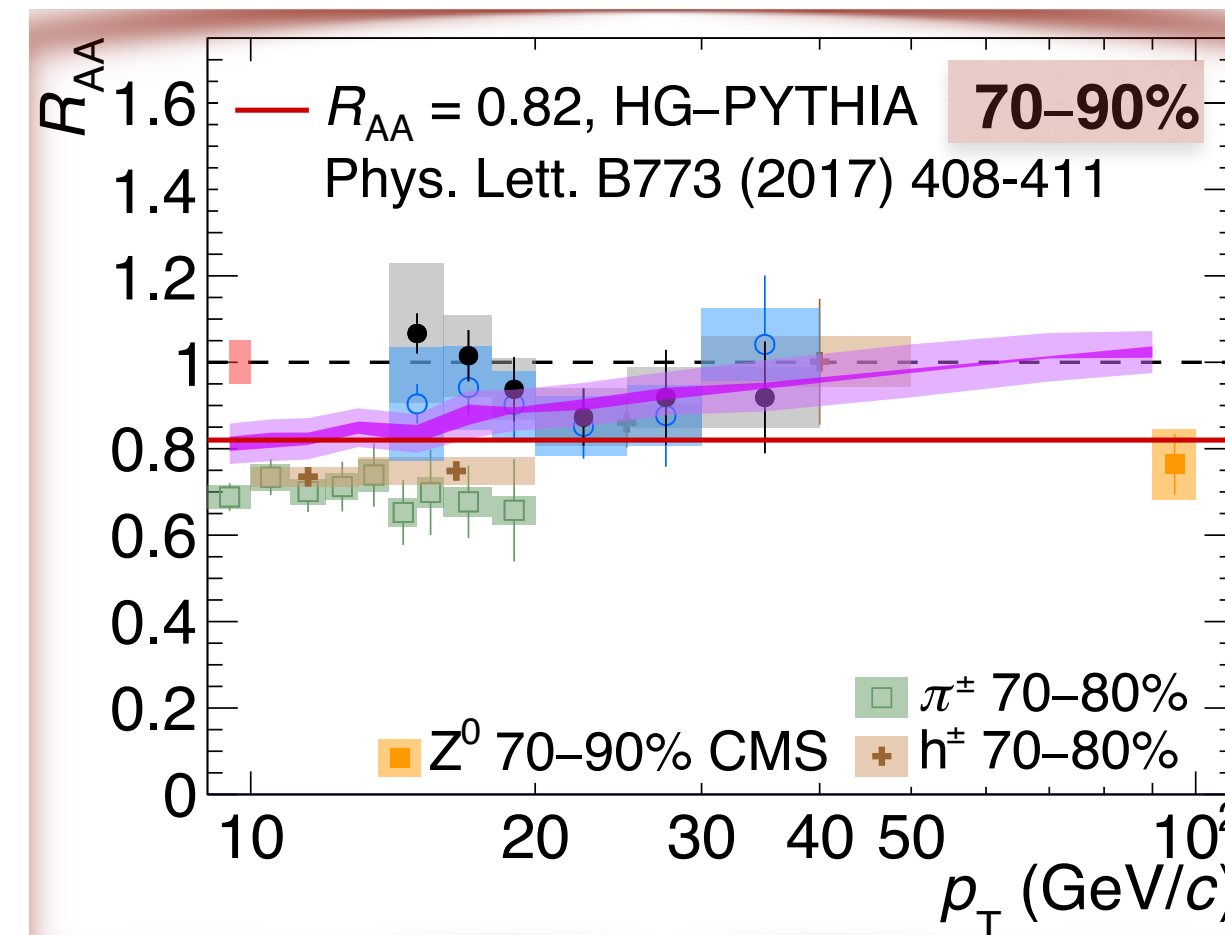
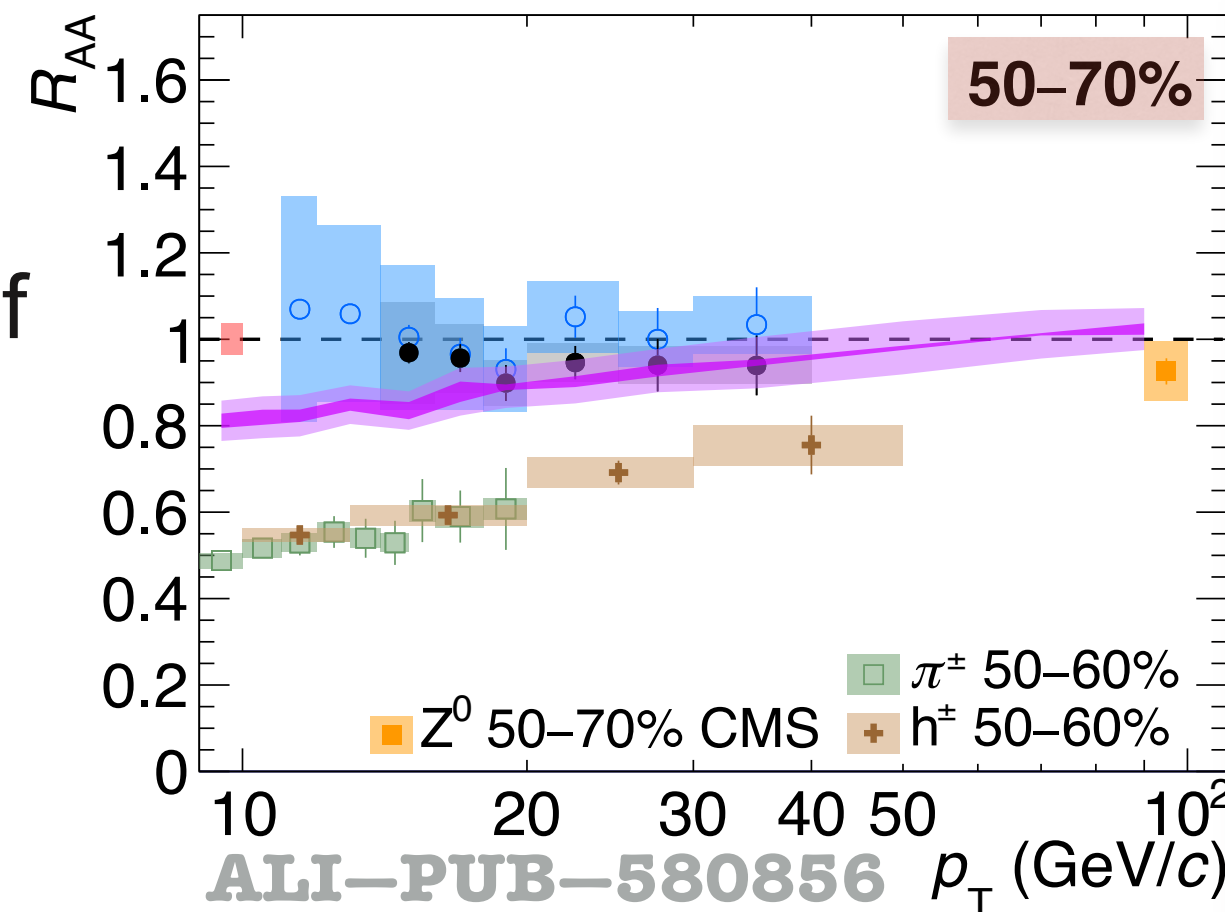
70-90%

Close to 0.9 than 1 for both R likely due to centrality selection bias of Glauber model

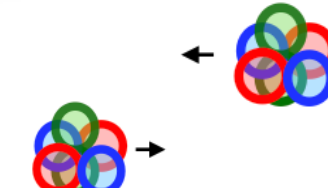
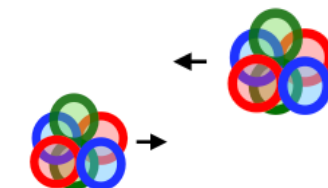
Model by C. Loizides & A. Morsch (Phys. Lett. B773 (2017) 408-411) yields a value at 0.82

In agreement within the uncertainties

Seen by CMS with Z^0 bosons



- $R = 0.2$ stat. unc. ◯ $R = 0.4$ stat. unc.
- $R = 0.2$ syst. unc. ■ $R = 0.4$ syst. unc.
- Normalisation unc.
- NLO (JETPHOX), 0-100%
 $p_T^{iso} < 2$ GeV/c, $R = 0.2$
pp : NNPFD40/BFG II FF
Pb-Pb: nNNPDF30/BFG II FF, 0-100%
- Scale unc. $p_T^\gamma/2 < \mu < 2p_T^\gamma$
- PDF unc.

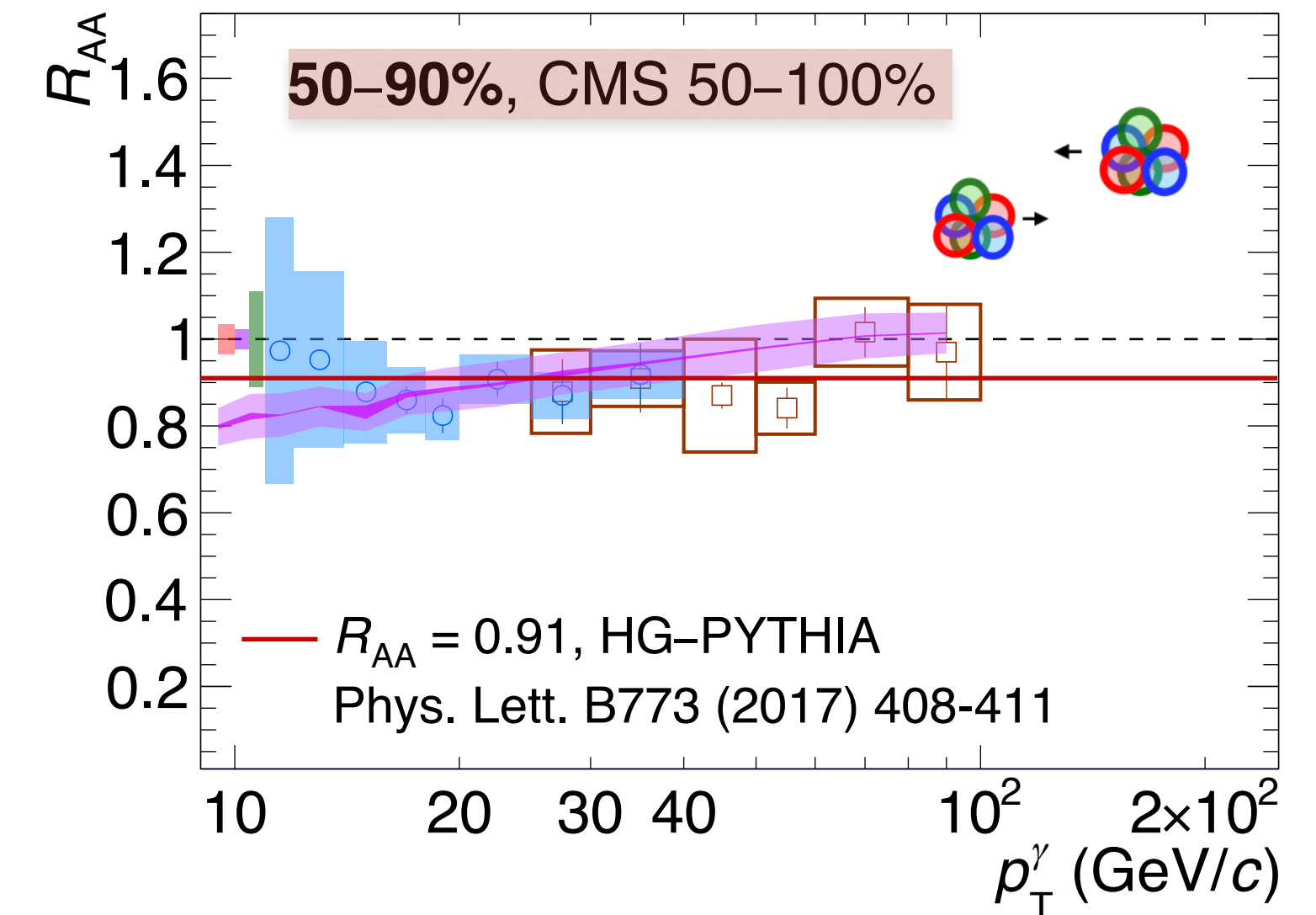
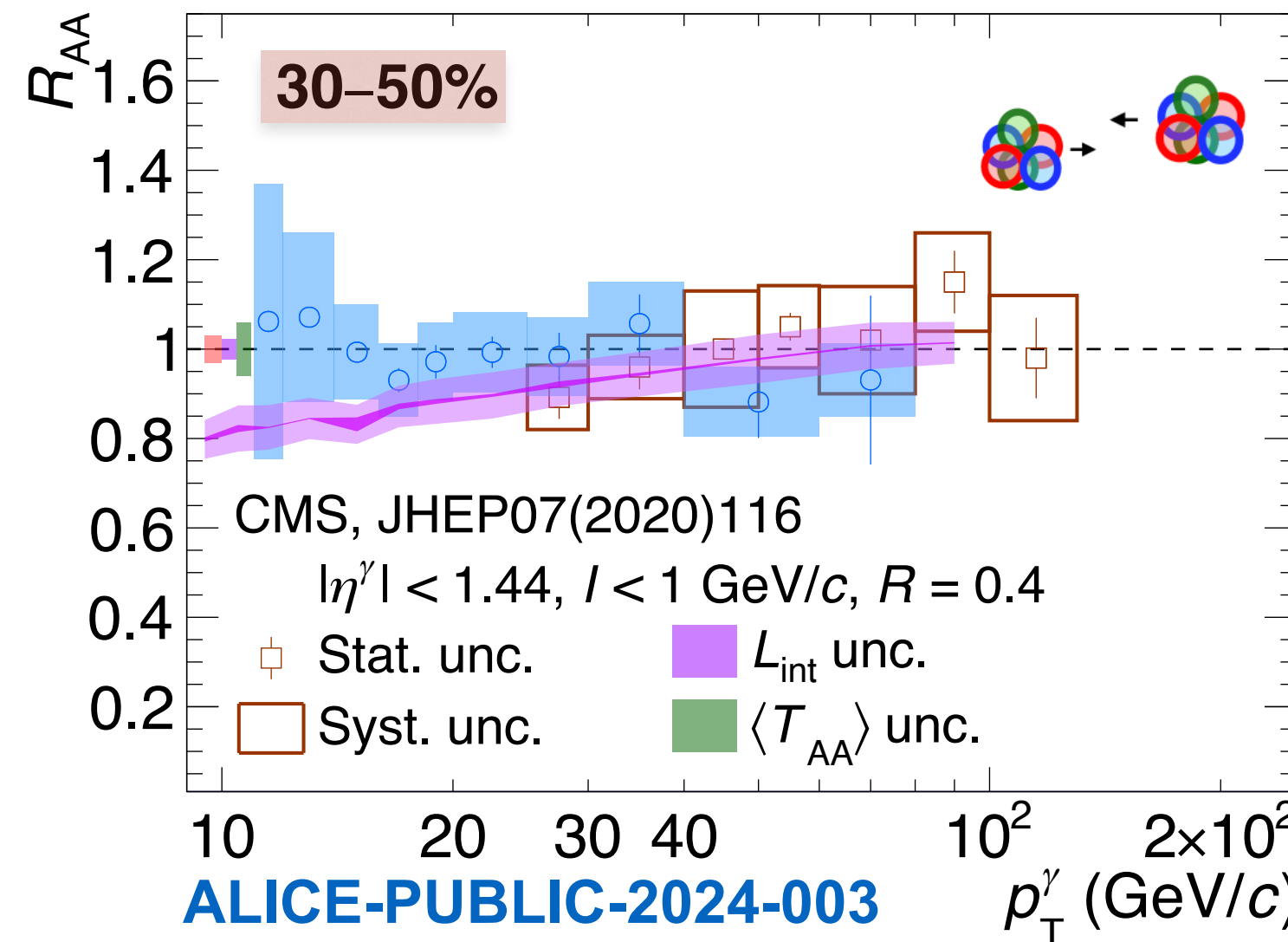
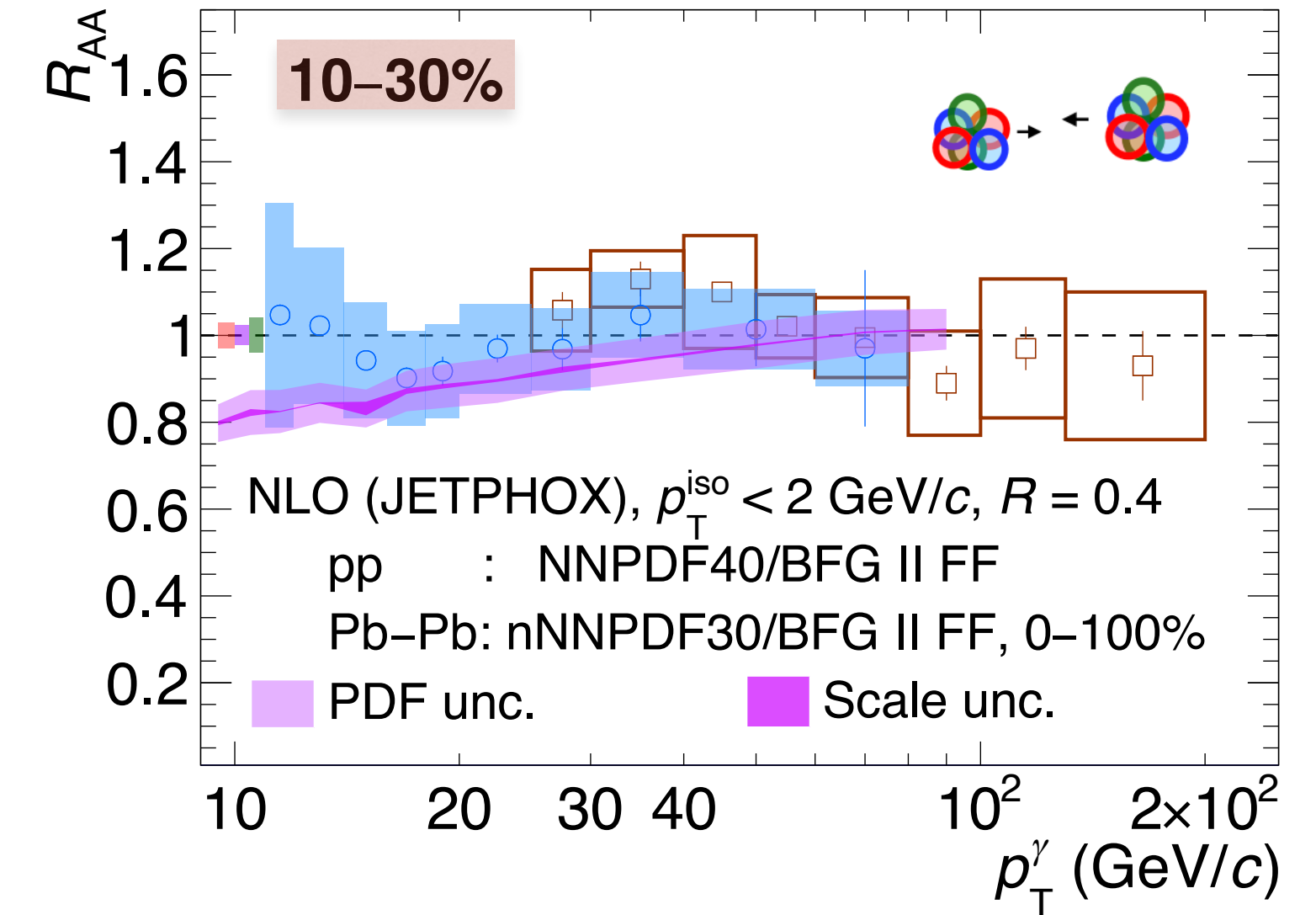
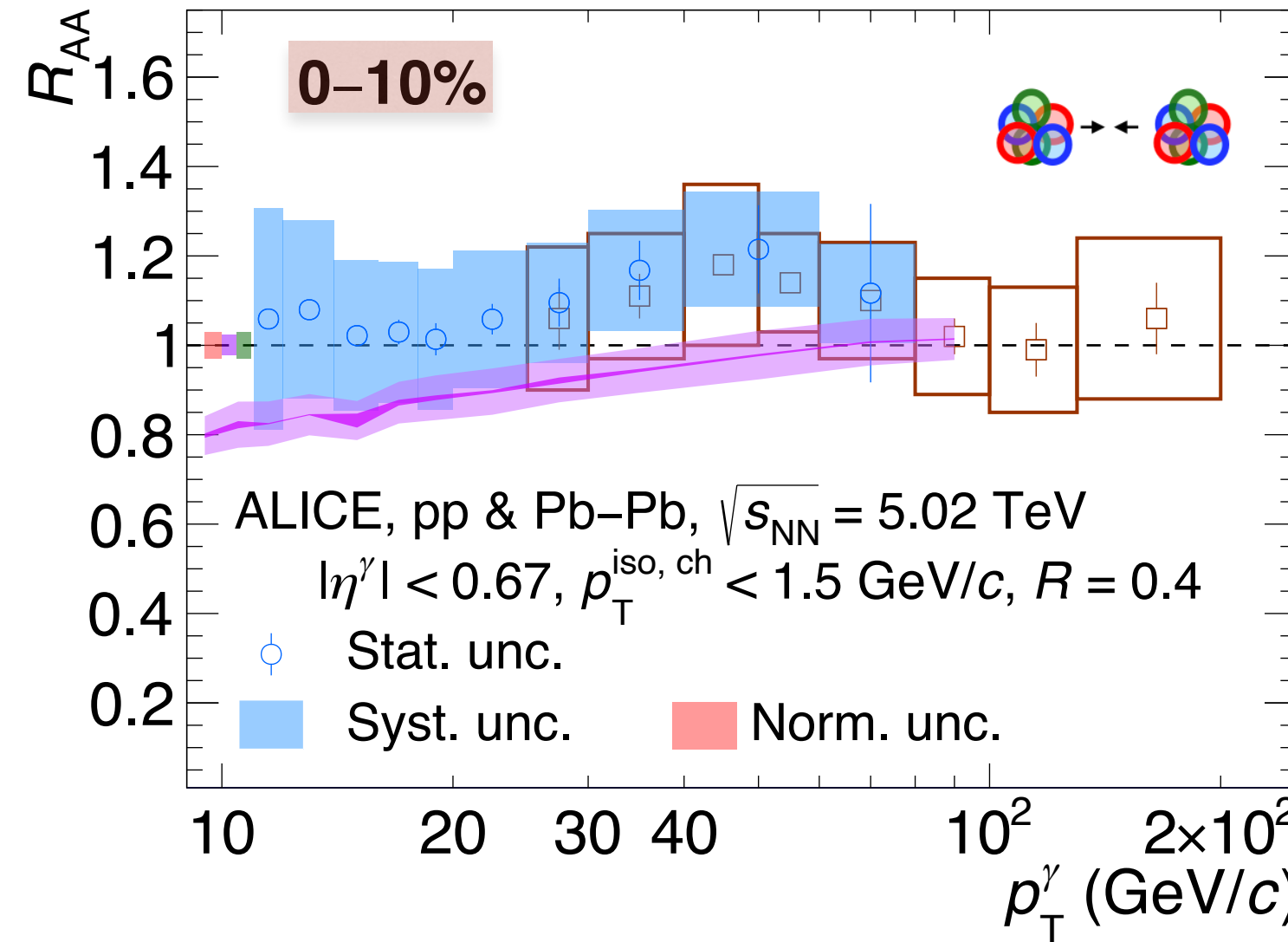


Nuclear modification factor R_{AA} , pp & Pb-Pb at $\sqrt{s_{NN}} = 5.02$ TeV



$$R_{AA} = \frac{1}{\langle N_{coll} \rangle} \frac{d^2\sigma_{AA} / (dp_T d\eta)}{d^2\sigma_{pp} / (dp_T d\eta)}$$

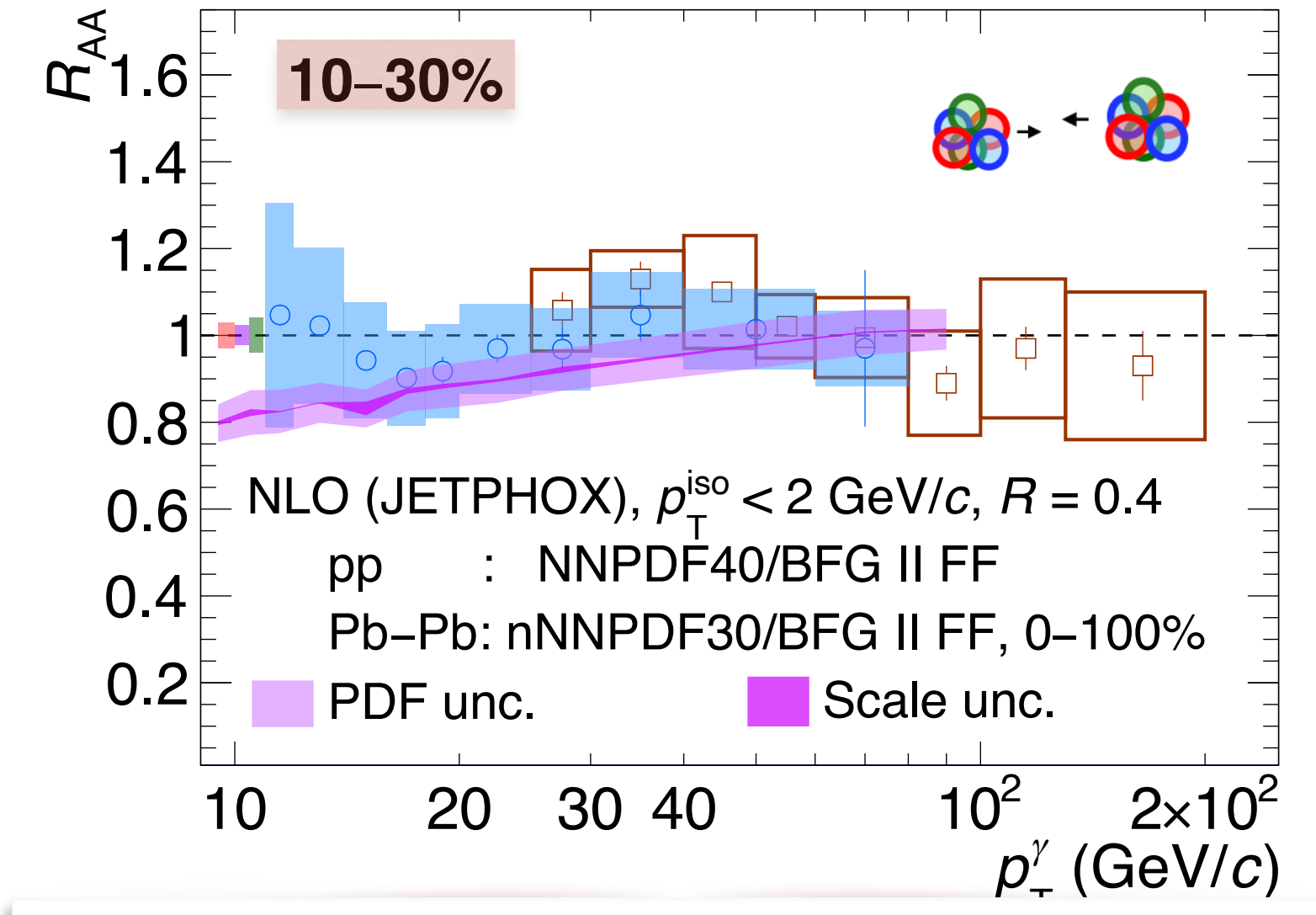
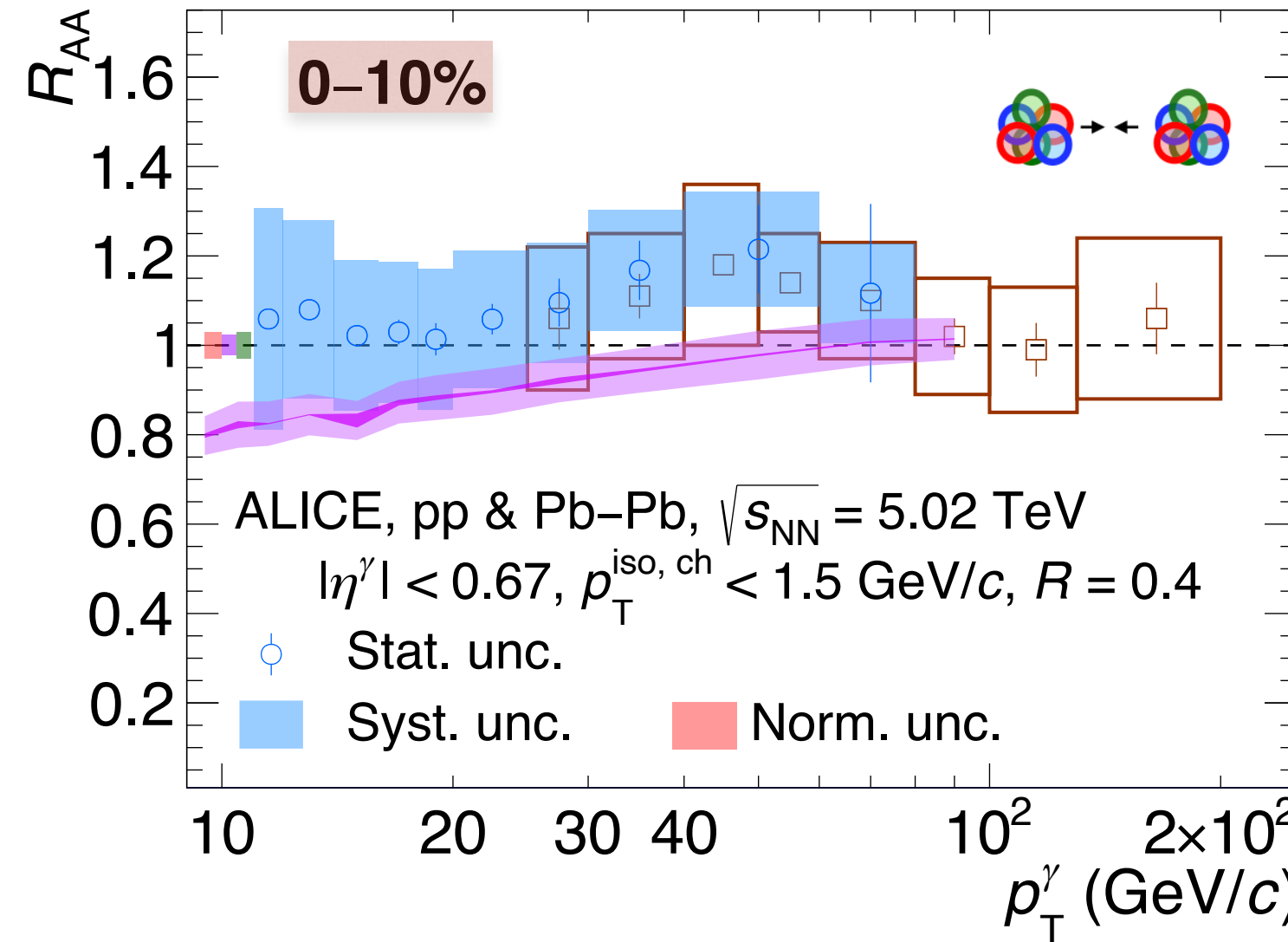
- **ALICE & CMS**: good agreement in the overlapping region $25 < p_T < 40-80$ GeV/c



Nuclear modification factor R_{AA} , pp & Pb-Pb at $\sqrt{s_{NN}} = 5.02$ TeV

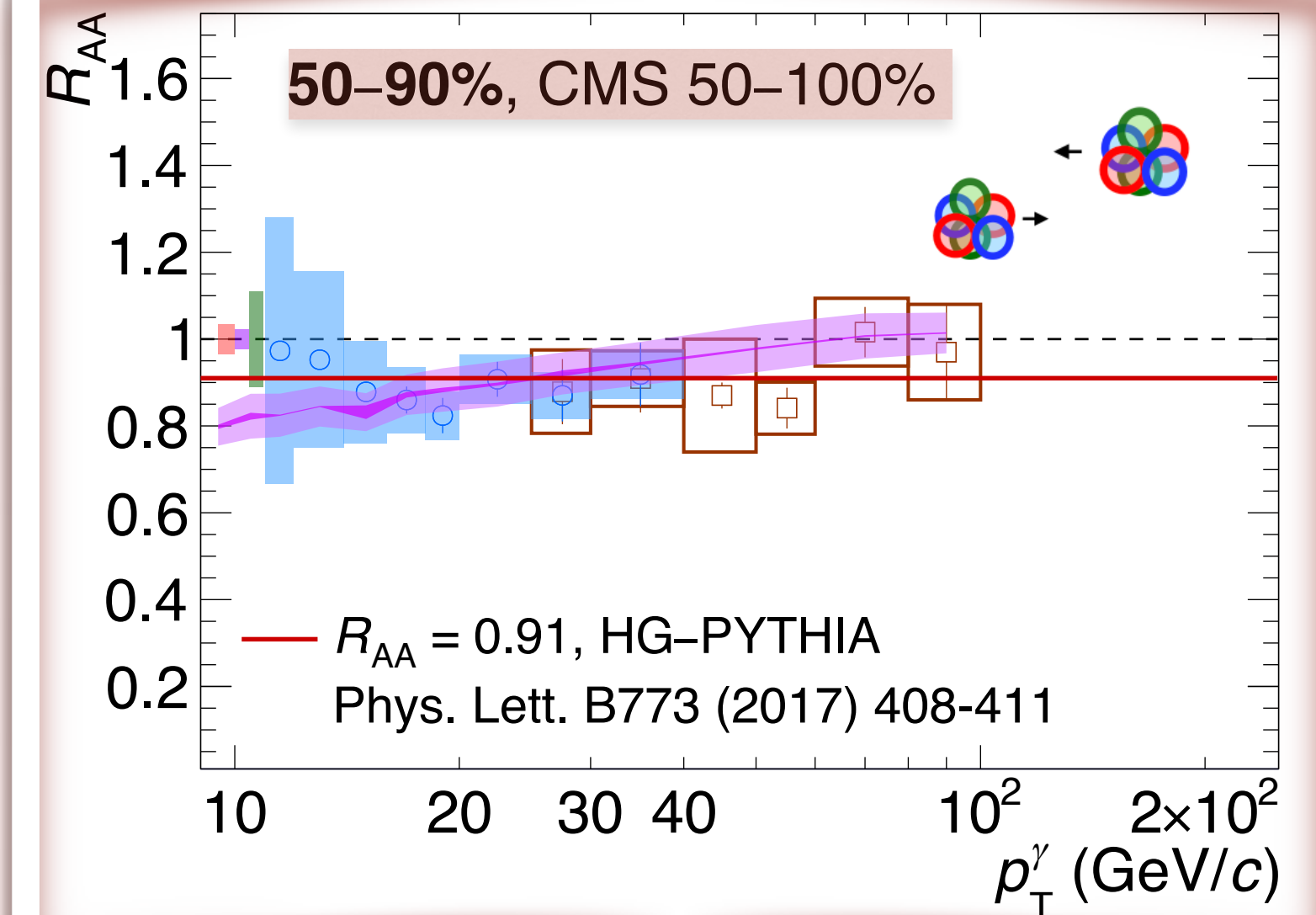
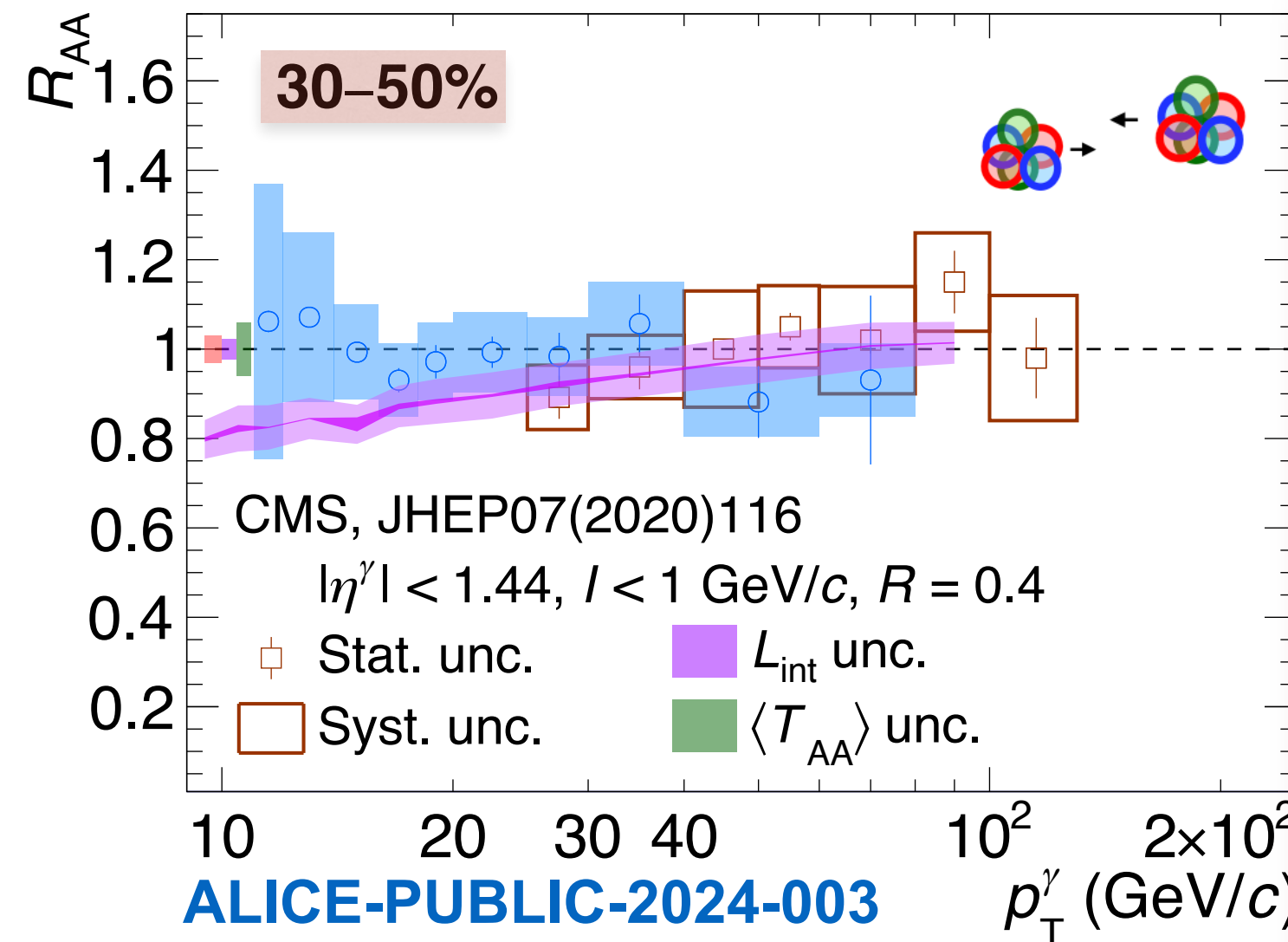
$$R_{AA} = \frac{1}{\langle N_{coll} \rangle} \frac{d^2\sigma_{AA} / (dp_T d\eta)}{d^2\sigma_{pp} / (dp_T d\eta)}$$

- ALICE & CMS: good agreement in the overlapping region $25 < p_T < 40-80$ GeV/c



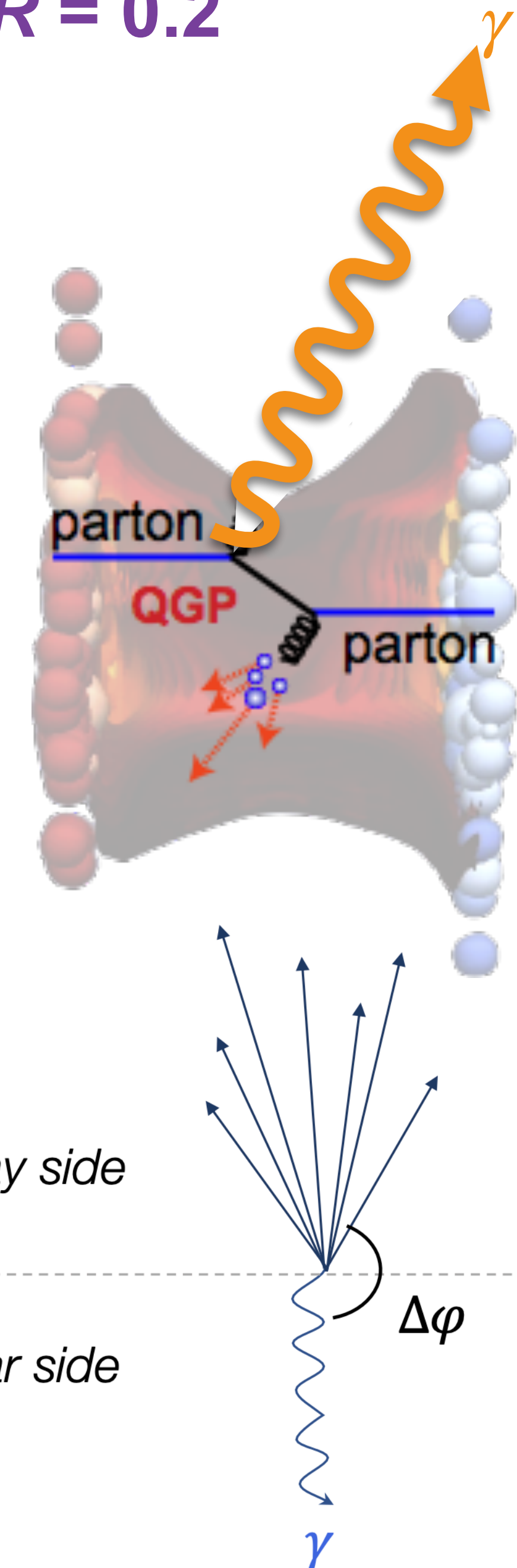
50-90%

- ➔ Closer to 0.9 than 1 for both R likely due to centrality selection bias of Glauber model
- ➔ Model by C. Loizides & A. Morsch (Phys. Lett. B773 (2017) 408-411) yields a value at **0.91**
- ❖ In agreement within the uncertainties



Isolated γ -hadron correlations in Pb-Pb at $\sqrt{s_{NN}} = 5.02$ TeV, $R = 0.2$

- Prompt γ associated to a parton emitted in opposite side
- **Tags the parton initial energy** $p_T^\gamma \simeq p_T^{\text{parton}}$, before losing ΔE in QGP
 - ➔ Aim: Measure FF modifications, where is the ΔE radiated?
- Observables:
 - ➔ Trigger: isolated narrow or wide clusters, $R = 0.2$ & $p_T^{\text{iso ch}} < 1.5$ GeV/c
 - ➔ Azimuthal correlation: $\Delta\varphi = \varphi^{\text{trigger}} - \varphi^{\text{track}}$ with
 - ➔ $z_T = \frac{p_T^{\text{track}}}{p_T^{\text{trigger}}}$ and $D(z_T) = \frac{1}{N^{\text{trigger}}} \frac{d N^{\text{track}}}{d z_T}$ for tracks in $|\Delta\varphi| > 3/5\pi$ rad (mirrored)
 - ➔ **When trigger = prompt γ , $D(z_T)$ is a proxy for FF**
 - ➔ Measurement: $18 < p_T^{\text{trigger}} < 40$ GeV/c & $p_T^{\text{track}} > 0.5$ GeV/c
 - ▶ Details in back-up



Such kind of analysis pursued by different thesis at LPSC and CCNU:
 Yaxian Mao (pp, 7 TeV, 2011), Nicolas Arbor (pp, 7 TeV, Pb-Pb, 2.76 TeV, 2013),
 Astrid Vauthier (p-Pb, 5 TeV, 2016) and Carolina Arata (Pb-Pb, 5 TeV, 2024)

Isolated γ -hadron correlations in Pb-Pb: Azimuthal distribution

- UE in $\Delta\varphi$: uncorrelated tracks shift up the distribution
- UE subtraction with mixed event: artificial dataset created combining the trigger cluster with tracks on different collisions



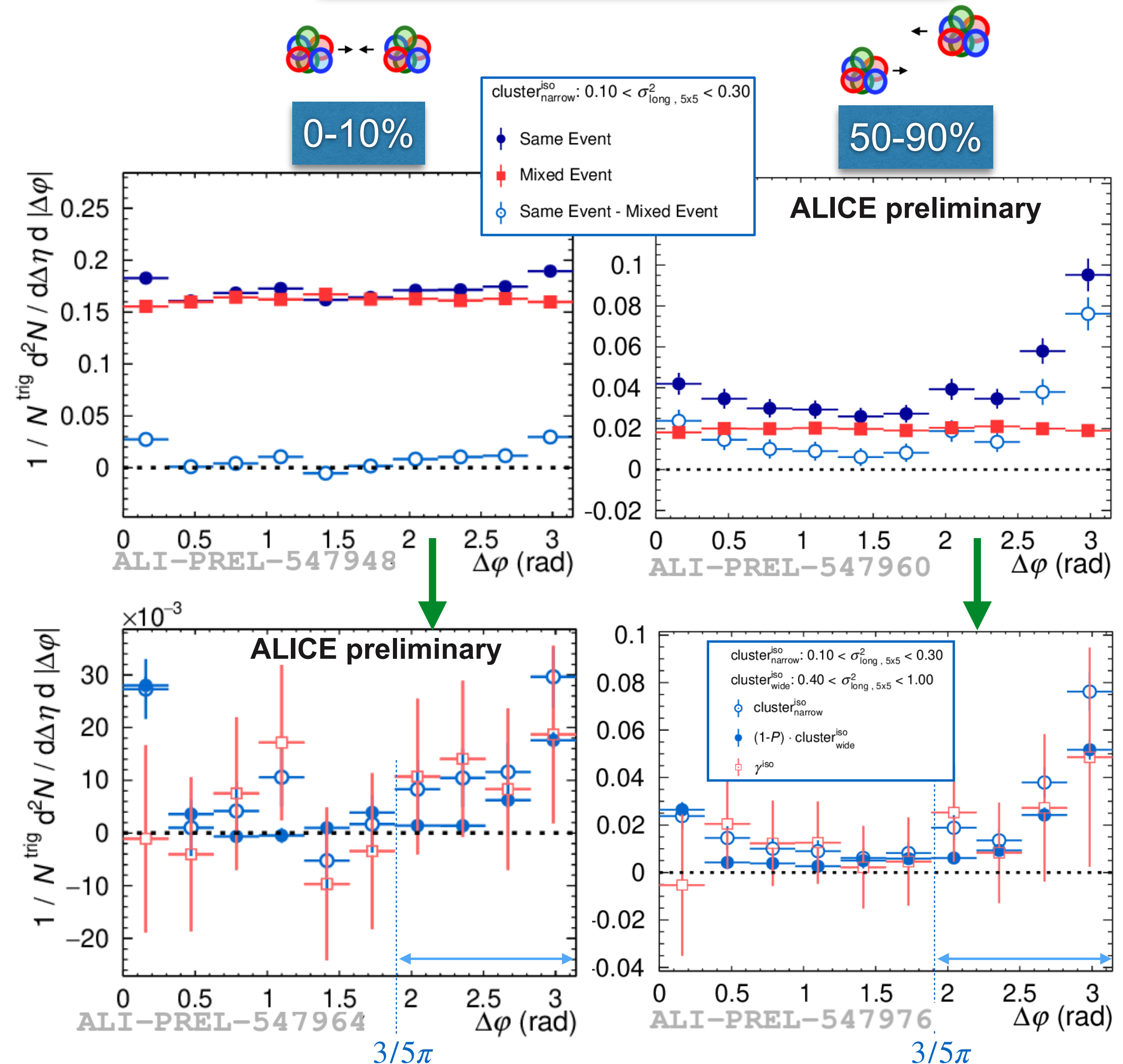
- Purity < 1 , considering

$$f(\Delta\varphi^{\text{cls}_{\text{narrow}}^{\text{iso}}}) \text{ bkg} = f(\Delta\varphi^{\text{cls}_{\text{wide}}^{\text{iso}}}):$$

$$f(\Delta\varphi^{\gamma^{\text{iso}}}) = \frac{f(\Delta\varphi^{\text{cls}_{\text{narrow}}^{\text{iso}}}) - (1 - P) \cdot f(\Delta\varphi^{\text{cls}_{\text{wide}}^{\text{iso}}})}{P}$$

- $D(z_T)$: Integrate $f(\Delta\varphi^{\gamma^{\text{iso}}})$ in $3/5\pi < |\Delta\varphi| < \pi$ rad

$20 < p_T < 25 \text{ GeV}/c$ & $0.2 < z_T < 0.3$



Isolated γ -hadron correlations in p-Pb & pp, $R = 0.4$: $D(z_T)$

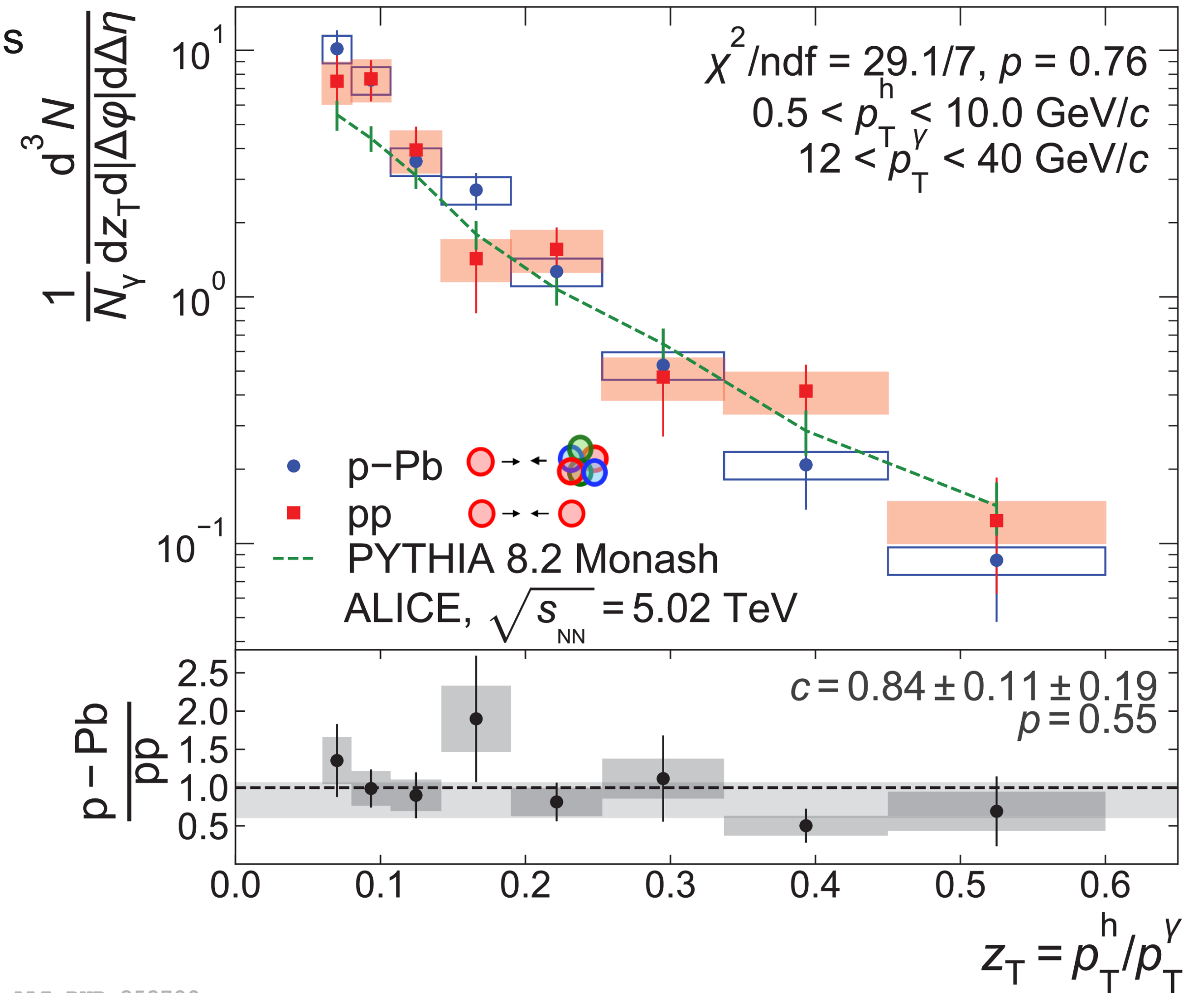
Phys Rev C 102 (2020) 044908

- Previous published results in p-Pb and pp collisions

→ Agreement between systems and with PYTHIA

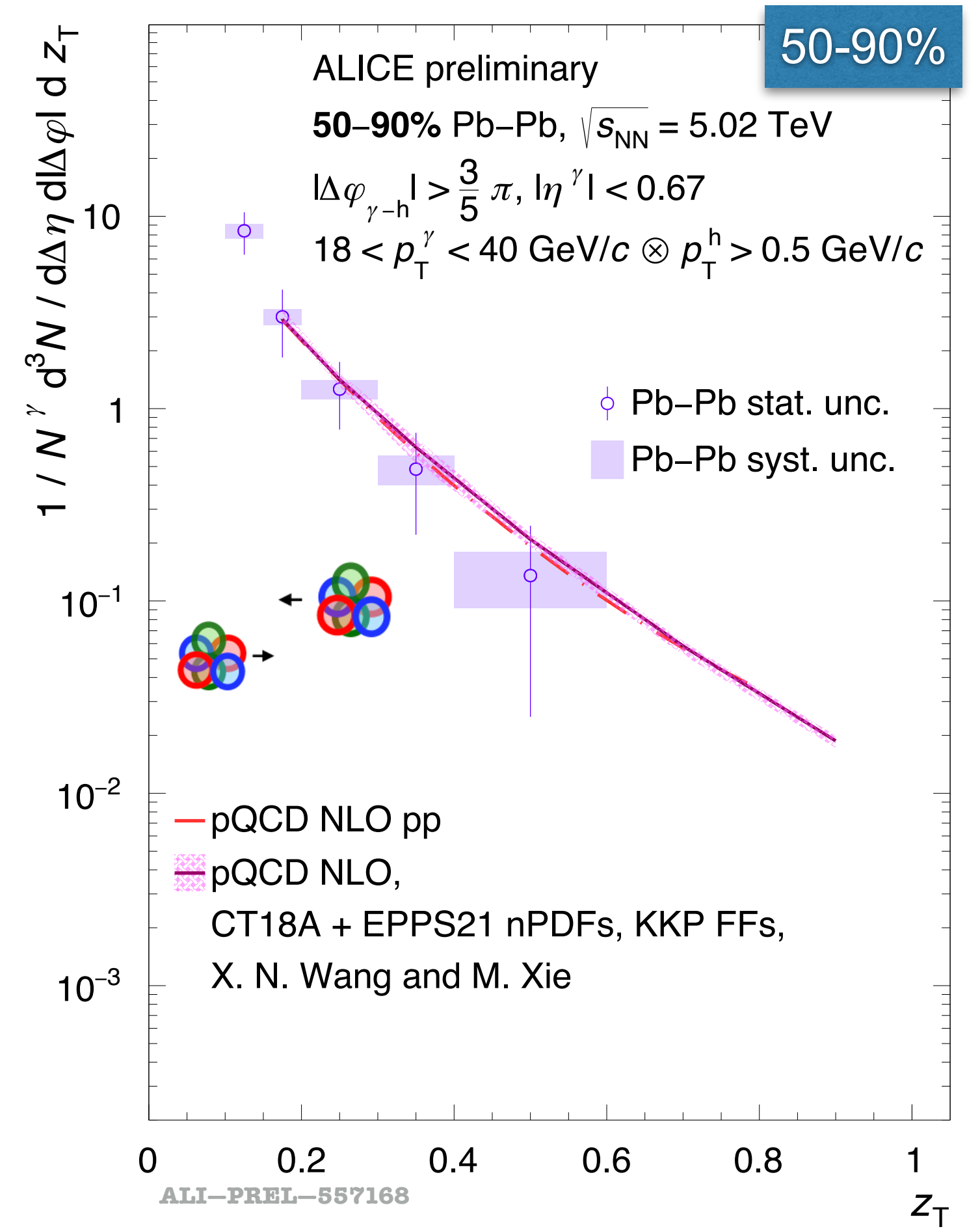
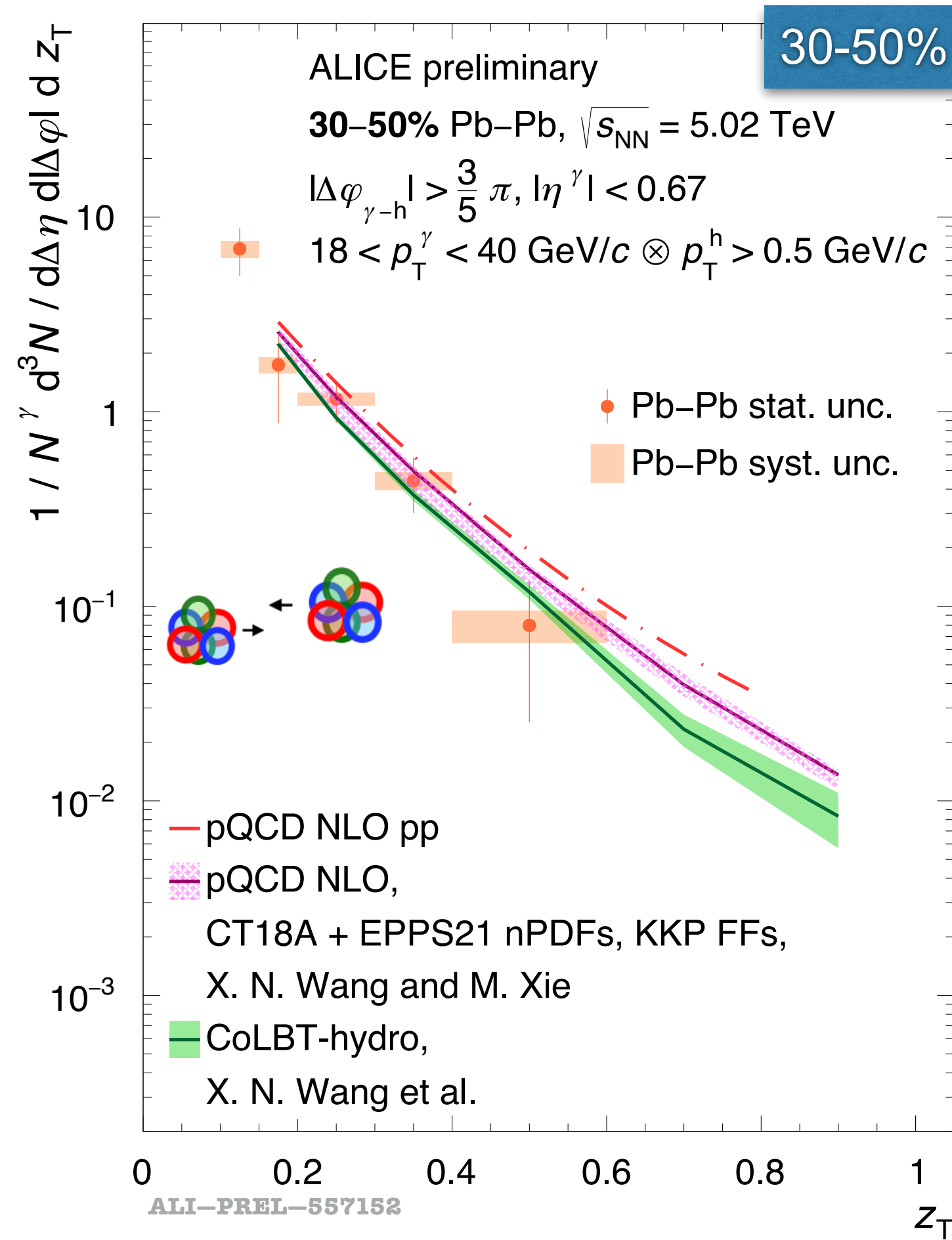
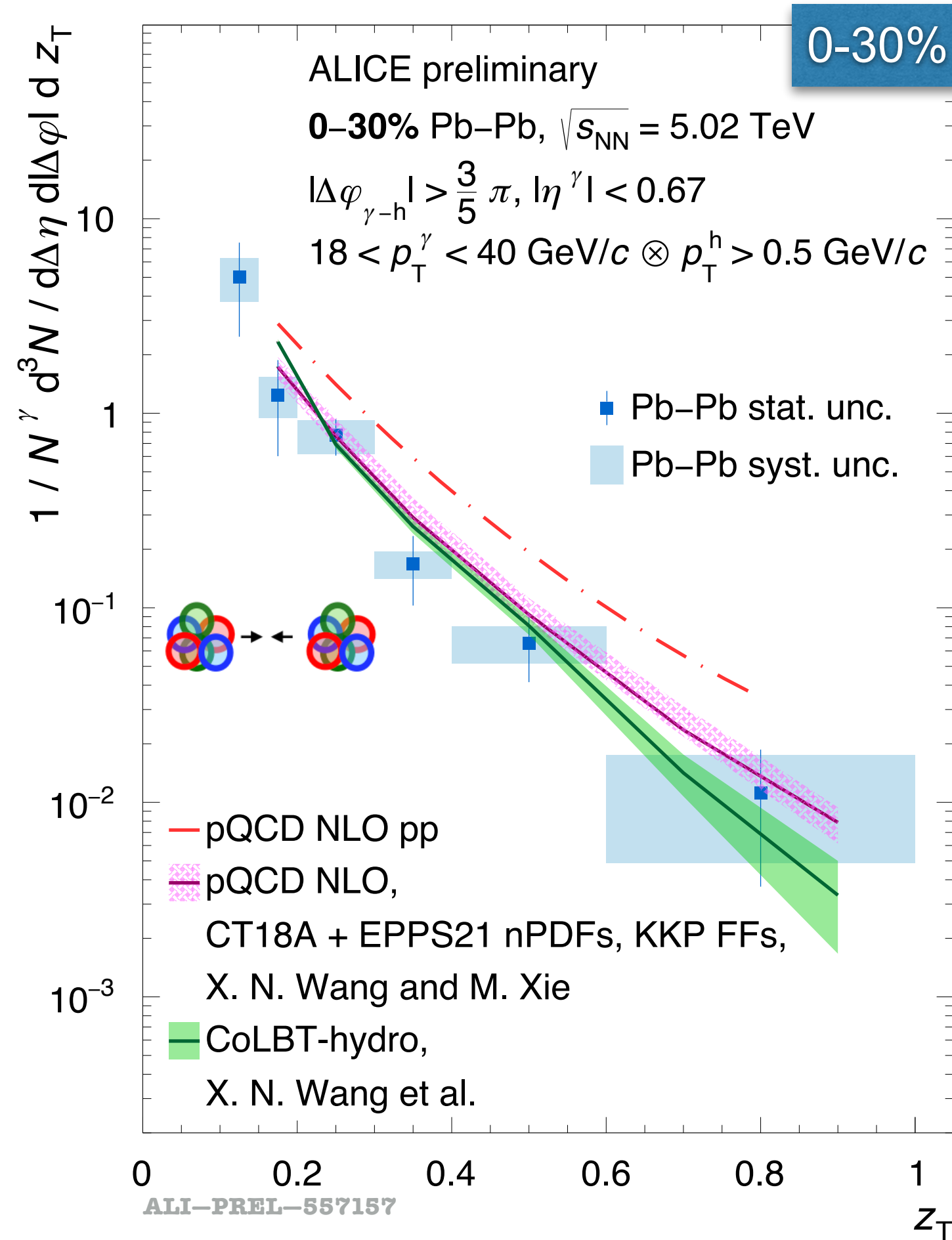
→ Note: Pb-Pb collisions measurement (next slides)

done in different p_T ranges and is compared directly to pQCD predictions



ALI-PUB-353789

Isolated γ -hadron correlations in Pb-Pb: $D(z_T)$



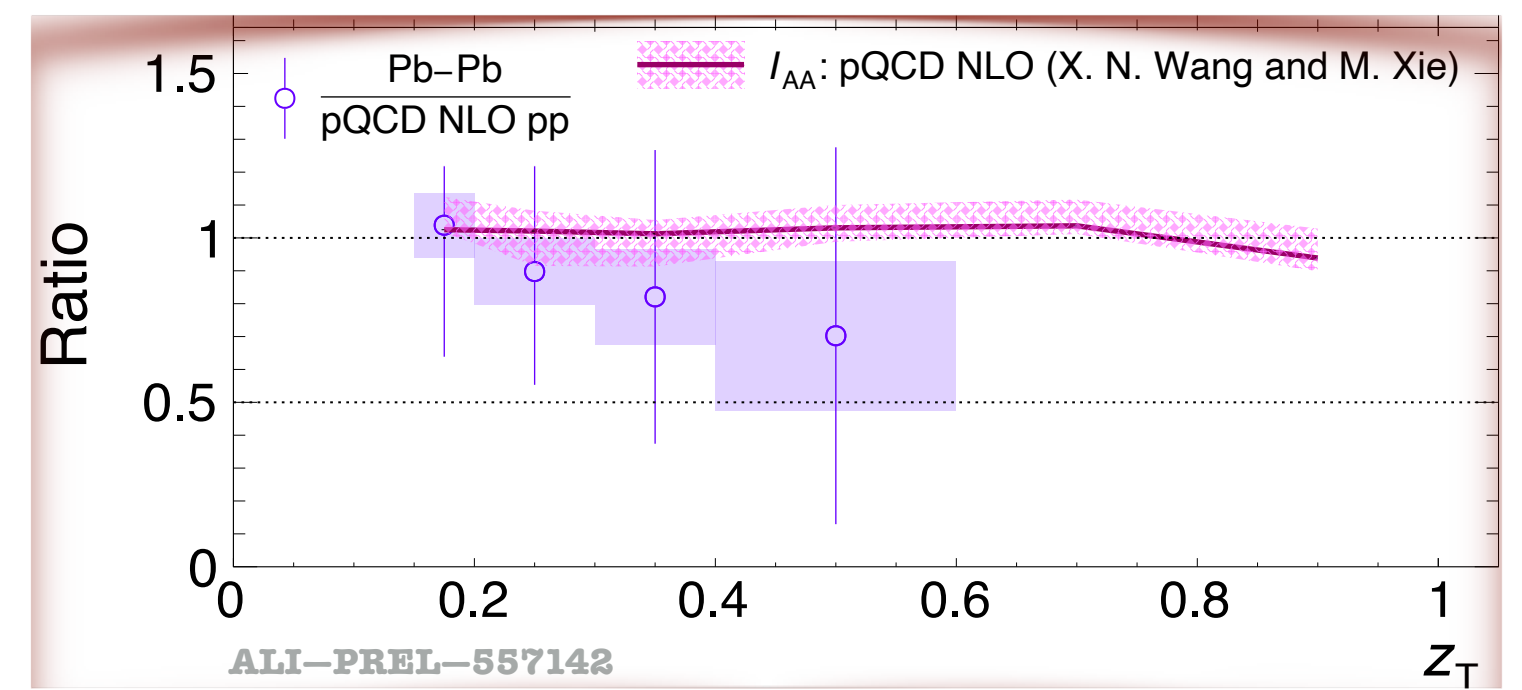
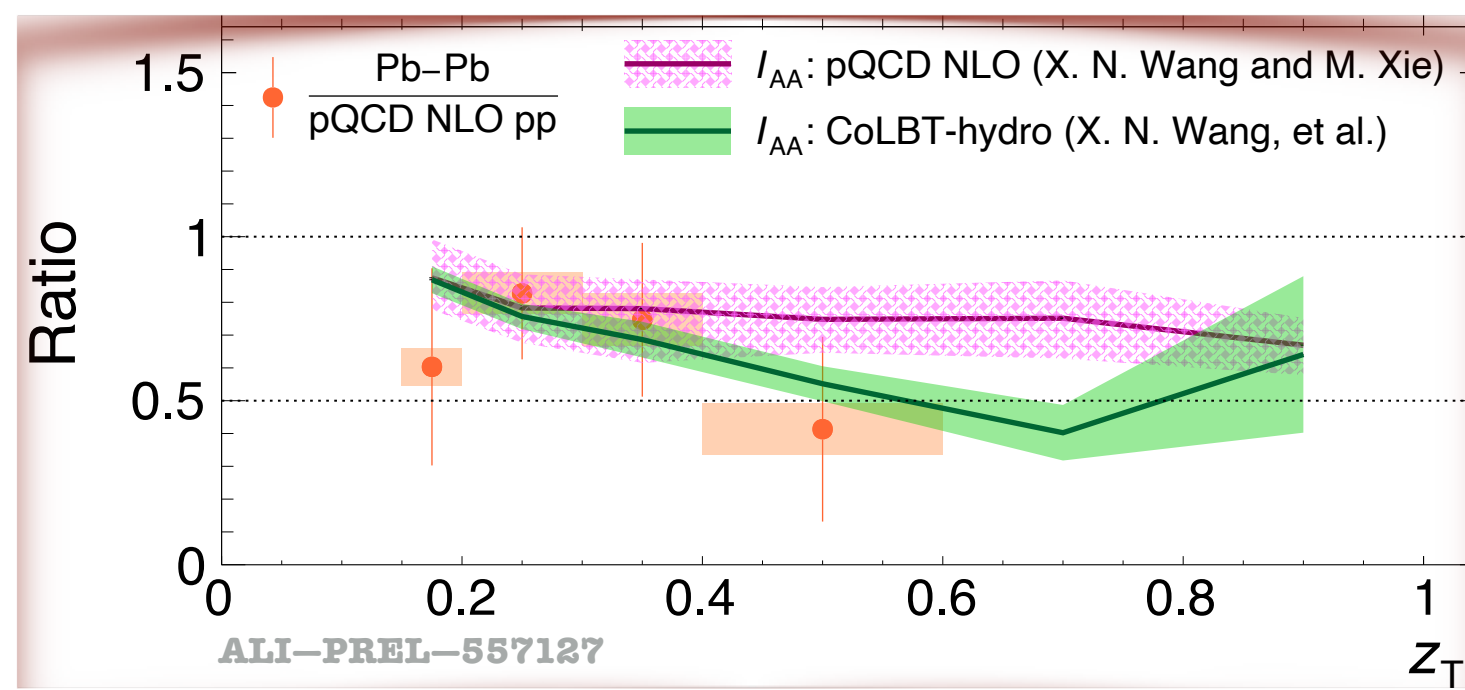
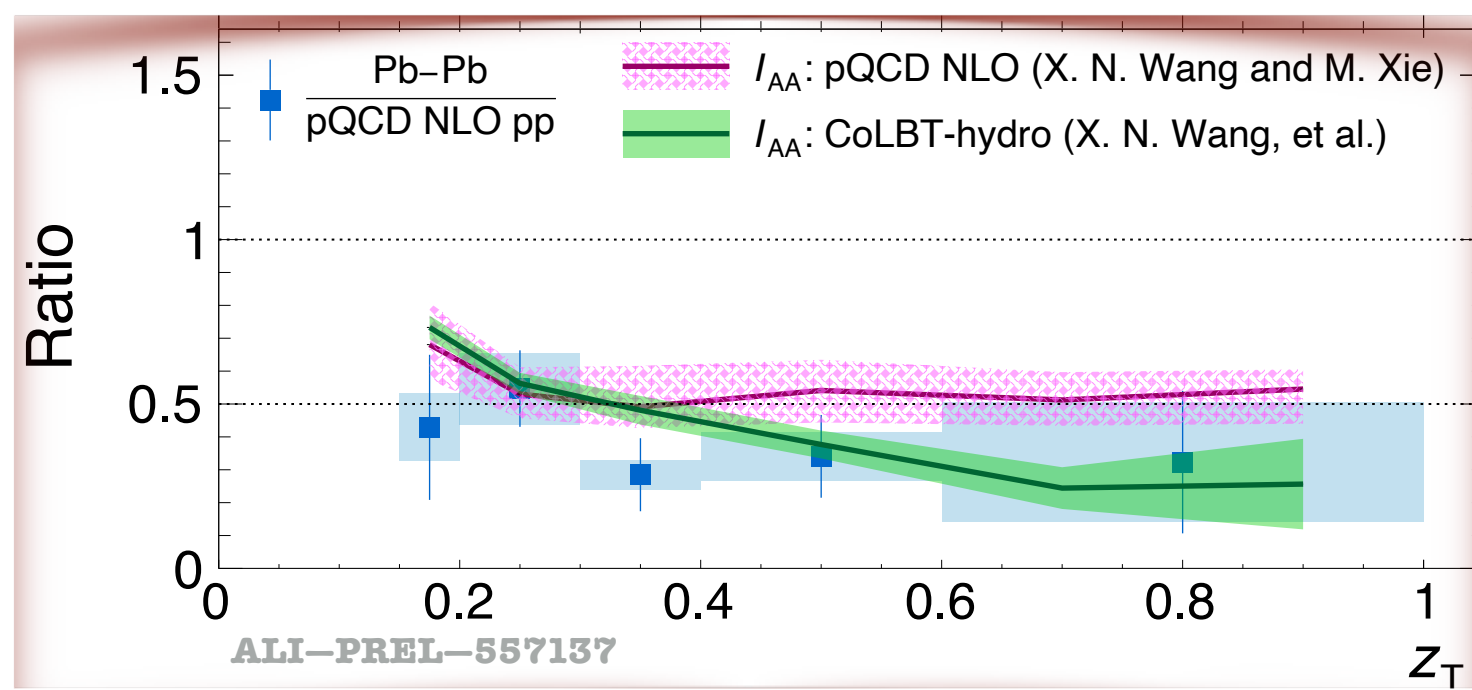
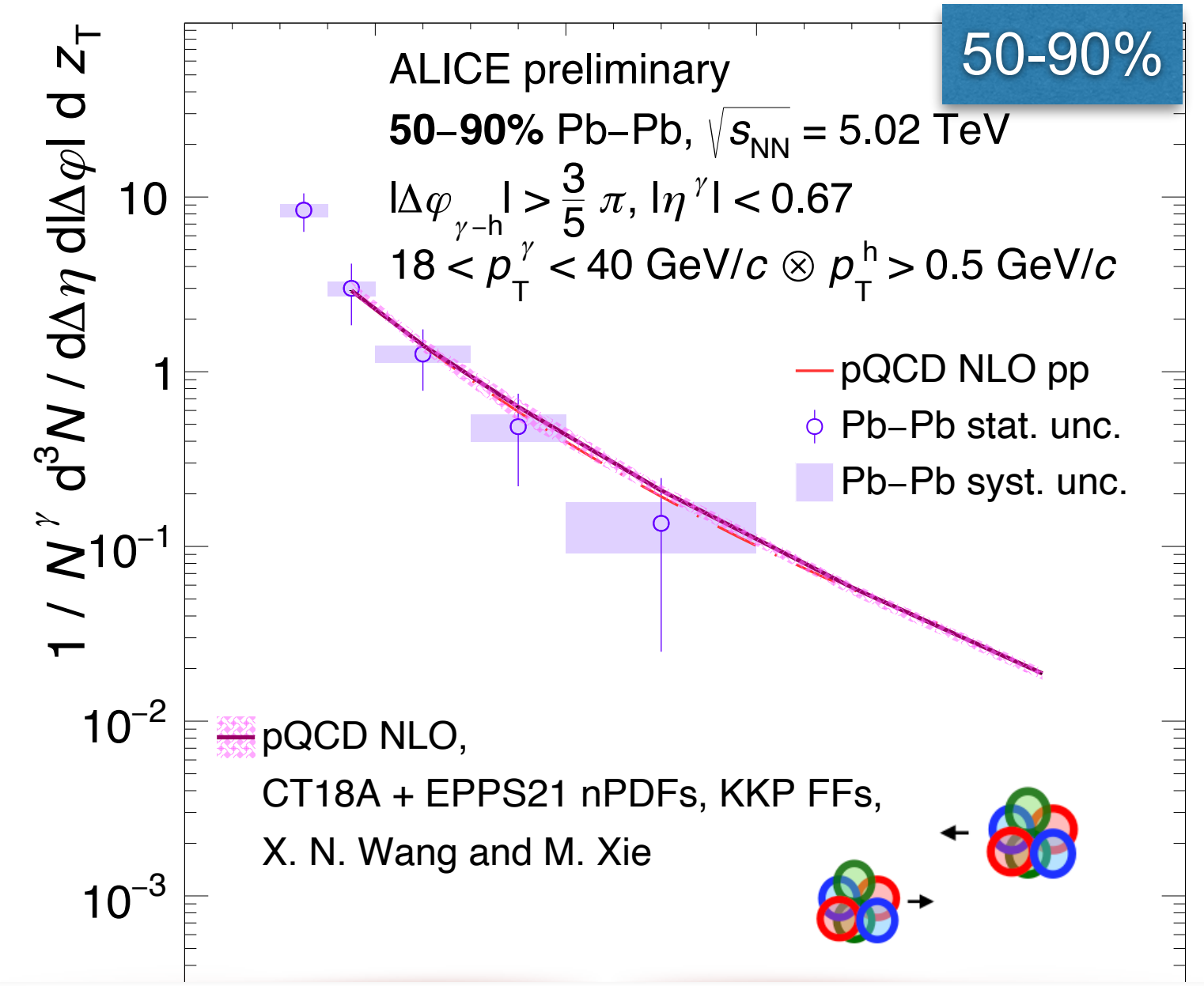
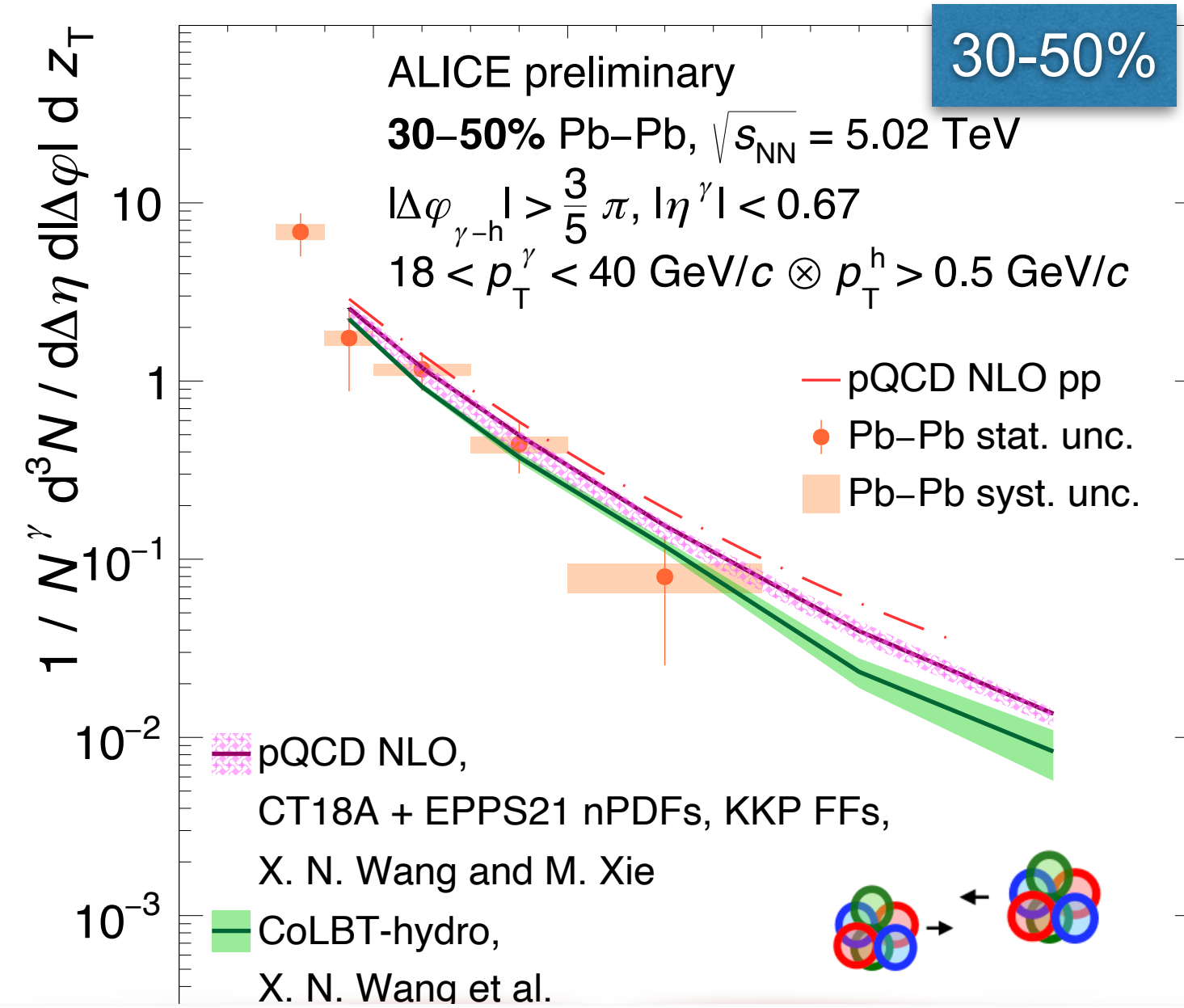
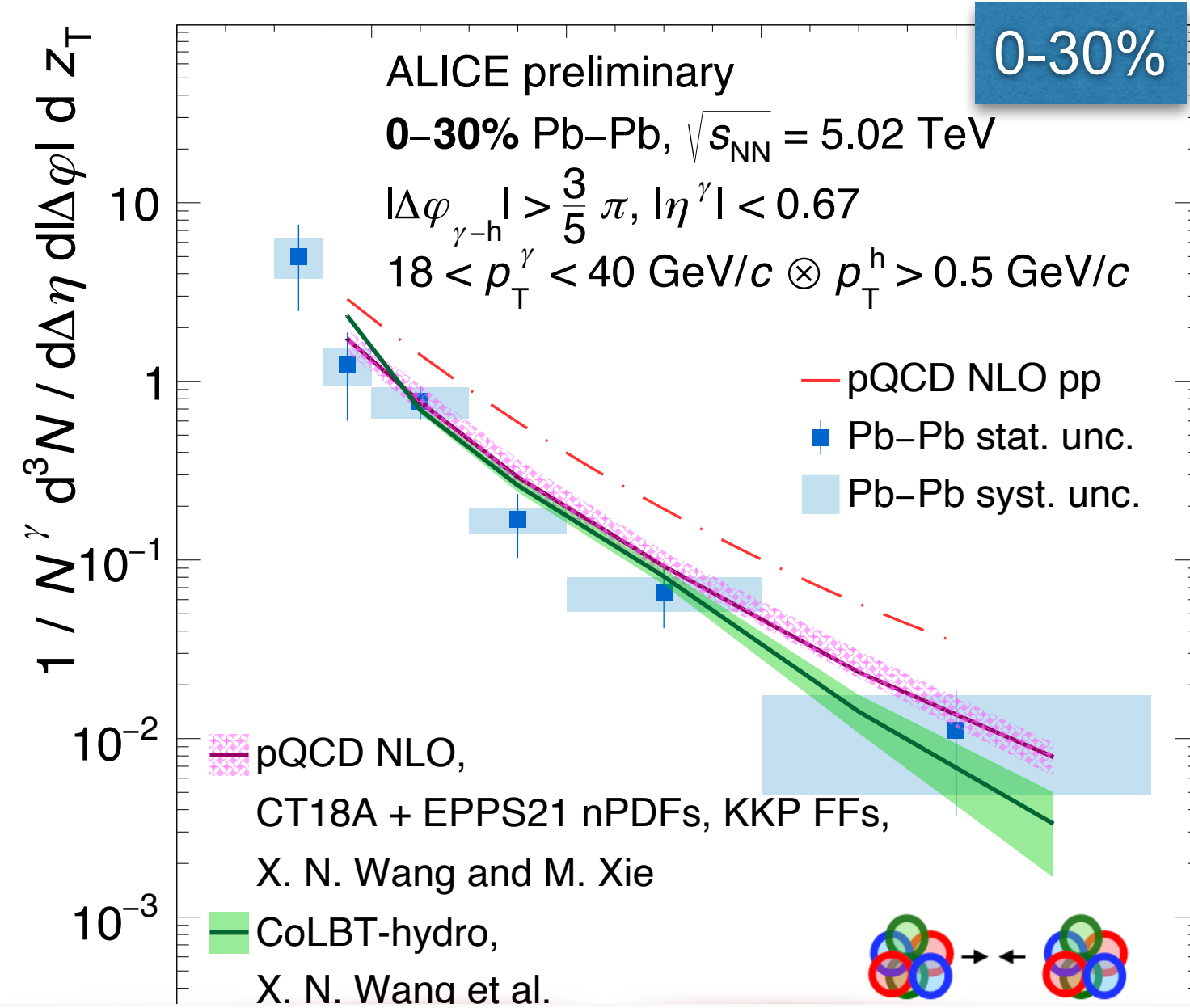
- Pb-Pb data compared with theory: **NLO pQCD** and **CoLBT (0-50% only)**

➔ In agreement with both models

➔ Discrimination not possible yet

- *Phys. Rev. C 103, 034911, Xie, Wang and Zhang,*
- *Phys. Rev. Lett. 103, 032302, Xie, Wang and Zhang*
- *Phys.Lett.B 777 (2018) 86-90, Chen et al.*

Isolated γ -hadron correlations in Pb-Pb: $D(z_T)$

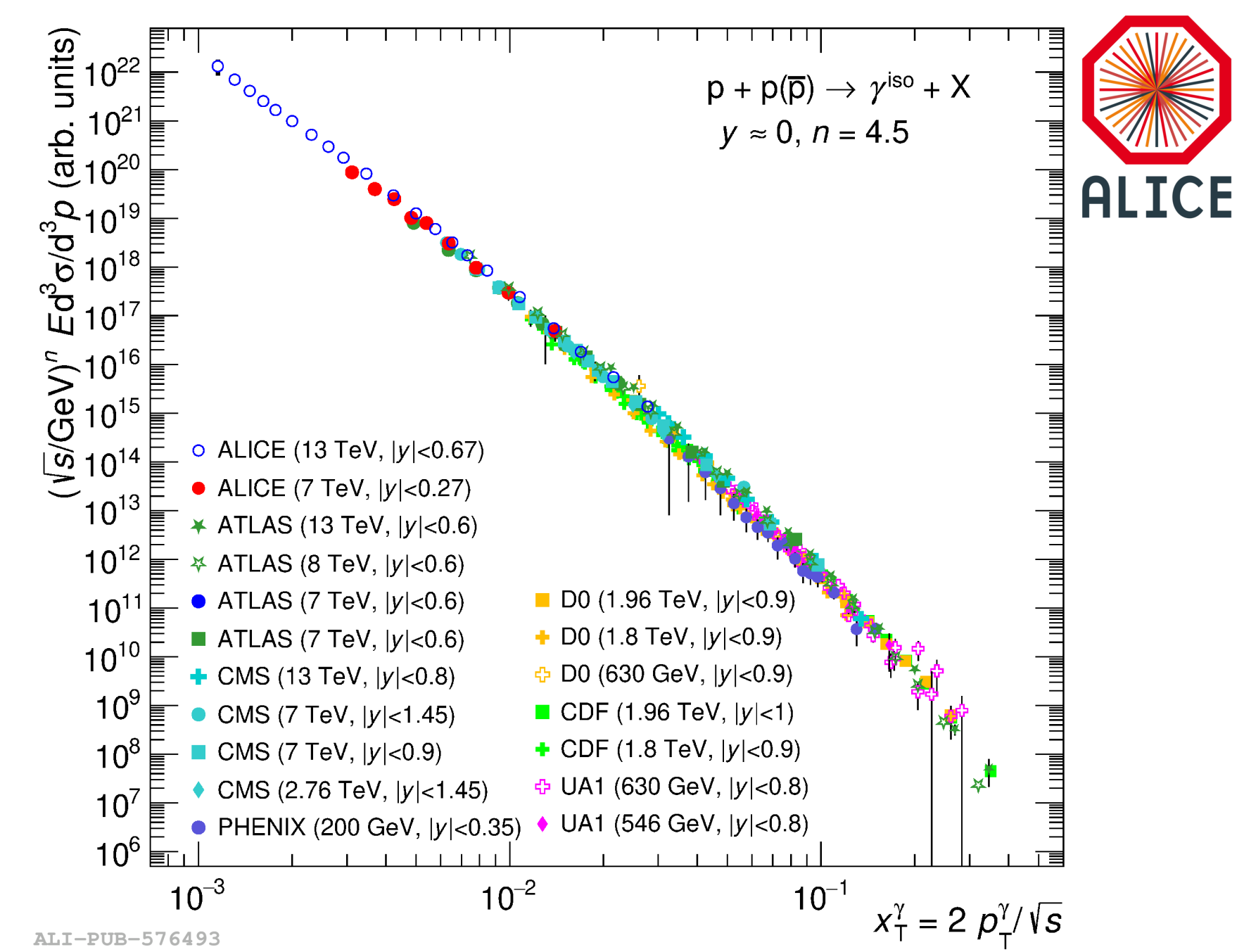


- Ratio with respect to **NLO pQCD pp collision simulation** → A proxy for $I_{AA} = \frac{D(z_T)_{Pb-Pb}}{D(z_T)_{pp}}$
- Clear modifications in data with respect to NLO pQCD pp simulation
- Comparison with I_{AA} from **NLO pQCD** and **CoLBT** models → agreement

Summary

→ Cross section

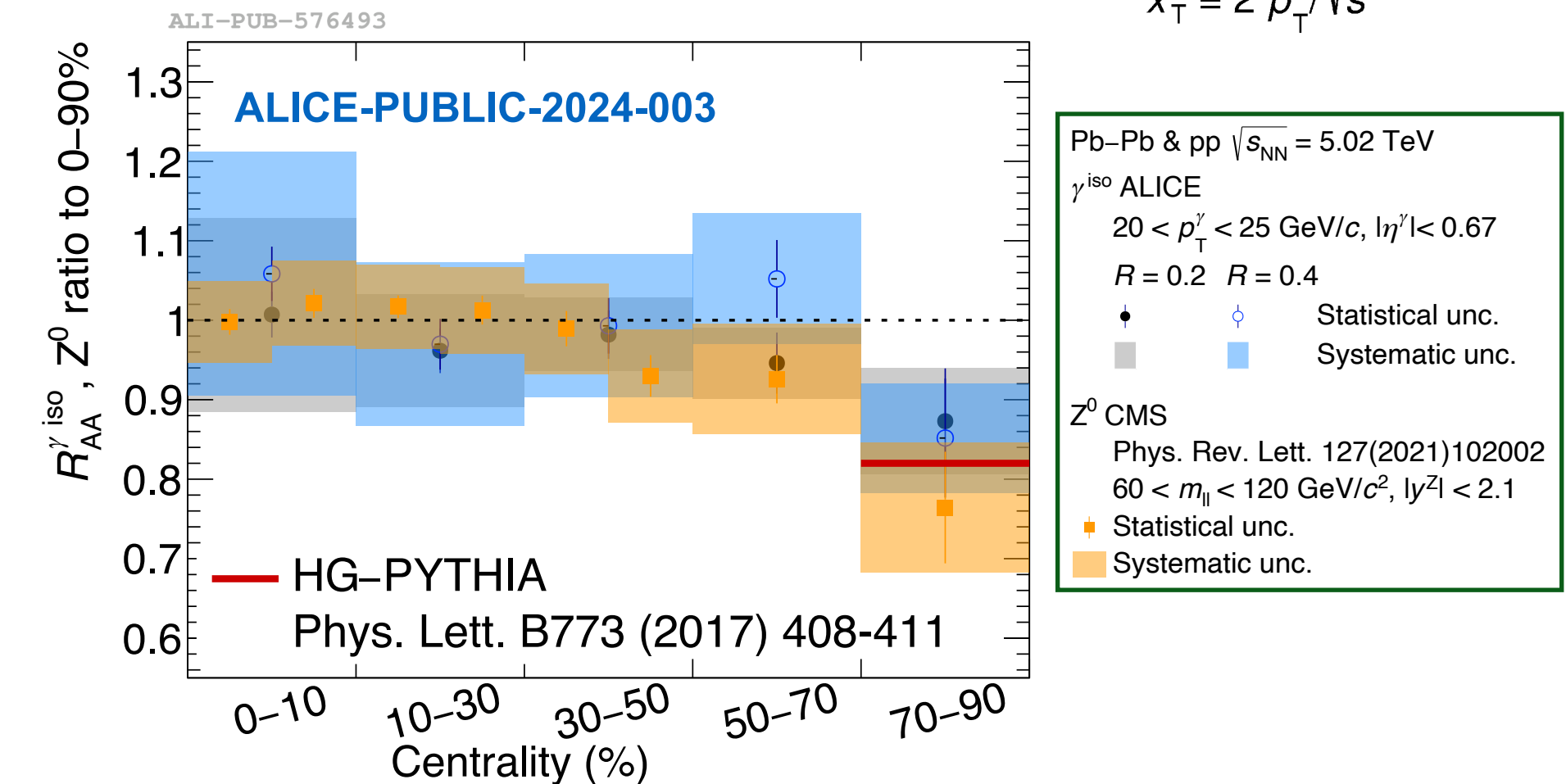
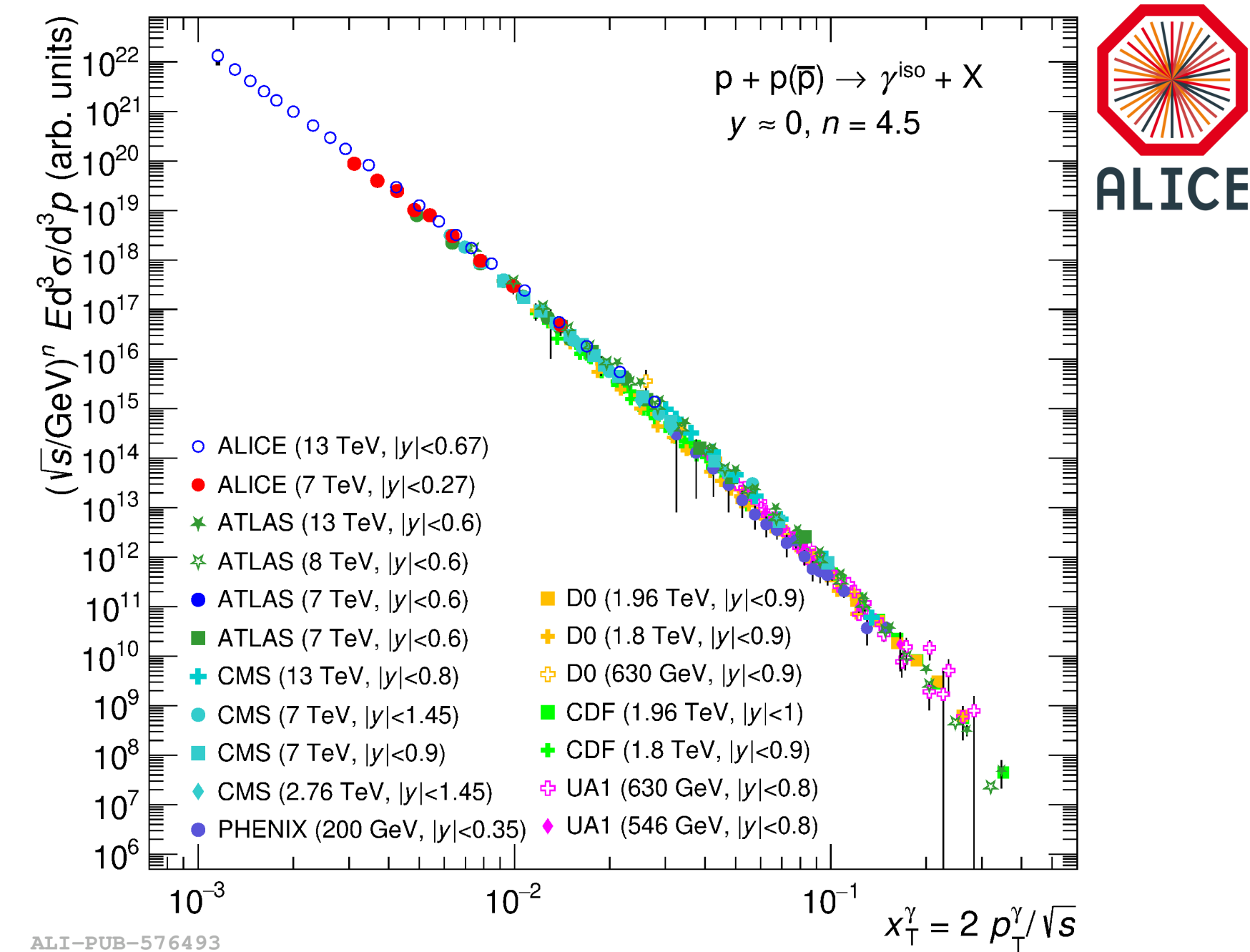
- * Data in agreement with NLO pQCD in multiple collision systems & $\sqrt{s_{NN}}$
- * Lowest measured x_T at mid-rapidity in pp collisions at $\sqrt{s} = 13$ TeV
- * Ratio of cross sections for different R in agreement with theory and within the different collision systems



Summary

→ Cross section

- * Data in agreement with NLO pQCD in multiple collision systems & $\sqrt{s_{NN}}$
- * Lowest measured x_T at mid-rapidity in pp collisions at $\sqrt{s} = 13$ TeV
- * Ratio of cross sections for different R in agreement with theory and within the different collision systems
- * Pb-Pb: $R_{AA} \simeq 1$, no γ production modification by QGP
 - ▶ but for 50–90% & 70–90%: $R_{AA} \simeq 0.9$, agreement (1σ) with HG-PYTHIA, model of the centrality selection bias
 - ▶ Pb-Pb col. agree with nPDF prediction
- * p-Pb: $R_{pA} \simeq 1$, no γ production modification
 - ▶ Hints of suppression for $p_T < 20$ GeV/c in p-Pb, in agreement with pQCD nPDF / PDF at low p_T



Summary

→ Cross section

* Data in agreement with NLO pQCD in multiple collision systems & $\sqrt{s_{NN}}$

* Lowest measured x_T at mid-rapidity in pp collisions at $\sqrt{s} = 13$ TeV

* Ratio of cross sections for different R in agreement with theory and within the different collision systems

* Pb-Pb: $R_{AA} \simeq 1$, no γ production modification by QGP

▶ but for 50–90% & 70–90%: $R_{AA} \simeq 0.9$, agreement (1σ) with HG-PYTHIA, model of the centrality selection bias

▶ Pb-Pb col. agree with nPDF prediction

* p-Pb: $R_{pA} \simeq 1$, no γ production modification

▶ Hints of suppression for $p_T < 20$ GeV/c in p-Pb, in agreement with pQCD nPDF / PDF at low p_T

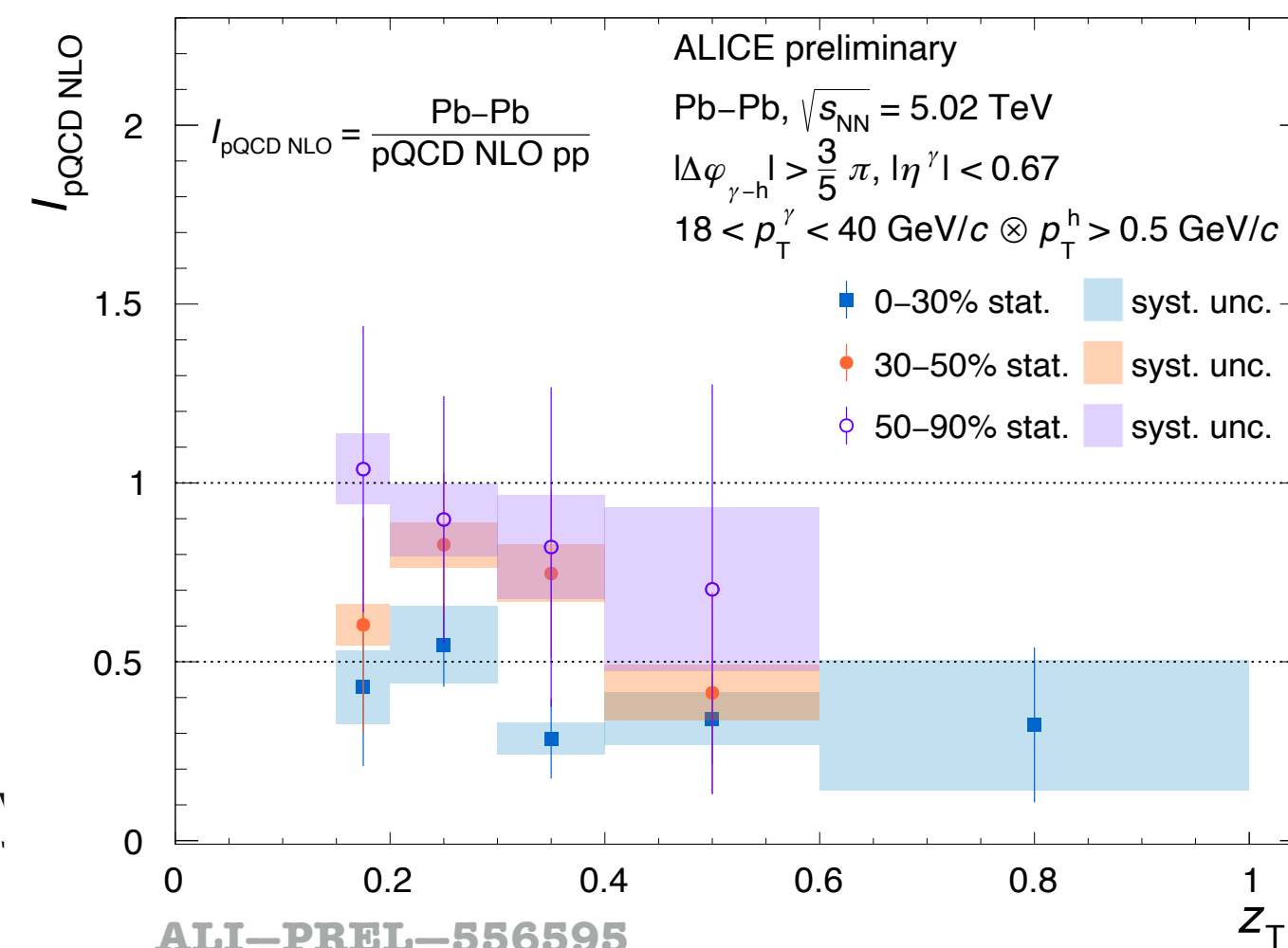
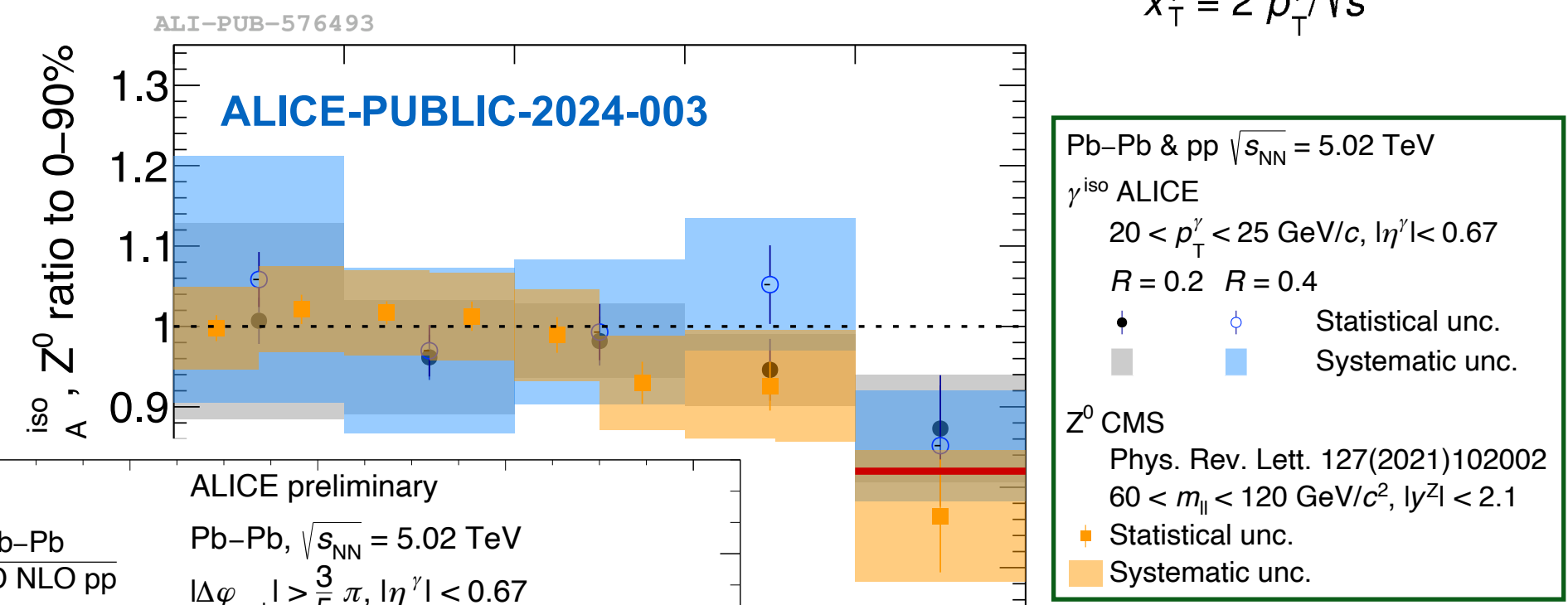
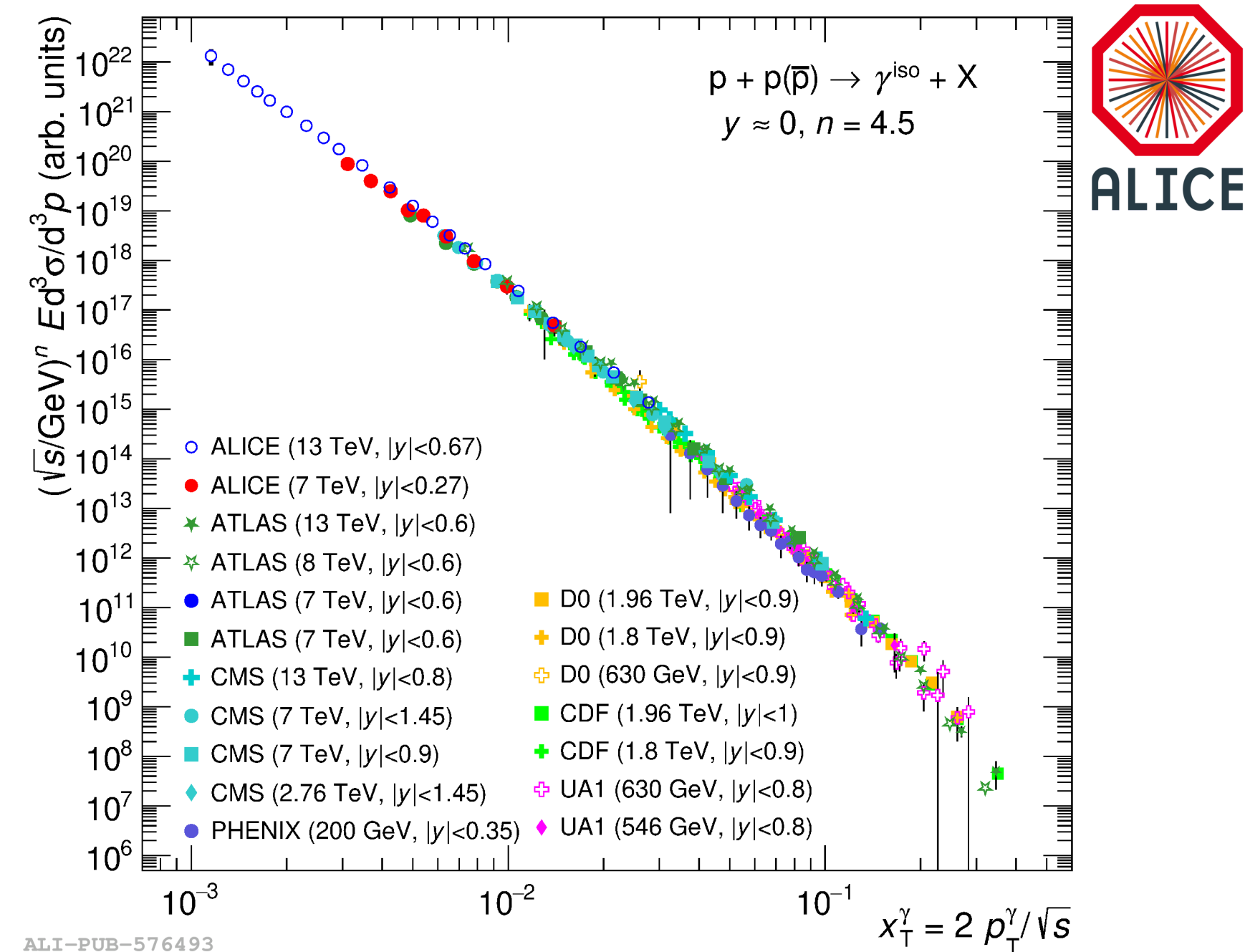
→ γ -hadron corr. in Pb-Pb at $\sqrt{s_{NN}} = 5.02$ TeV

* Very statistically limited, challenging!

* z_T distribution significantly lower than pp NLO pQCD in central

▶ FF modification: stronger for central compared to peripheral

* Results described by two models, model discrimination not possible



Expected improvement with Run 3 + Run 4 data samples, in particular γ -hadron correlations

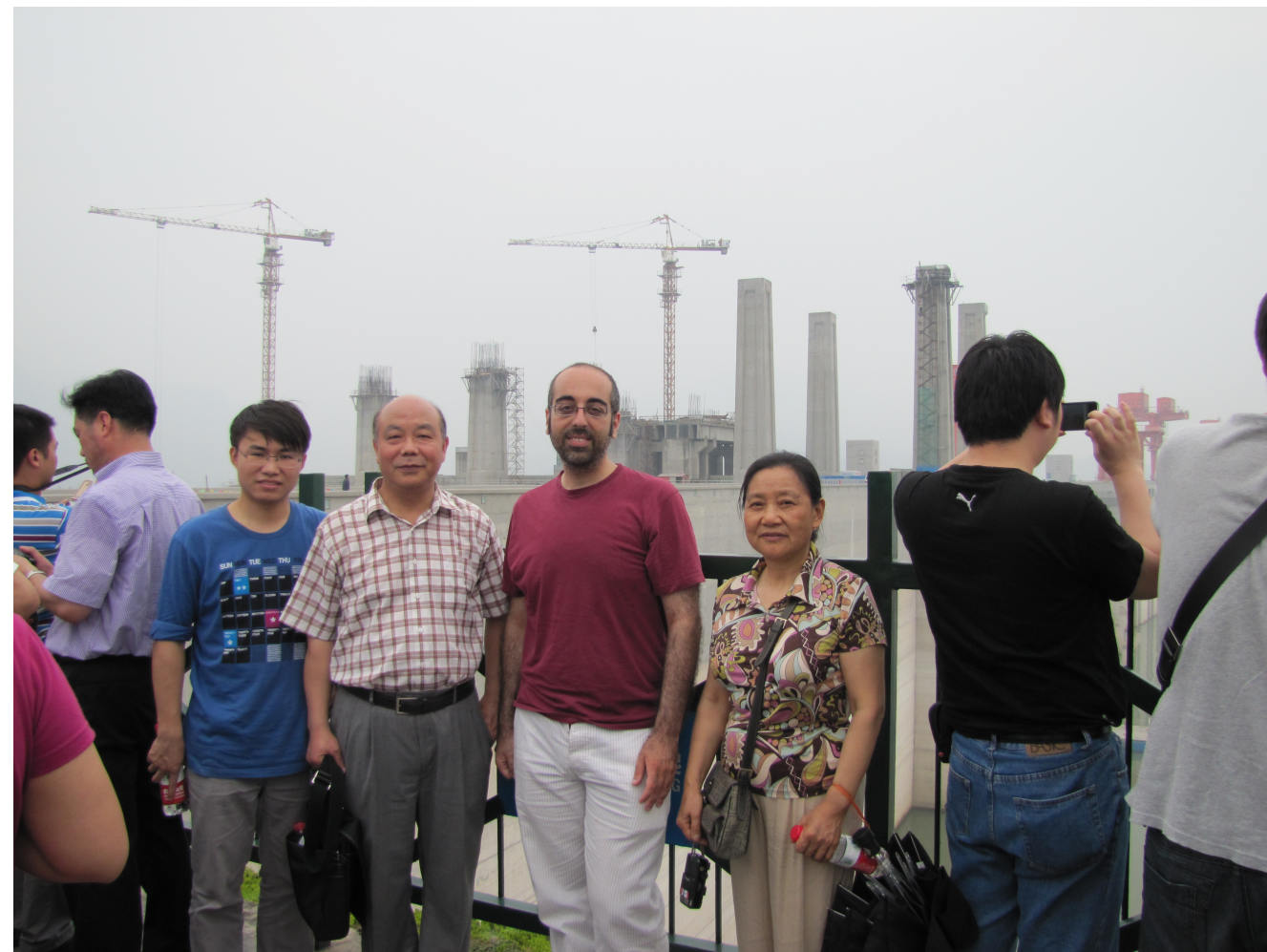
2002 Xiaomei + PHOS rusian friends



2011 Renzhuo & Yaxian Thesis



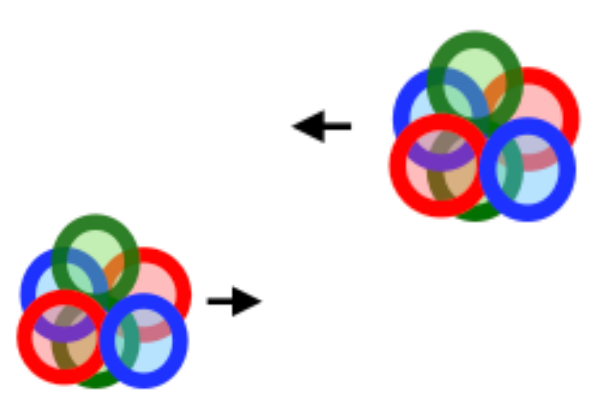
LICE



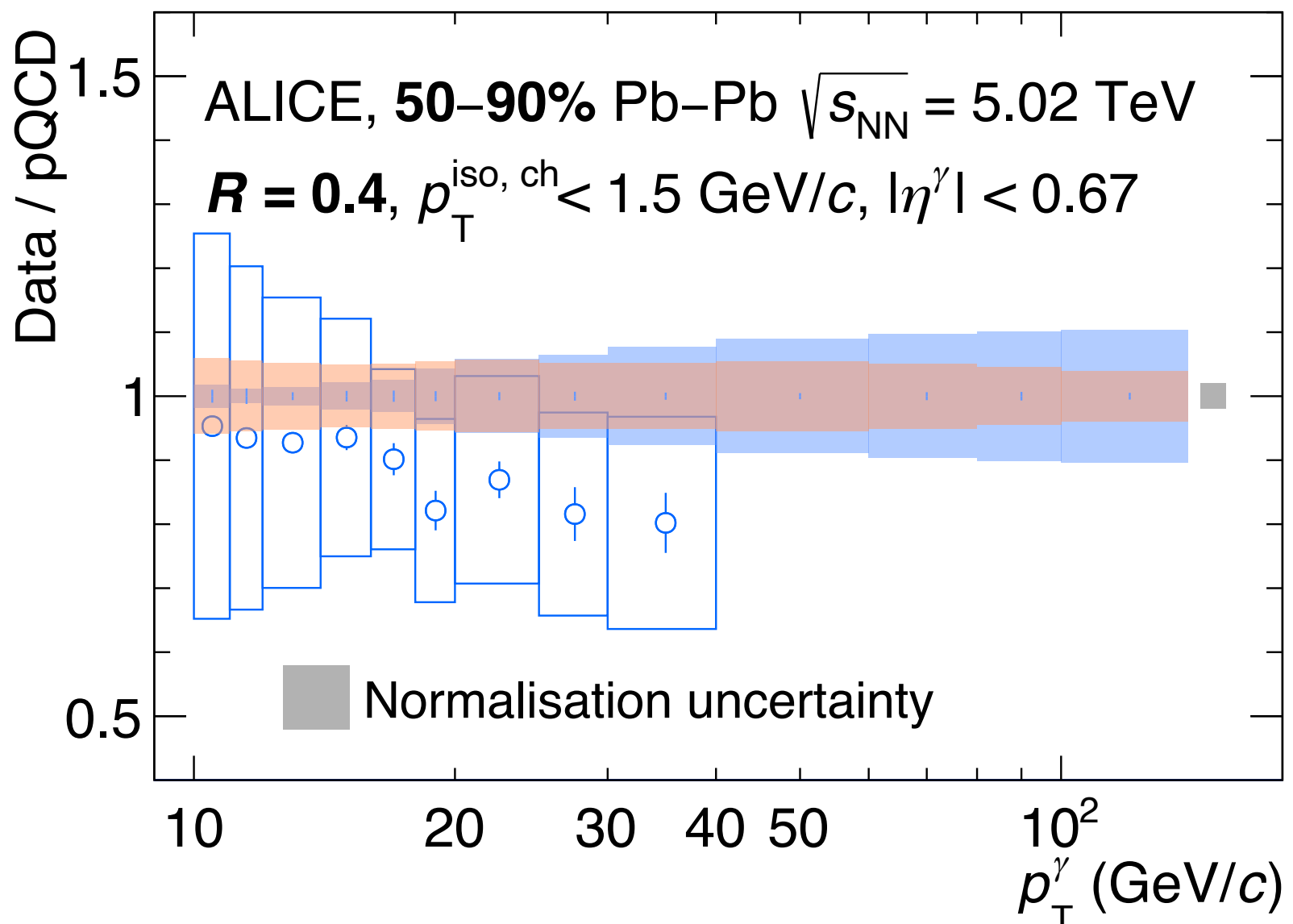
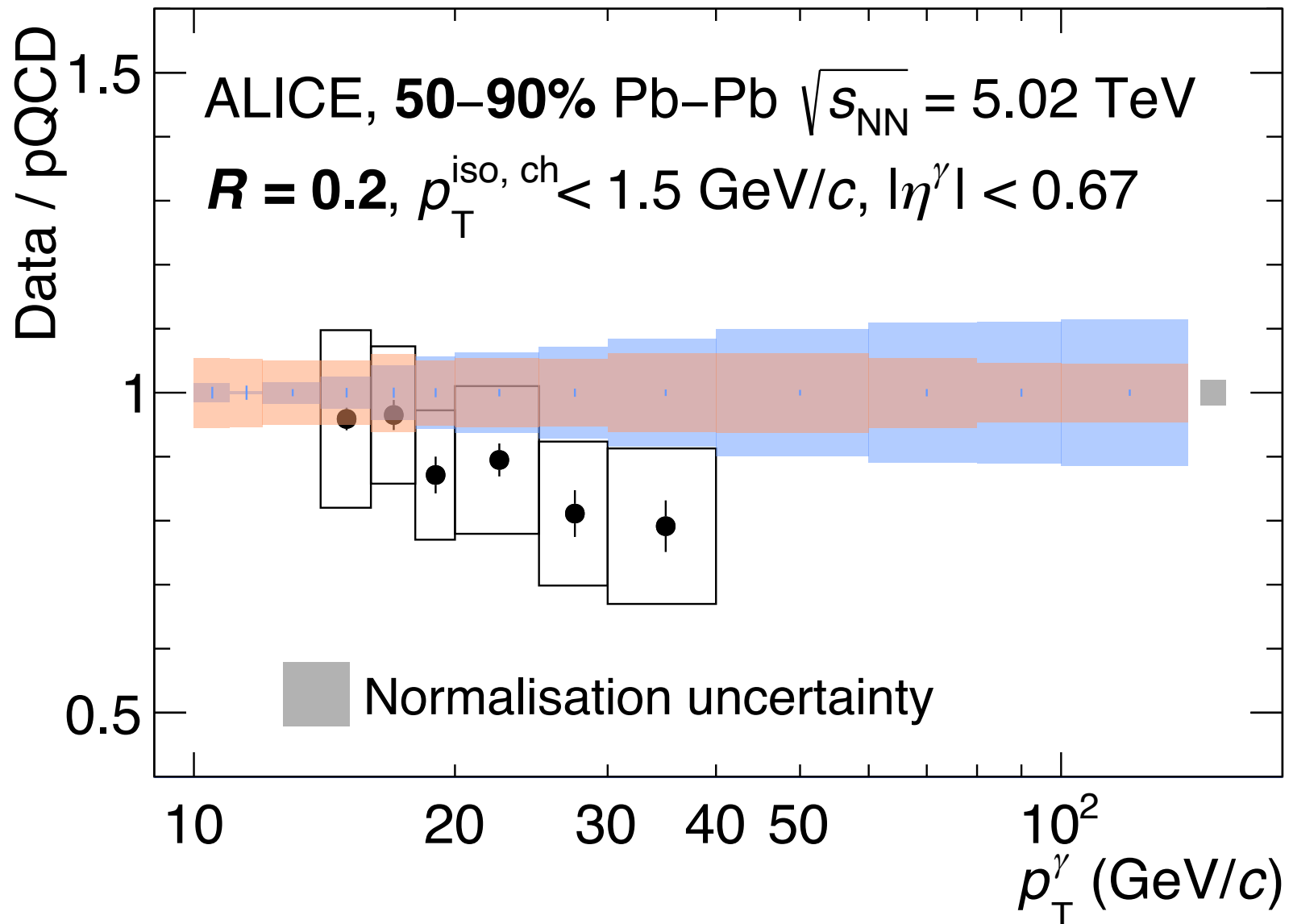
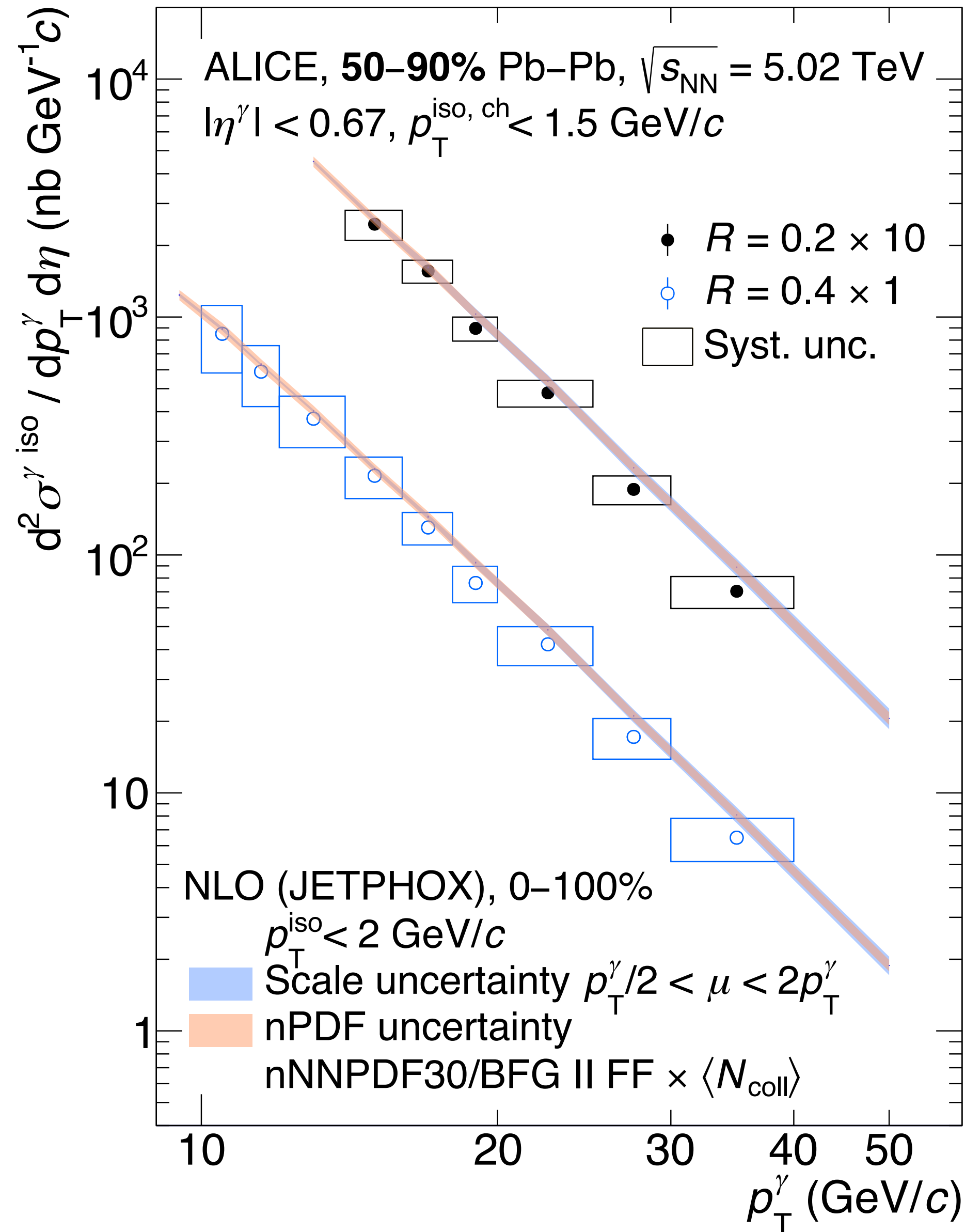
Thanks to all our chinese colleagues and students all over the many years!



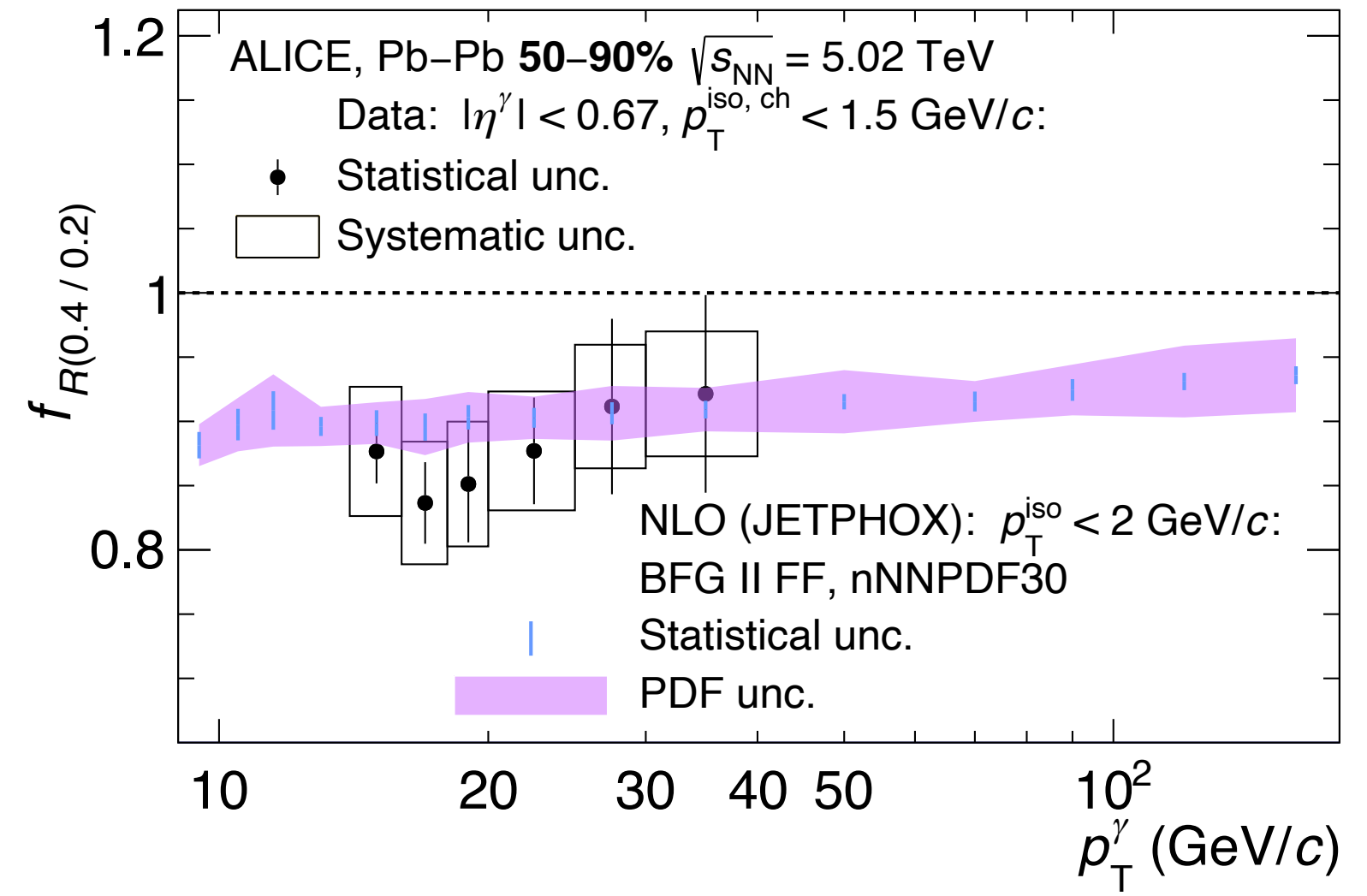
+ the students Xianrong, Haitao, Xinye, Ran and many others



Pb-Pb 50-90%: cross section and ratios



ALICE-PUBLIC-2024-003



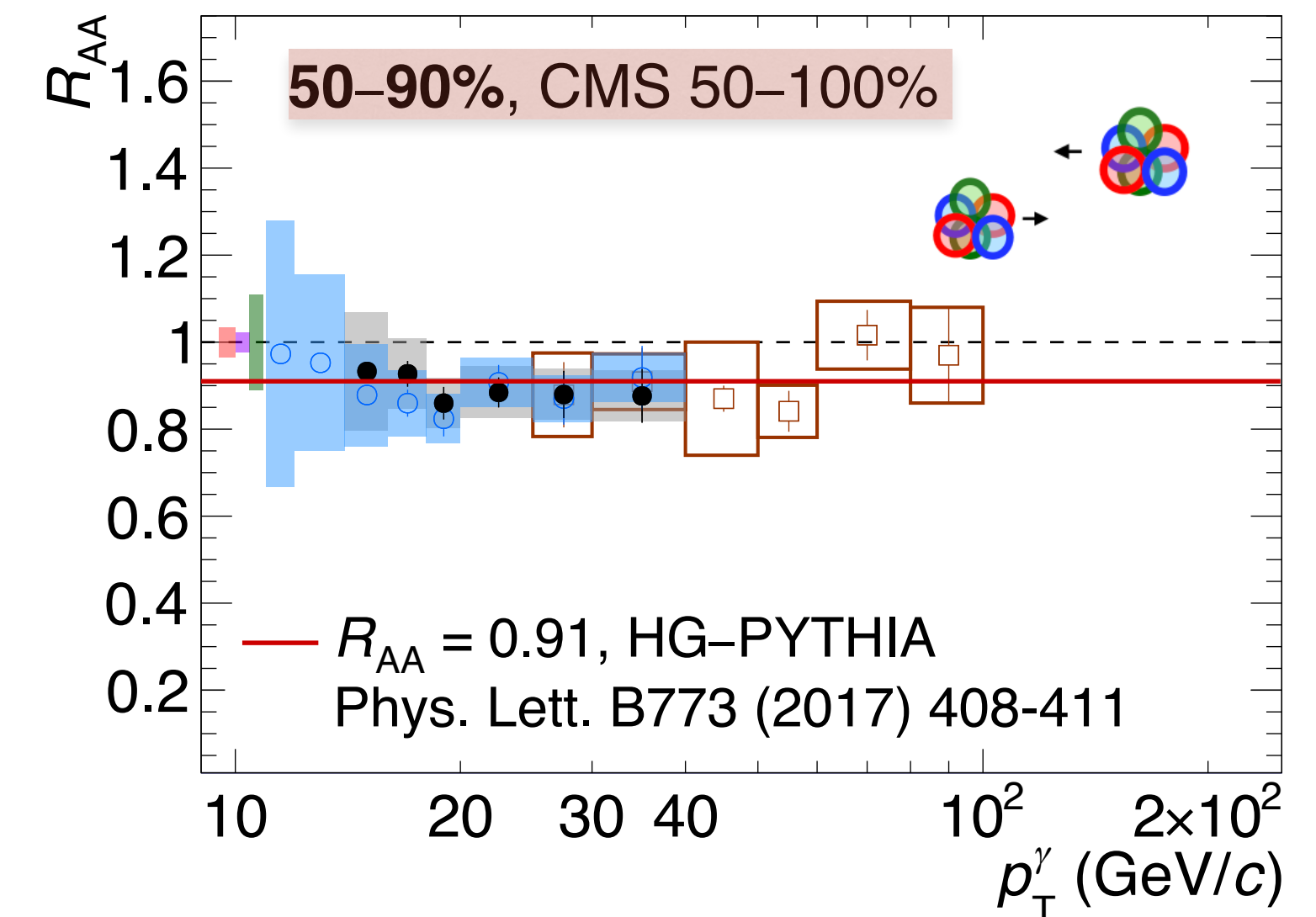
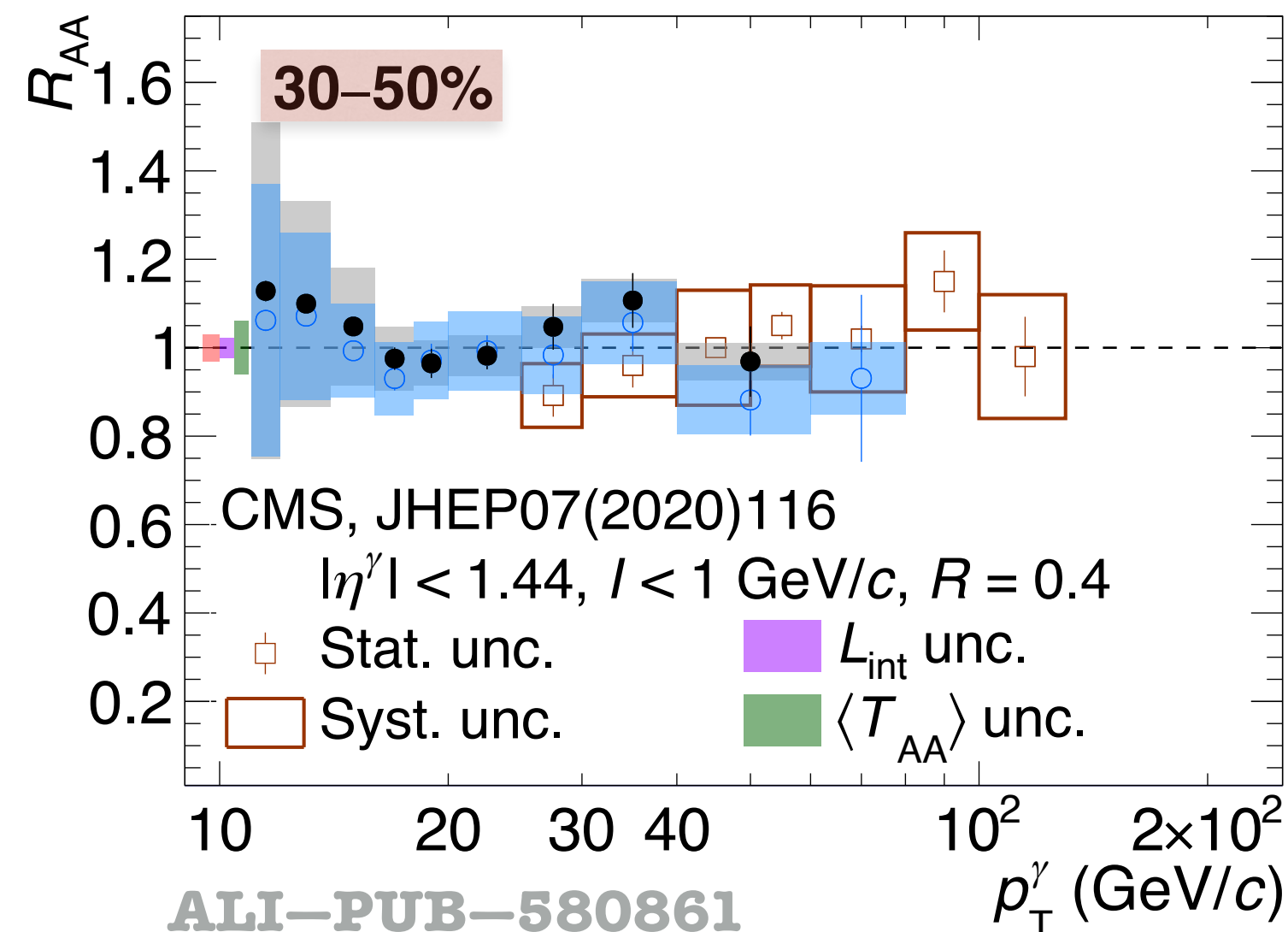
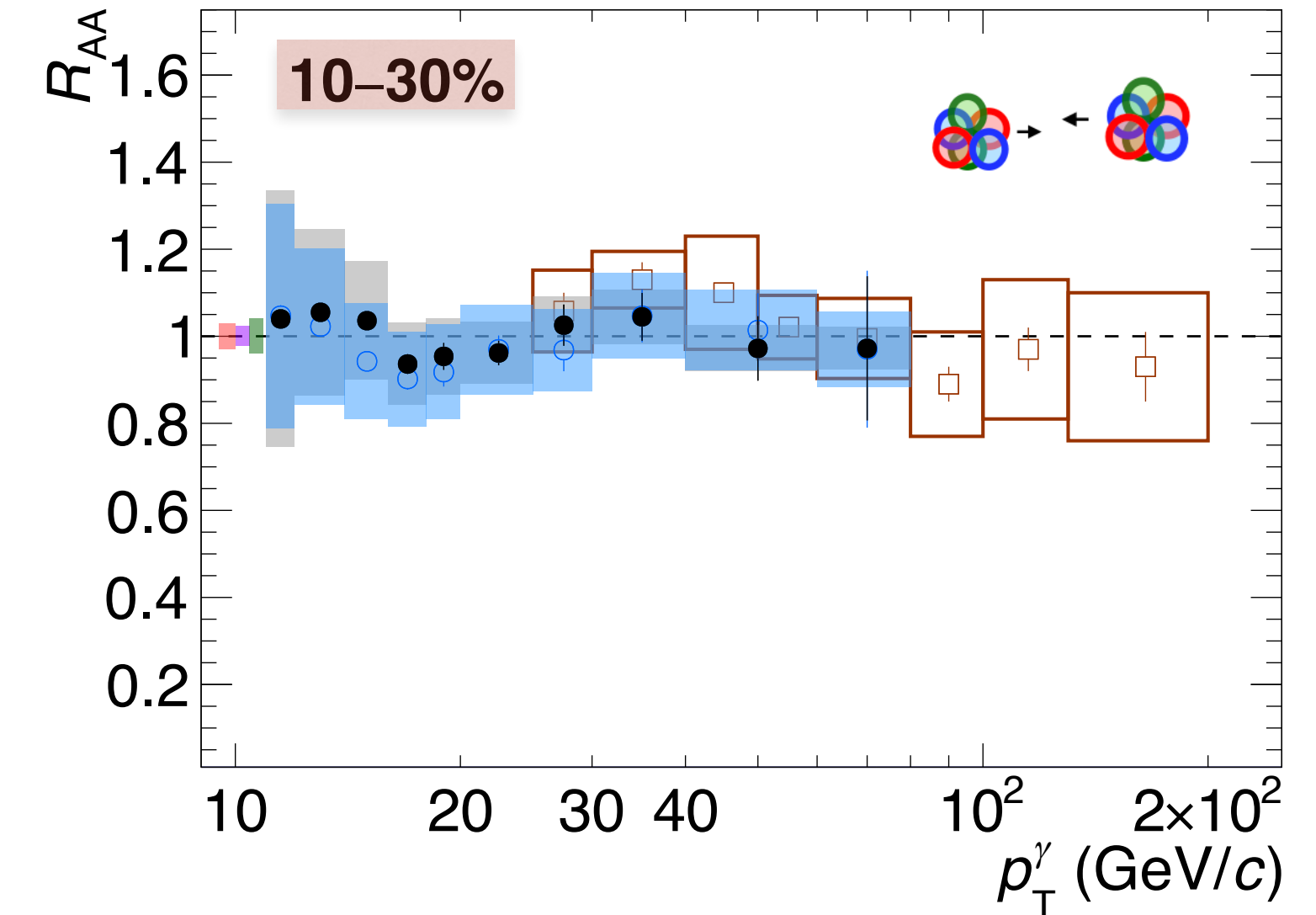
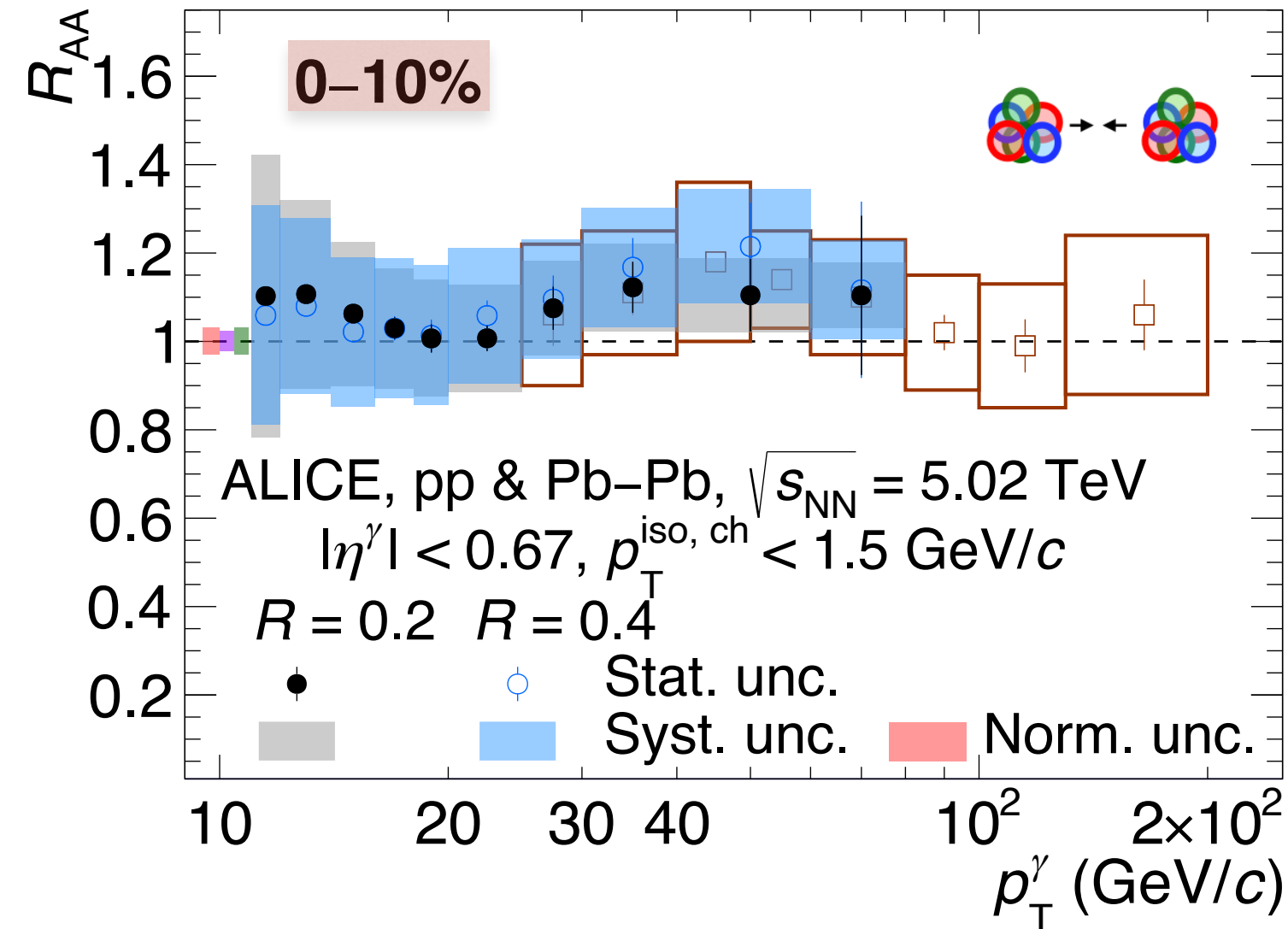
Nuclear modification factor R_{AA} , pp & Pb-Pb at $\sqrt{s_{NN}} = 5.02$ TeV

$$R_{AA} = \frac{1}{\langle N_{coll} \rangle} \frac{d^2\sigma_{AA} / (dp_T d\eta)}{d^2\sigma_{pp} / (dp_T d\eta)}$$

- **ALICE & CMS:** good agreement in the overlapping region $25 < p_T < 40-80$ GeV/c

50-90%

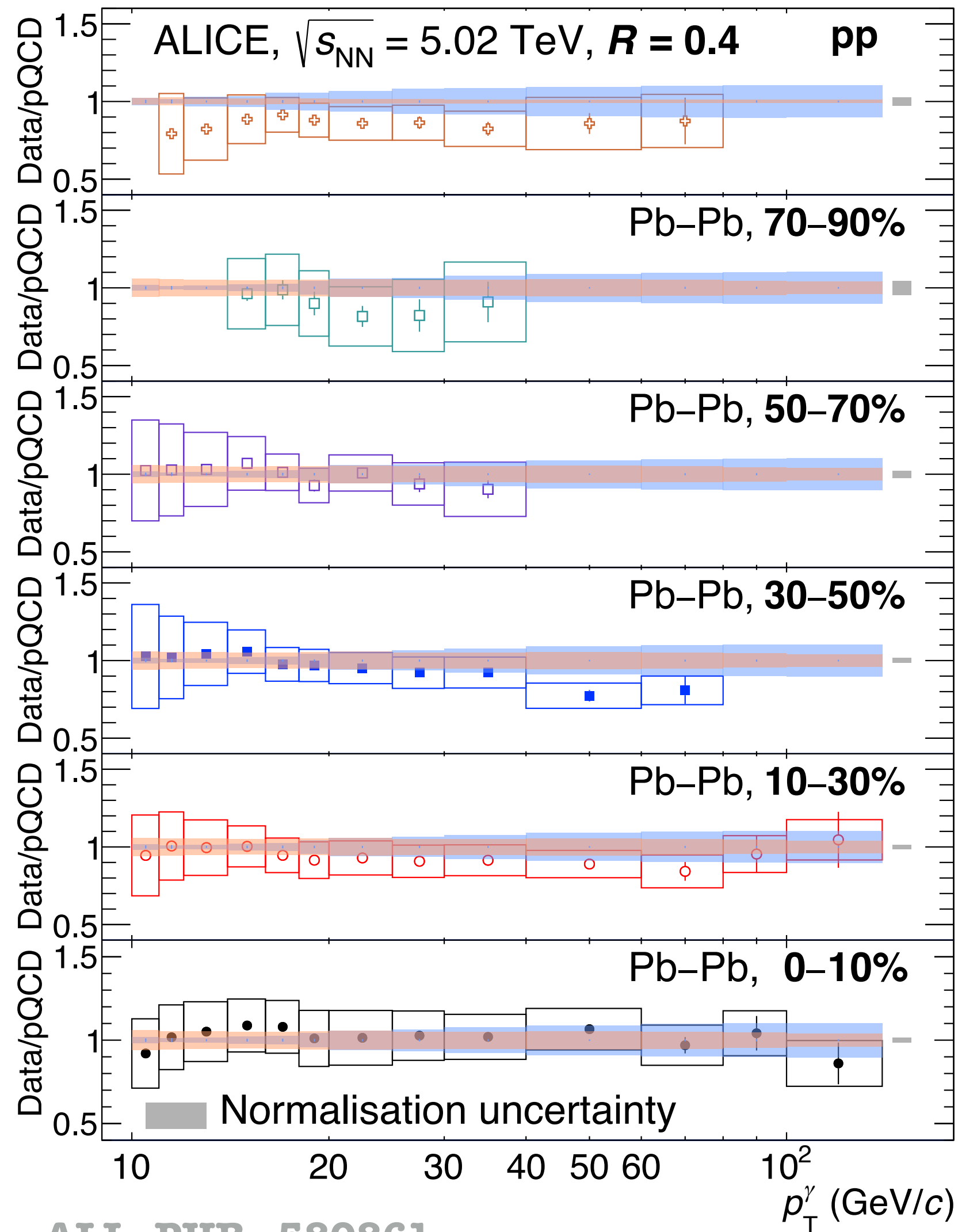
- ➔ Closer to 0.9 than 1 for both R likely due to centrality selection bias of Glauber model
- ➔ Model by C. Loizides & A. Morsch (Phys. Lett. B773 (2017) 408-411) yields a value at **0.91**
- ❖ In agreement within the uncertainties



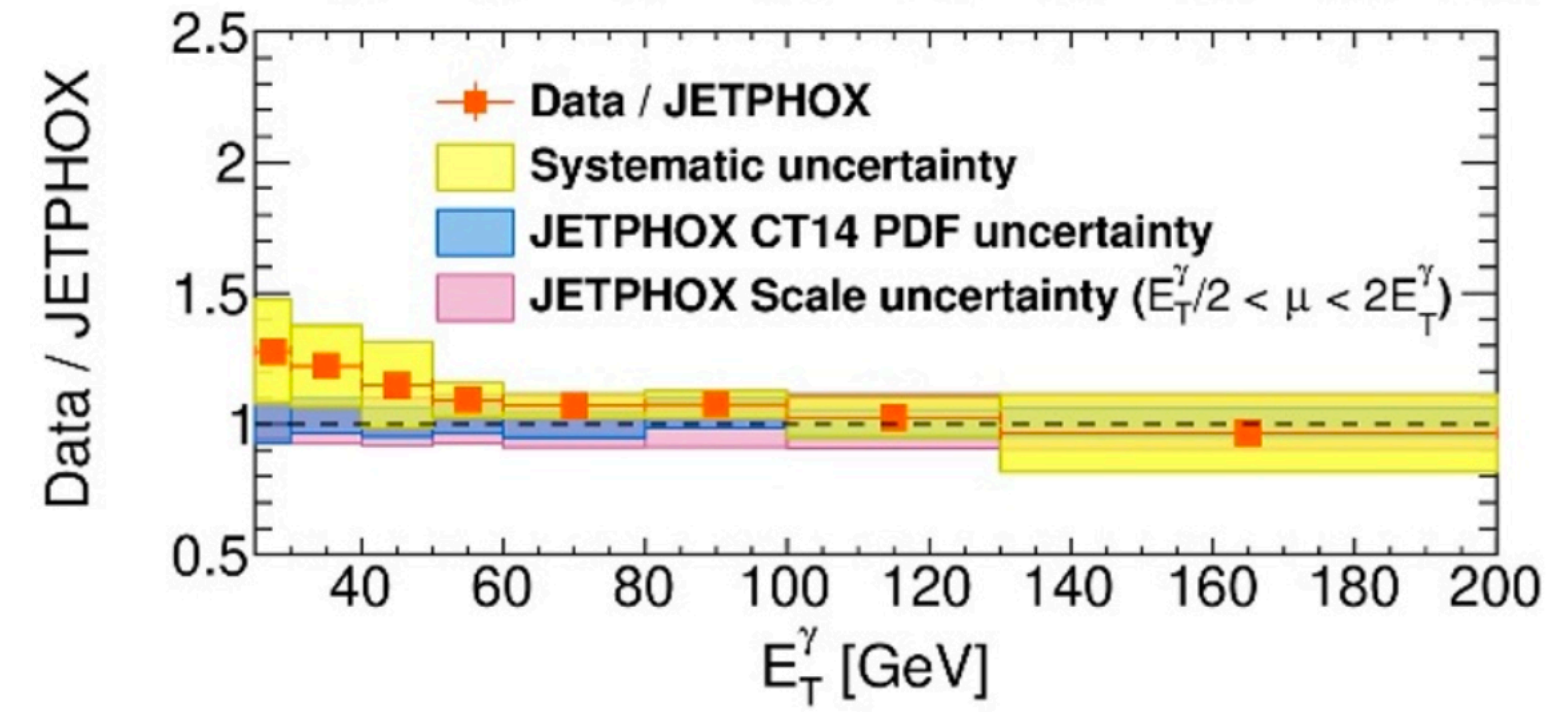
Data over theory, $R = 0.4$, pp & Pb–Pb at $\sqrt{s_{NN}} = 5.02$ TeV



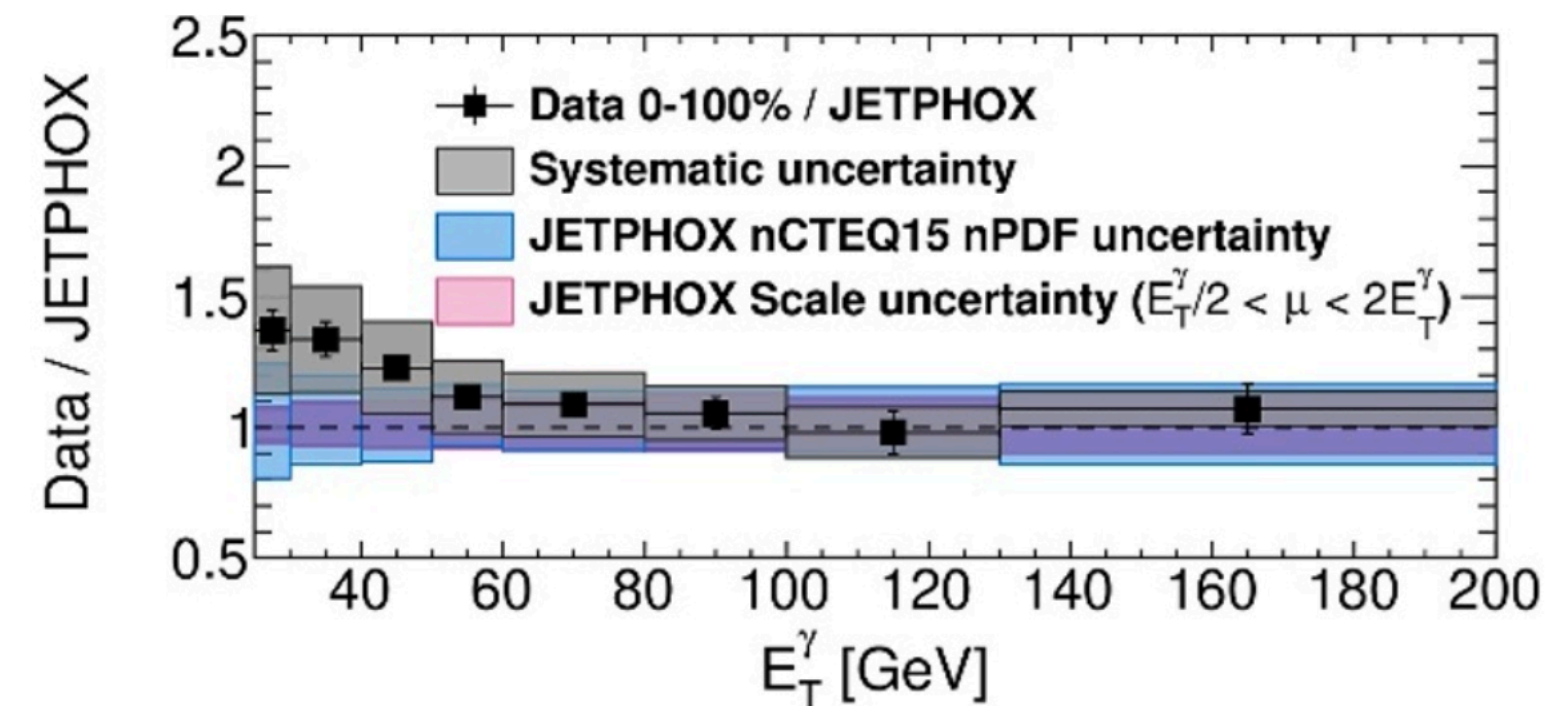
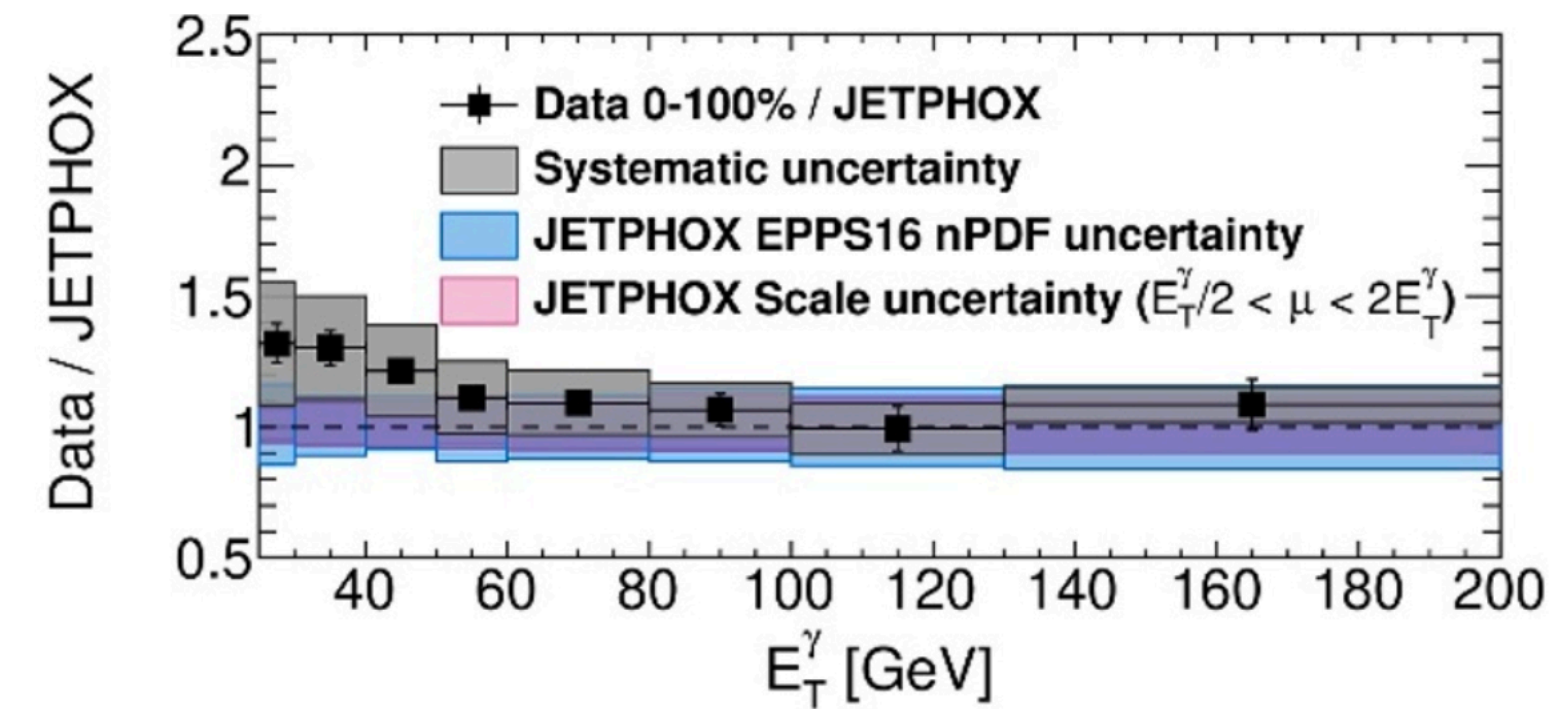
ALICE



CMS



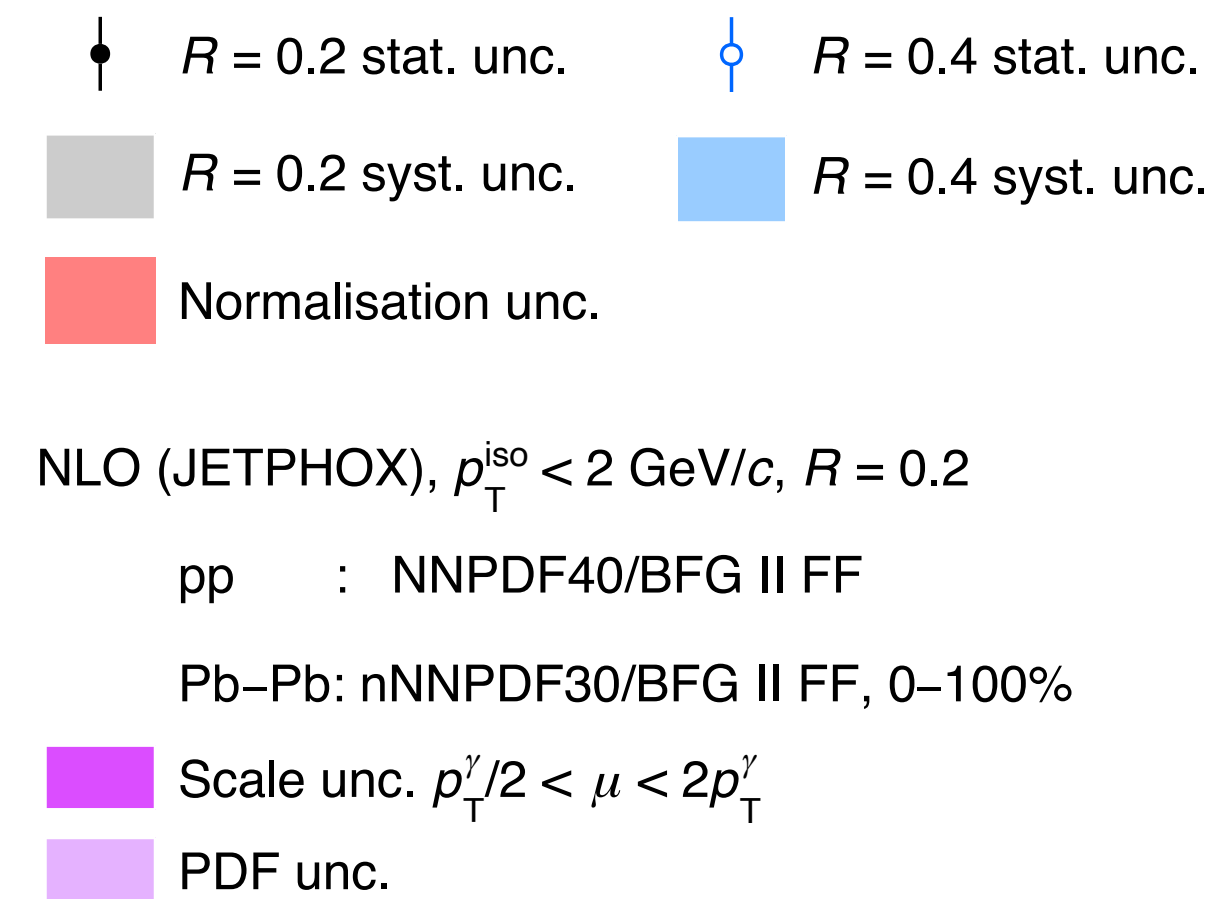
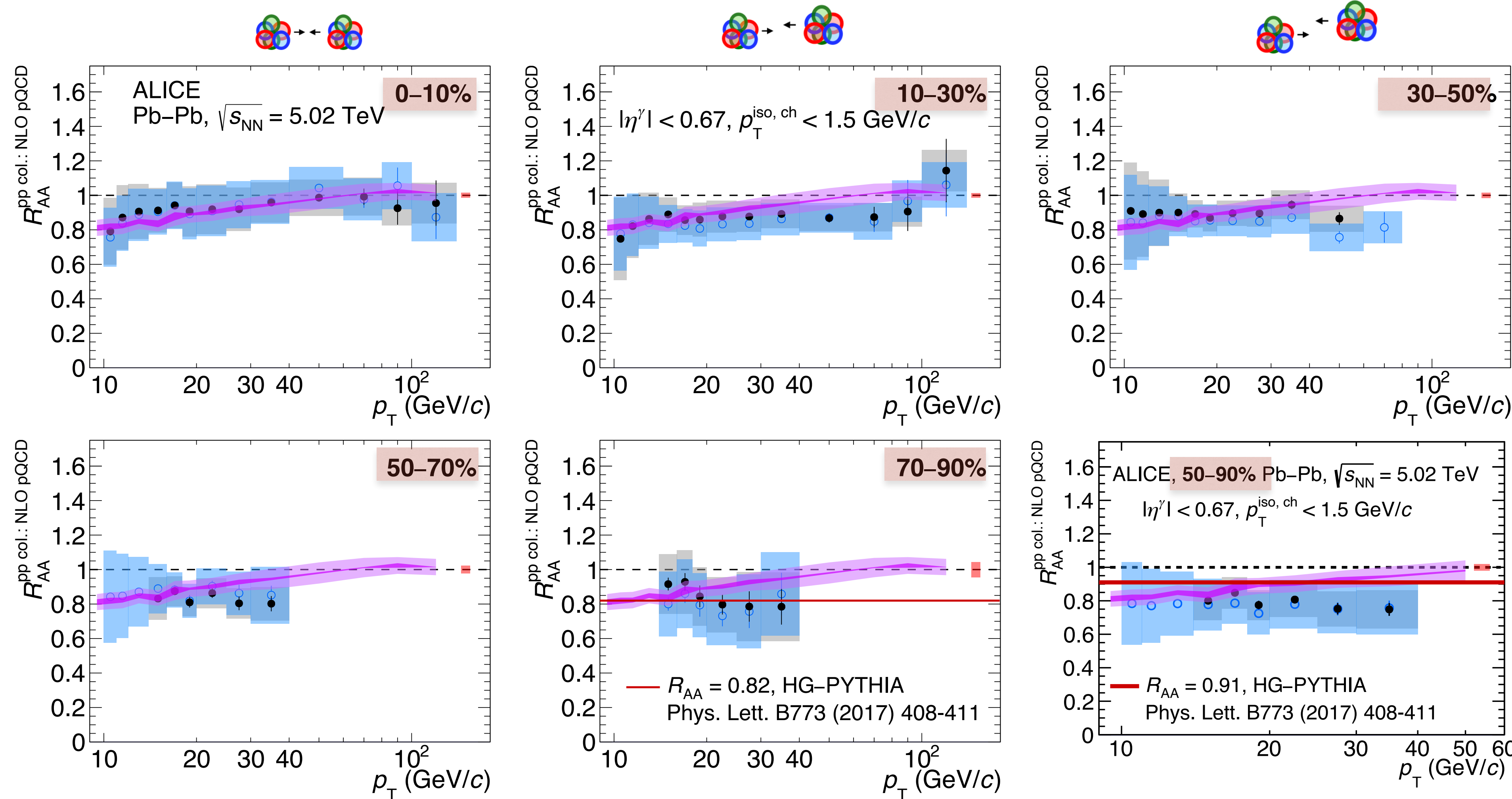
CMS JHEP 07 (2020) 116
arXiv:2003.12797 [hep-ex]



ALI-PUB-580861

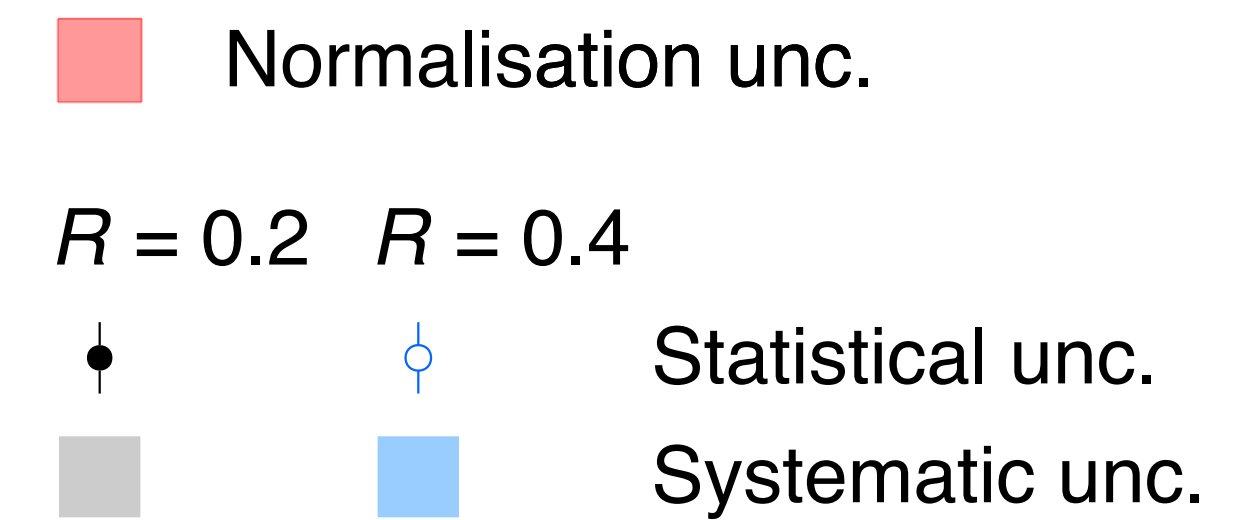
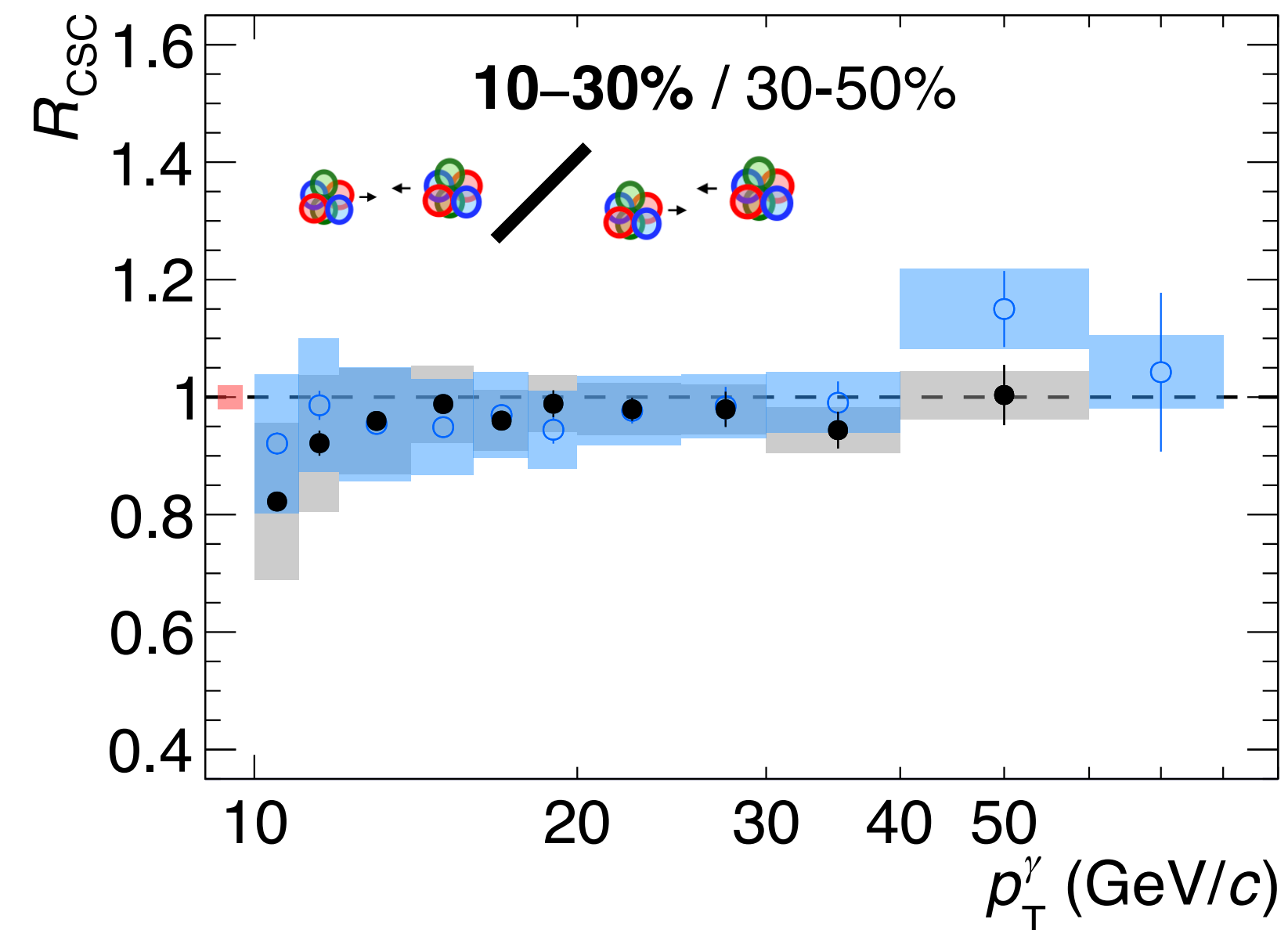
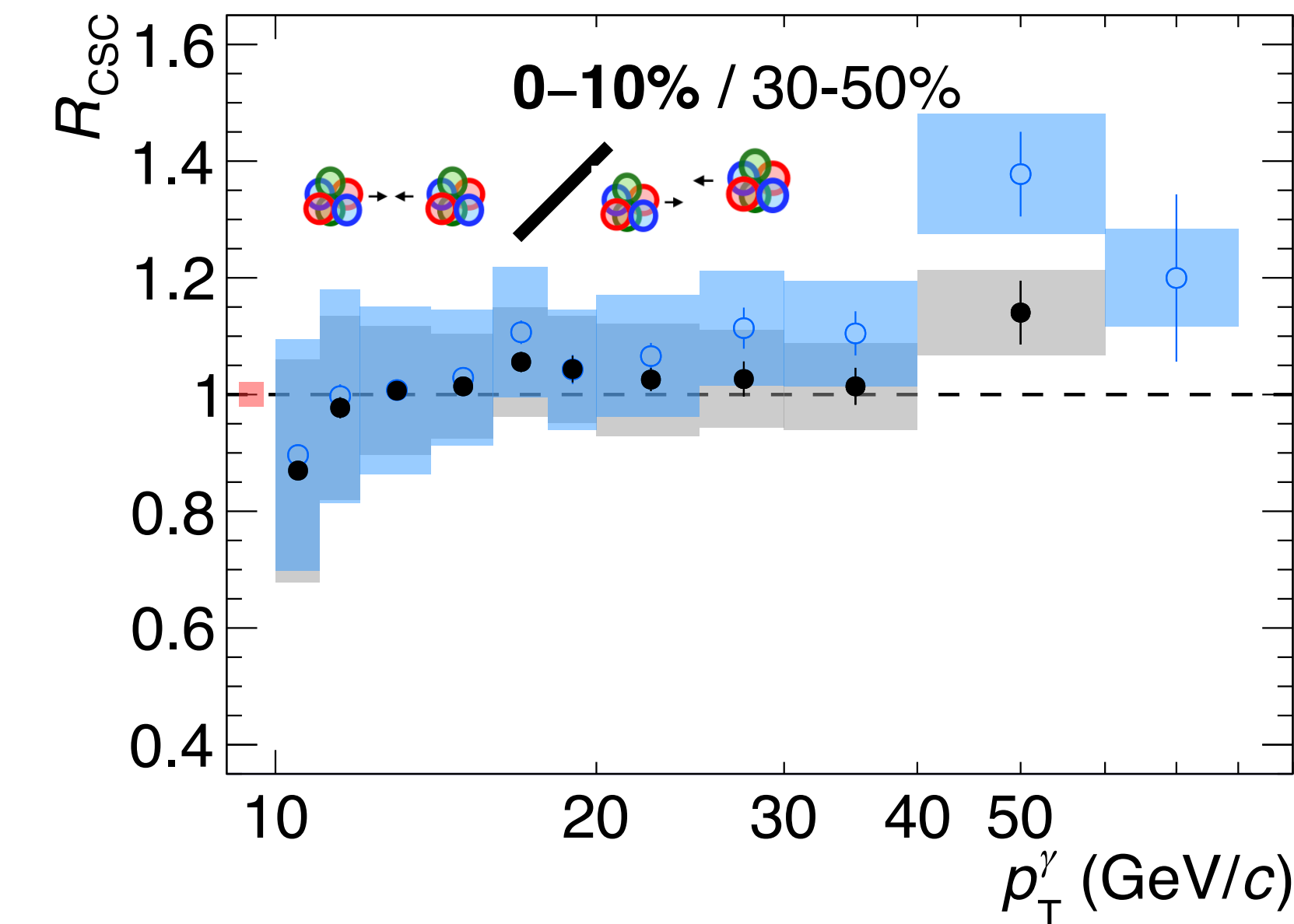
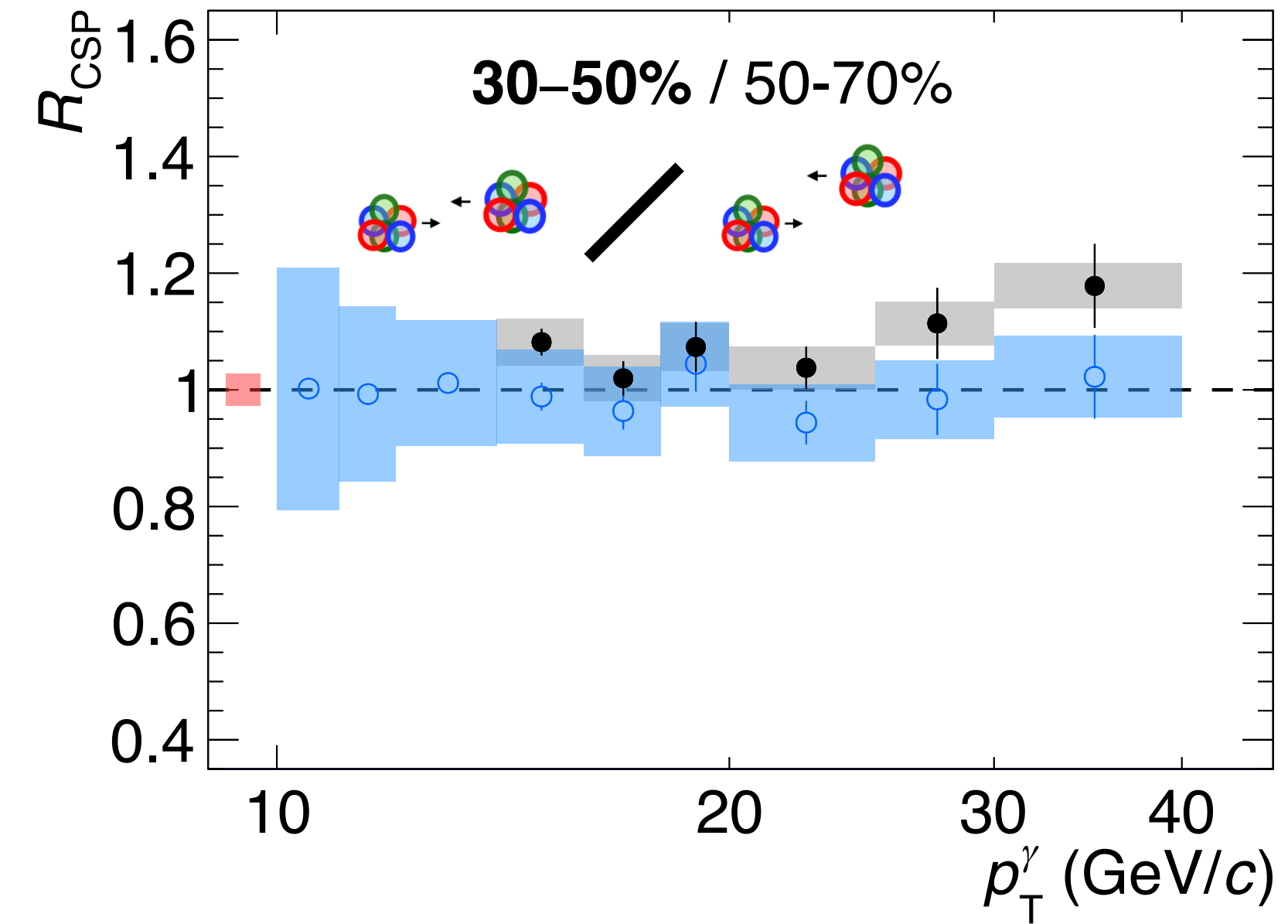
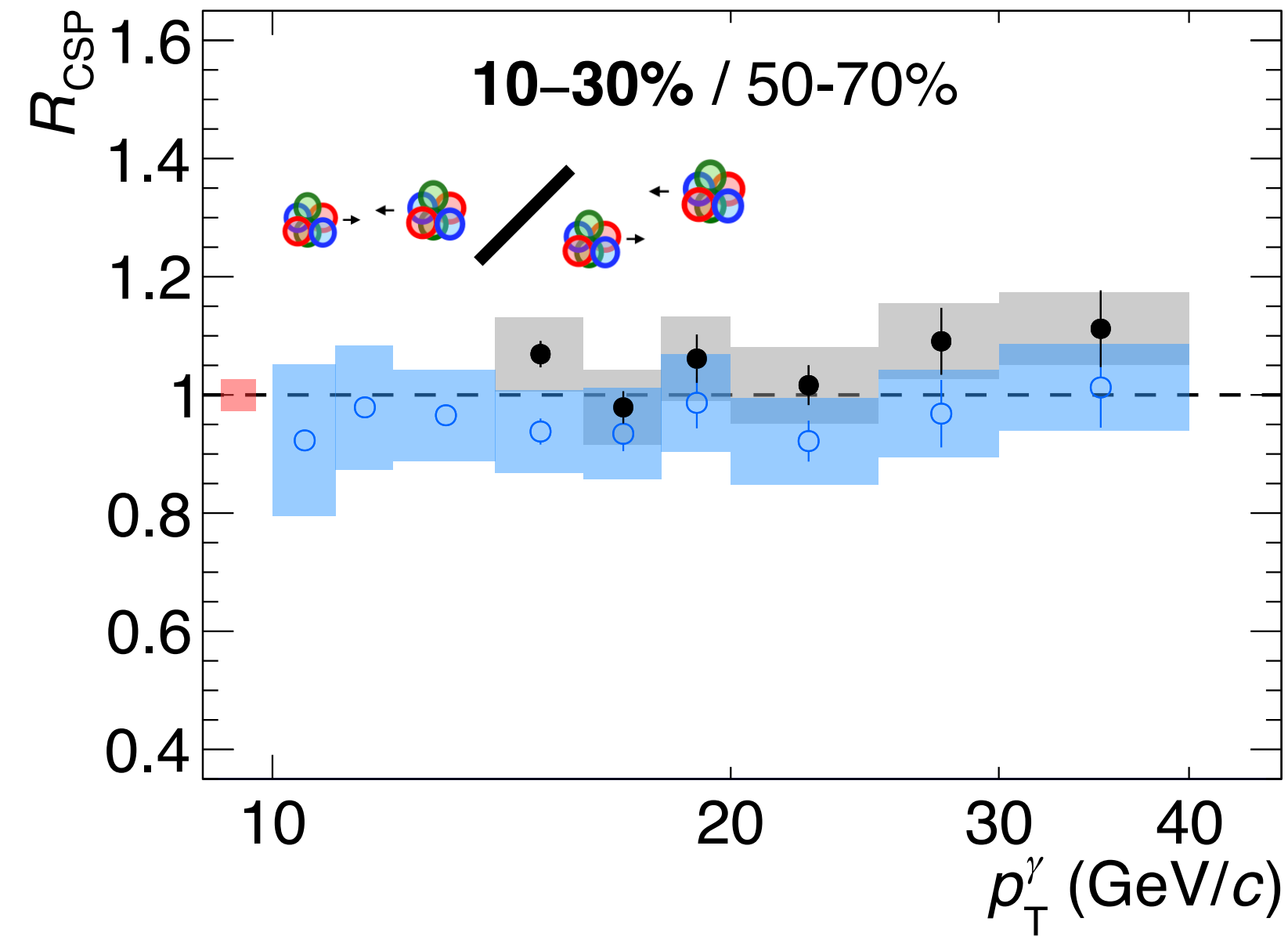
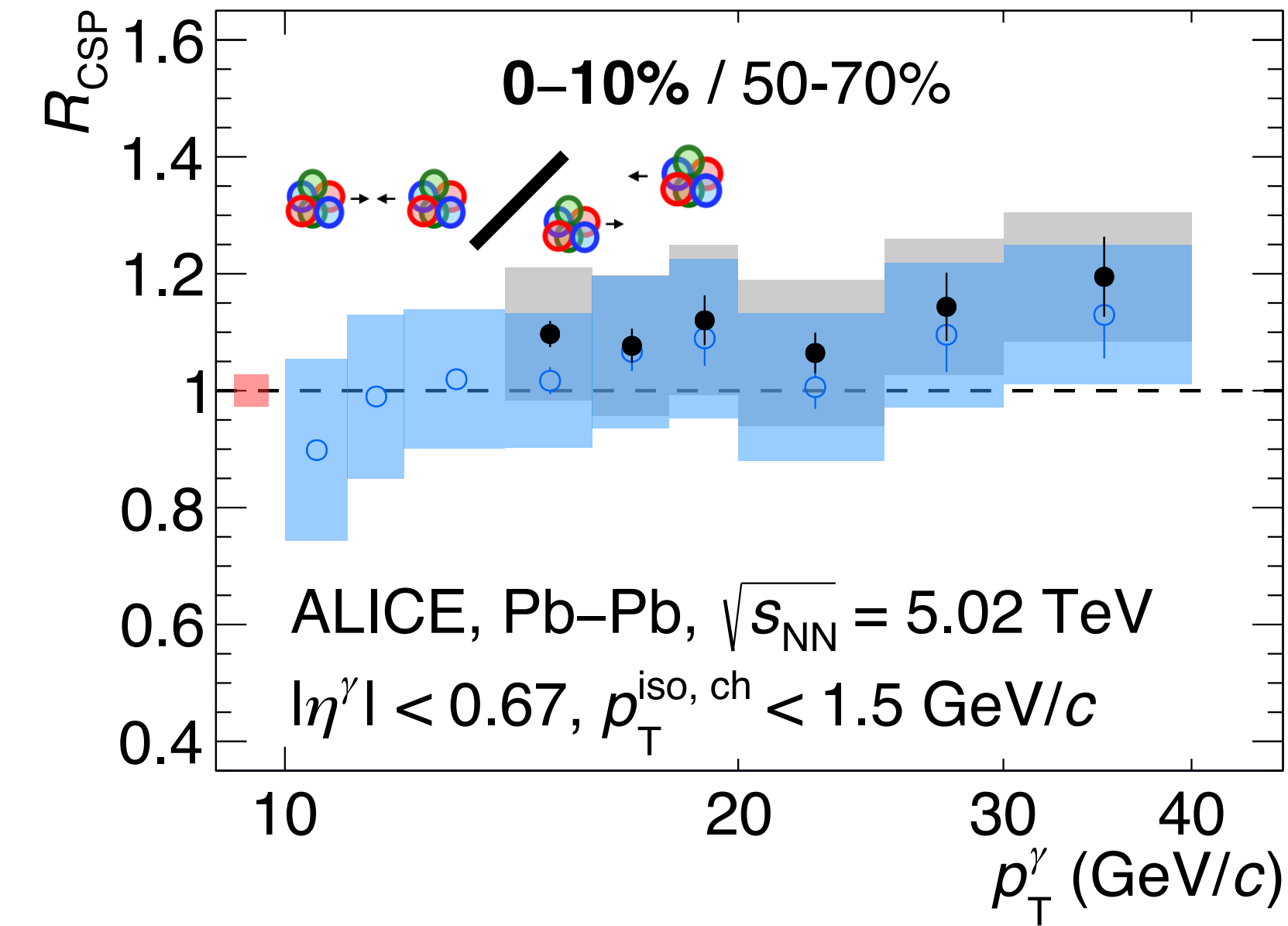
Nuclear modification factor pp data denominator replaced by pp NLO pQCD

ALICE-PUBLIC-2024-003



Pb-Pb cross section ratios

$$R_{\text{CSP}} = \frac{\langle N_{\text{coll}} \rangle^{50-70\%}}{\langle N_{\text{coll}} \rangle^k} \frac{d^2 \sigma_{\text{Pb-Pb}}^{\gamma \text{ iso}} / (dp_T d\eta)|_k}{d^2 \sigma_{\text{Pb-Pb}}^{\gamma \text{ iso}} / (dp_T d\eta)|_{50-70\%}}, \quad R_{\text{CSC}} = \frac{\langle N_{\text{coll}} \rangle^{30-50\%}}{\langle N_{\text{coll}} \rangle^k} \frac{d^2 \sigma_{\text{Pb-Pb}}^{\gamma \text{ iso}} / (dp_T d\eta)|_k}{d^2 \sigma_{\text{Pb-Pb}}^{\gamma \text{ iso}} / (dp_T d\eta)|_{30-50\%}}$$

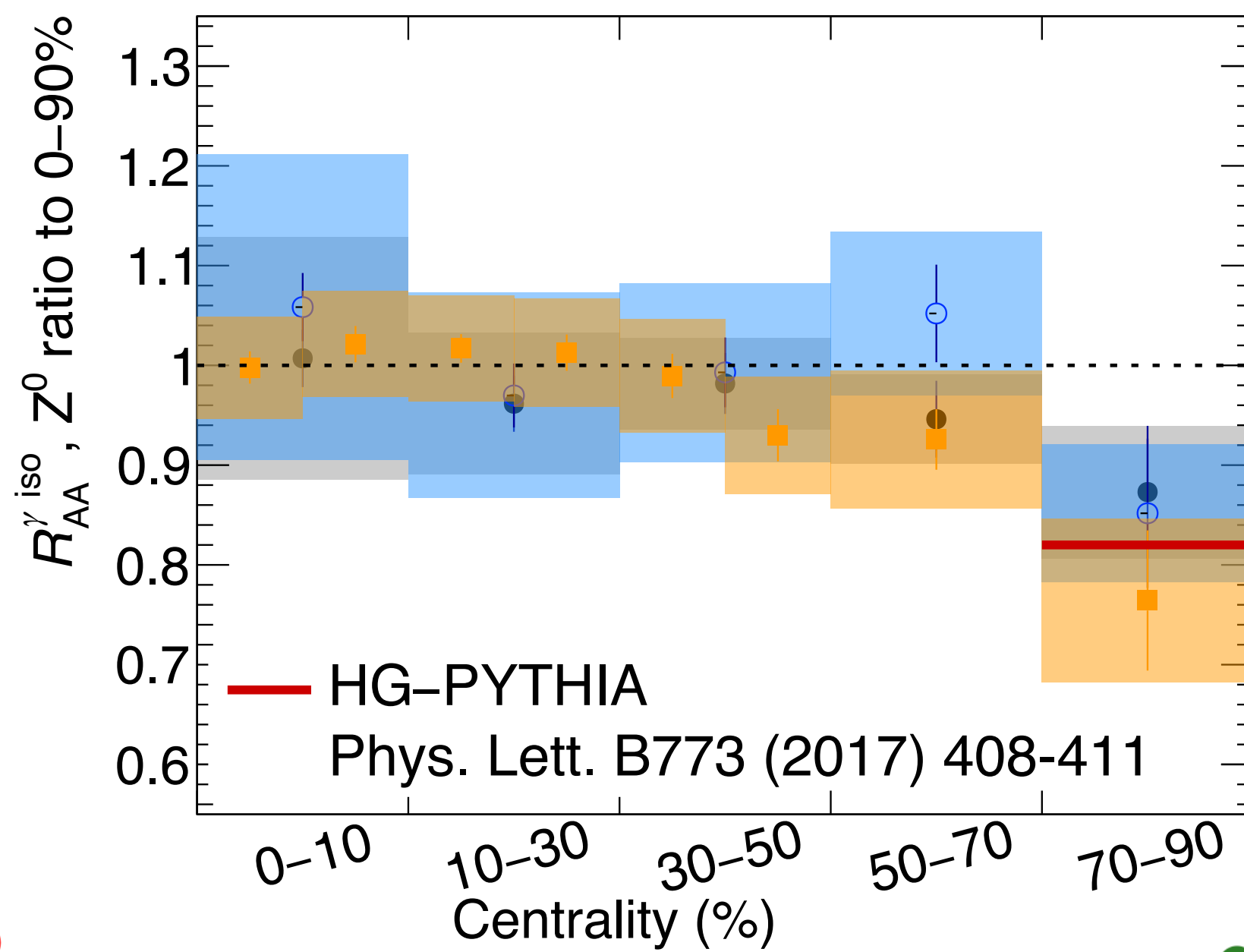
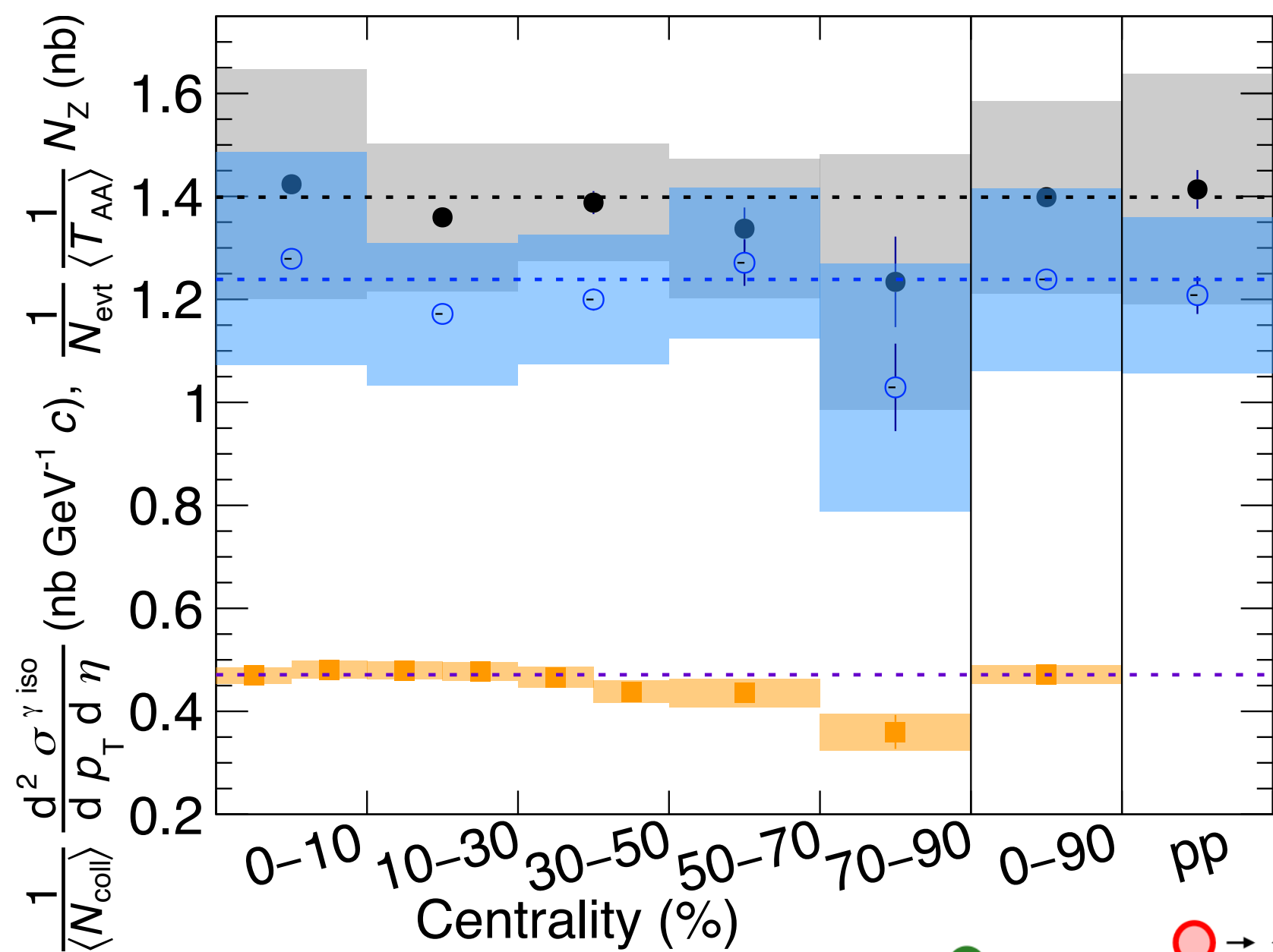


ALICE-PUBLIC-2024-003

Nuclear modification factor R_{AA} , pp & Pb-Pb at $\sqrt{s_{NN}} = 5.02$ TeV



ALICE-PUBLIC-2024-003



Pb-Pb & pp $\sqrt{s_{NN}} = 5.02$ TeV

γ^{iso} ALICE

$20 < p_T^\gamma < 25$ GeV/c, $|\eta^\gamma| < 0.67$

$R = 0.2$ $R = 0.4$

● ○ Statistical unc.
 ■ Systematic unc.

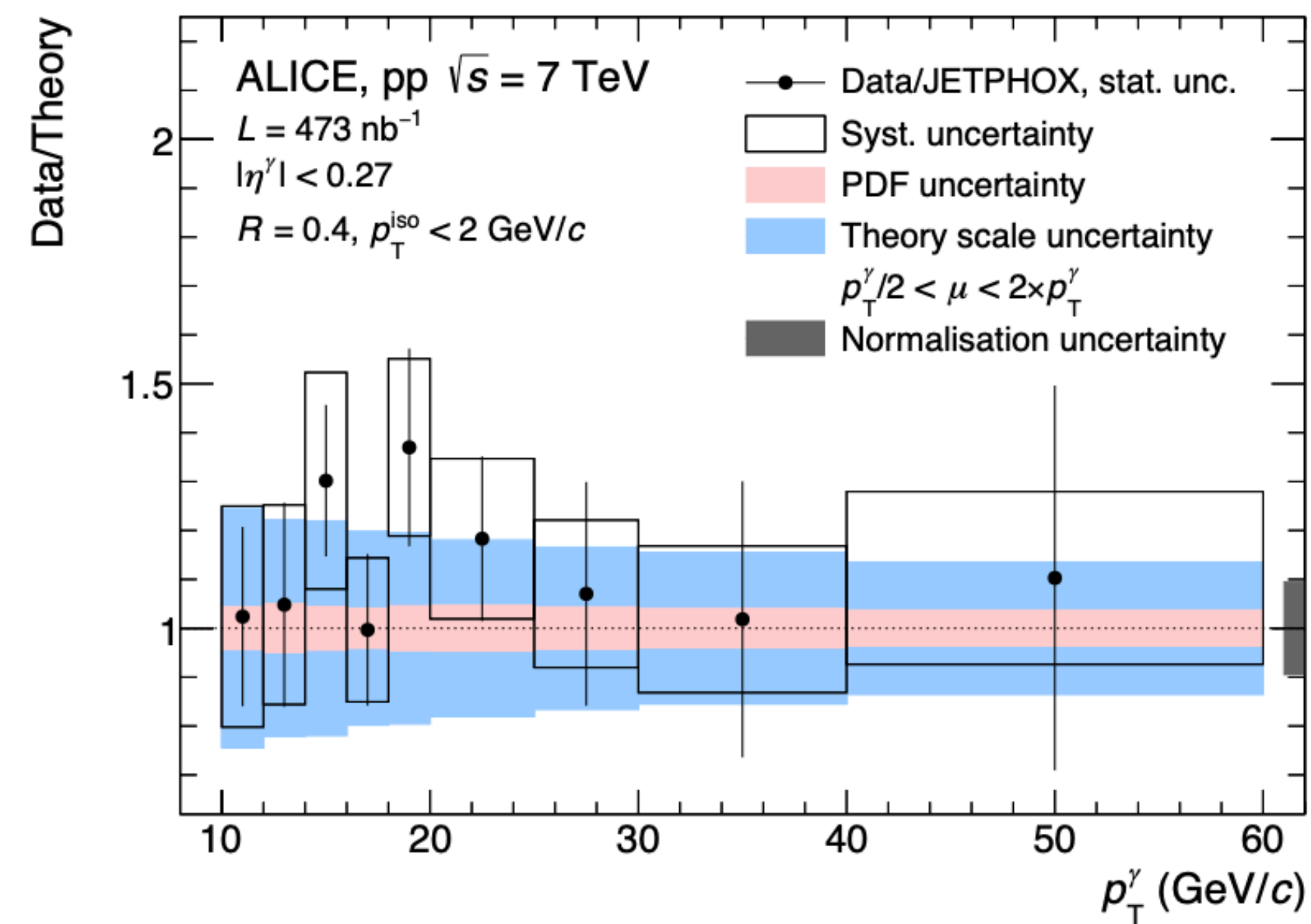
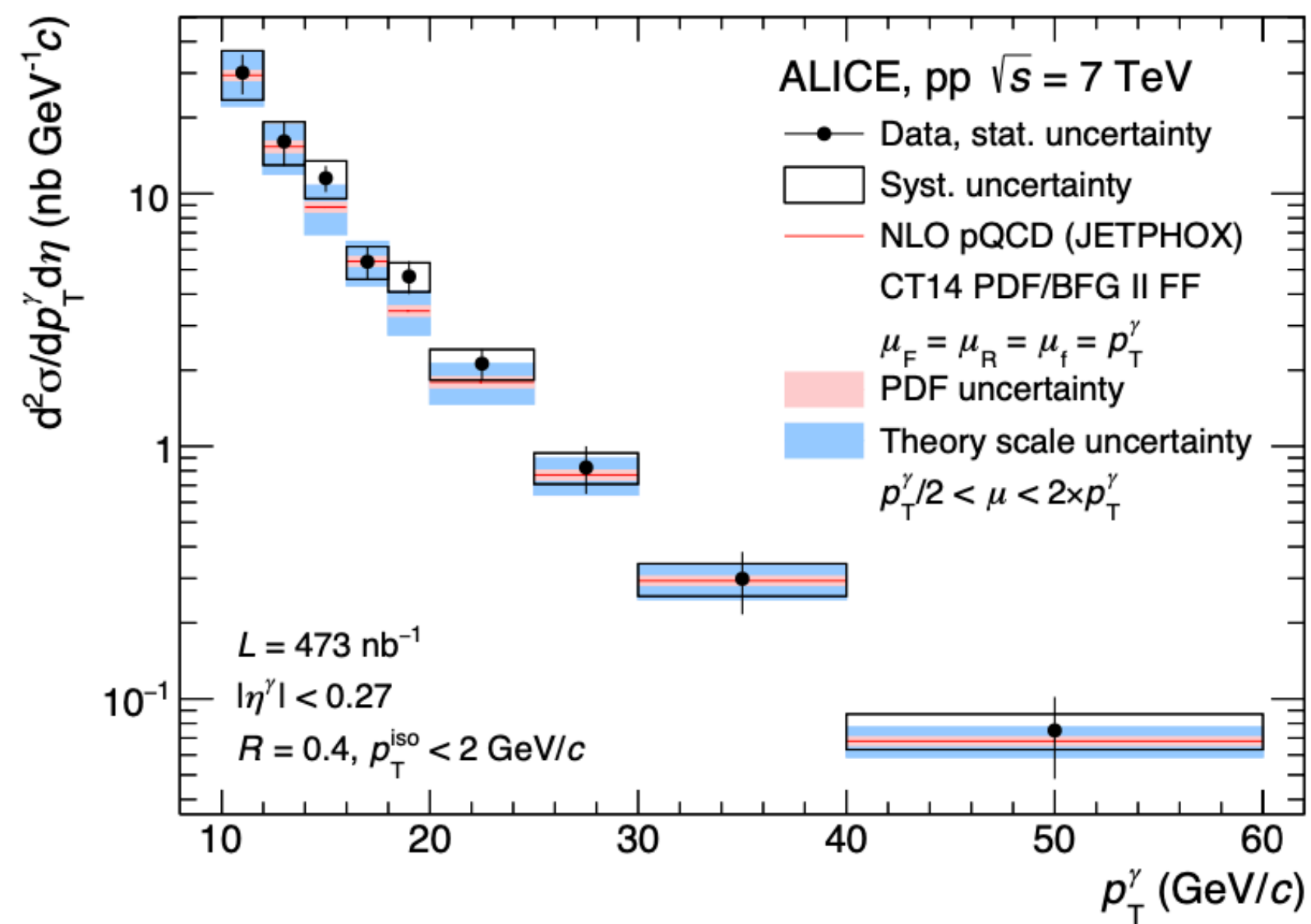
Z^0 CMS

Phys. Rev. Lett. 127(2021)102002

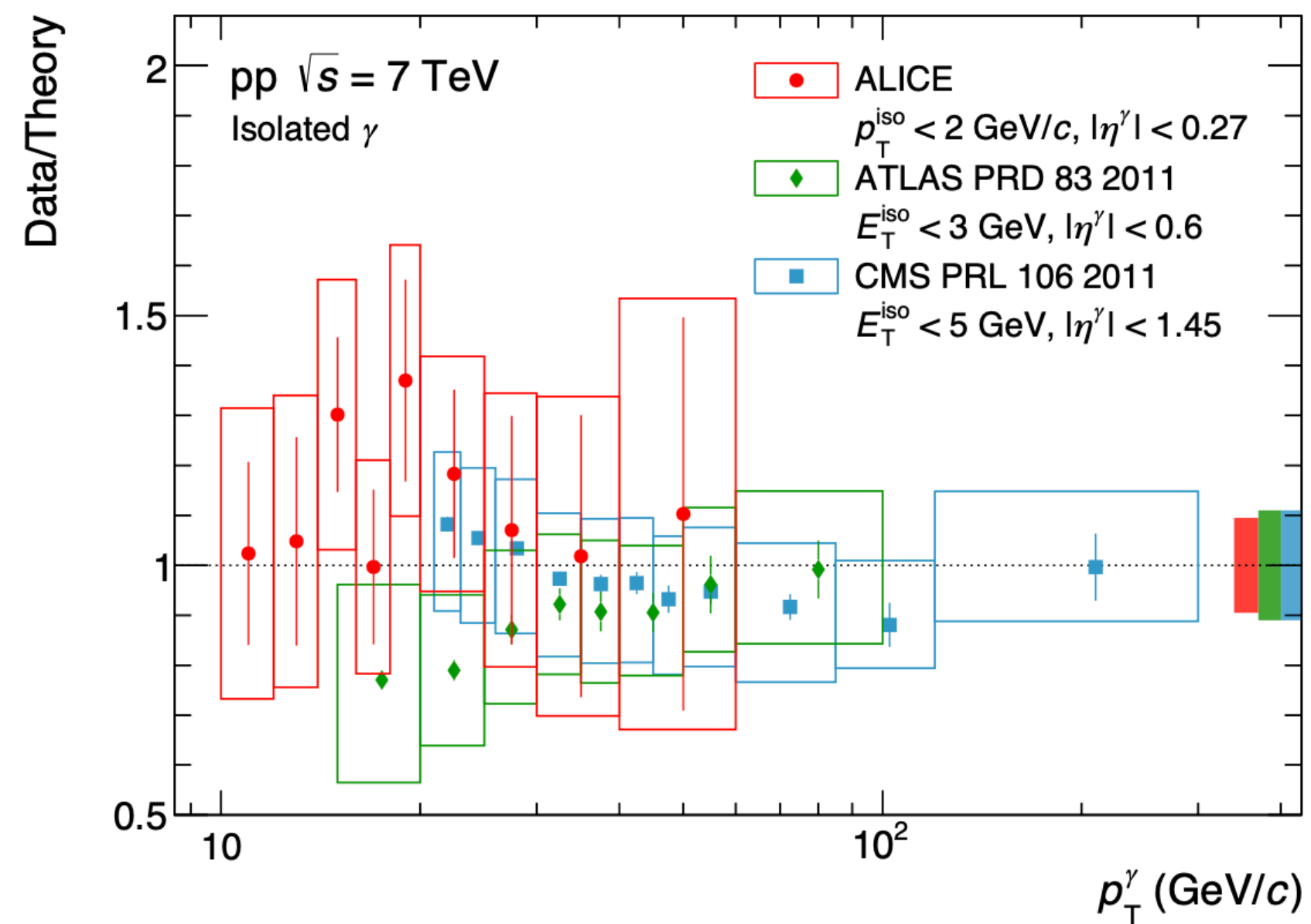
$60 < m_{||} < 120$ GeV/c², $|\eta^{Z^0}| < 2.1$

■ Statistical unc.
 ■ Systematic unc.

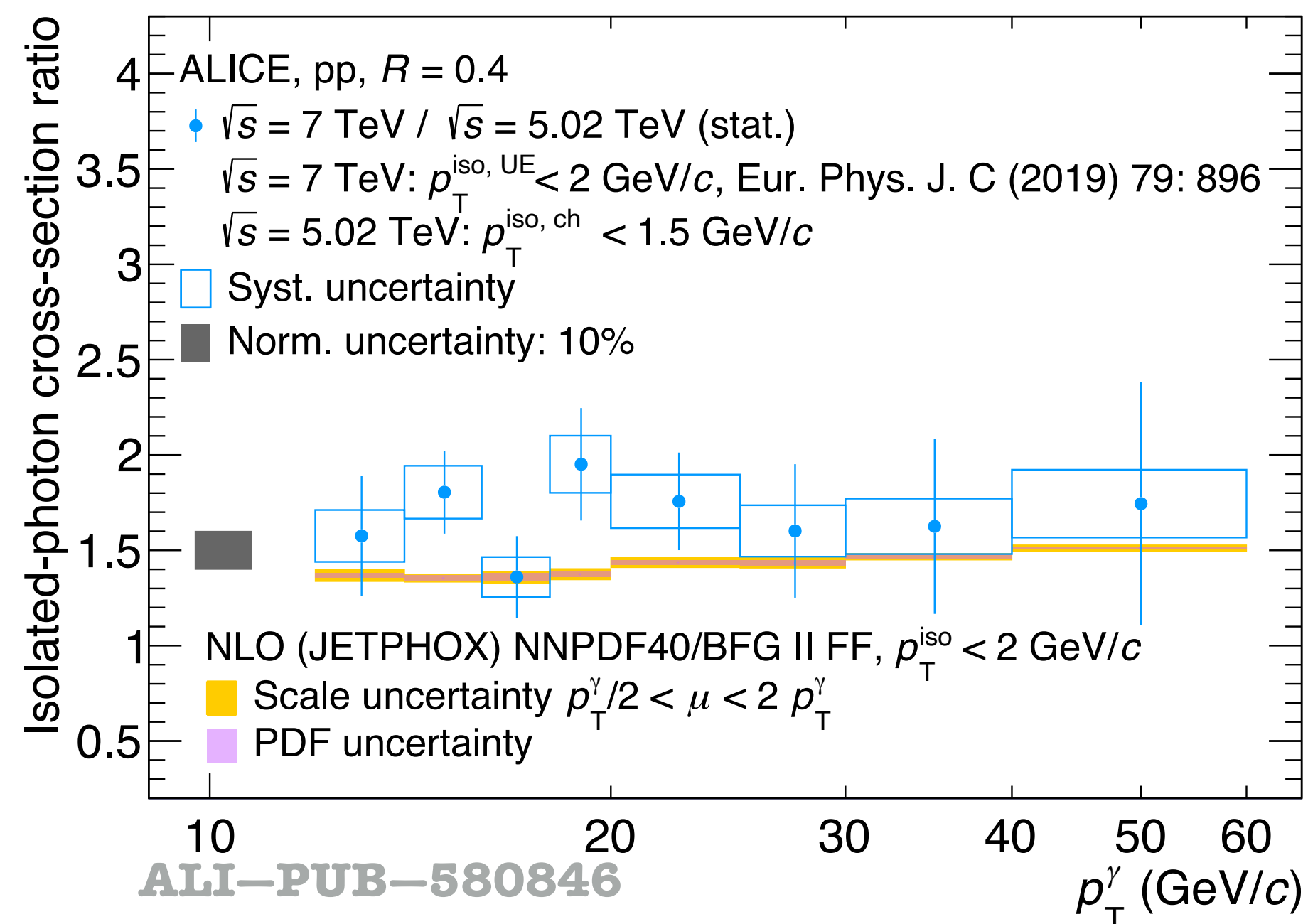
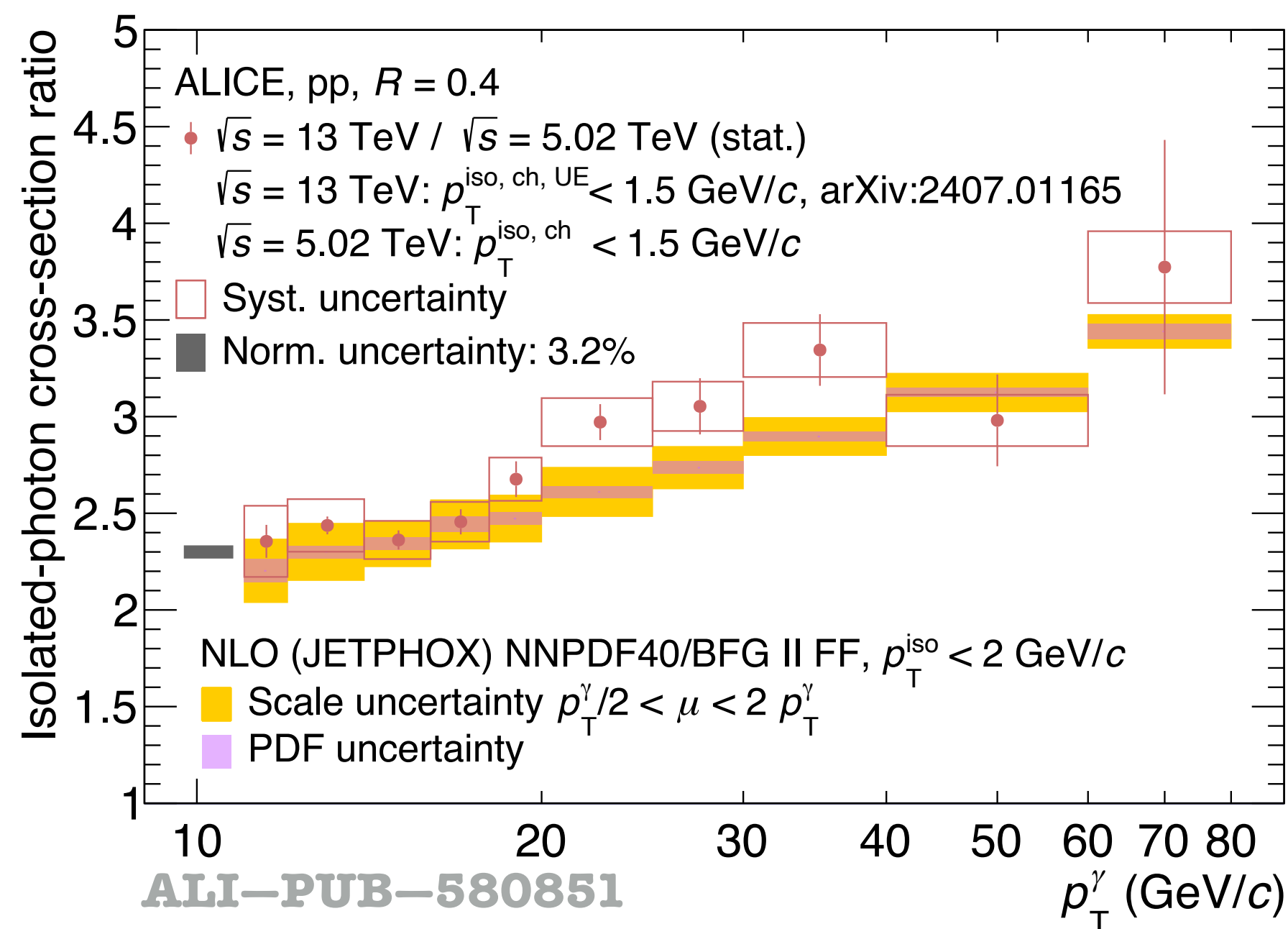
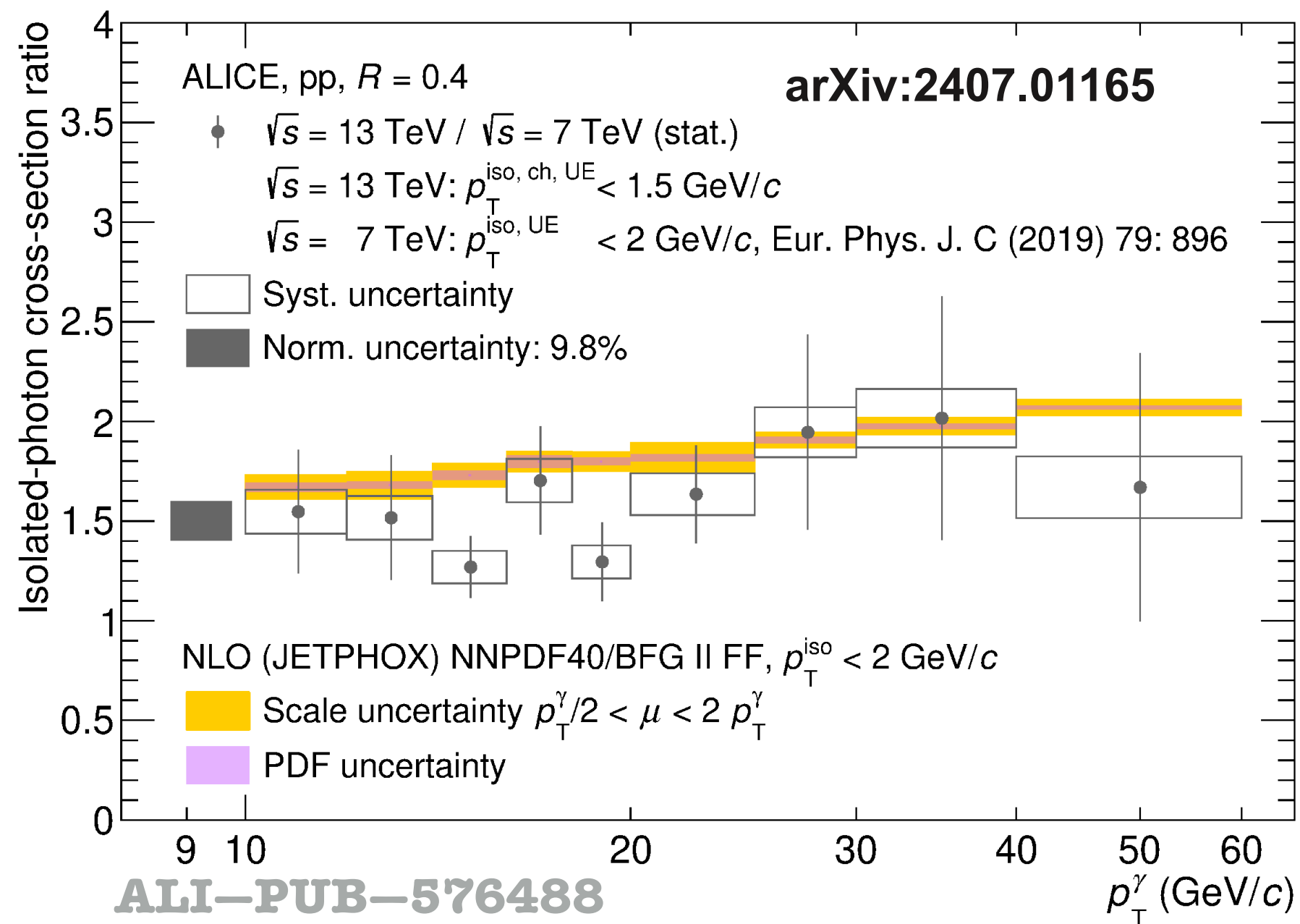
Cross section, pp $\sqrt{s} = 7$ TeV



- ➔ arXiv:1906.01371
- ➔ Eur. Phys. J. C 79, 896 (2019)



Cross section ratios in pp collisions



- γ measurement

- ➔ Calorimeters

- EMCal: Pb/scintillator towers (6×6 cm)
 - 4.4 m from interaction point (IP)
 - $|\eta| < 0.67$ for $\Delta\varphi = 107^\circ$, $0.22 < |\eta| < 0.67$ for $\Delta\varphi = 60^\circ$ (DCal);
 - Identification via EM shower dispersion selection
 - $E_\gamma > 700$ MeV

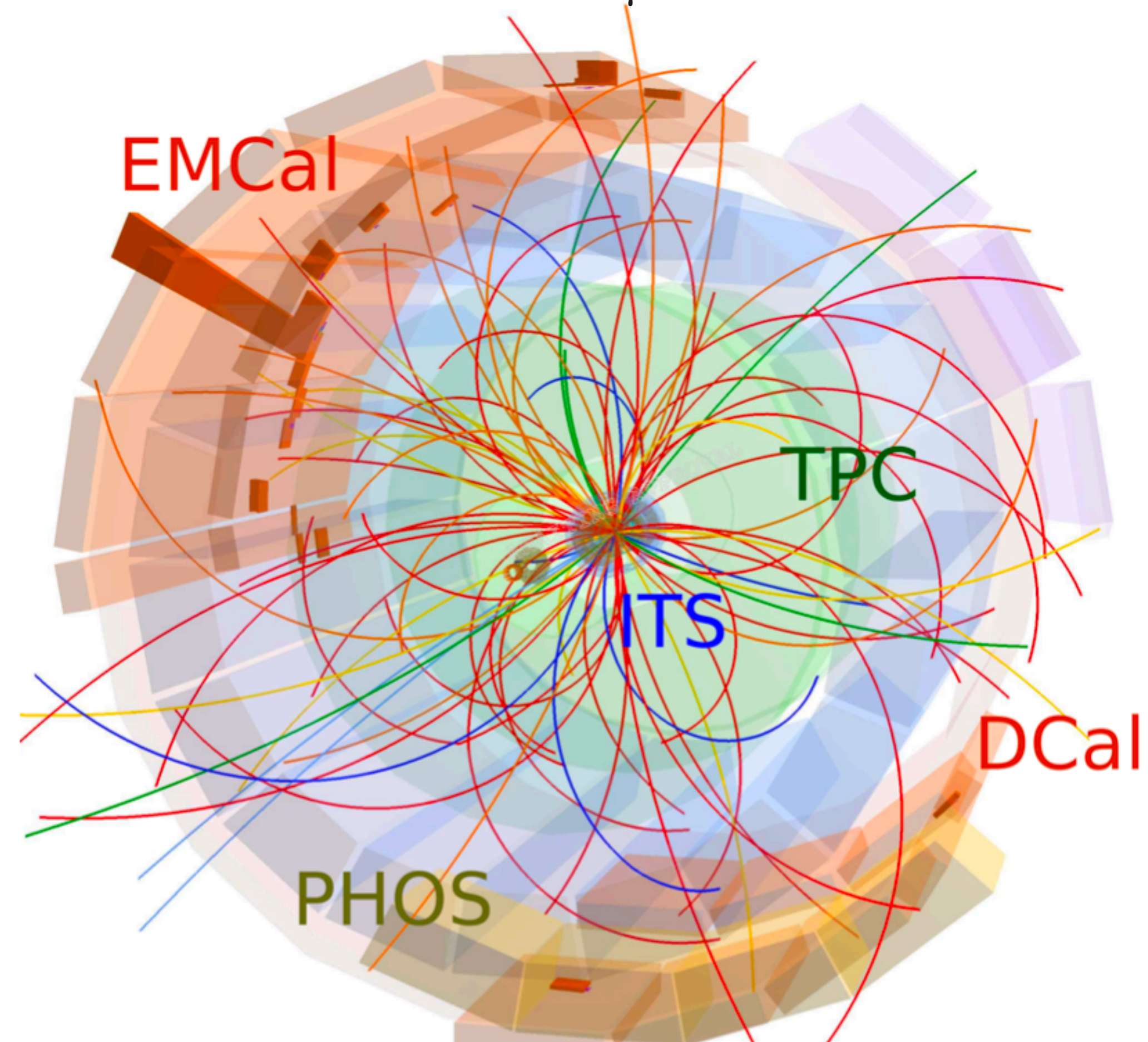
- ➔ Tracking, TPC & ITS

- γ conversion method (PCM)
 - $R < 180$ cm
 - 8% conversion probability
 - $|\eta| < 0.9$ for $\Delta\varphi = 360^\circ$
 - $E_\gamma > 100$ MeV

- γ identification combining tracking+calorimeter

- ➔ Inclusive γ : Charged particle veto
- ➔ Prompt γ : Isolation (next slides)

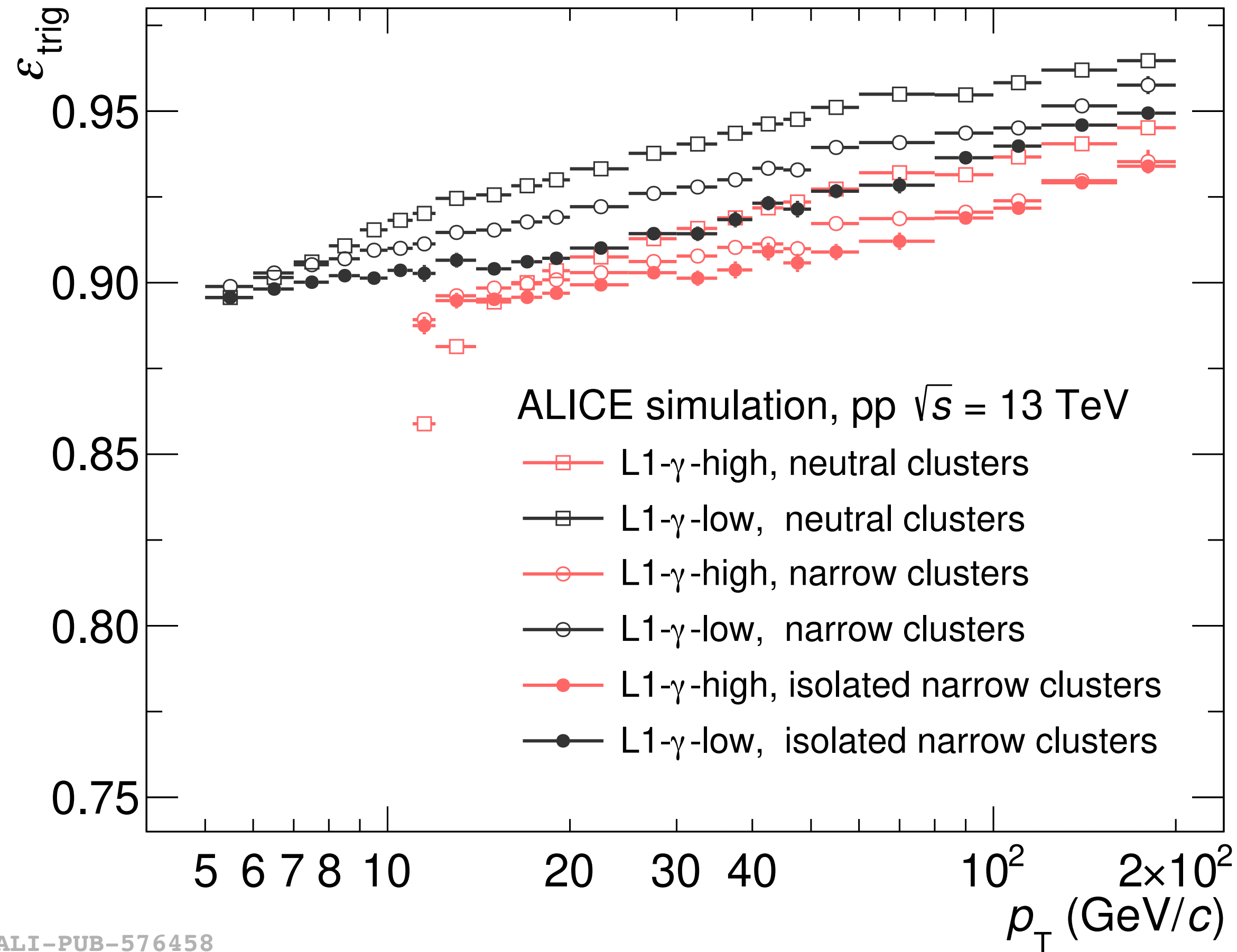
- PHOS: PWO_4 crystals (2.2×2.2 cm)
 - 4.6 m from IP
 - $|\eta| < 0.13$ for $\Delta\varphi = 70^\circ$
 - Identification via EM shower dispersion selection
 - $E_\gamma > 200$ MeV



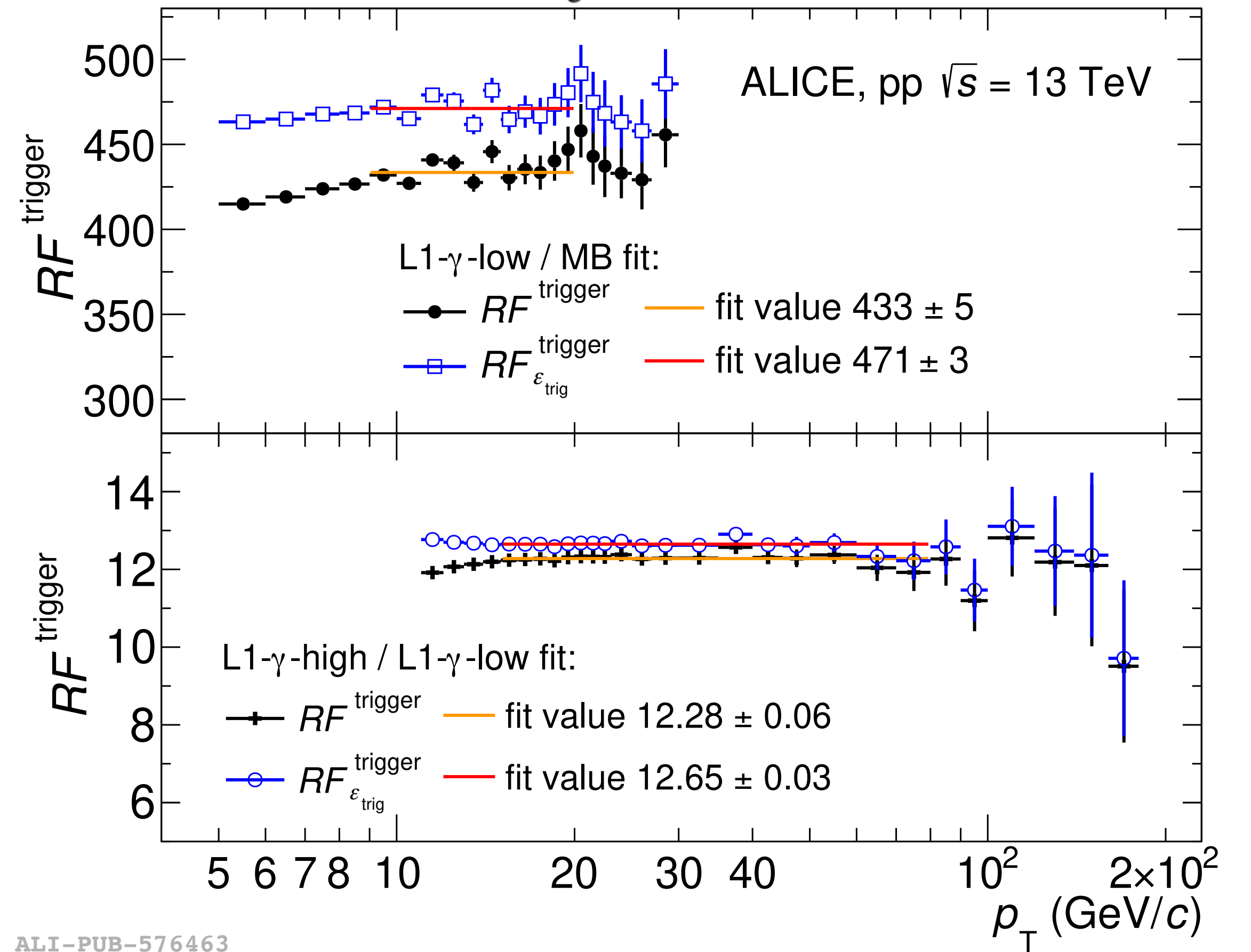
EMCal trigger performance, pp $\sqrt{s} = 13$ TeV



$$RF_{\epsilon_{\text{trig}}^{\text{trig}}} = \frac{1}{\epsilon_{\text{trig}}^{\text{clus}}} \frac{1/N_{\text{evt}}^{\text{L1-}\gamma} \times dN^{\text{L1-}\gamma}/dp_T}{1/N_{\text{evt}}^{\text{MB}} \times dN^{\text{MB}}/dp_T}$$



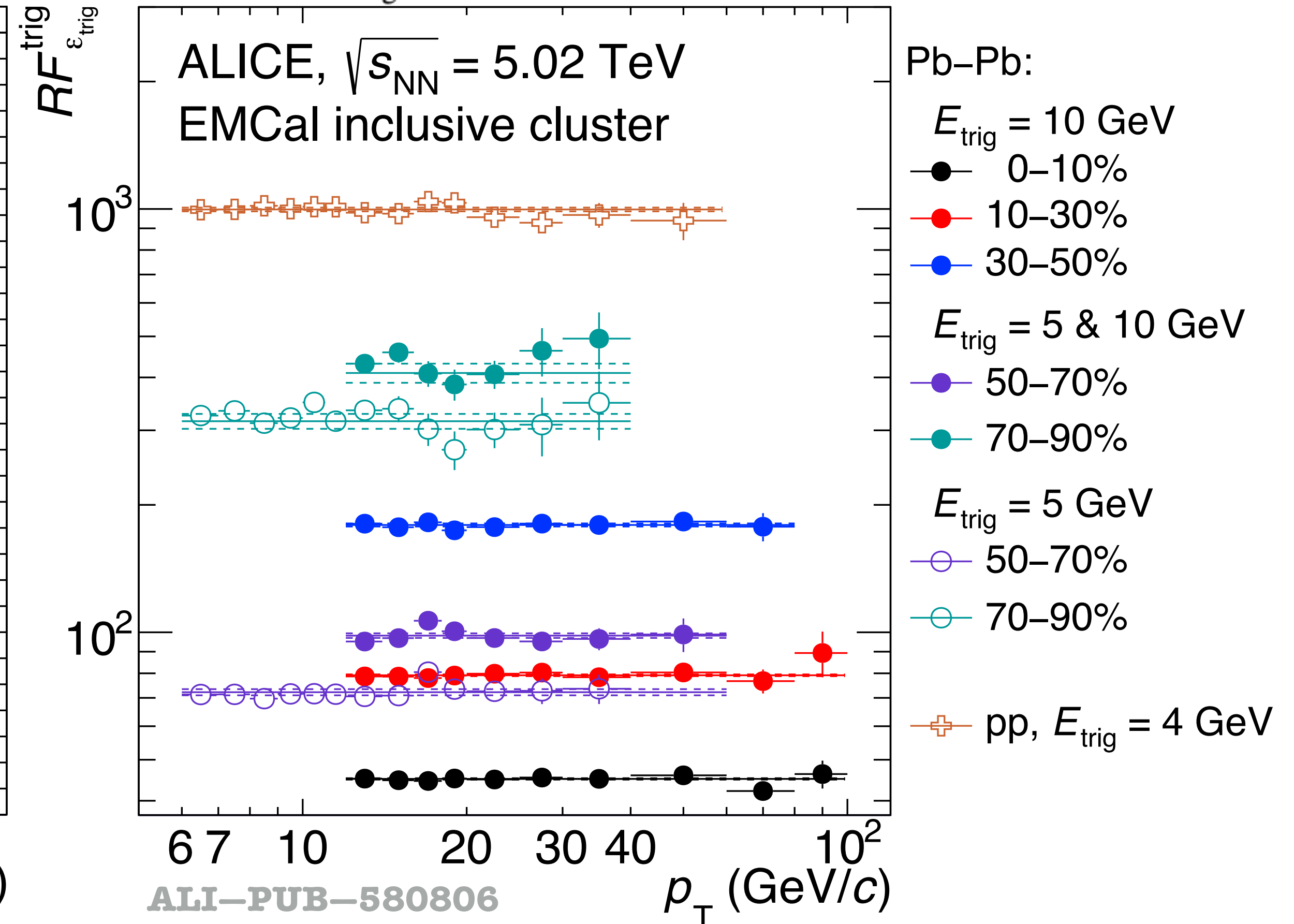
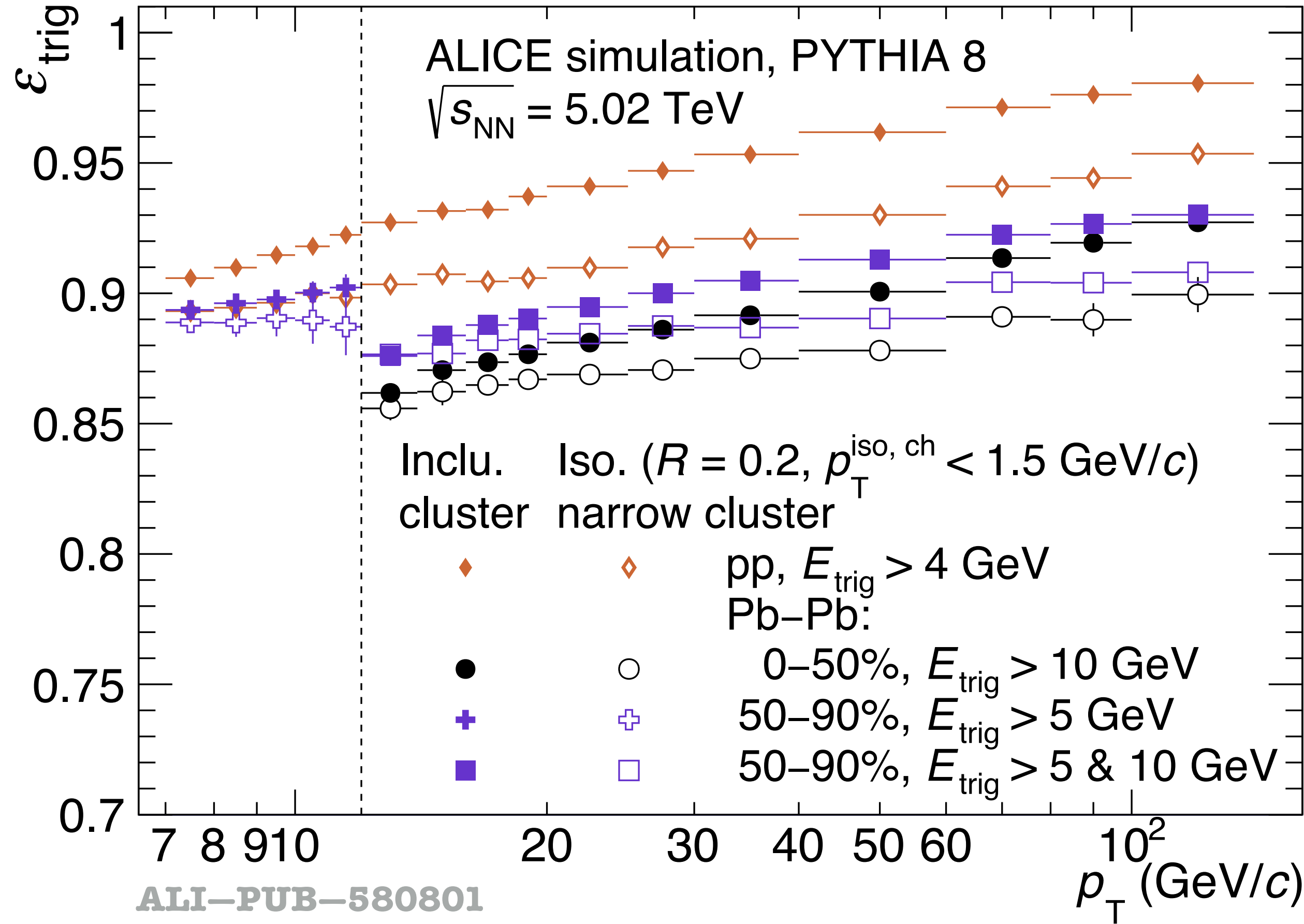
ALI-PUB-576463



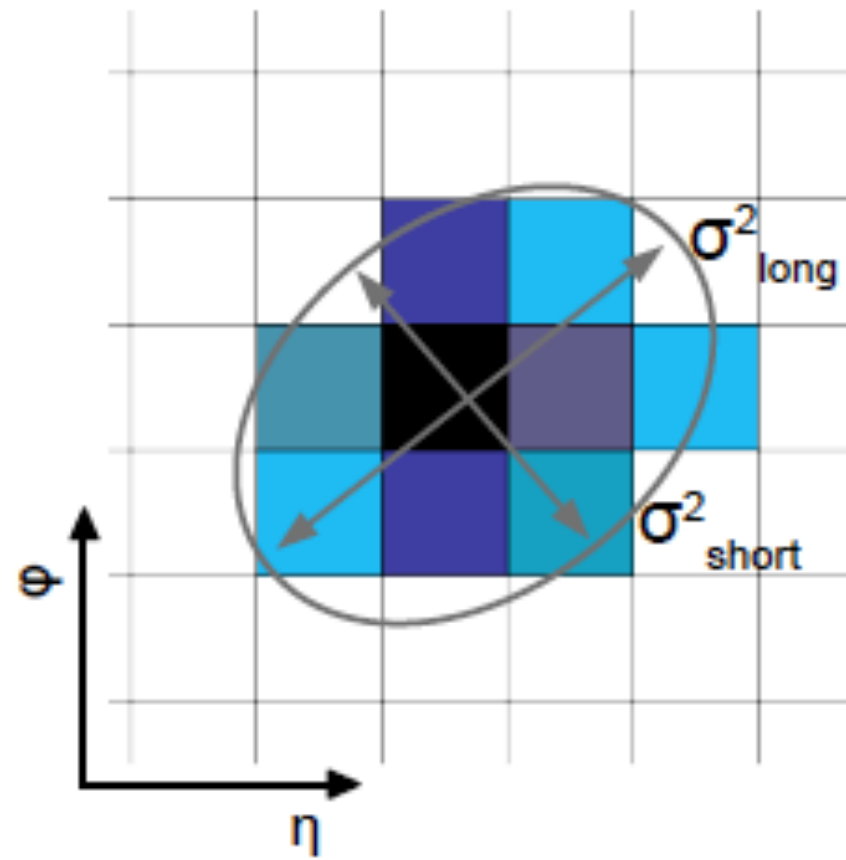
EMCal trigger performance, pp & Pb-Pb $\sqrt{s_{NN}} = 5.02$ TeV



$$RF_{\epsilon_{\text{trig}}}^{\text{trig}} = \frac{1}{\epsilon_{\text{trig}}^{\text{clus}}} \frac{1/N_{\text{evt}}^{\text{L1-}\gamma} \times dN^{\text{L1-}\gamma}/dp_T}{1/N_{\text{evt}}^{\text{MB}} \times dN^{\text{MB}}/dp_T}$$



EMCal cluster shower lateral dispersion parameter



- Shower shape parameter σ^2_{long} is related to the longer axis of the cluster ellipse
- Parameter depends on cluster cells location and its energy

$$w_i = \text{Maximum}(0, w_0 + \ln(E_{\text{cell}, i}/E))$$

$$\sigma_{\alpha\beta}^2 = \sum_i \frac{w_i \alpha_i \beta_i}{w_{\text{tot}}} - \sum_i \frac{w_i \alpha_i}{w_{\text{tot}}} \sum_i \frac{w_i \beta_i}{w_{\text{tot}}}$$

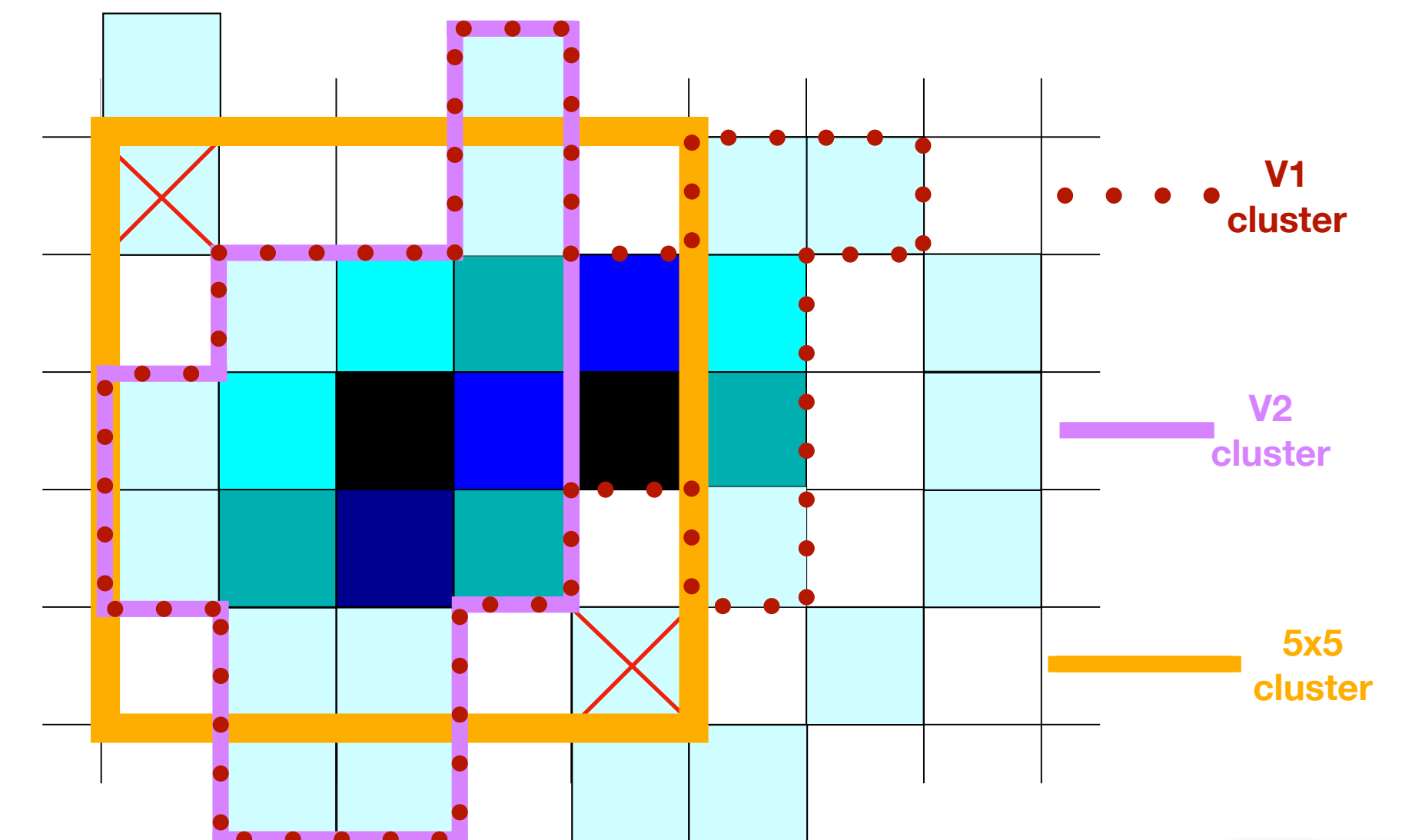
$$w_{\text{tot}} = \sum_i w_i,$$

$$\sigma_{\text{long}}^2 = 0.5(\sigma_{\phi\phi}^2 + \sigma_{\eta\eta}^2) + \sqrt{0.25(\sigma_{\phi\phi}^2 - \sigma_{\eta\eta}^2)^2 + \sigma_{\eta\phi}^2},$$

$$\sigma_{\text{short}}^2 = 0.5(\sigma_{\phi\phi}^2 + \sigma_{\eta\eta}^2) - \sqrt{0.25(\sigma_{\phi\phi}^2 - \sigma_{\eta\eta}^2)^2 + \sigma_{\eta\phi}^2},$$

- V2 clusters: Used in pp & Pb-Pb at $\sqrt{s_{\text{NN}}} = 5.02$ TeV to get E and position
 - ▶ In other pp and p-Pb measurements V1 clusters are used
- For the σ^2_{long} calculation: consider the neighbour cells around the highest energy cell in a 5x5 fixed window
 - ▶ Increase meson decay merging but limiting UE merging

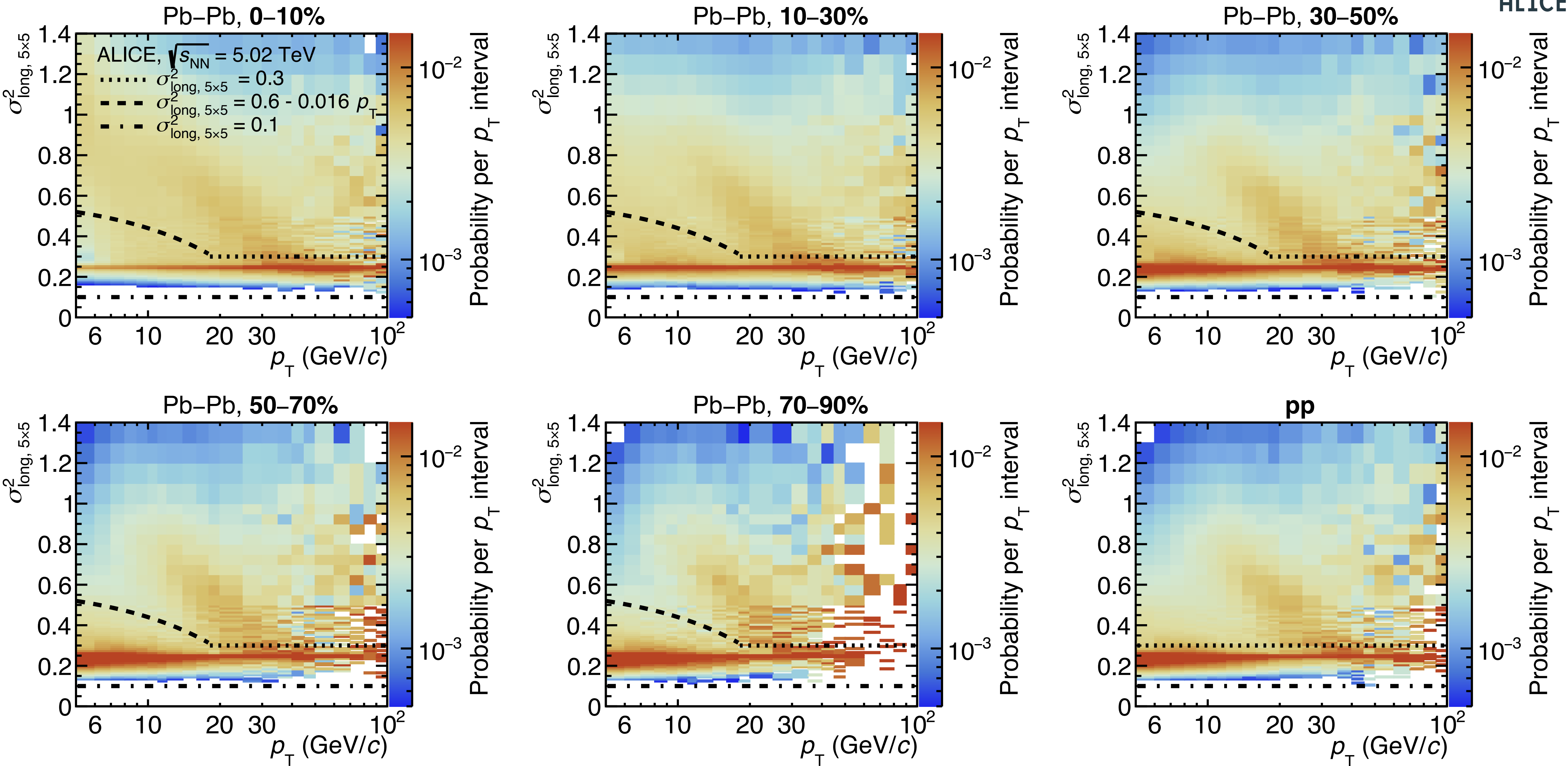
ALICE-PUBLIC-2024-003



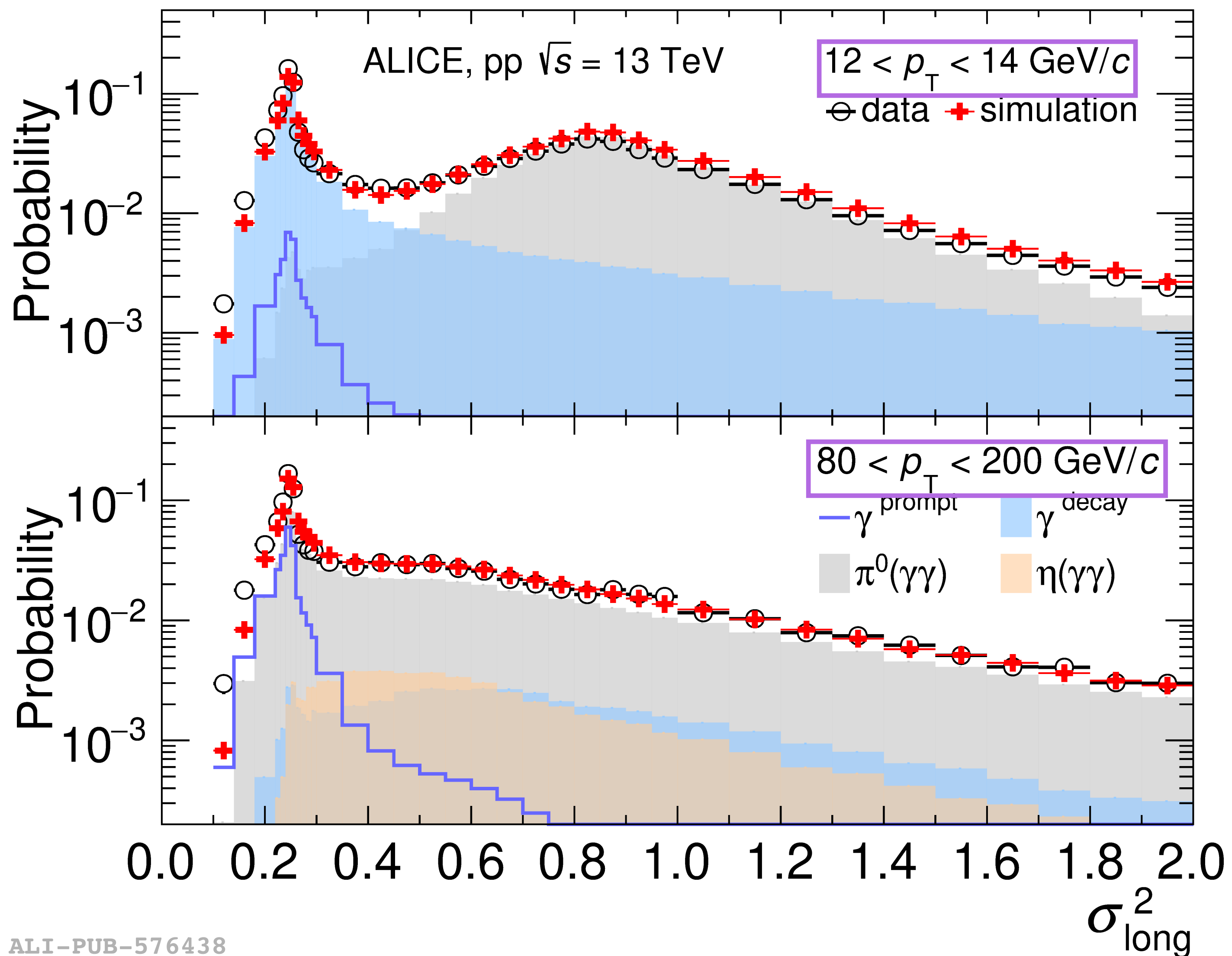
EMCal cluster shower shape, pp & Pb-Pb $\sqrt{s_{NN}} = 5.02$ TeV



ALICE

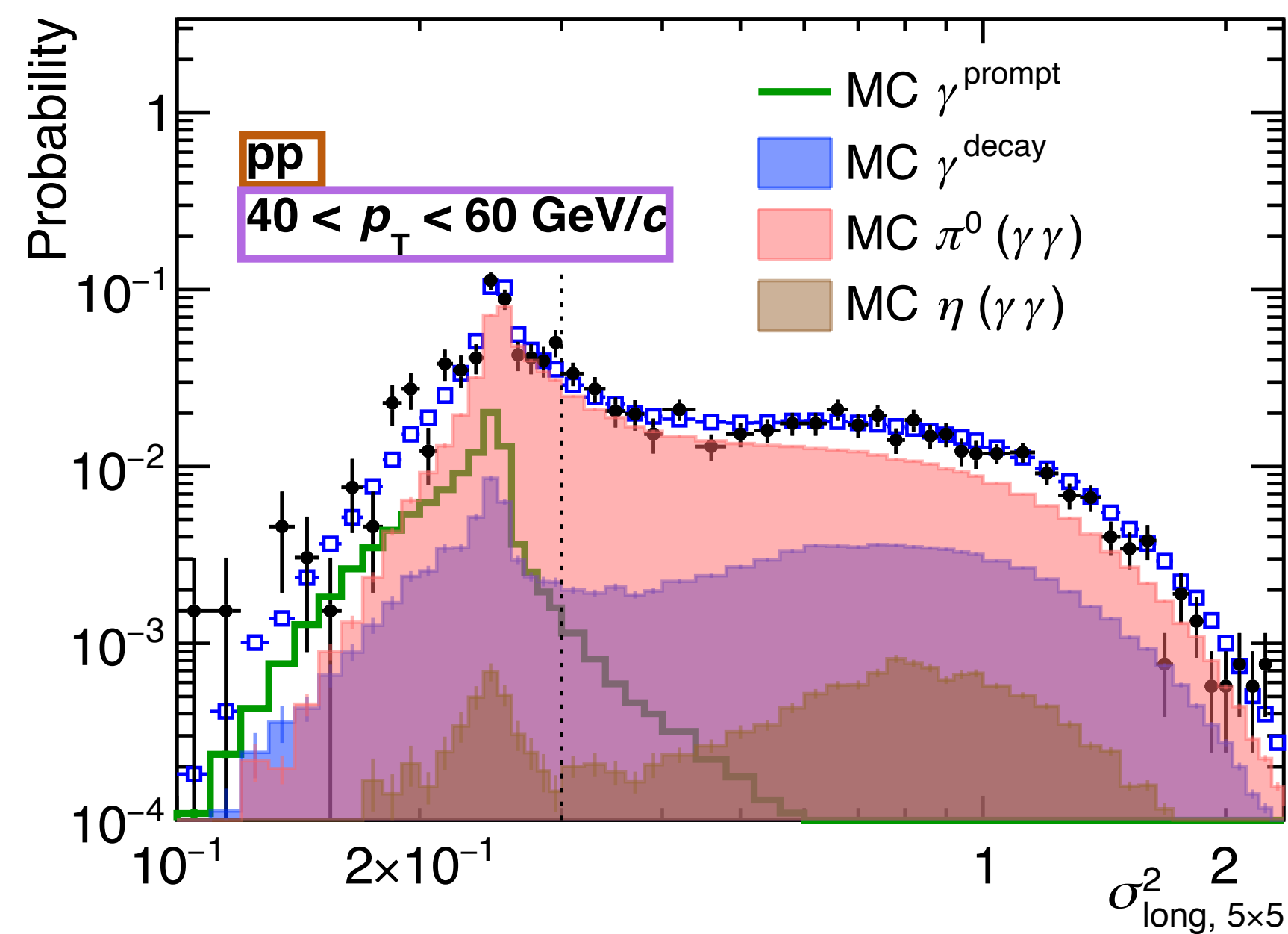
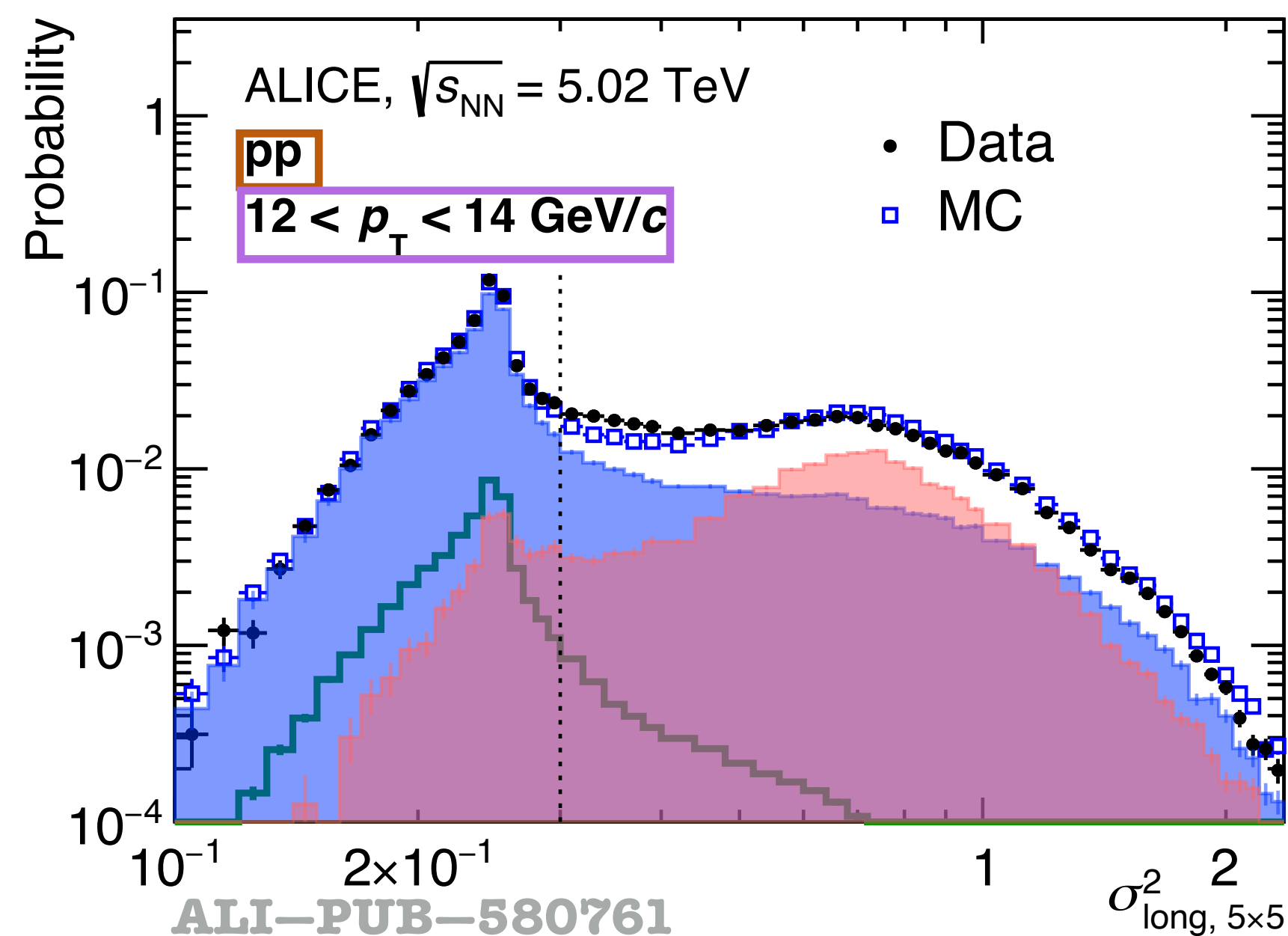
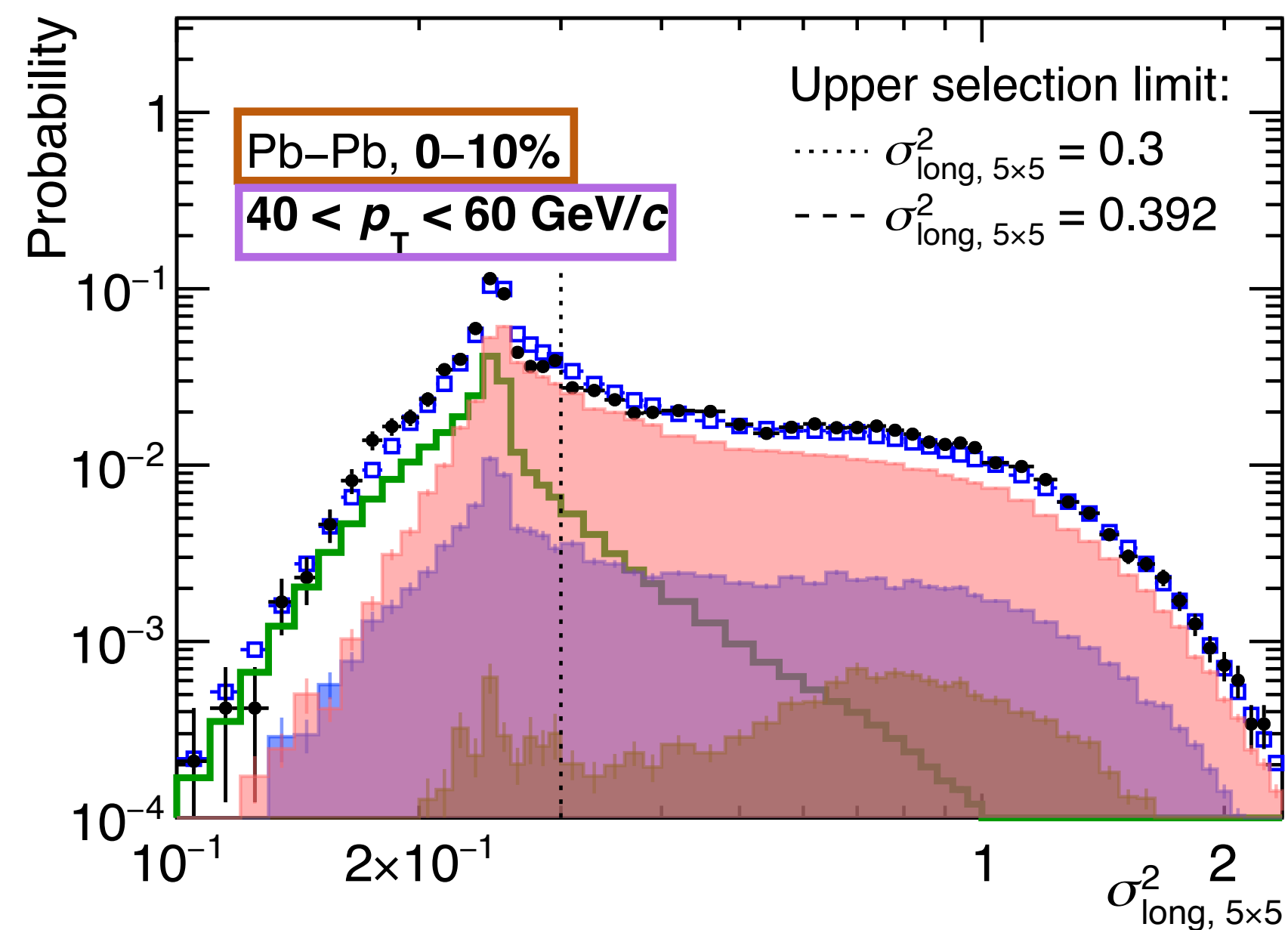
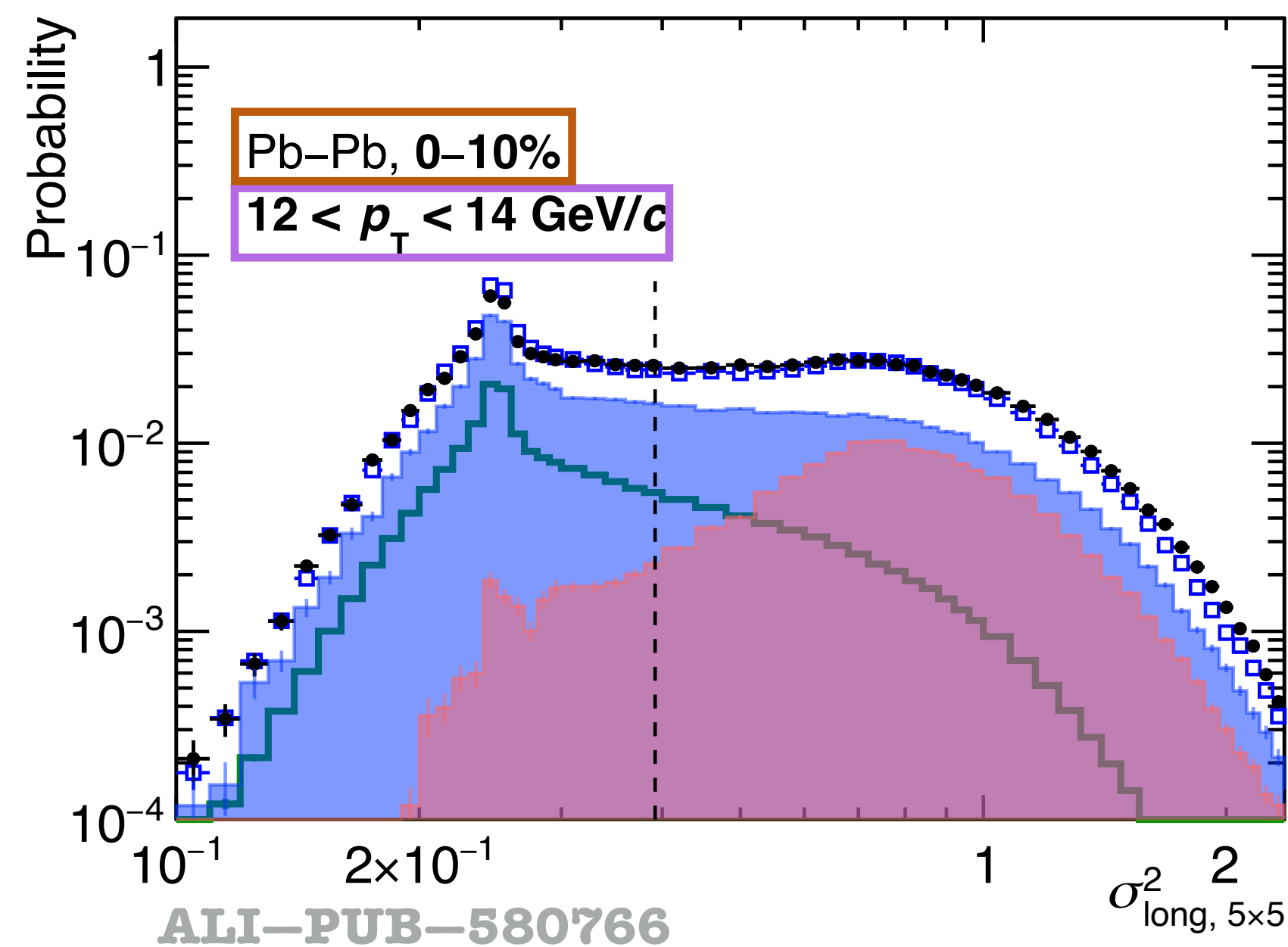


EMCal cluster shower shape, pp $\sqrt{s} = 13$ TeV

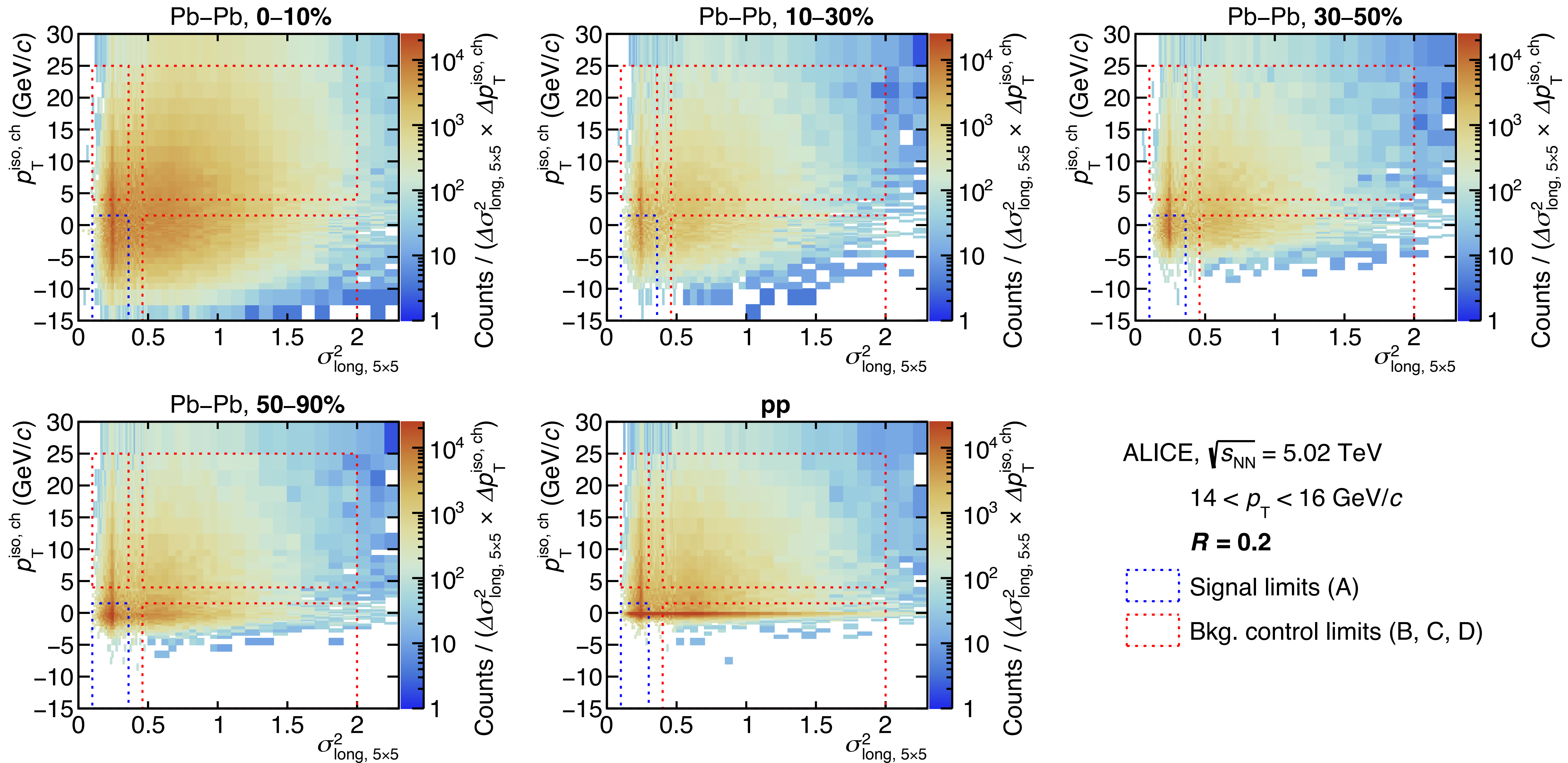


ALI-PUB-576438

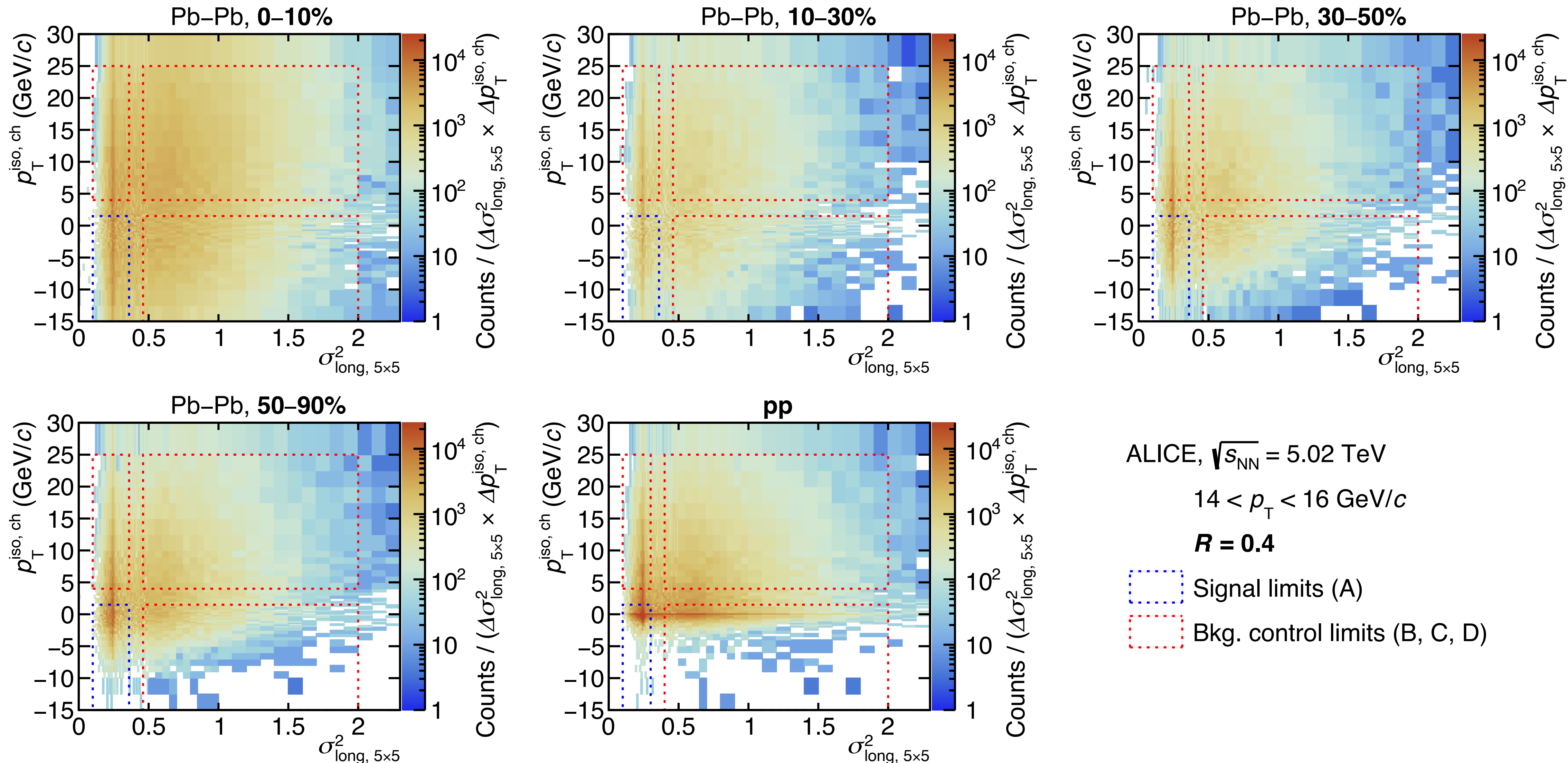
EMCal cluster shower shape, pp & Pb-Pb $\sqrt{s_{NN}} = 5.02$ TeV



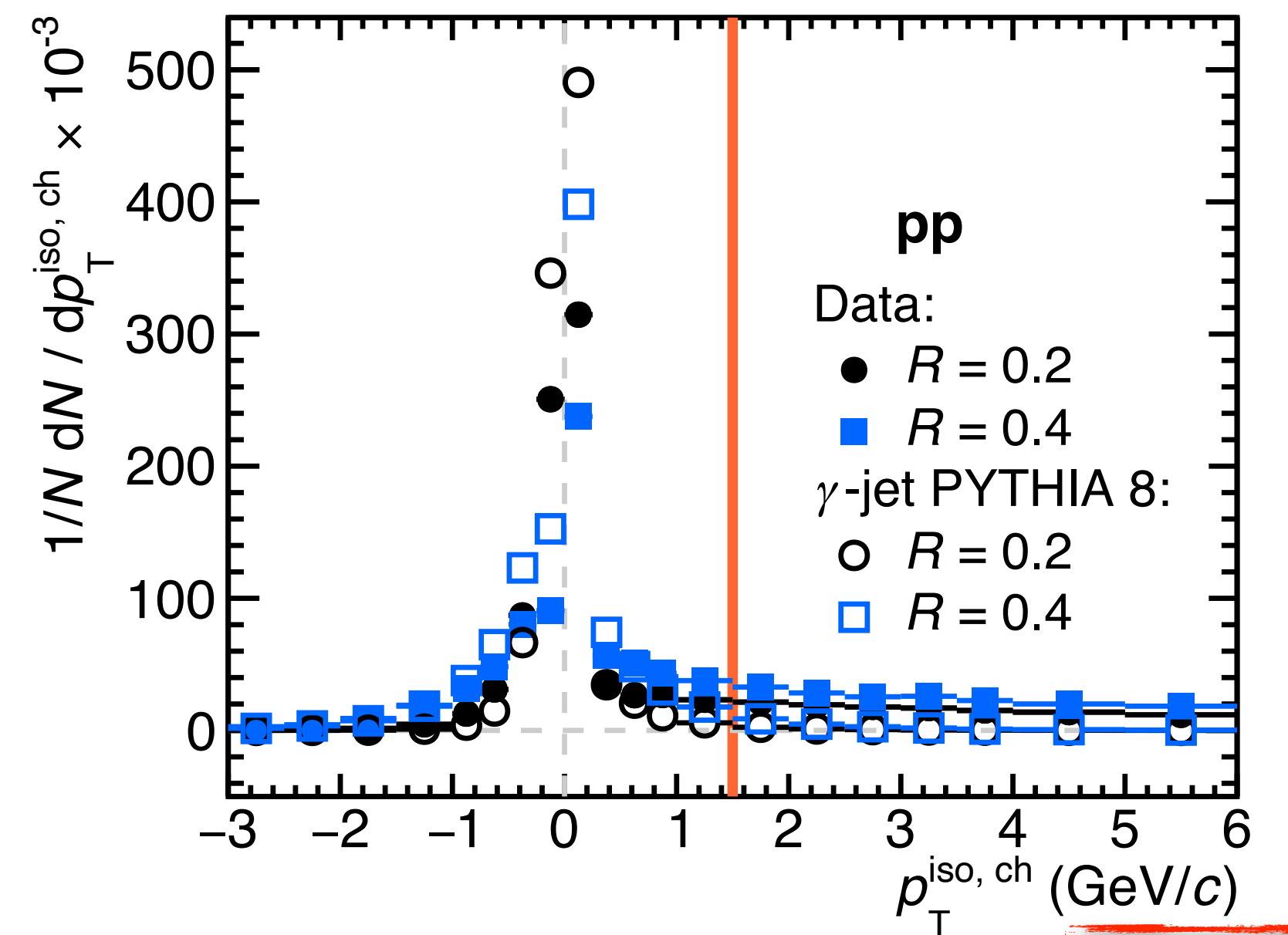
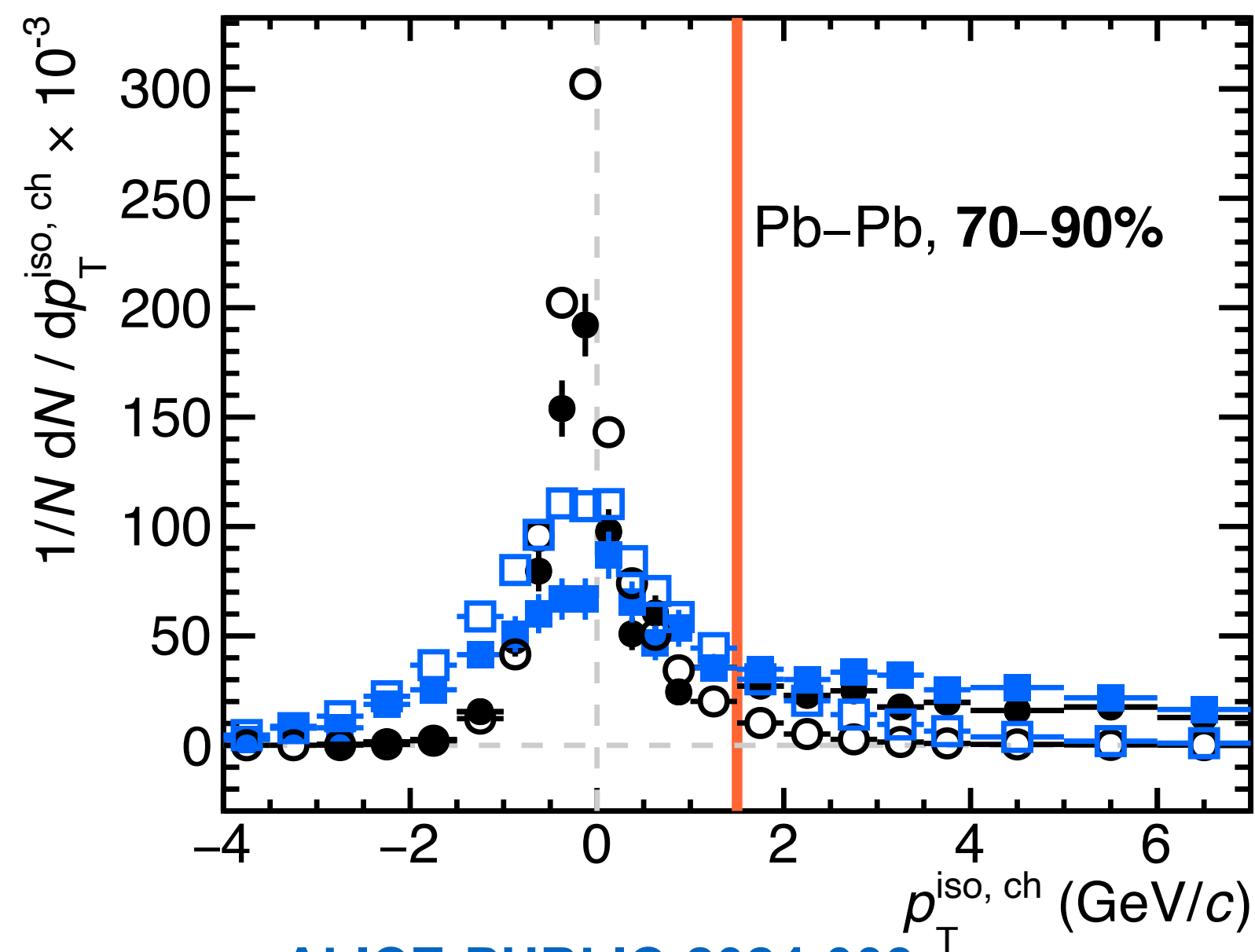
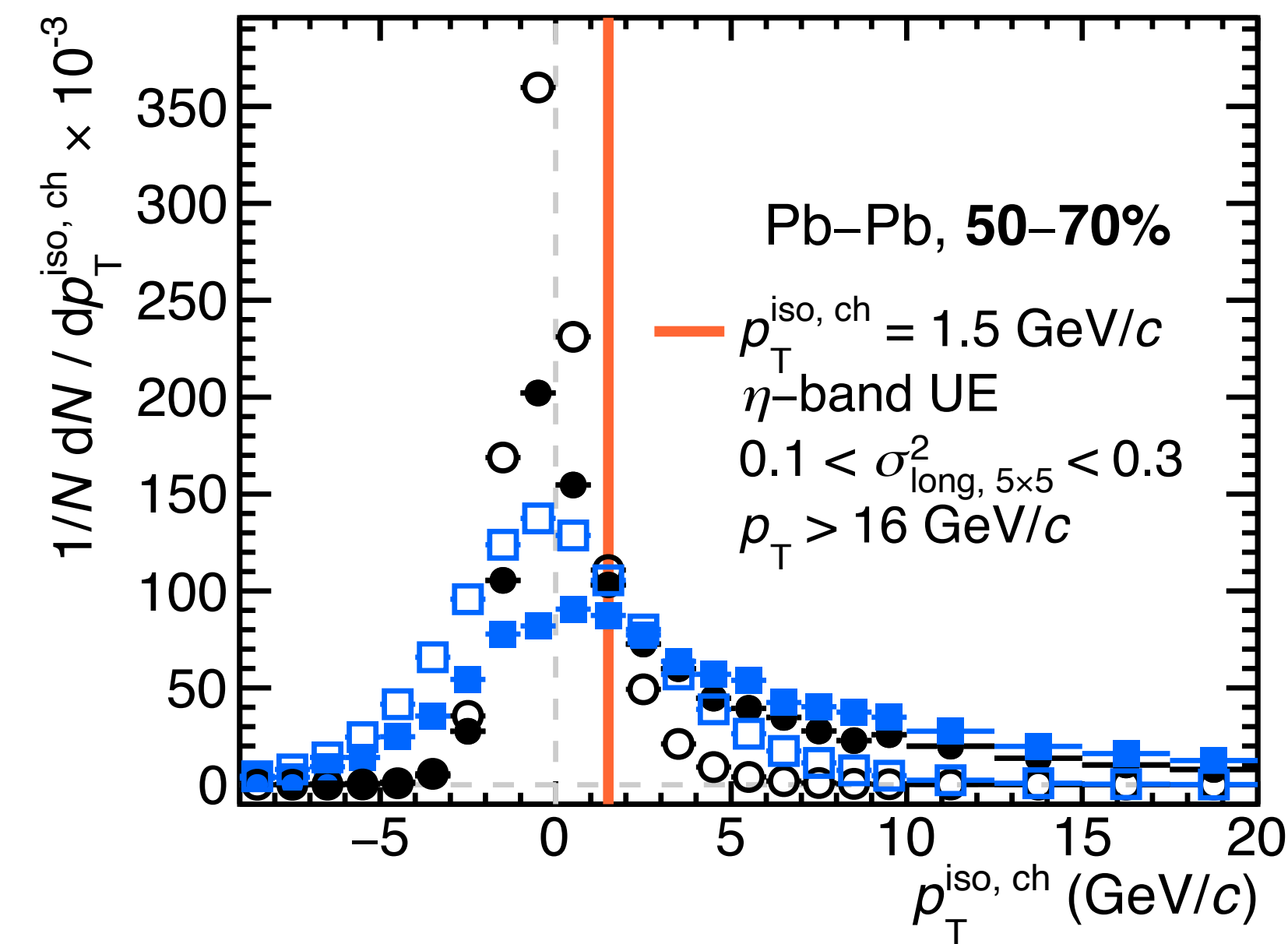
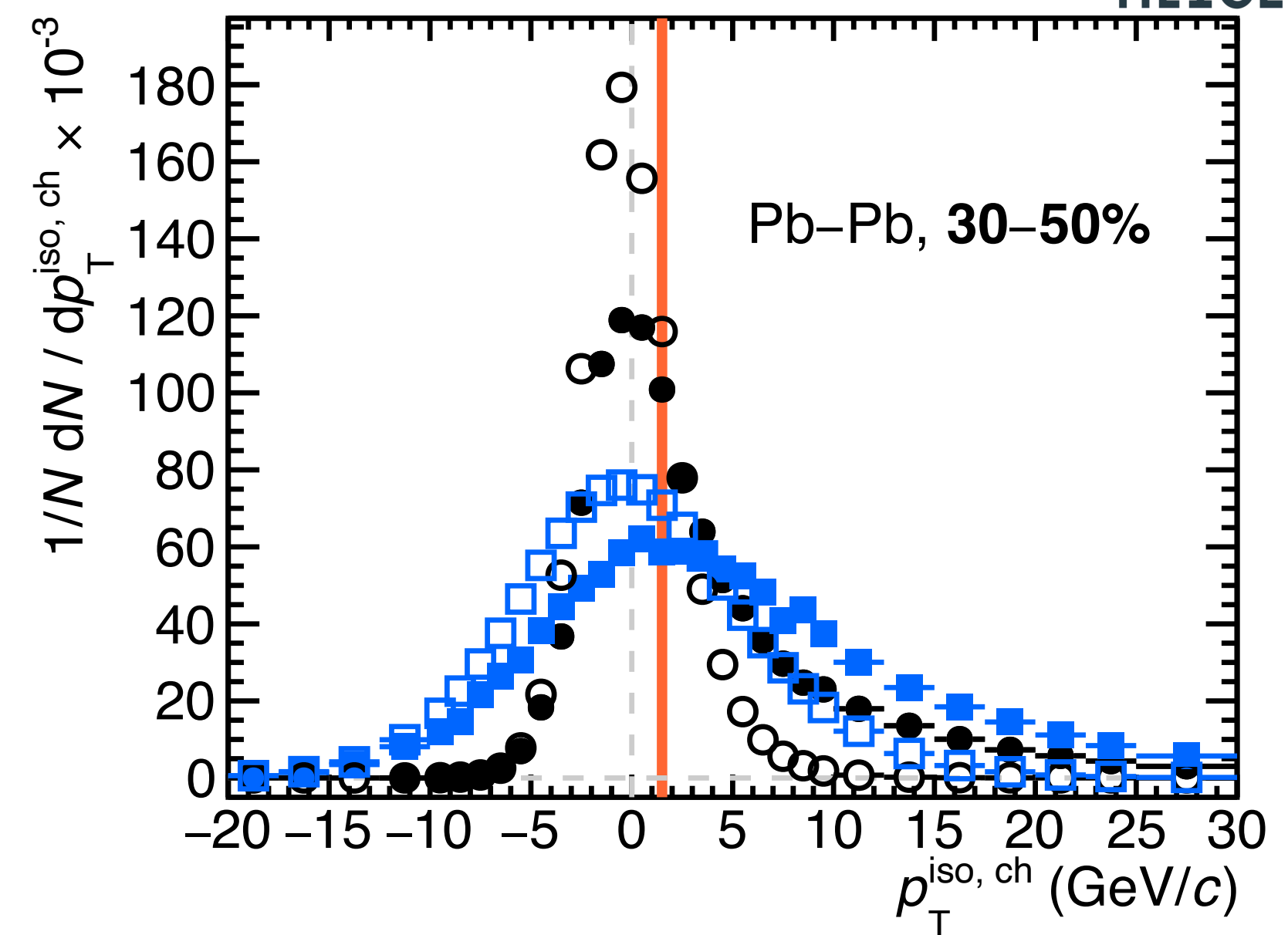
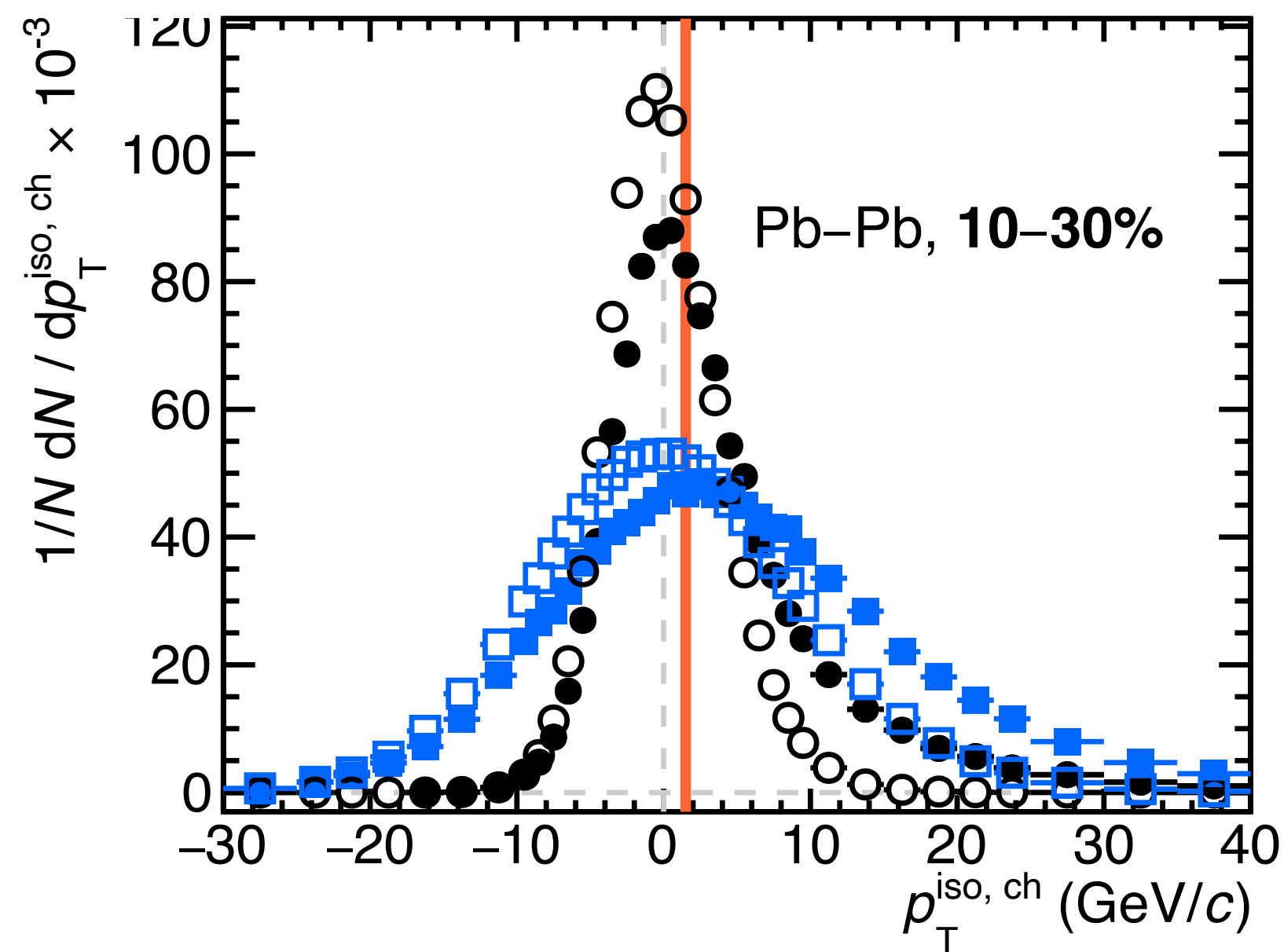
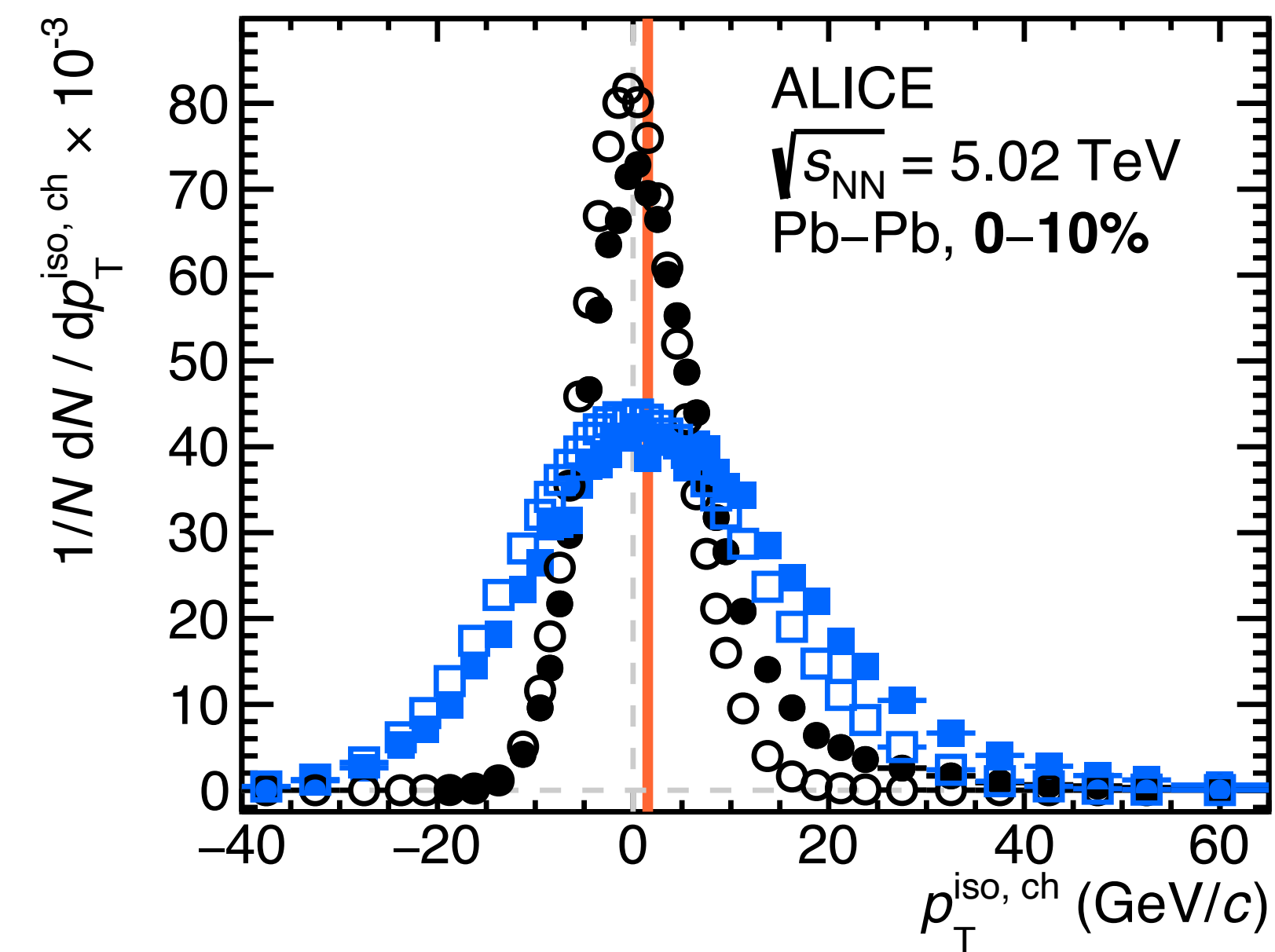
ABCD regions, $R = 0.2$, pp & Pb-Pb $\sqrt{s_{NN}} = 5.02$ TeV



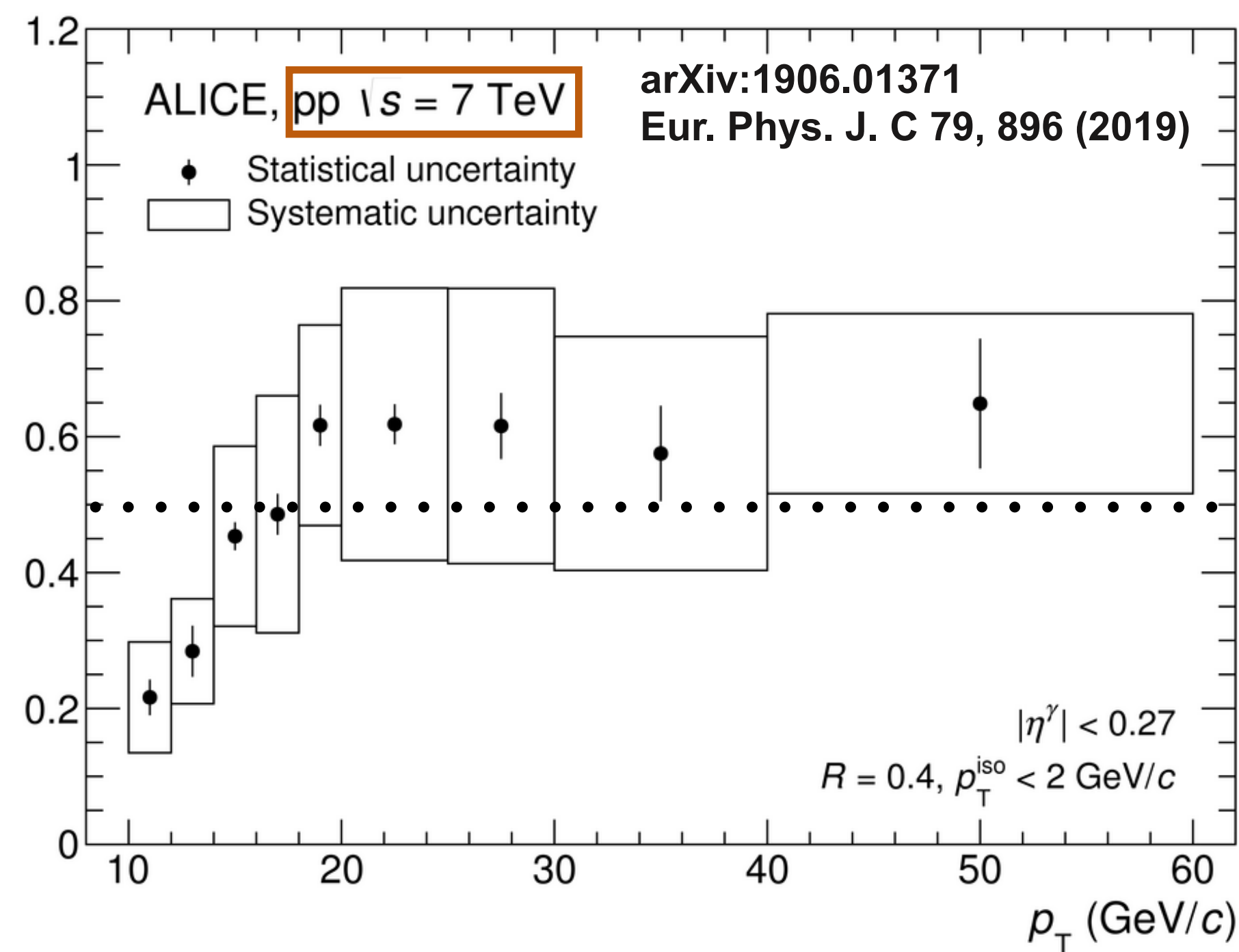
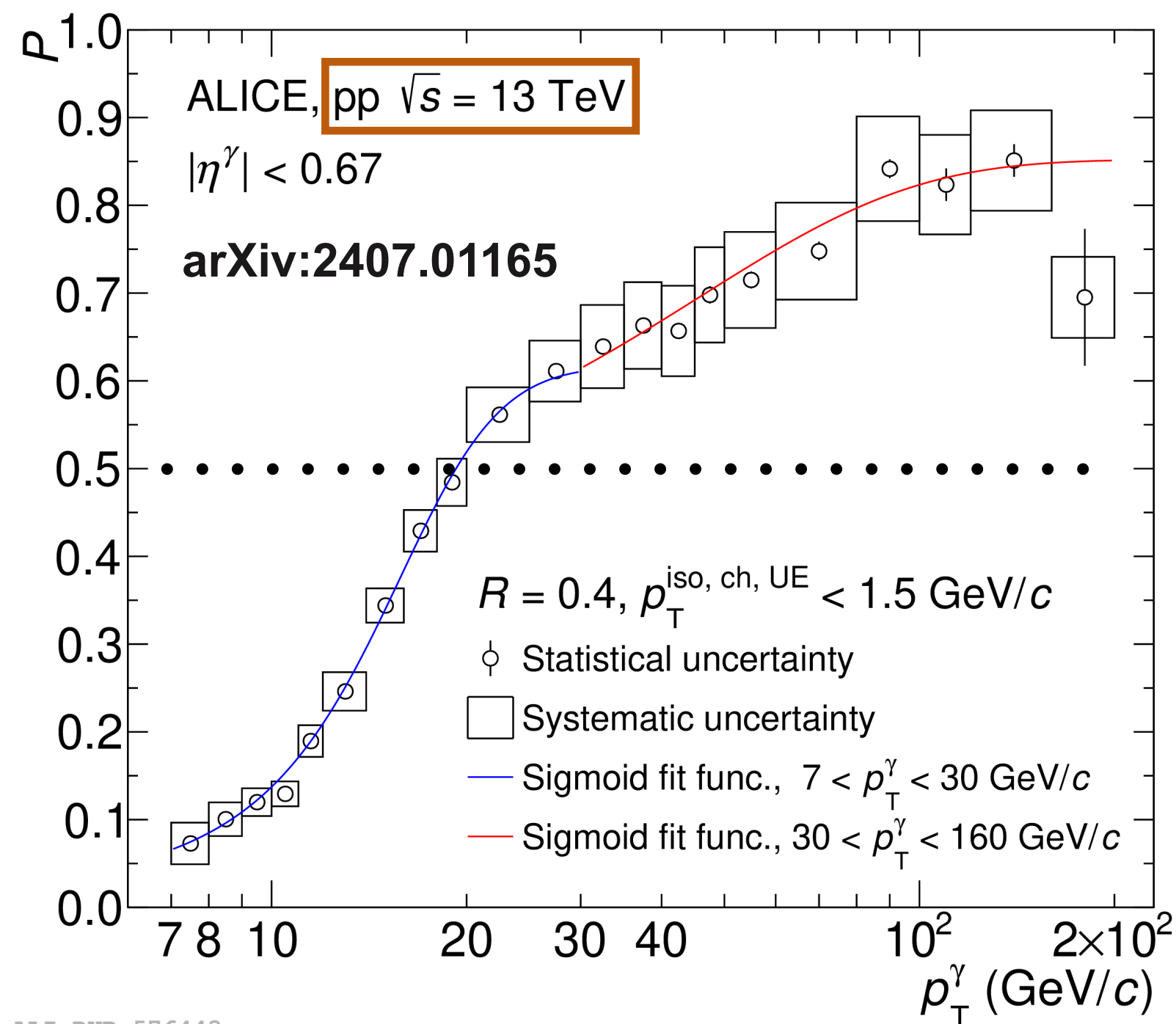
ABCD regions, $R = 0.4$, pp & Pb-Pb $\sqrt{s_{NN}} = 5.02$ TeV



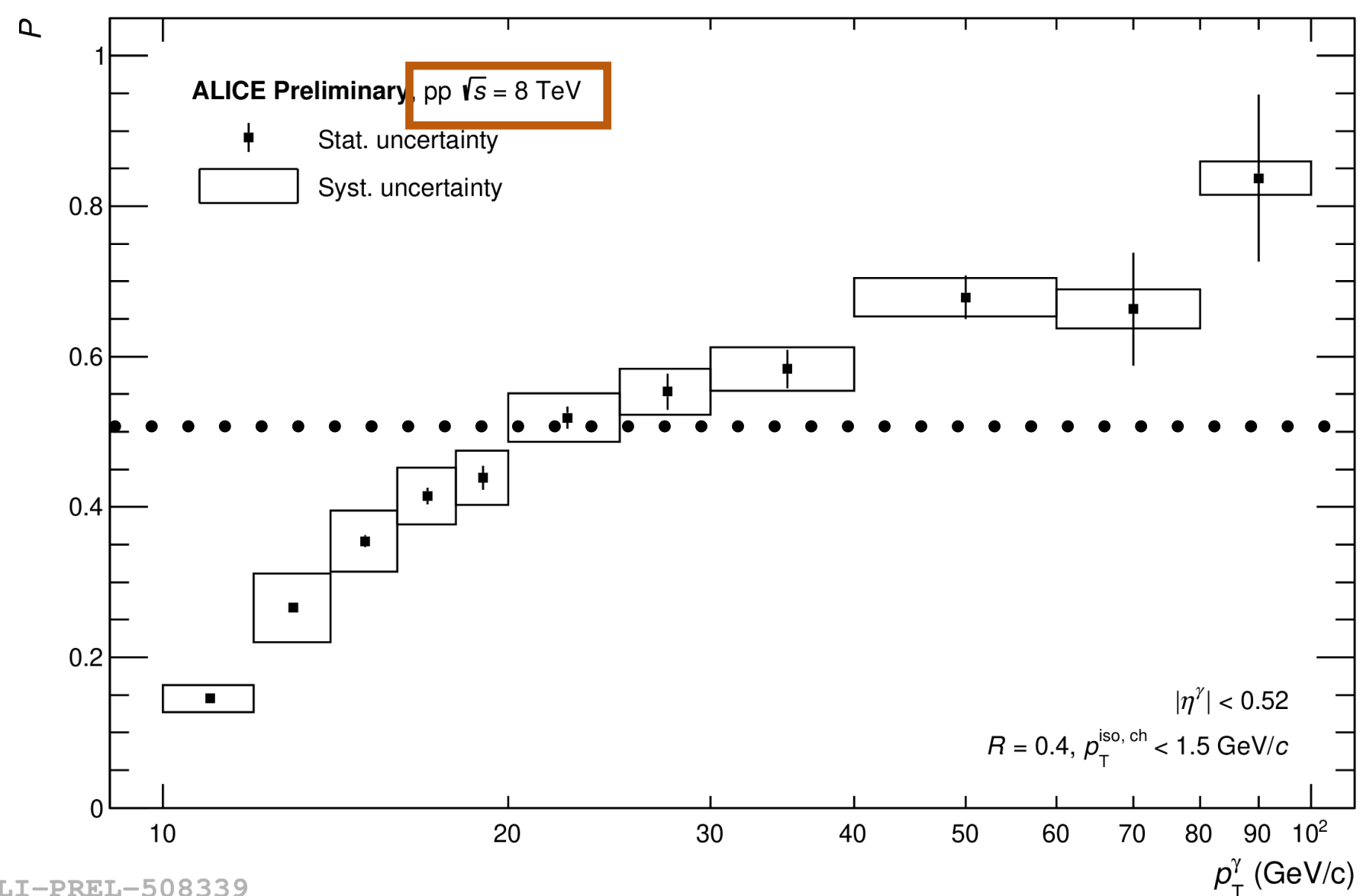
Isolation momentum in cone, pp & Pb-Pb $\sqrt{s_{NN}} = 5.02$ TeV



Isolated γ purity in pp collisions, $R = 0.4$

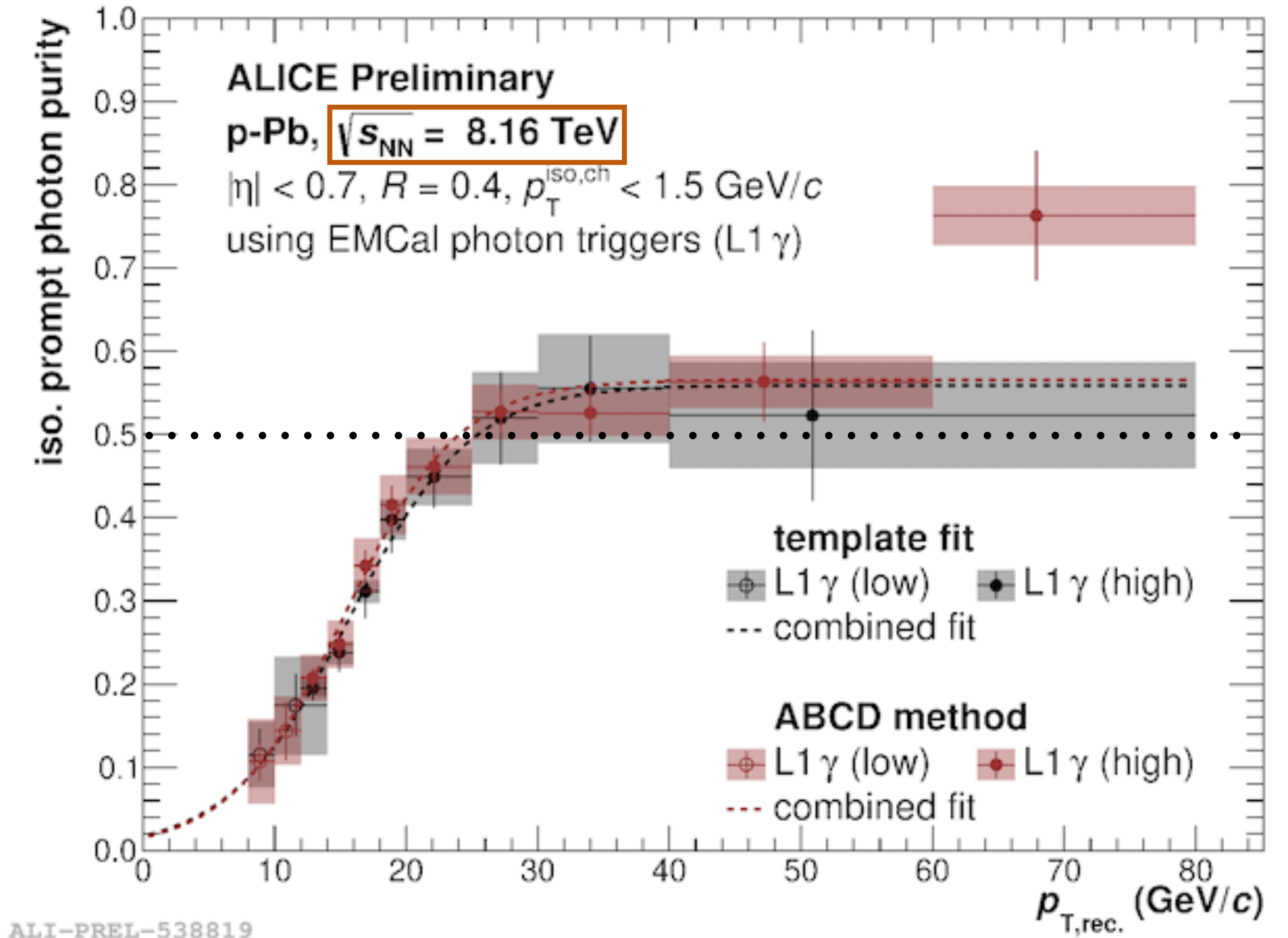
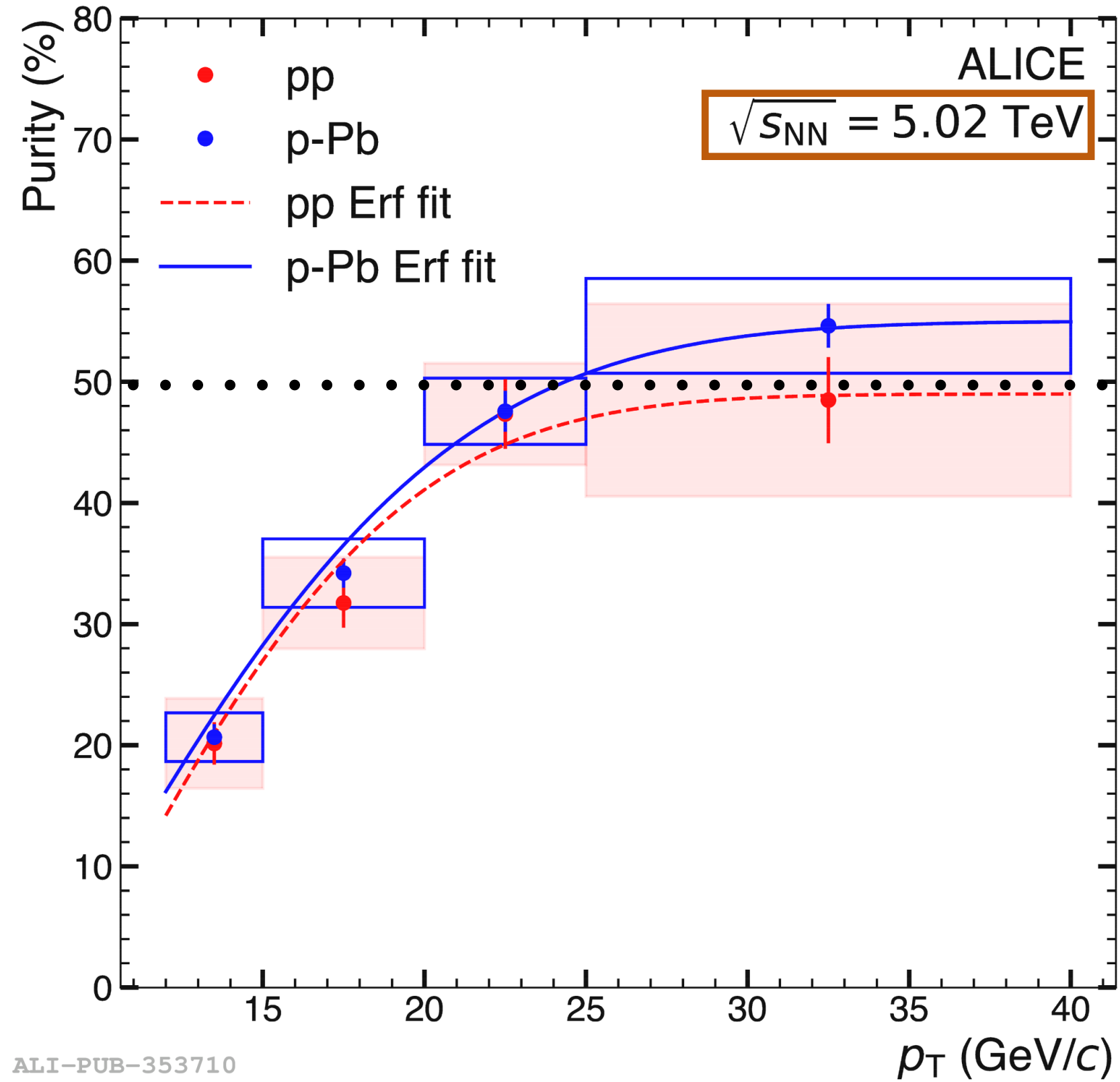


ALI-PUB-576443

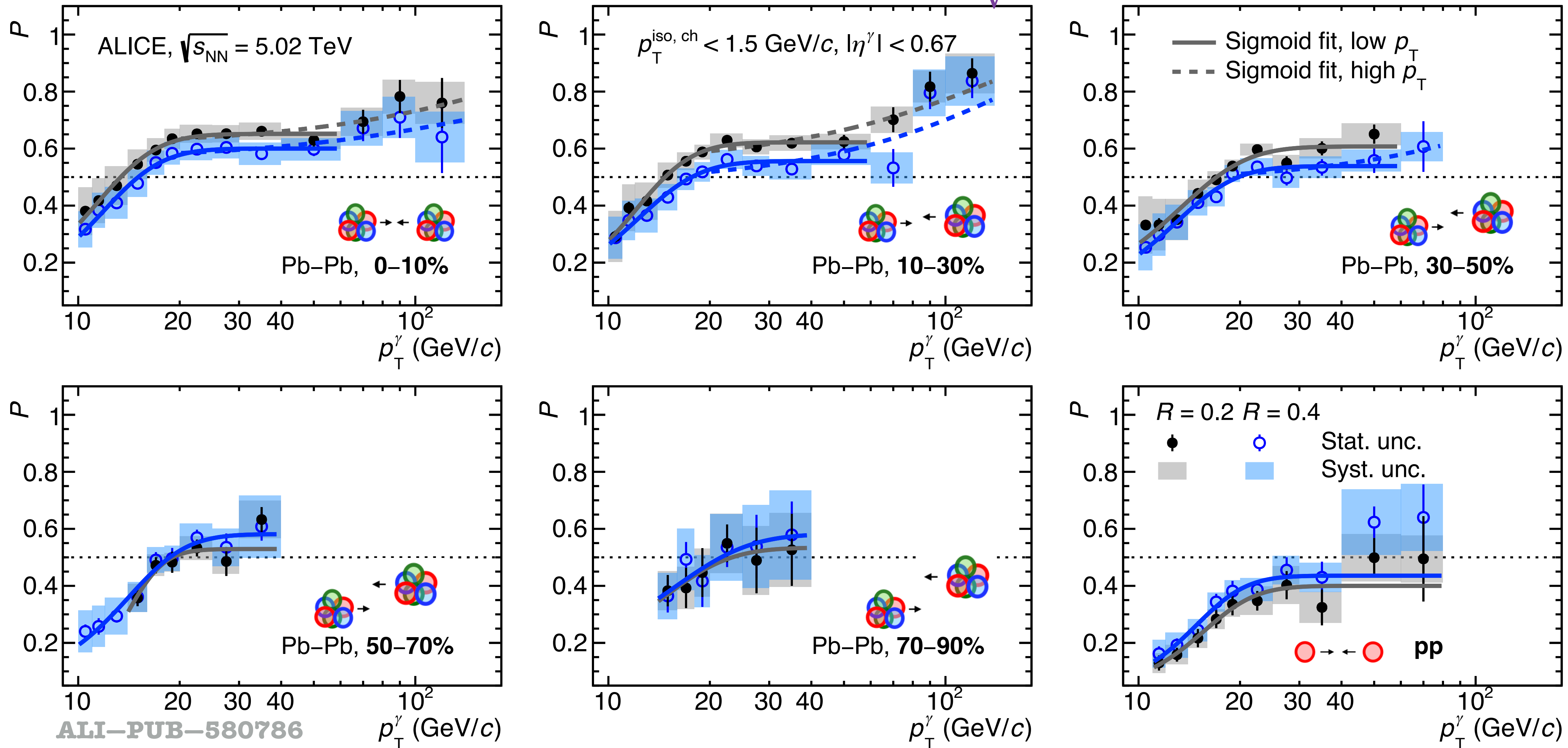


ALI-PREL-508339

Isolated γ purity in p-Pb collisions, $R = 0.4$



Purity for $R = 0.2$ & 0.4 , pp & Pb-Pb $\sqrt{s_{NN}} = 5.02$ TeV

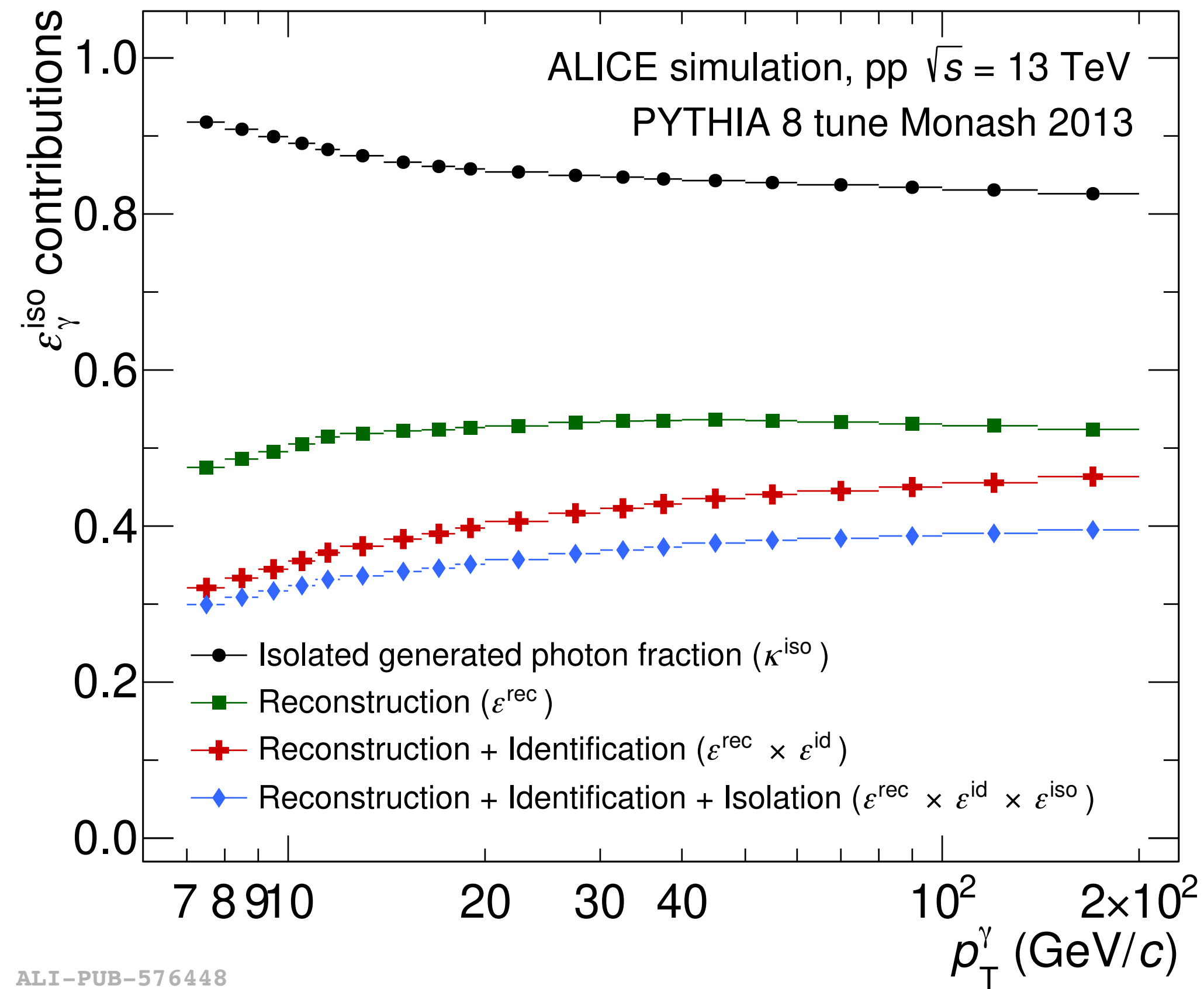


- Distributions fitted to sigmoid function to reduce influence of fluctuations, fits used to correct the spectra
- $P(R = 0.4) > P(R = 0.2)$ in pp collisions, more jet particles in cone, but decreasing centrality $P(R = 0.2) > P(R = 0.4)$, due to UE fluctuations, although not significantly different
- $P(\text{Pb-Pb}) > P(\text{pp})$ due to better tracking and higher $N(\gamma) / N(\pi^0)$ ratio ($R_{AA}(\pi^0) \ll 1$)

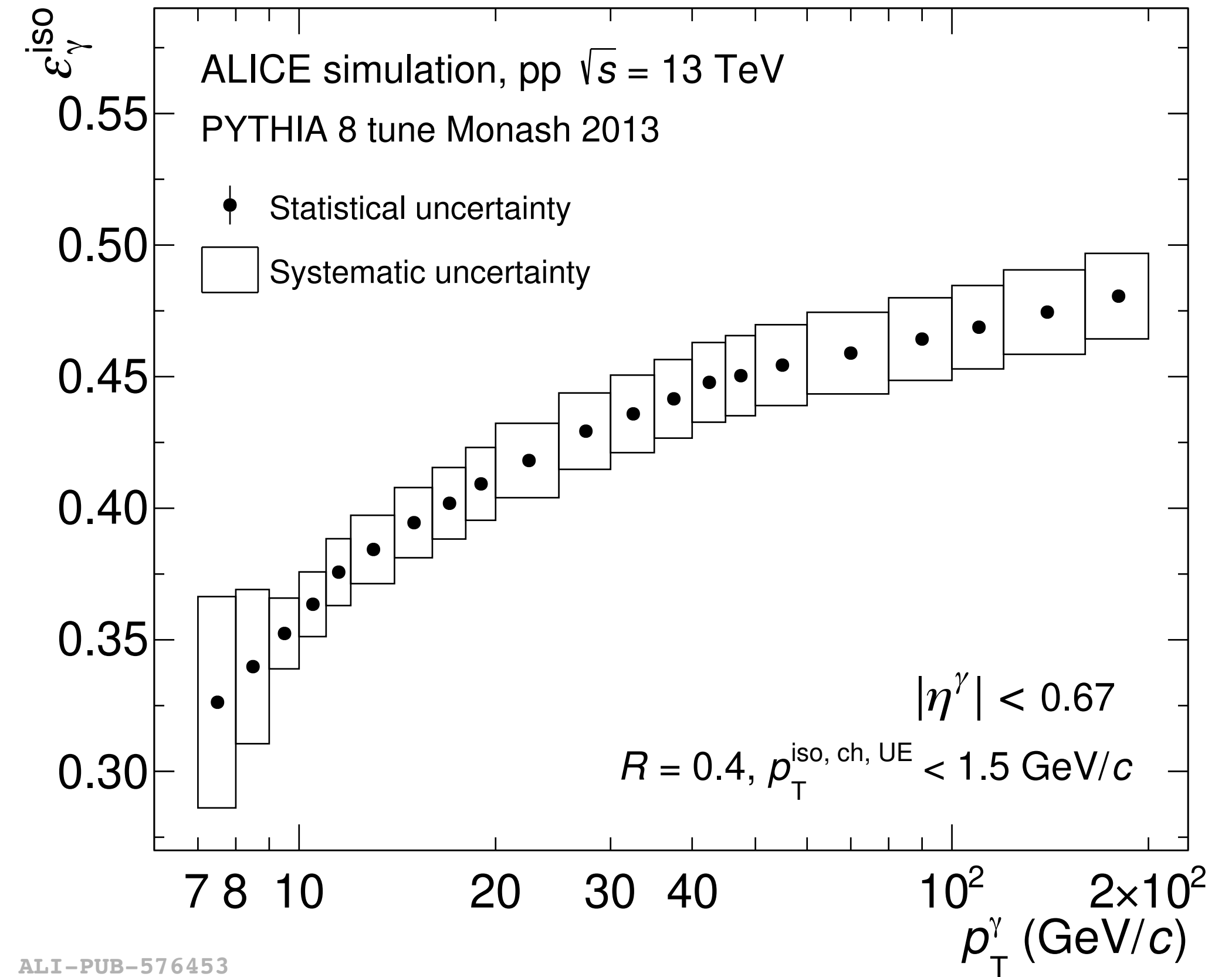
Isolated γ efficiency components, pp $\sqrt{s} = 13$ TeV

$$\varepsilon^{\text{sel}} = \frac{dN_{\gamma_{\text{prompt}}}^{\text{cluster sel.}}/dp_{\text{T}}^{\text{rec}}}{dN_{\gamma_{\text{prompt}}}^{\text{gener.}}/dp_{\text{T}}^{\text{gen}}}$$

$$\varepsilon_{\gamma}^{\text{iso}} = \frac{dN_{\gamma_{\text{prompt}}}^{\text{cluster iso. narrow}}/dp_{\text{T}}^{\text{rec}}}{dN_{\gamma_{\text{prompt}}}^{\text{gener. iso.}}/dp_{\text{T}}^{\text{gen}}}$$



ALI-PUB-576448



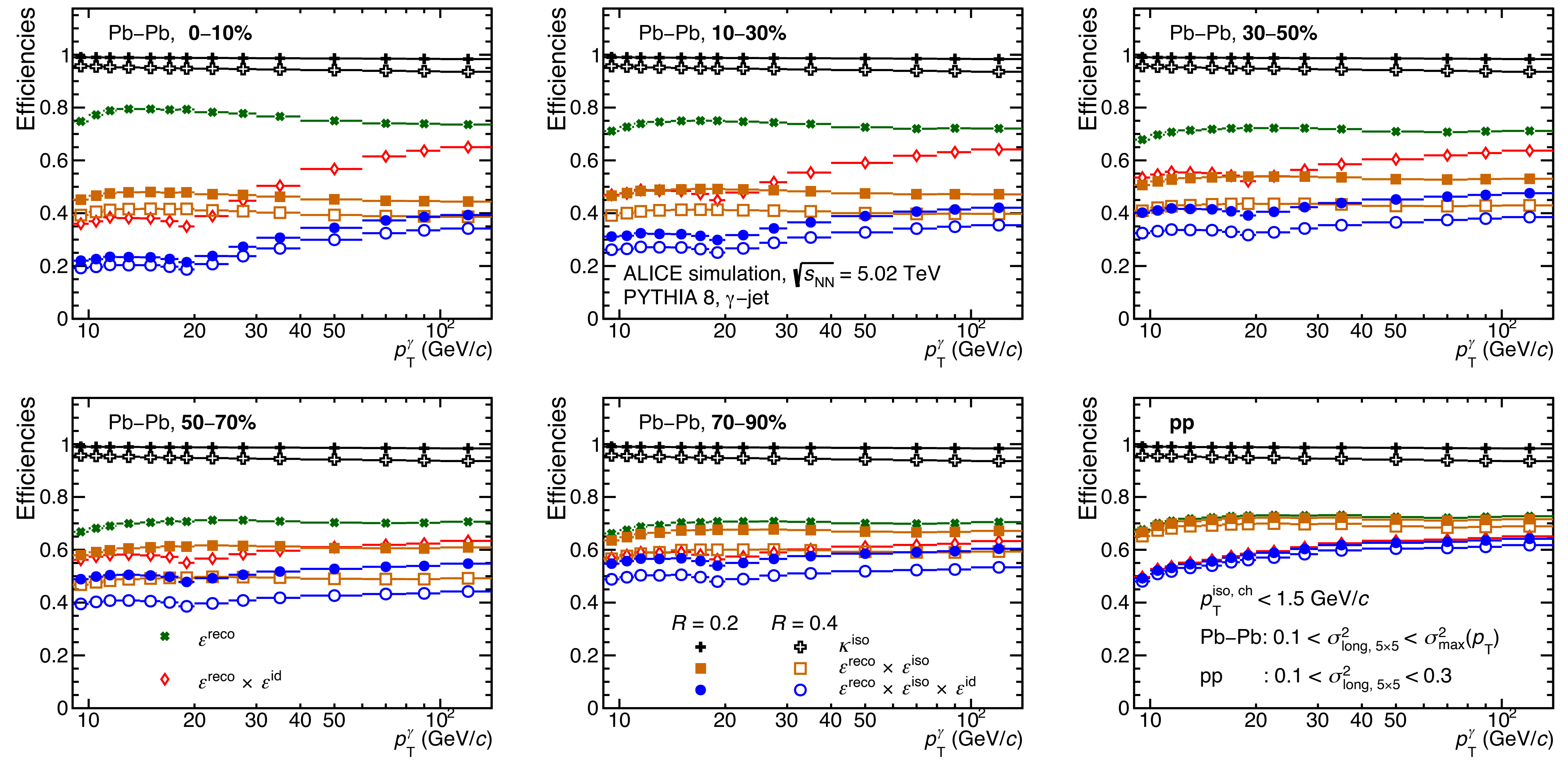
ALI-PUB-576453

Isolated γ efficiency components, pp & Pb-Pb $\sqrt{s_{NN}} = 5.02$ TeV



$$\epsilon^{\text{sel}} = \frac{dN_{\gamma_{\text{prompt}}^{\text{cluster sel.}}/dp_T^{\text{rec}}}{dN_{\gamma_{\text{prompt}}^{\text{gener.}}/dp_T^{\text{gen}}}$$

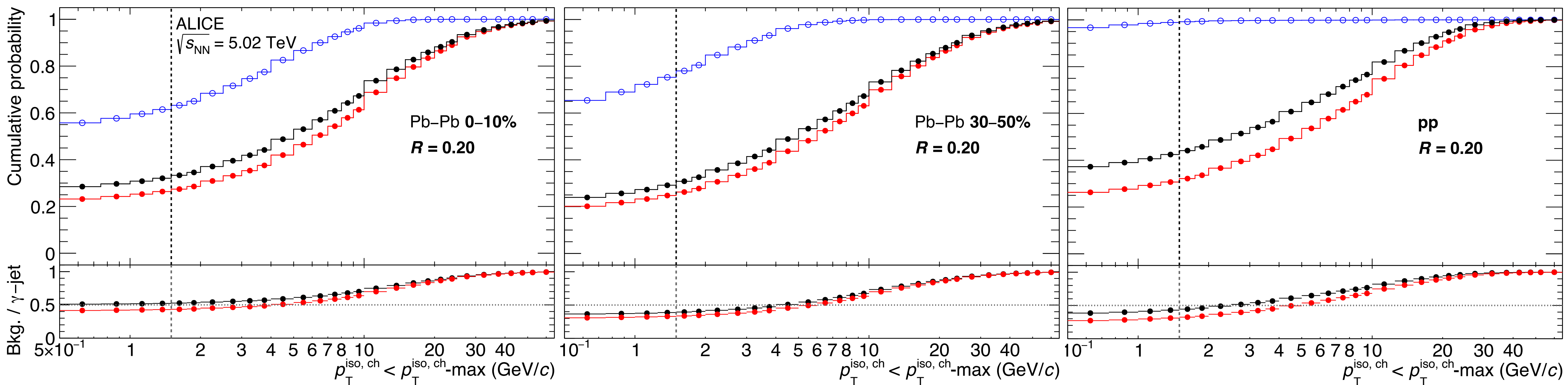
ALICE-PUBLIC-2024-003



Selection probability depending isolation threshold, $R = 0.2$, pp & Pb-Pb $\sqrt{s_{NN}} = 5.02$ TeV



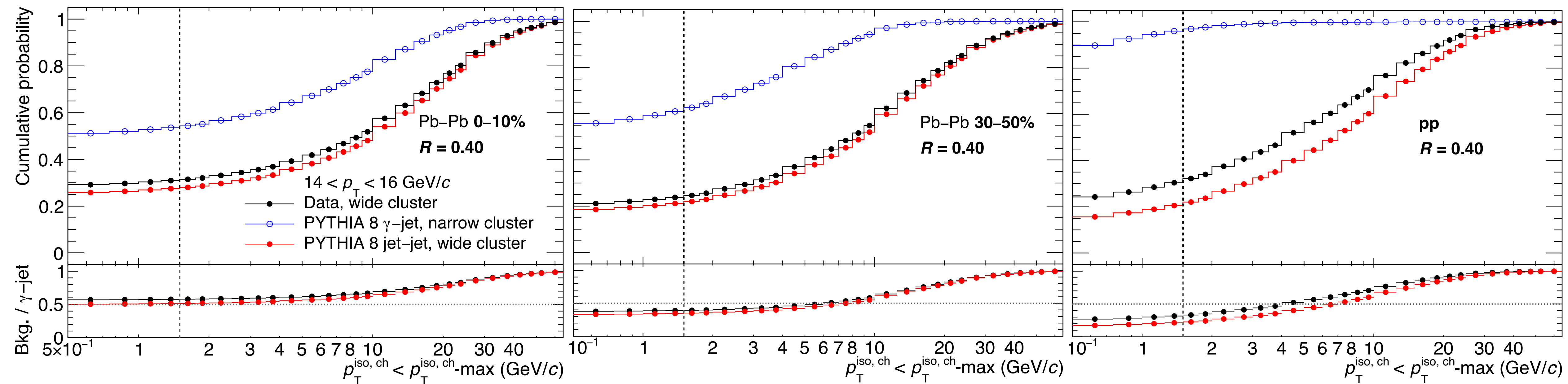
ALICE-PUBLIC-2024-003



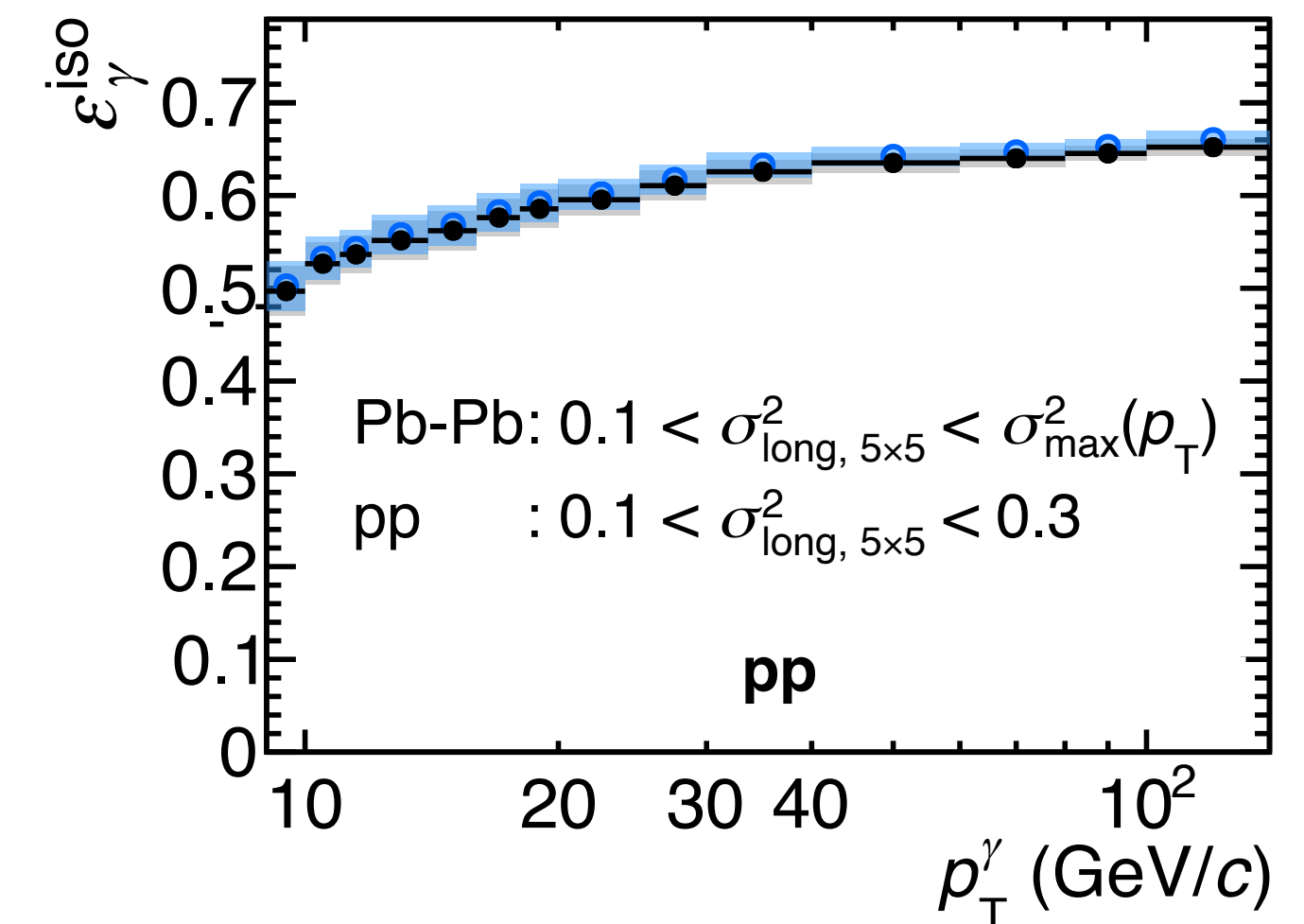
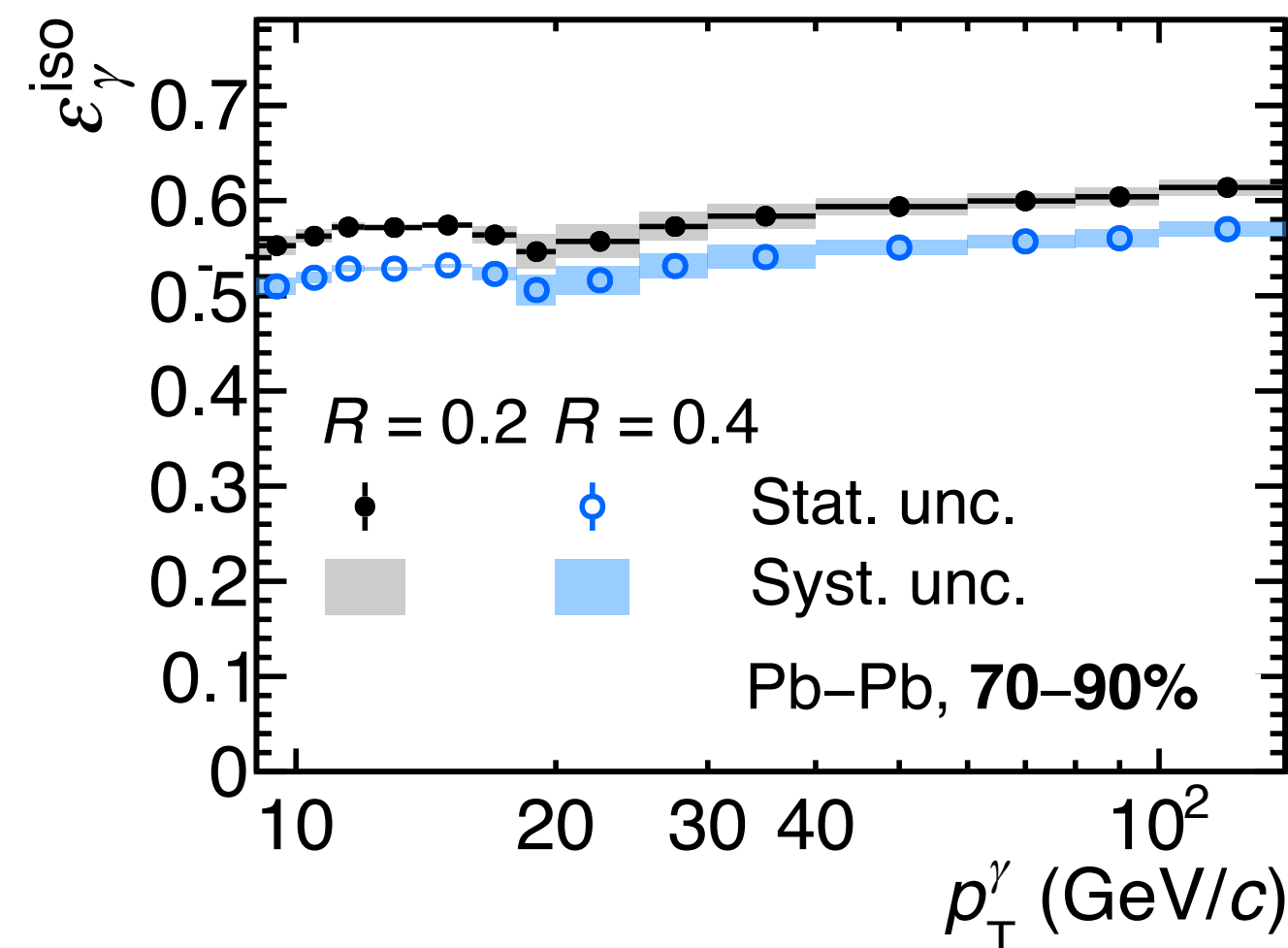
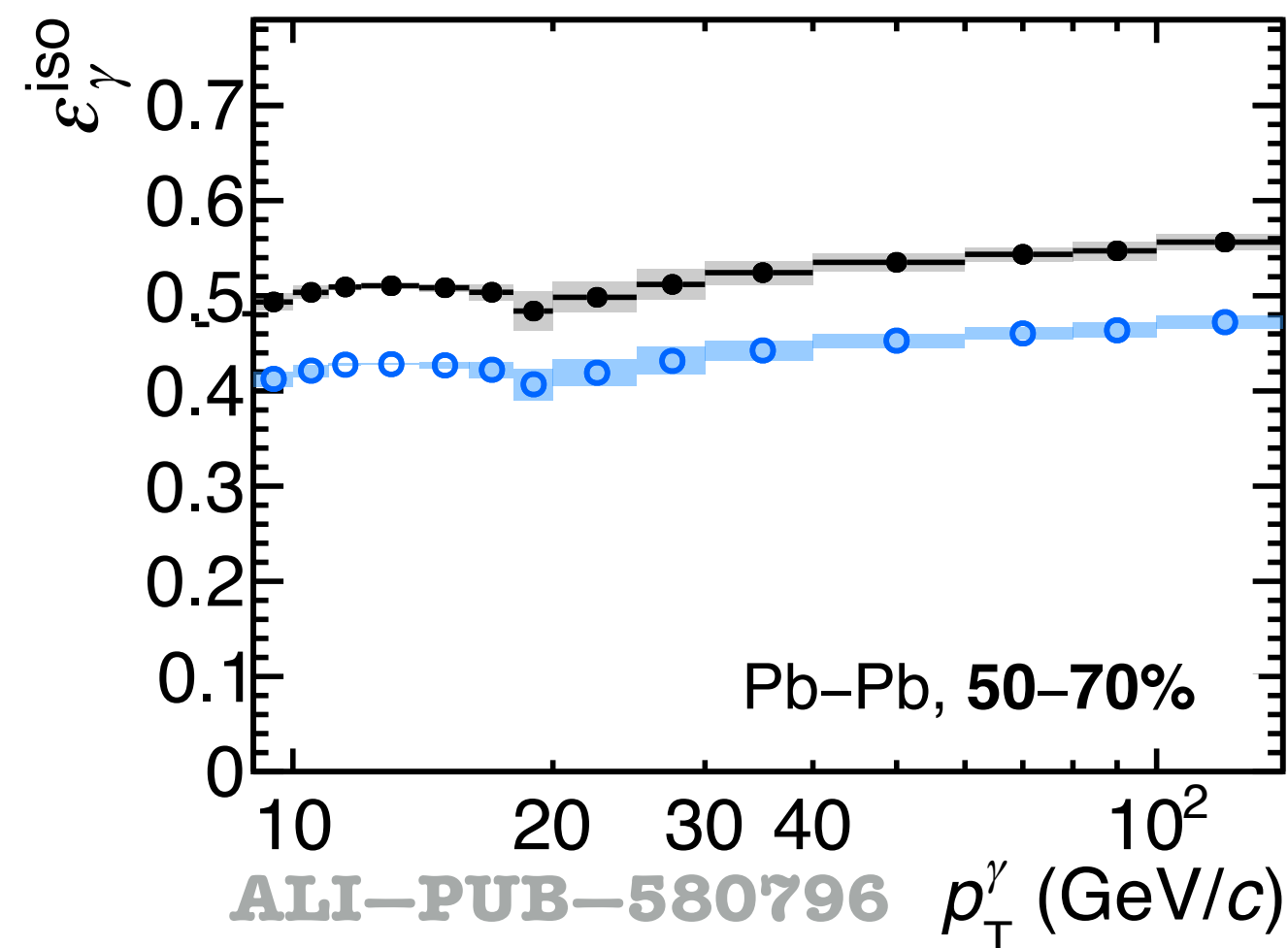
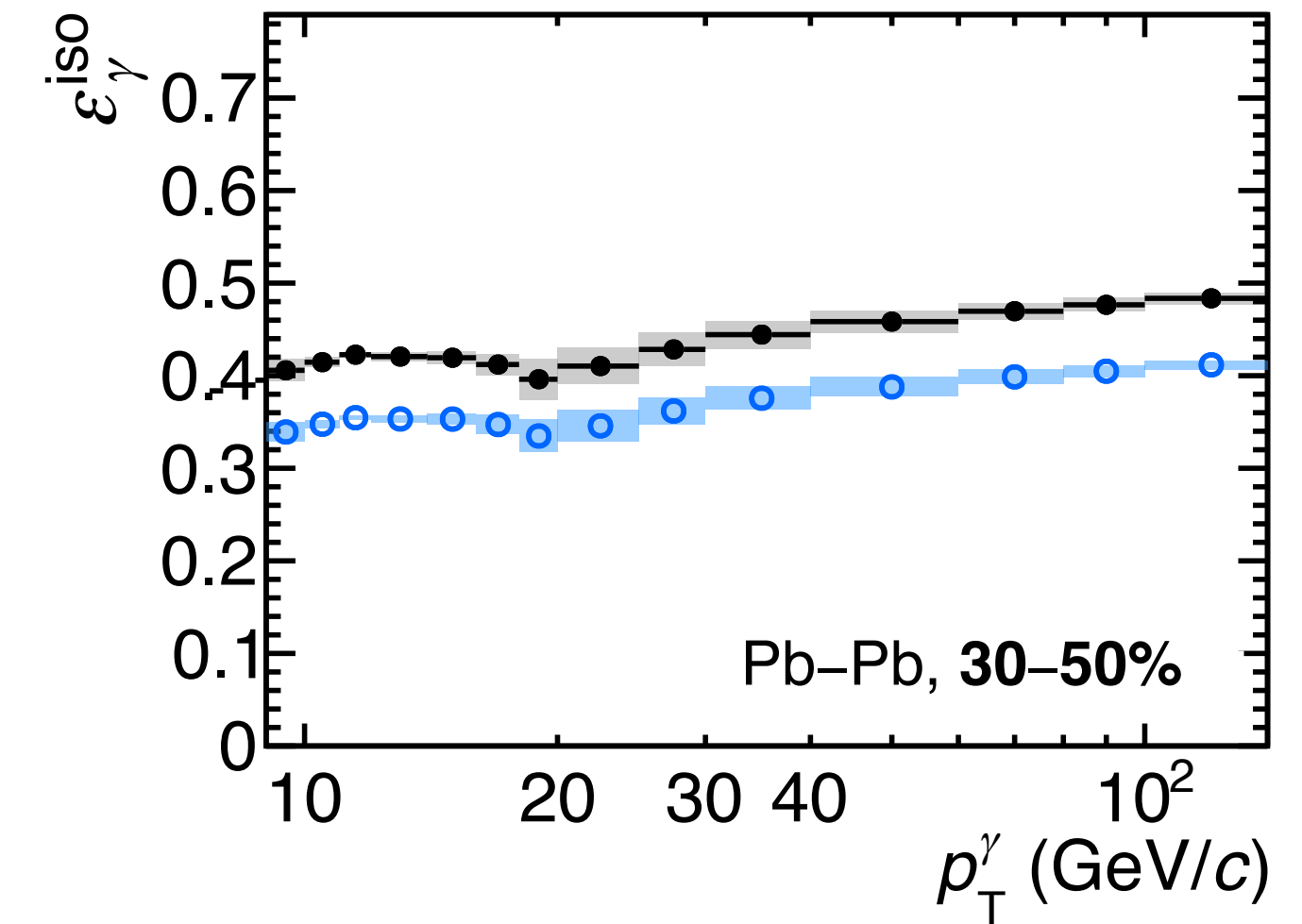
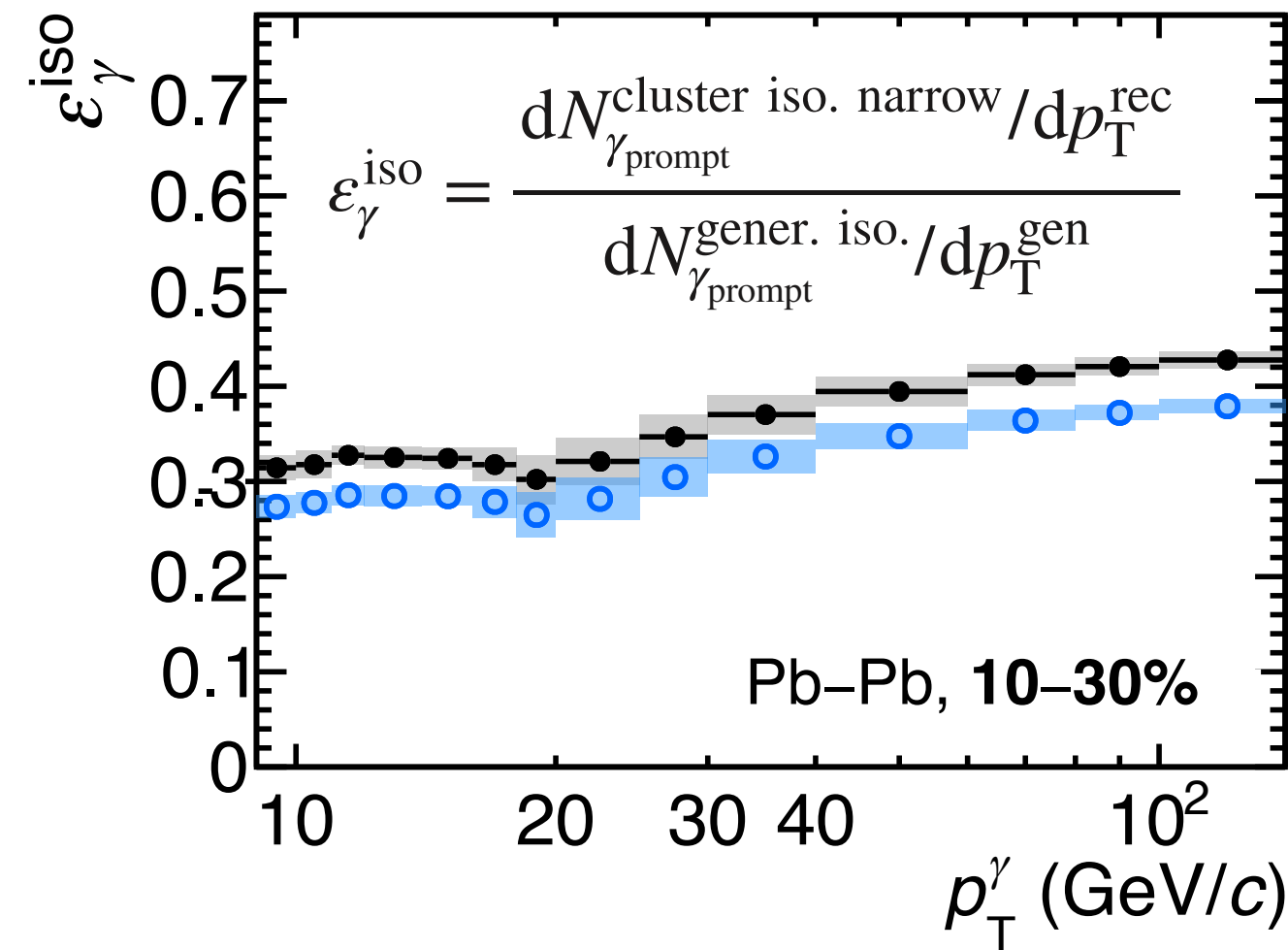
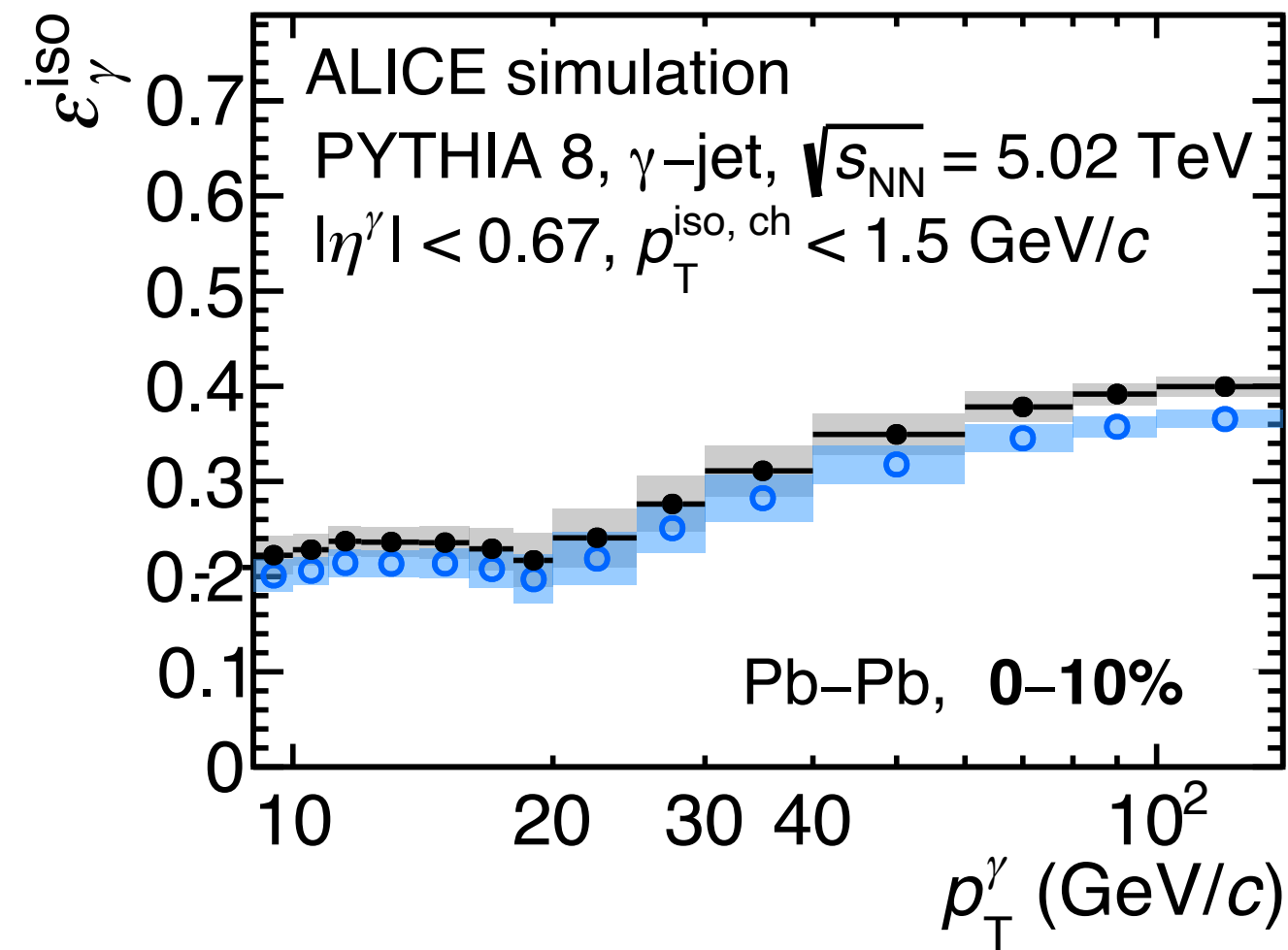
Selection probability depending isolation threshold, $R = 0.4$, pp & Pb-Pb $\sqrt{s_{NN}} = 5.02$ TeV



ALICE-PUBLIC-2024-003



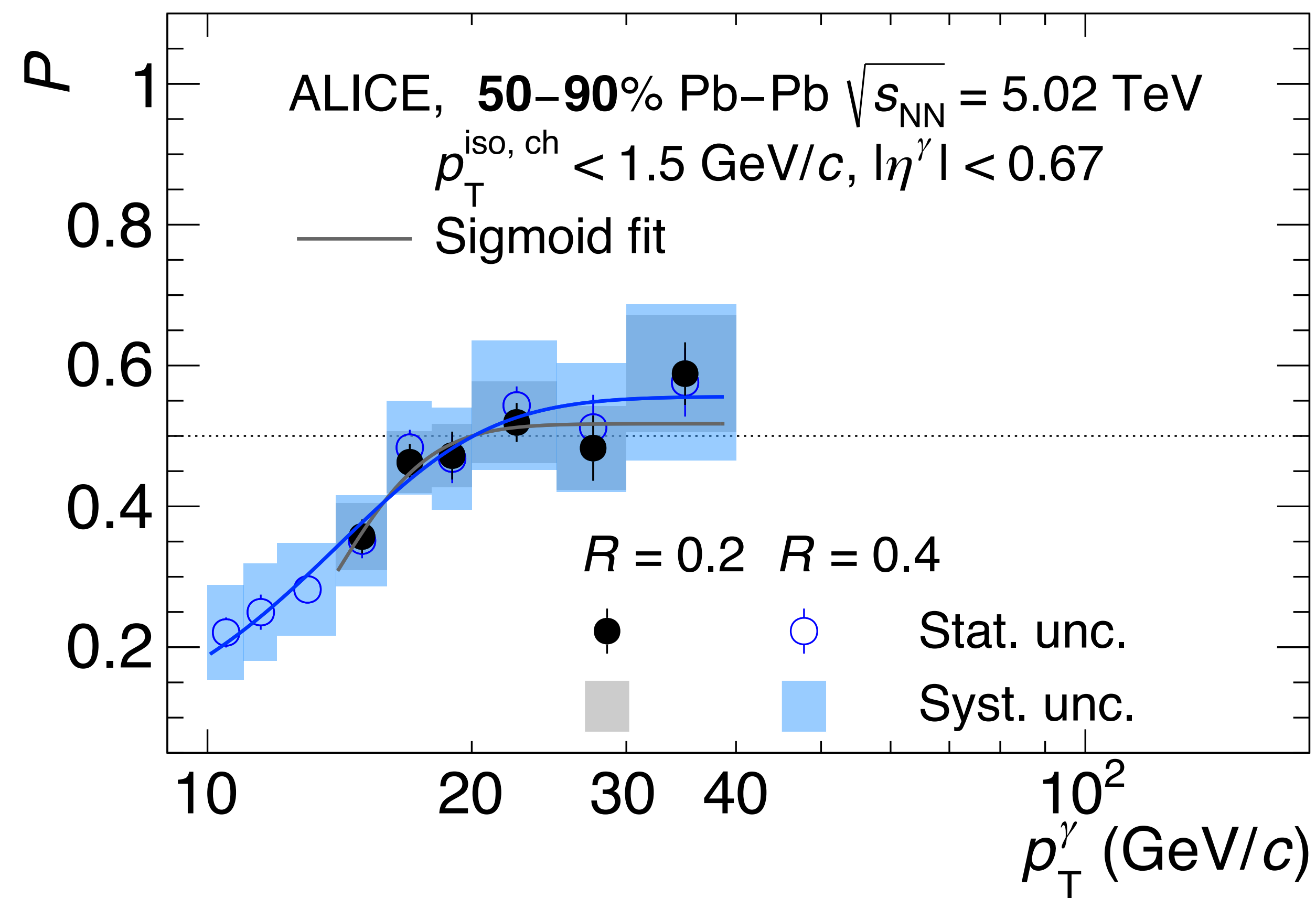
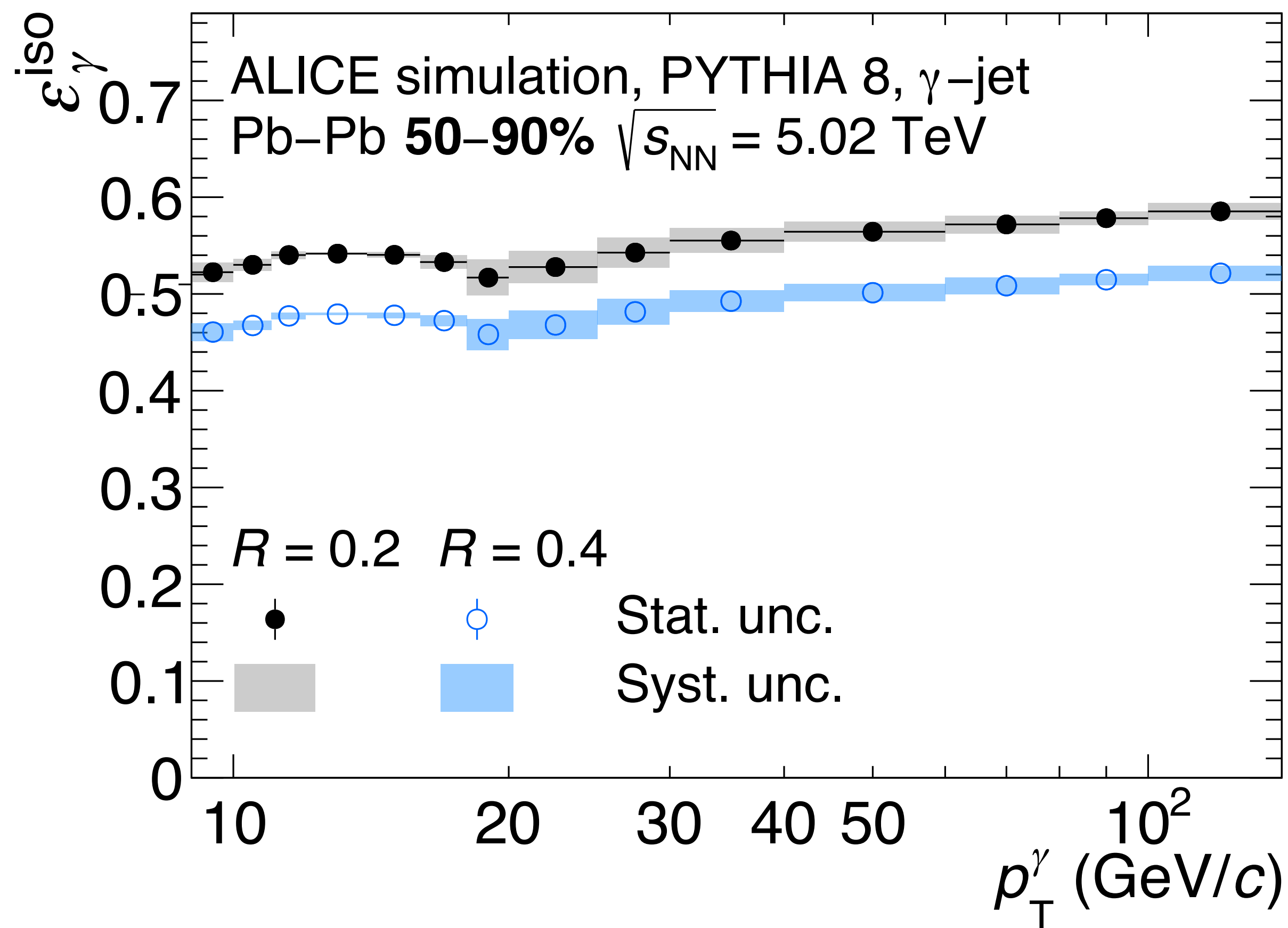
Efficiency, $R = 0.2$ & 0.4 , pp & Pb-Pb $\sqrt{s_{NN}} = 5.02$ TeV



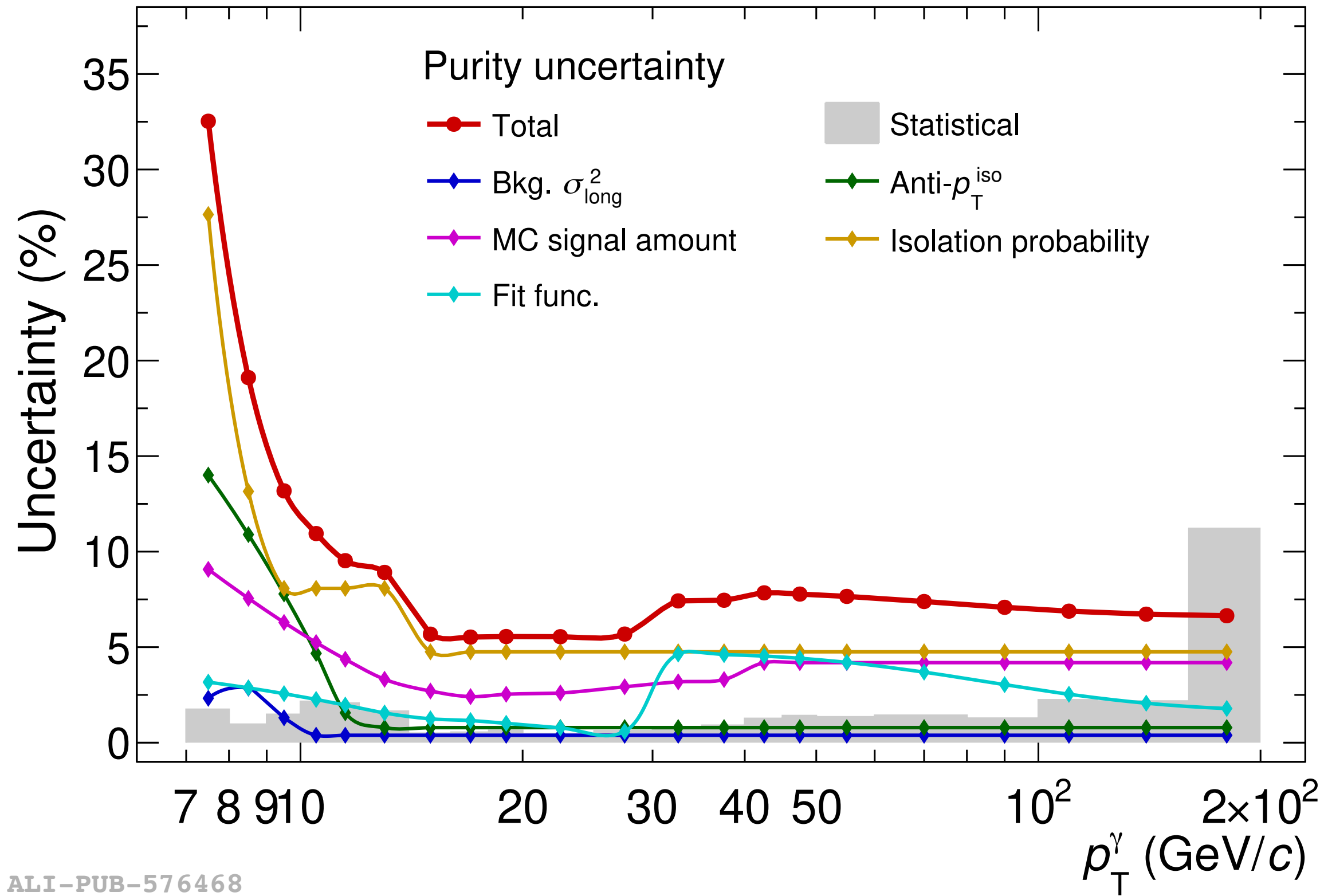
- $\epsilon_{\gamma}^{\text{iso}} (0-10\%) < \epsilon_{\gamma}^{\text{iso}} (50-90\%)$: UE increases cluster size in more central collisions
- In Pb-Pb, $\epsilon_{\gamma}^{\text{iso}} (R = 0.2) > \epsilon_{\gamma}^{\text{iso}} (R = 0.4)$ a factor ~ 0.9 due to lower UE fluctuations
- In pp, $\epsilon_{\gamma}^{\text{iso}} (R = 0.2) \approx \epsilon_{\gamma}^{\text{iso}} (R = 0.4)$, due to the less performing ITS-only tracks

Pb-Pb 50-90%: efficiency and purity

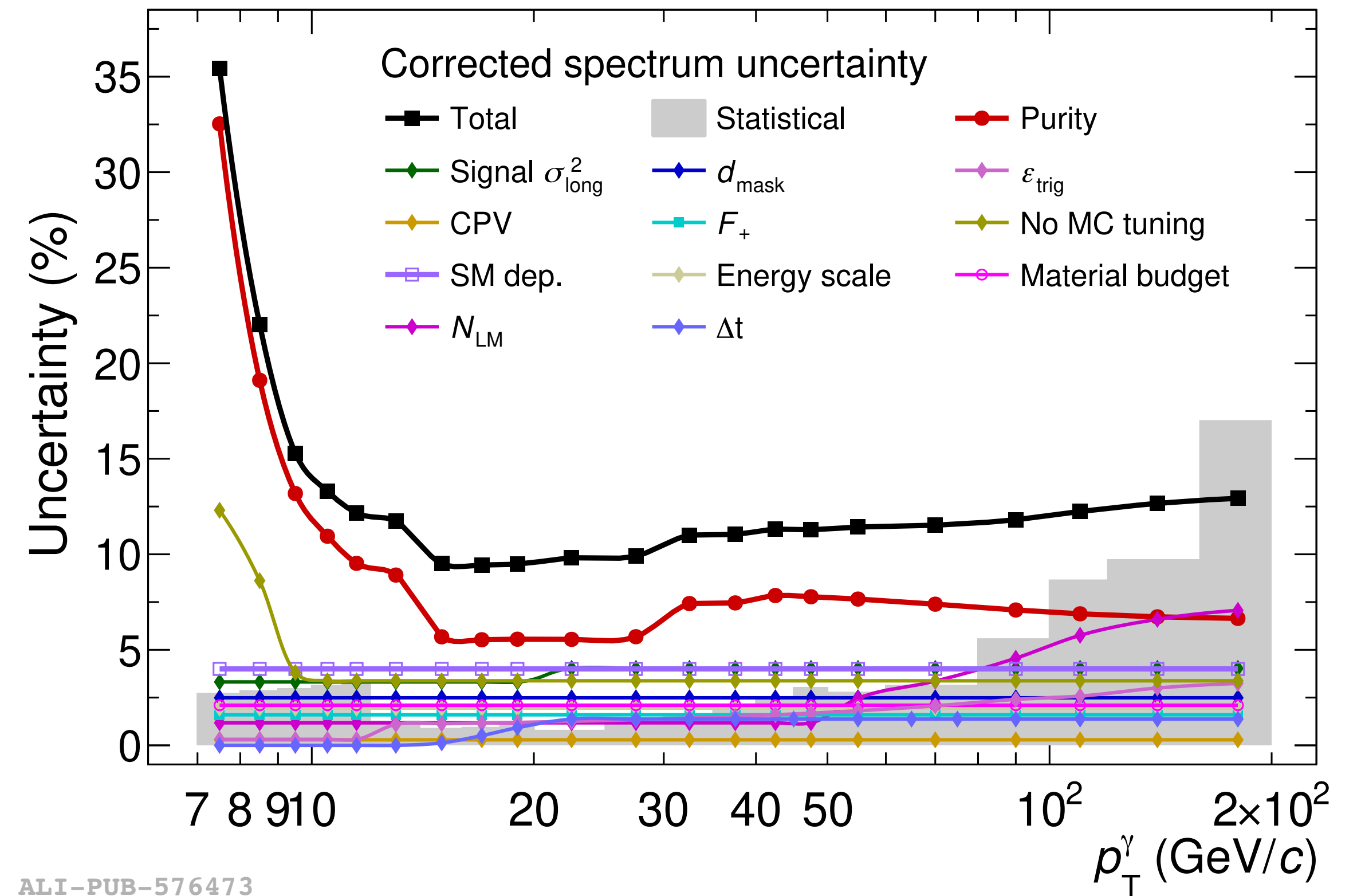
ALICE-PUBLIC-2024-003



Uncertainties, pp $\sqrt{s} = 13$ TeV

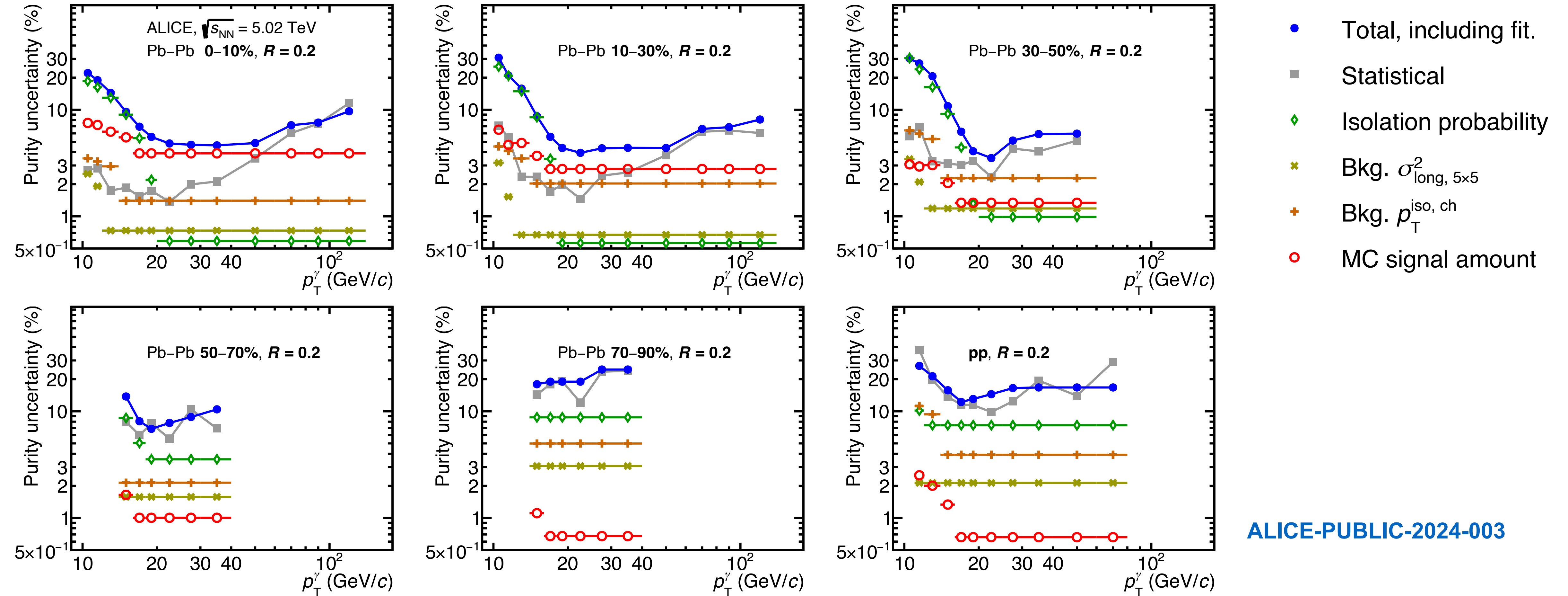


ALI-PUB-576468



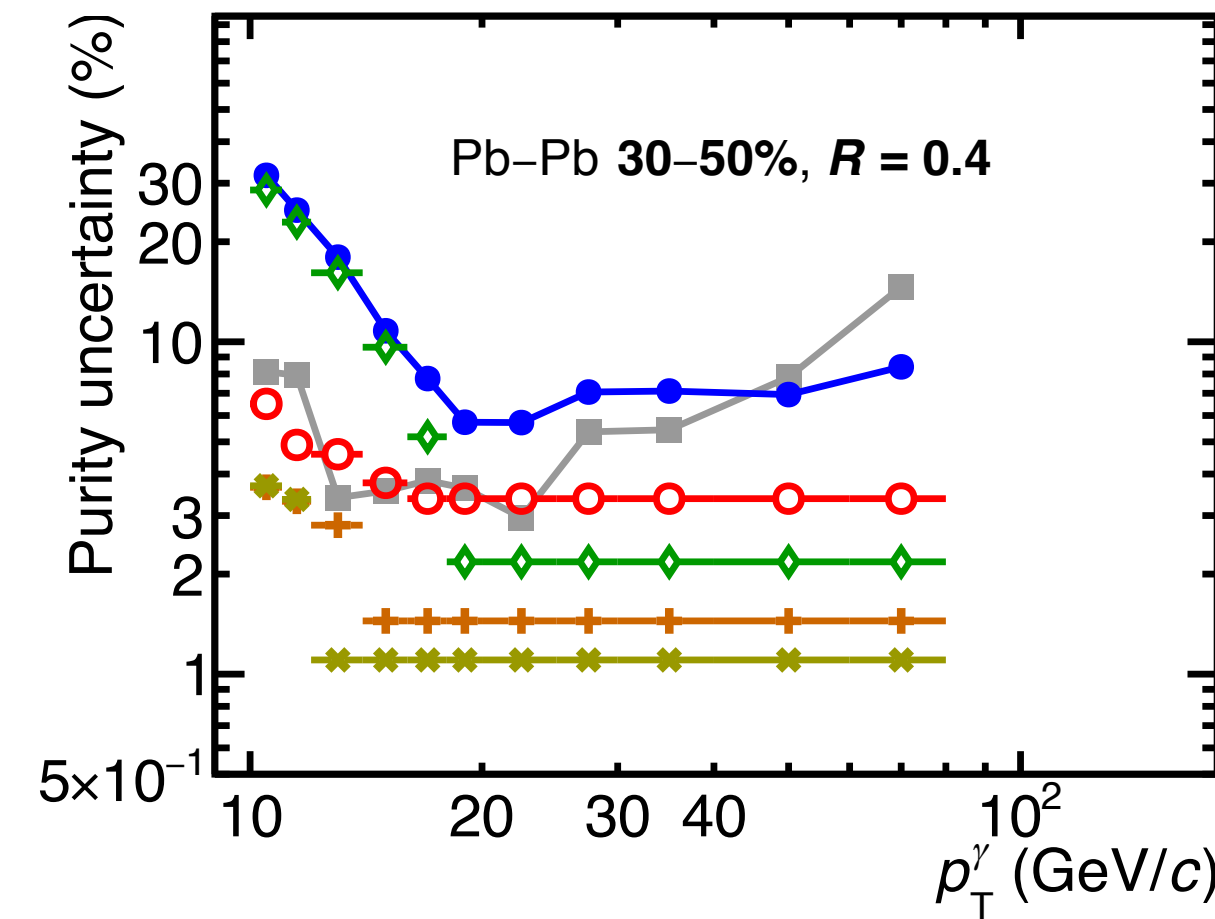
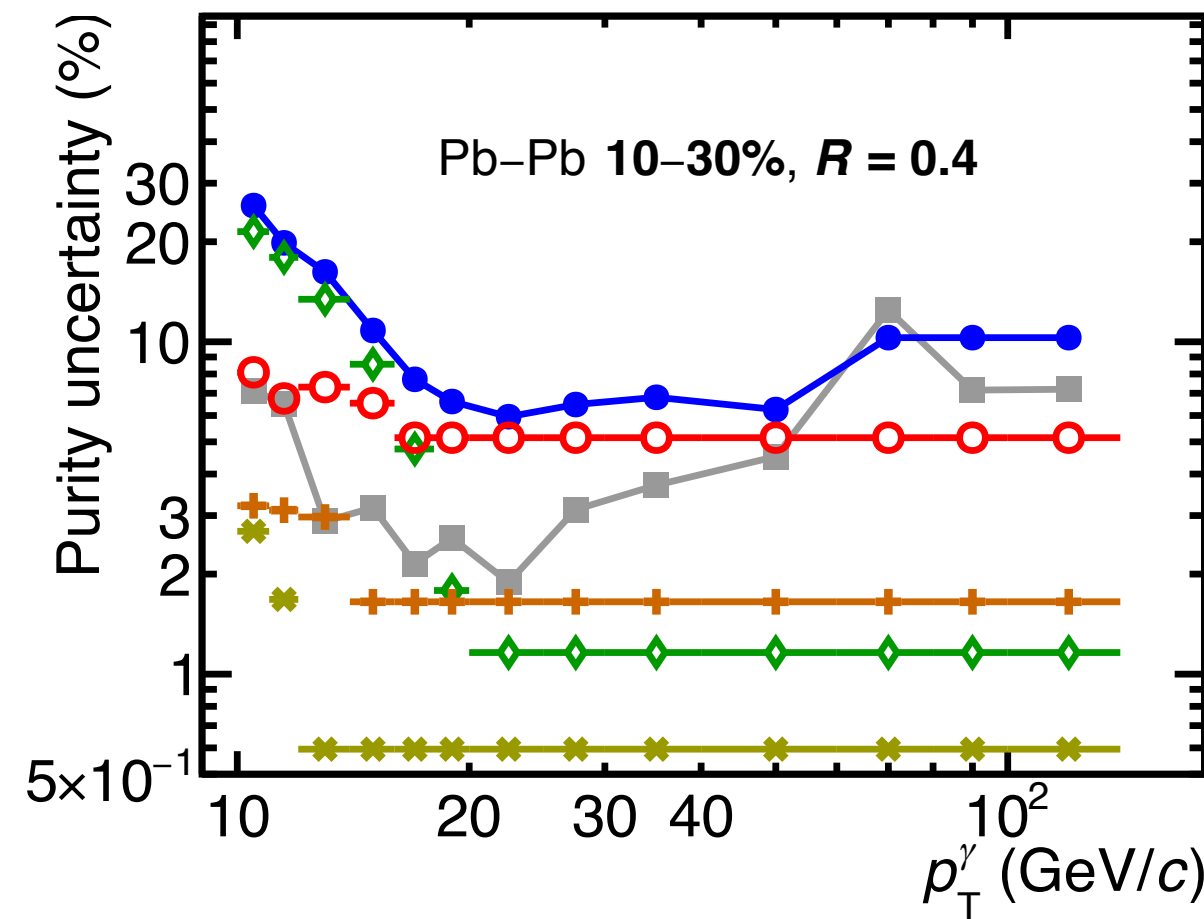
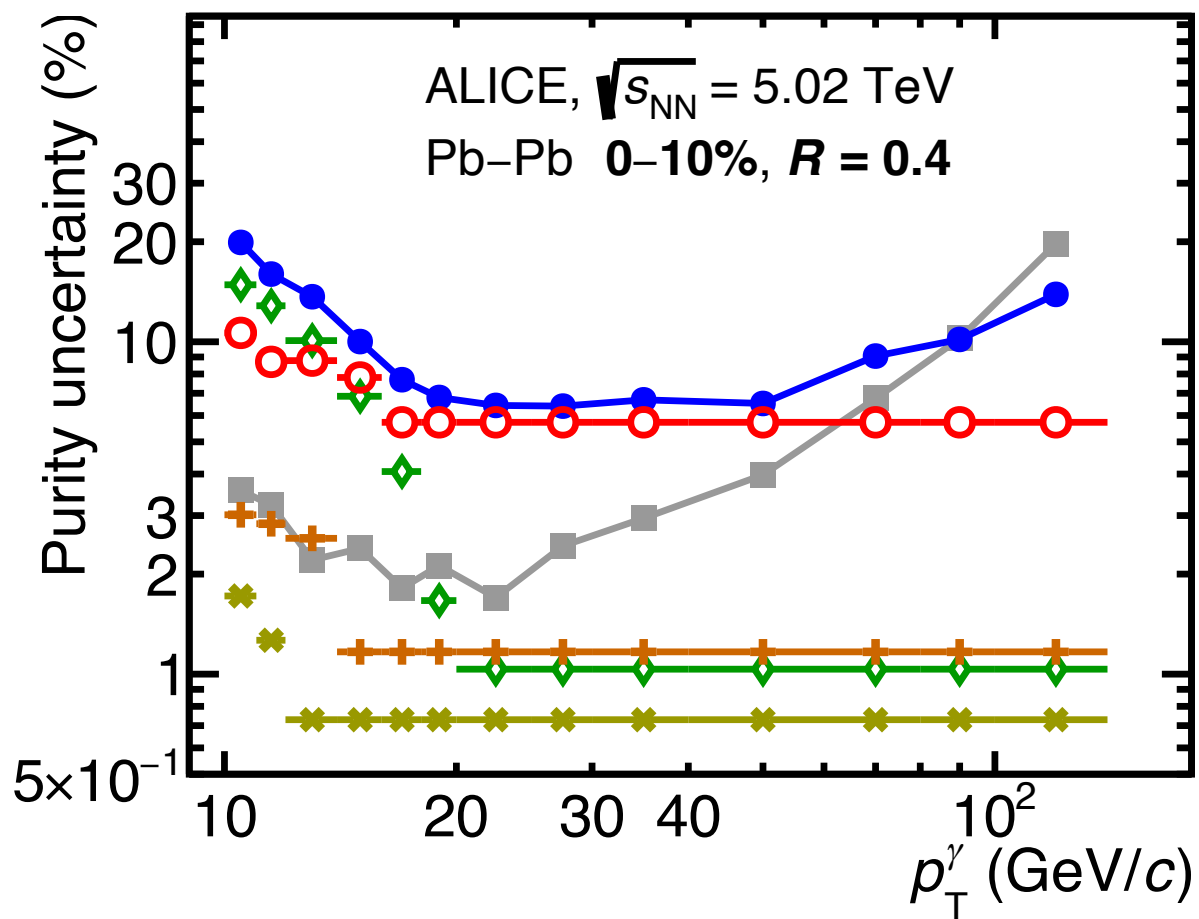
ALI-PUB-576473

Purity uncertainties, pp & Pb-Pb $\sqrt{s_{NN}} = 5.02$ TeV, $R = 0.2$

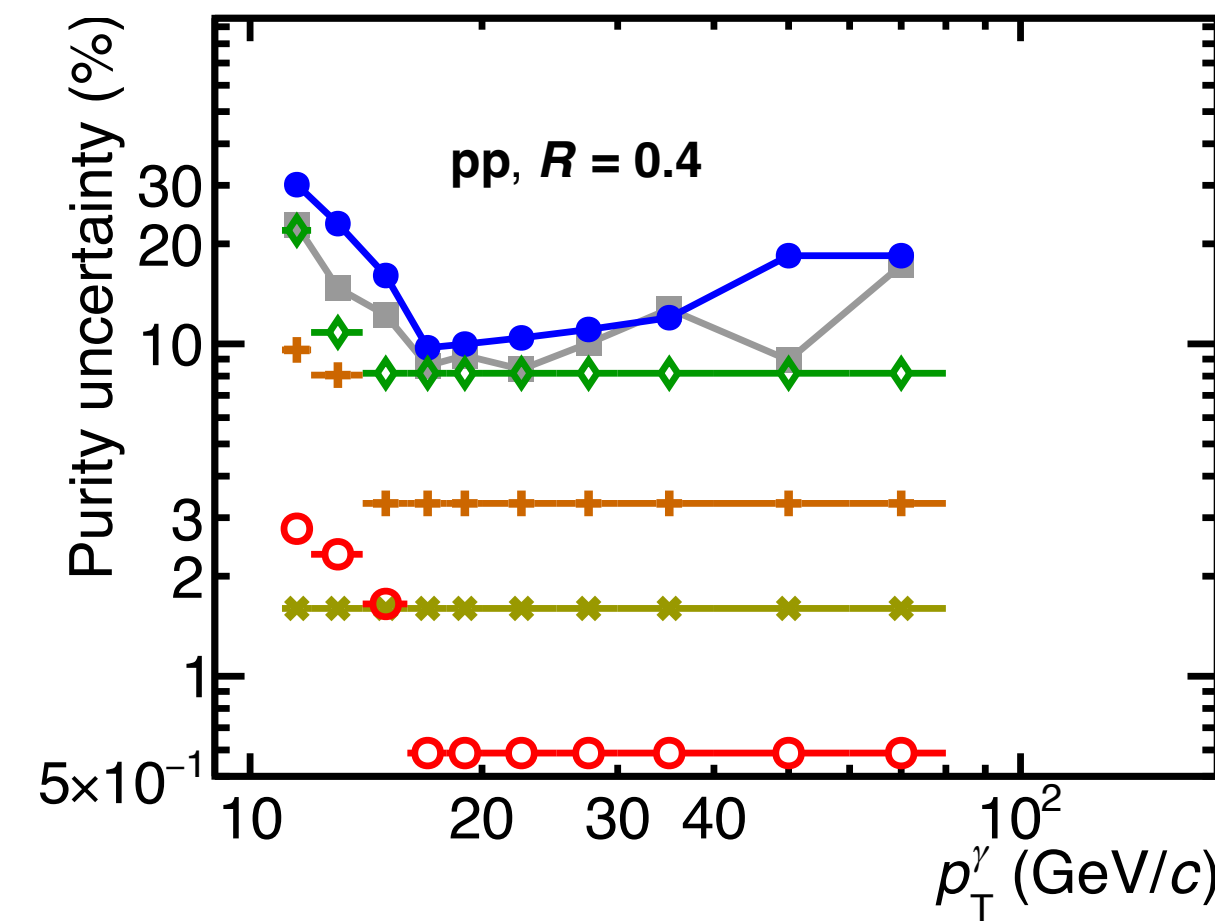
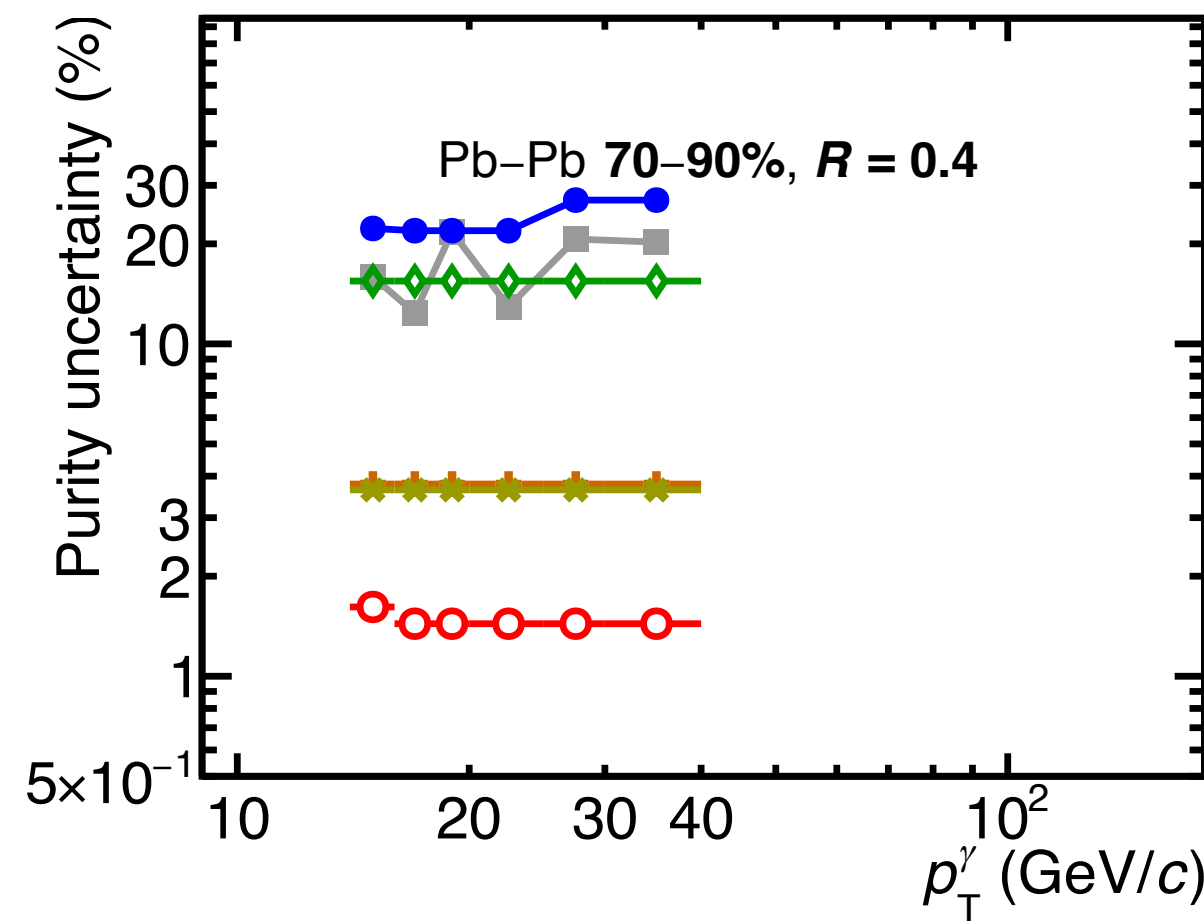
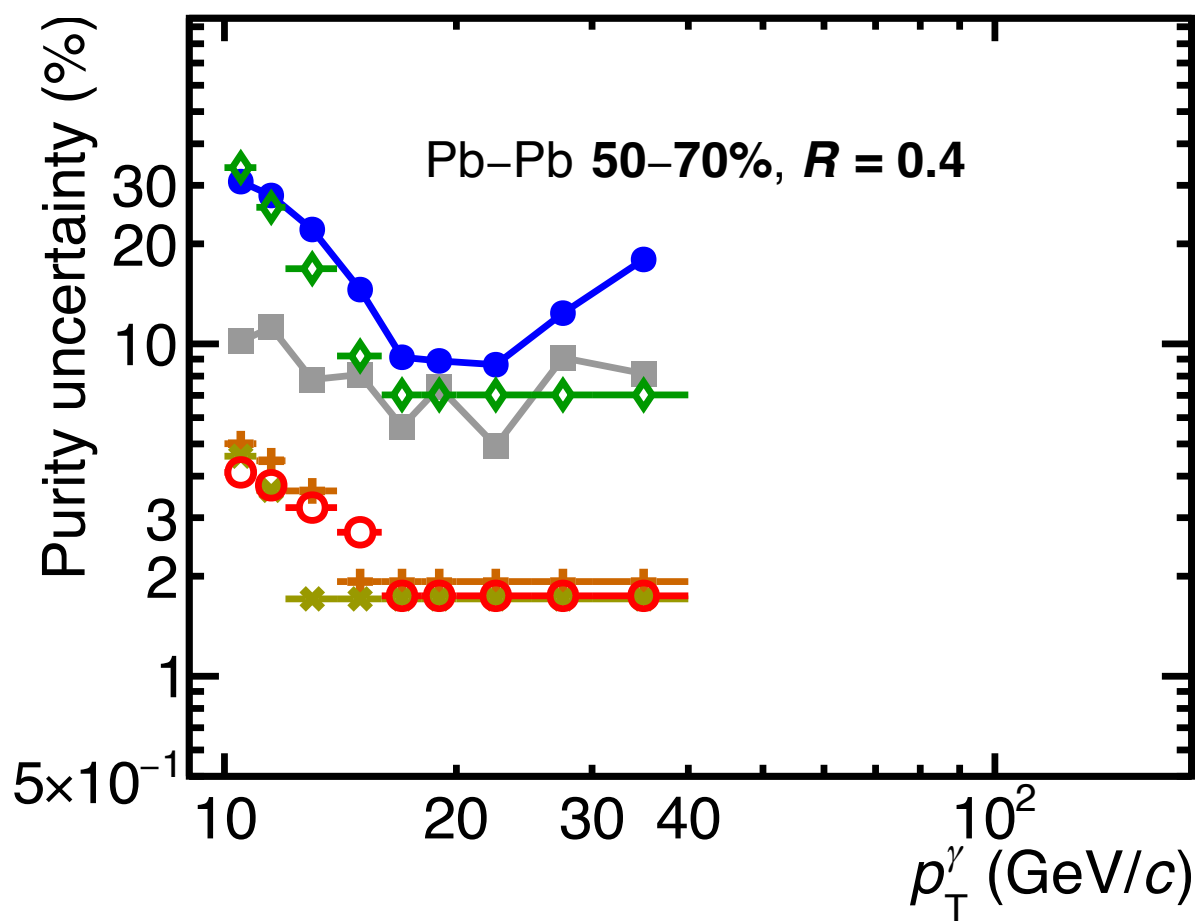


ALICE-PUBLIC-2024-003

Purity uncertainties, pp & Pb-Pb $\sqrt{s_{NN}} = 5.02$ TeV, $R = 0.4$

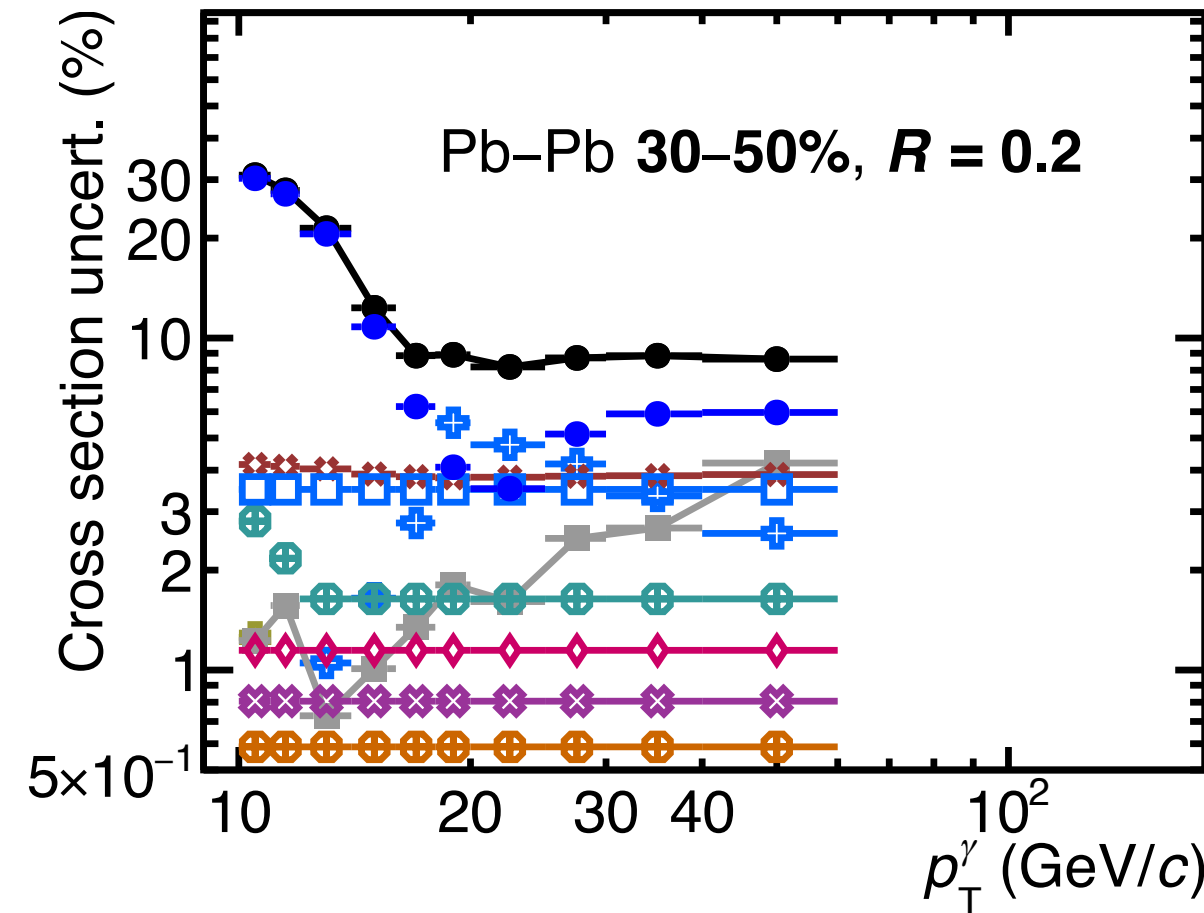
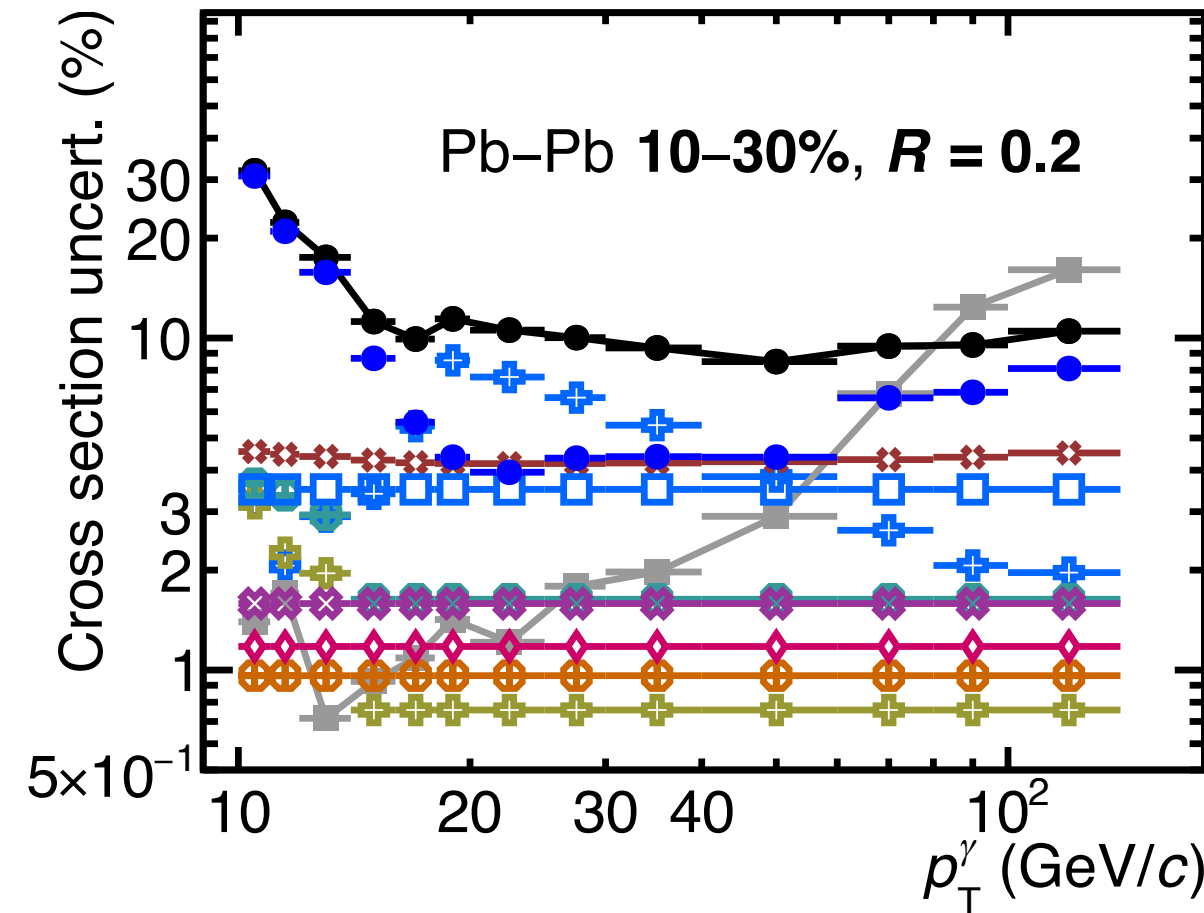
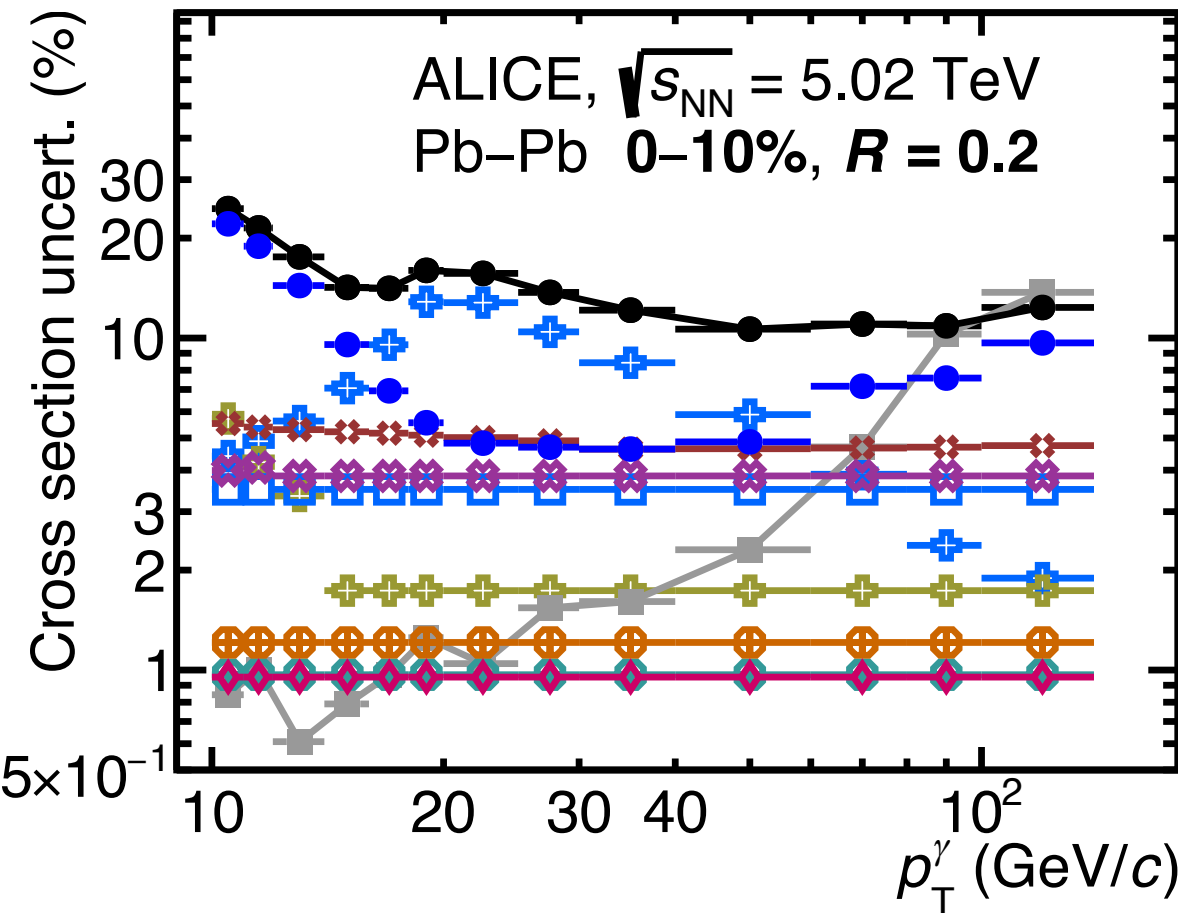


- Total, including fit.
- Statistical
- ◆ Isolation probability
- * Bkg. $\sigma_{long}^2, 5 \times 5$
- + Bkg. $p_T^{iso, ch}$
- MC signal amount

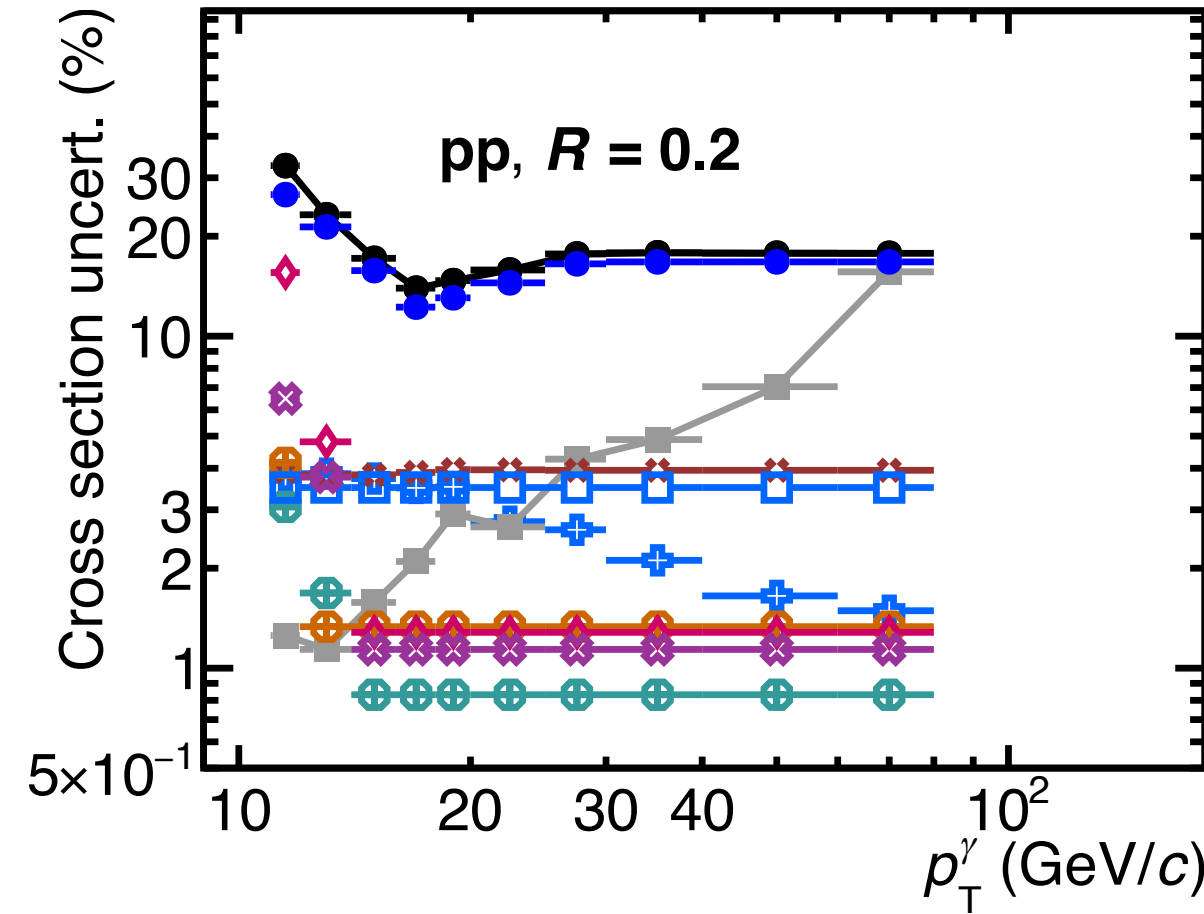
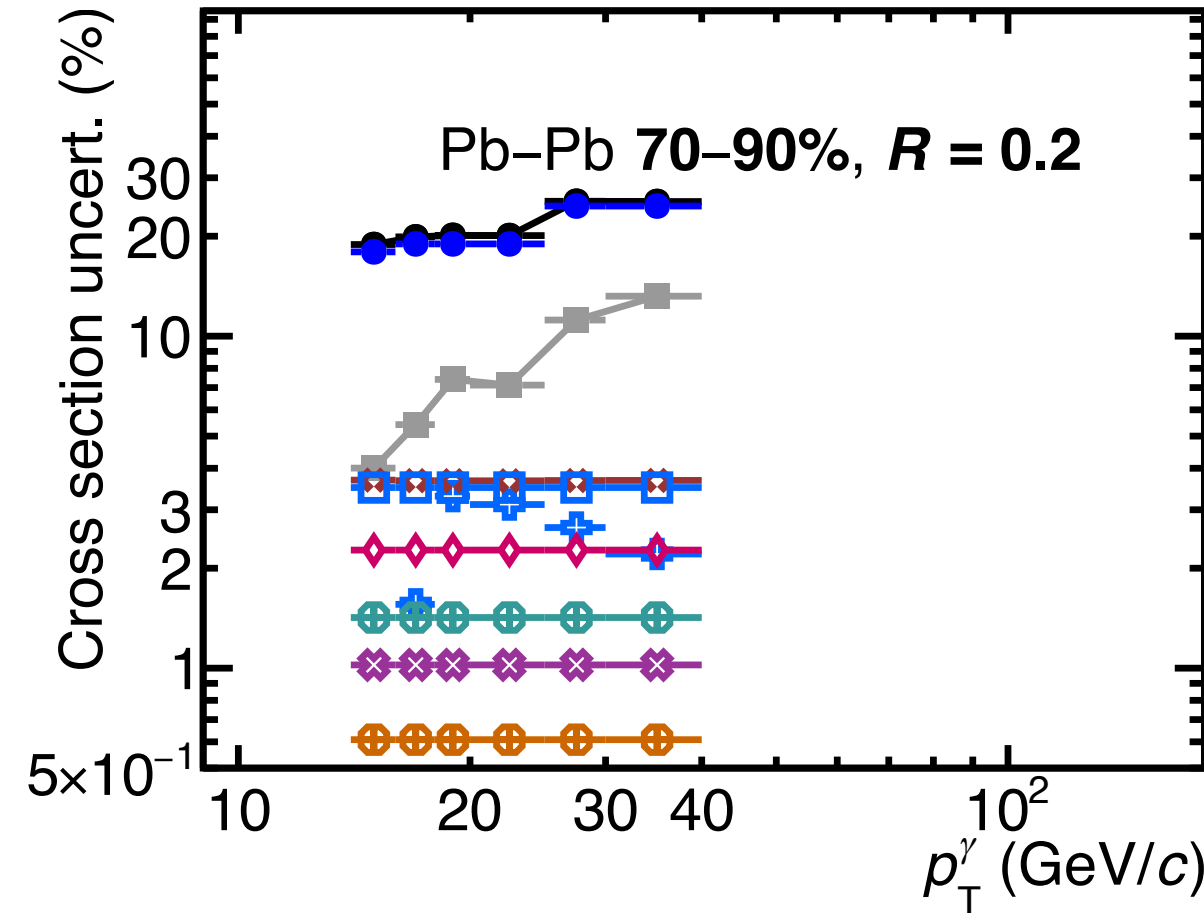
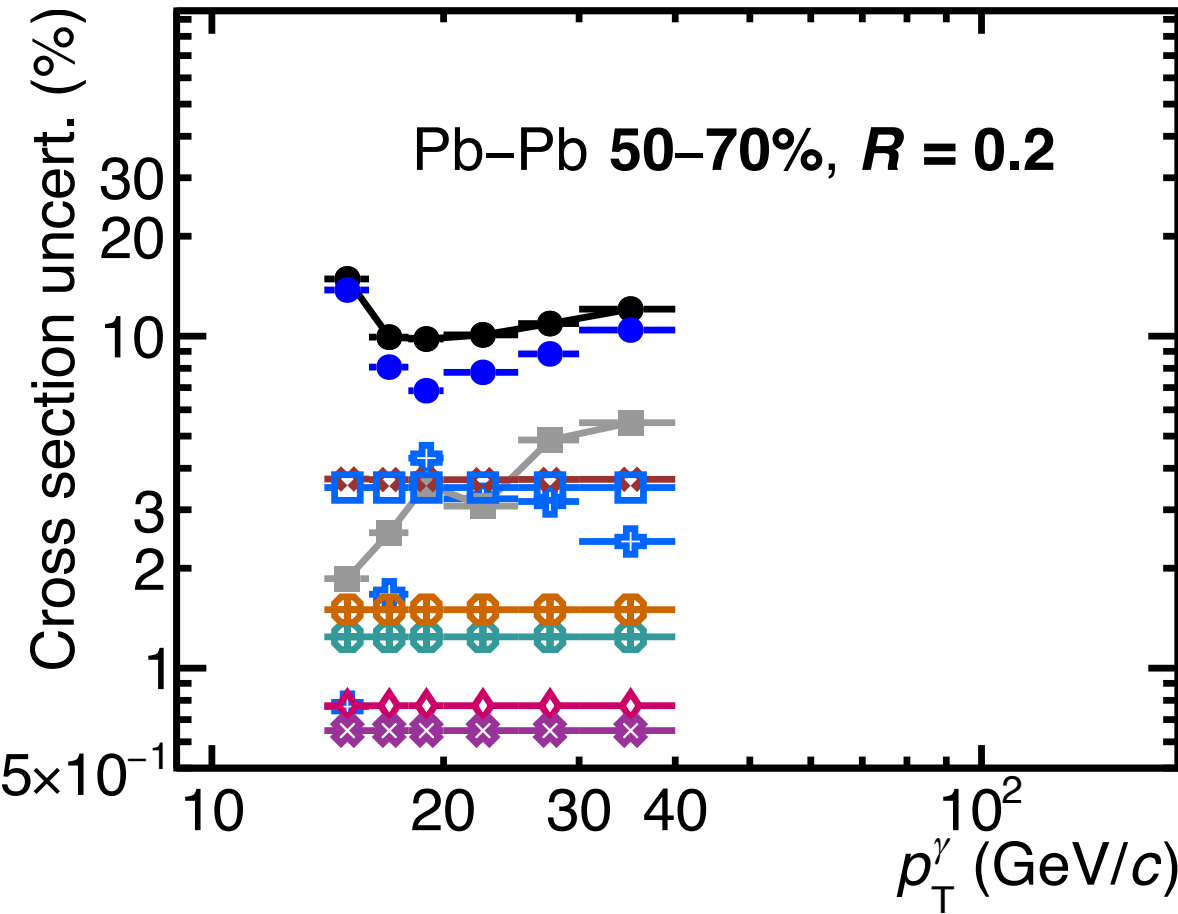


ALICE-PUBLIC-2024-003

Cross section uncertainties, pp & Pb-Pb $\sqrt{s_{NN}} = 5.02$ TeV, $R = 0.2$

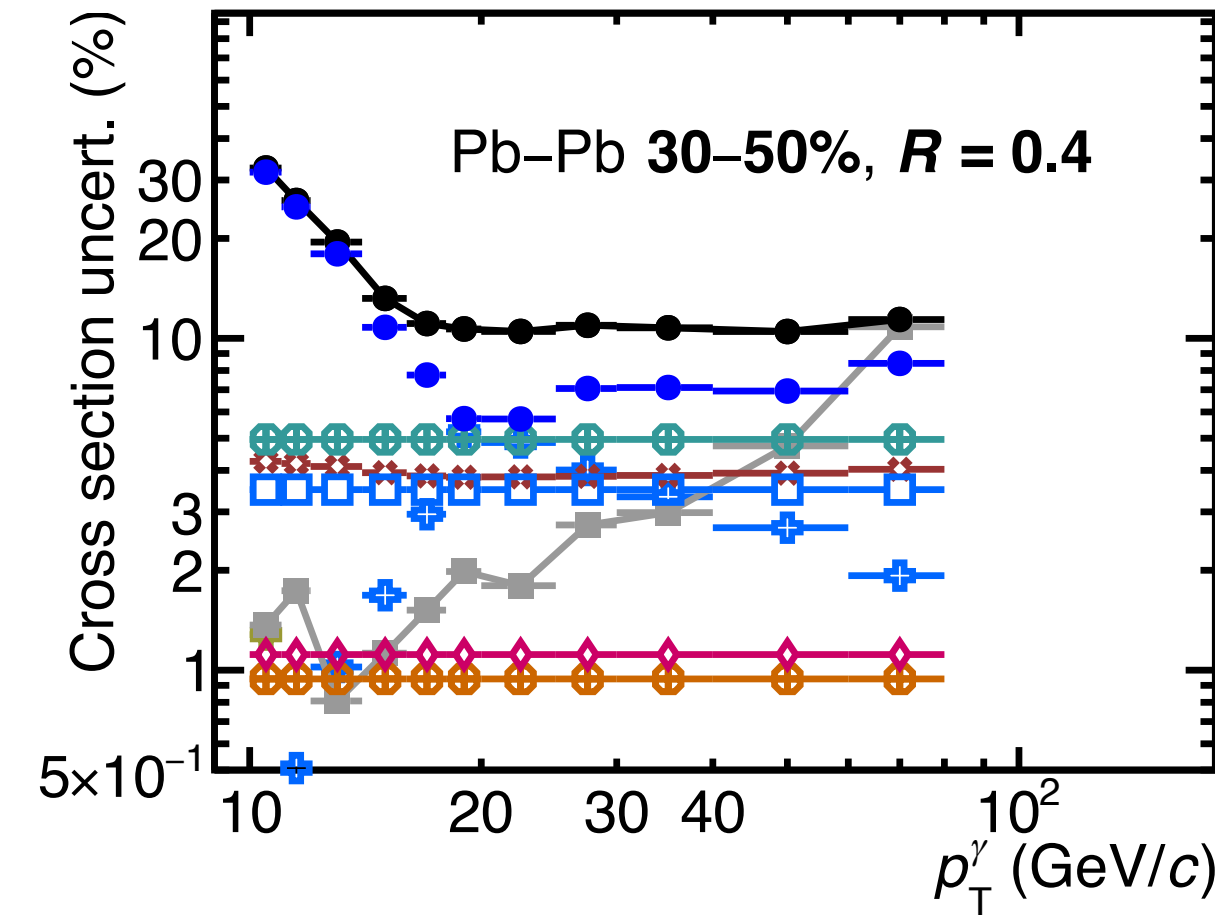
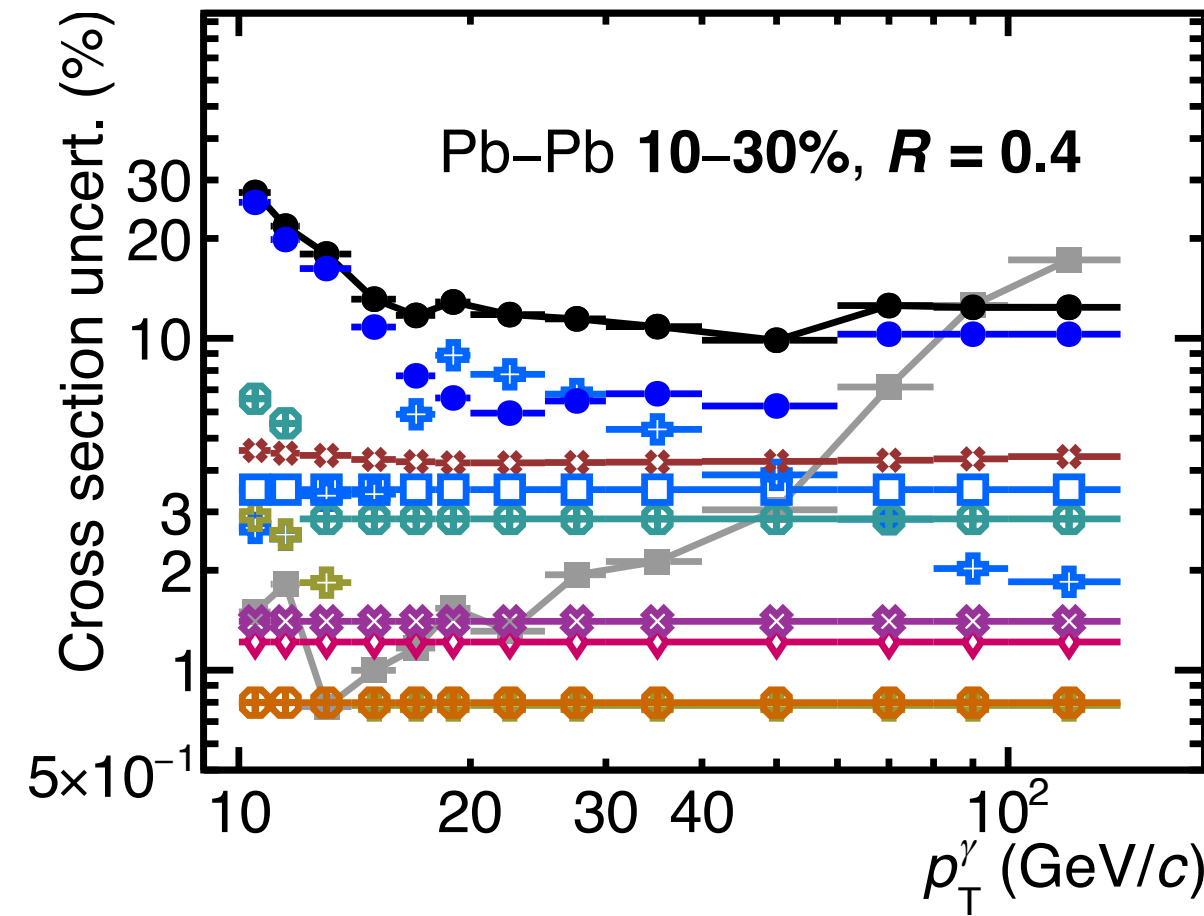
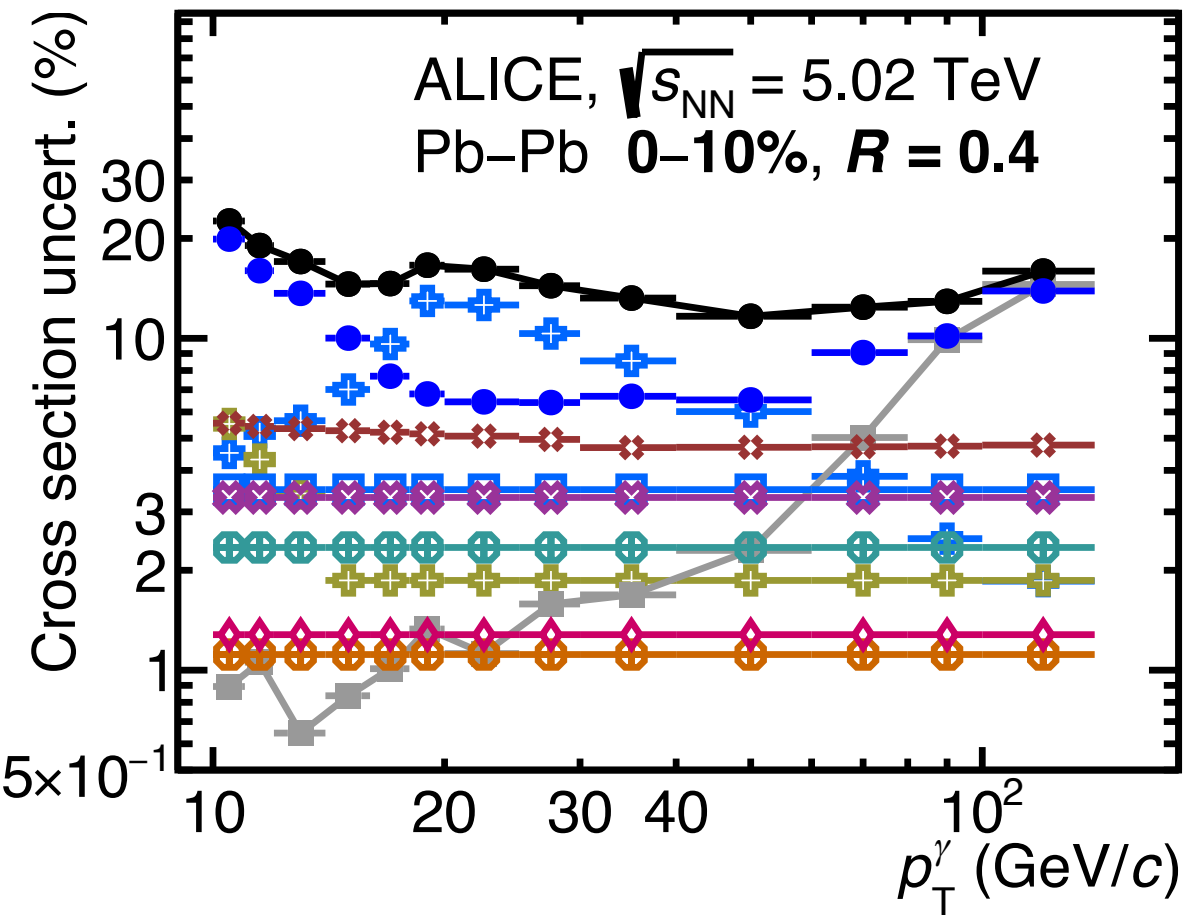


- Total systematic
- Statistical
- Purity
- ⊕ No MC tuning
- ⊕ Spectra shape
- ⊕ UE area
- ⊕ UE gap
- ◇ Sig. $\sigma_{long}^2, 5 \times 5$
- ⊗ F_+
- SM dependence
- ⊕ Other systematic

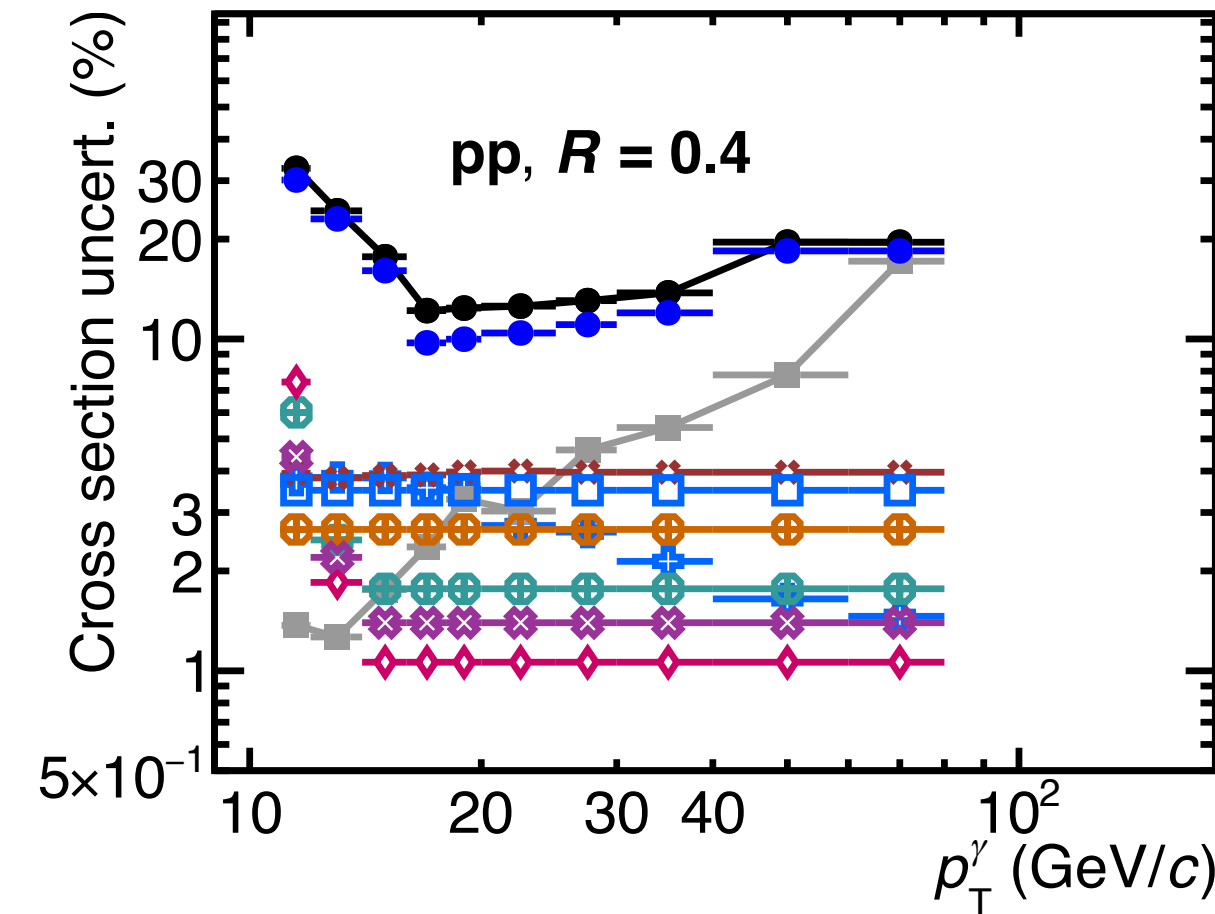
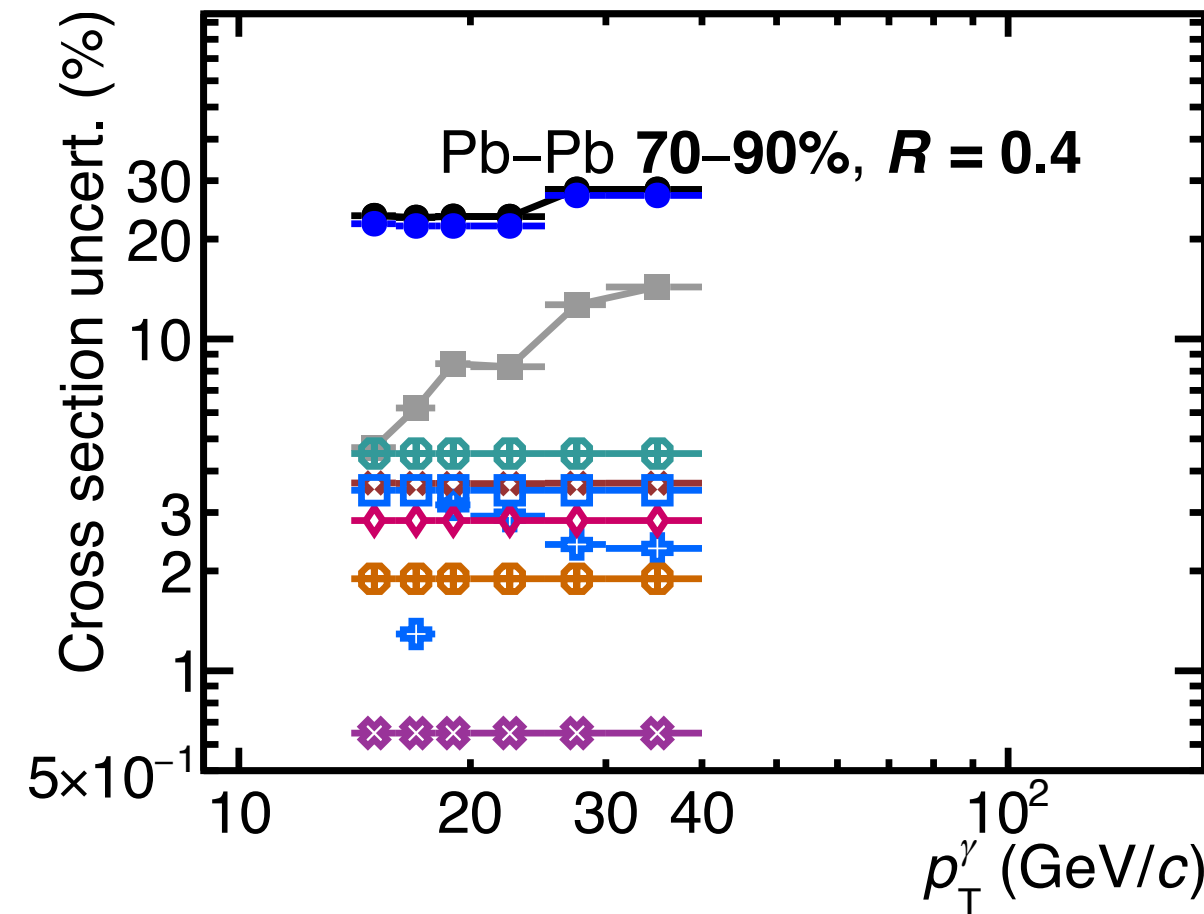
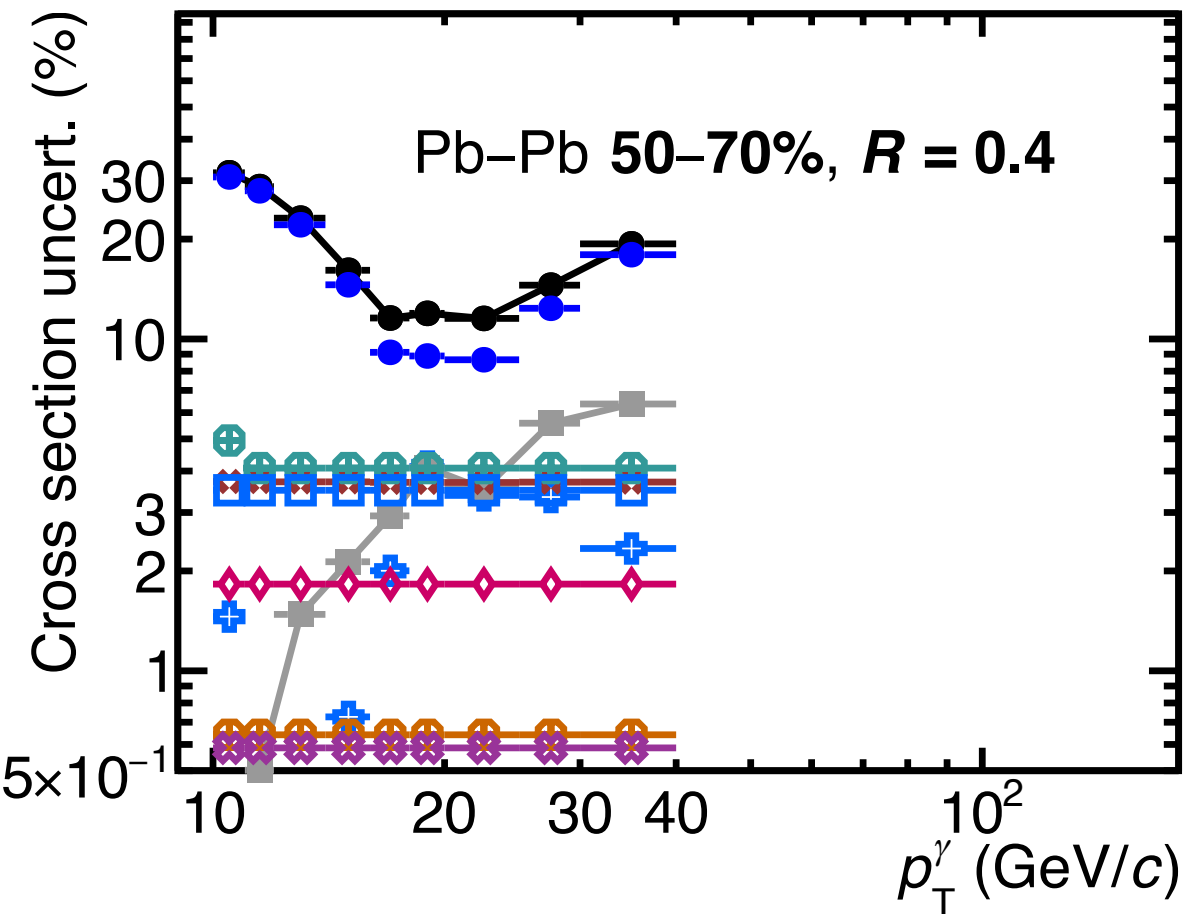


ALICE-PUBLIC-2024-003

Cross section uncertainties, pp & Pb-Pb $\sqrt{s_{NN}} = 5.02$ TeV, $R = 0.4$

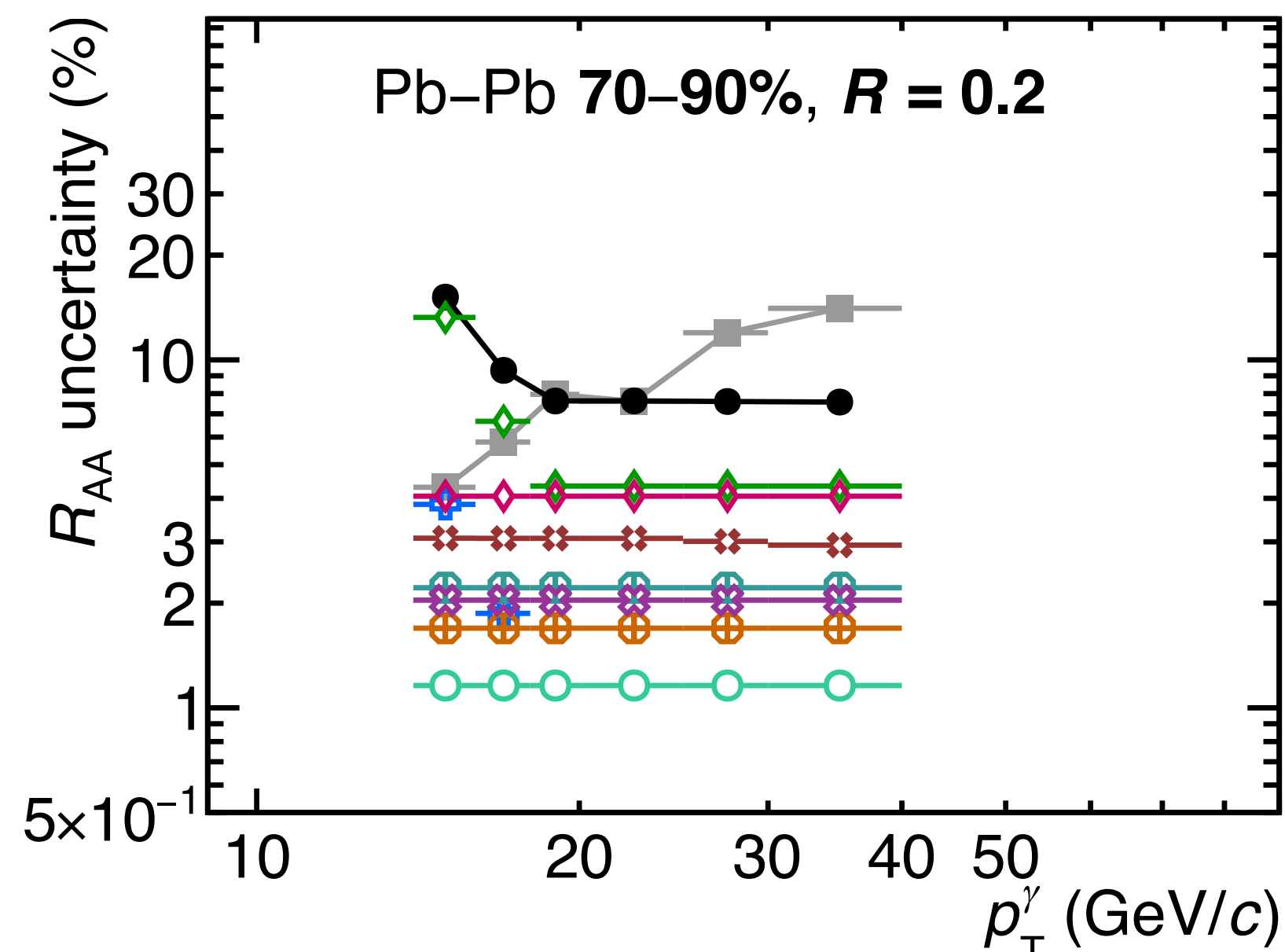
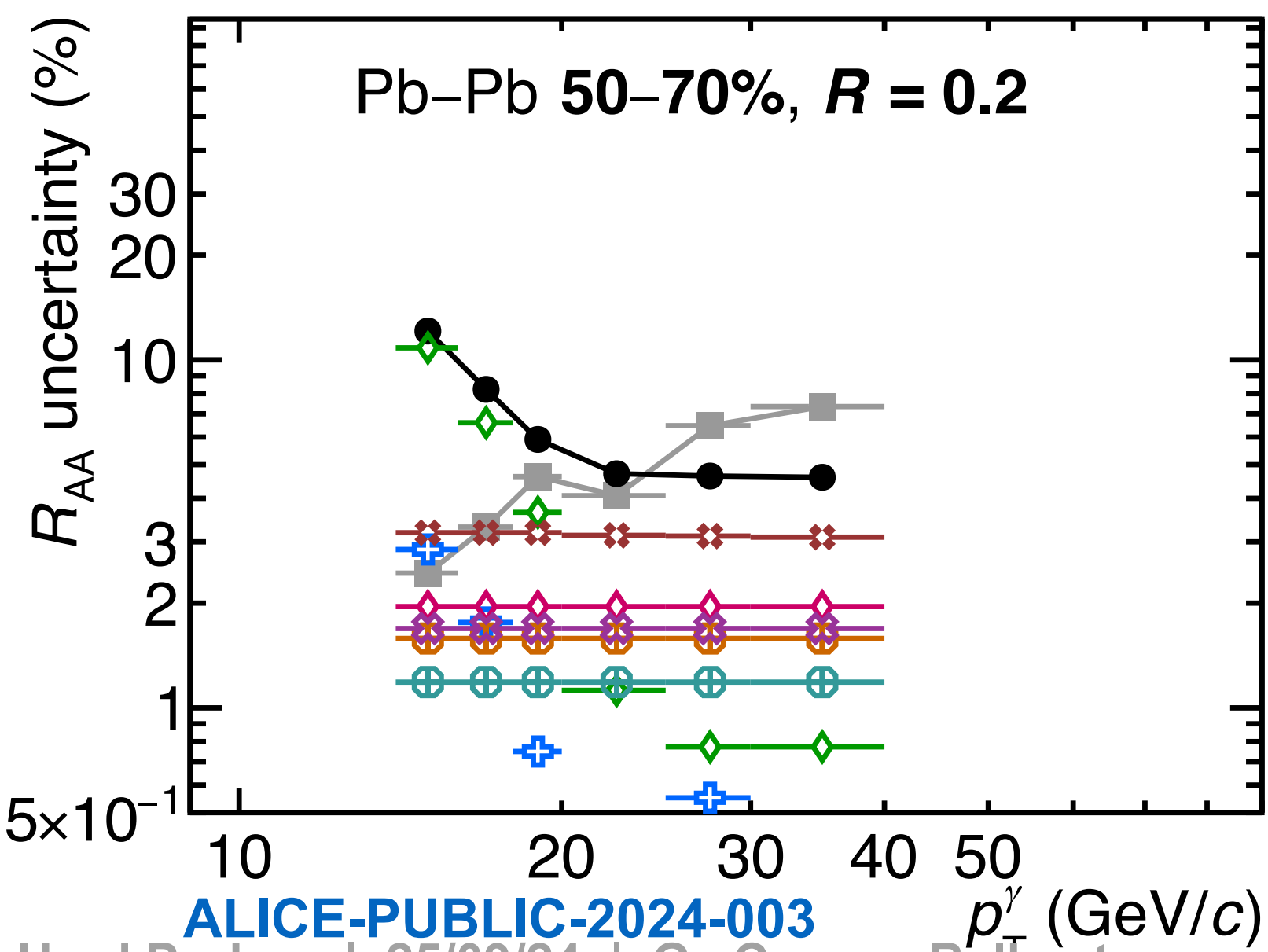
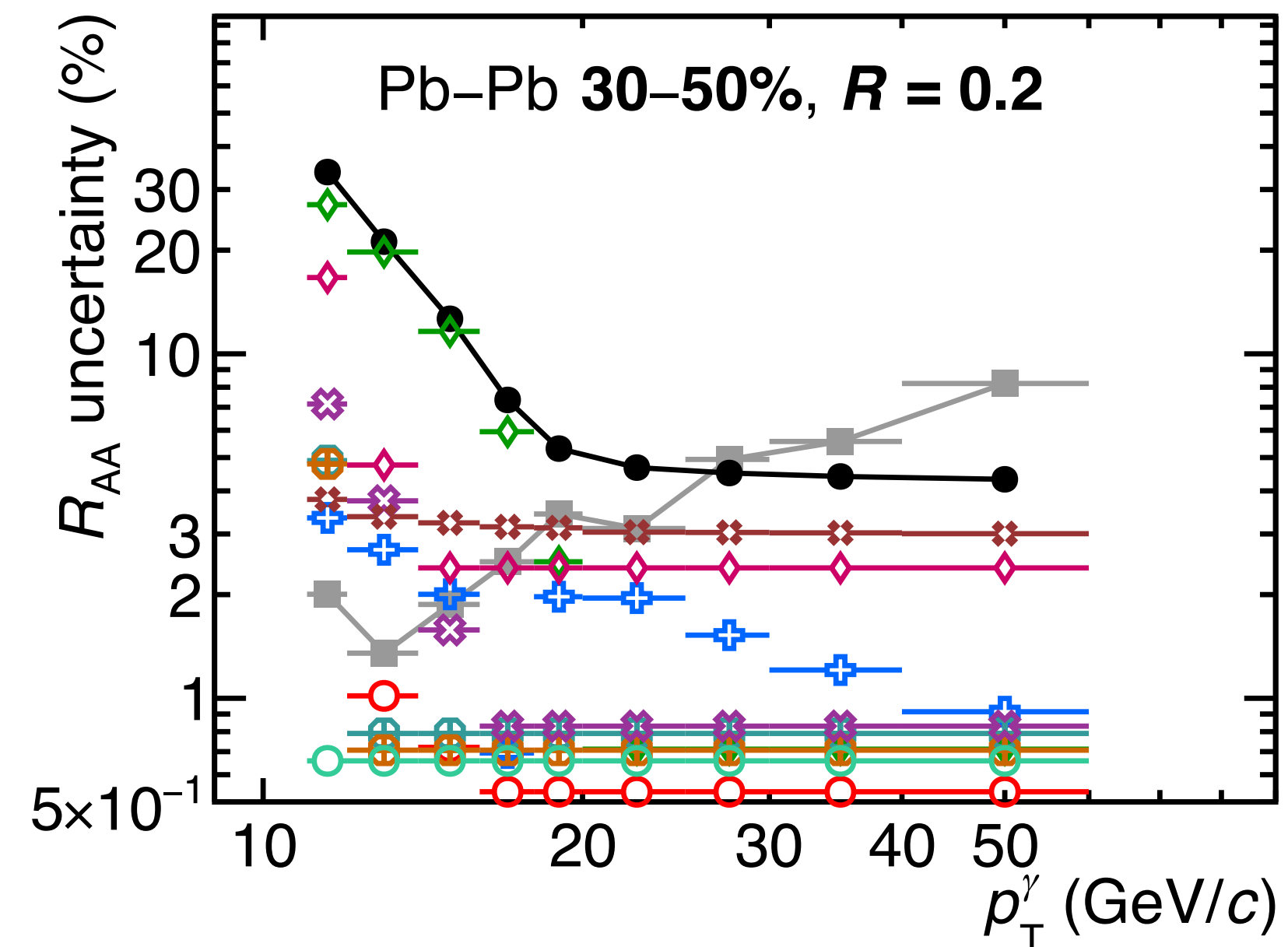
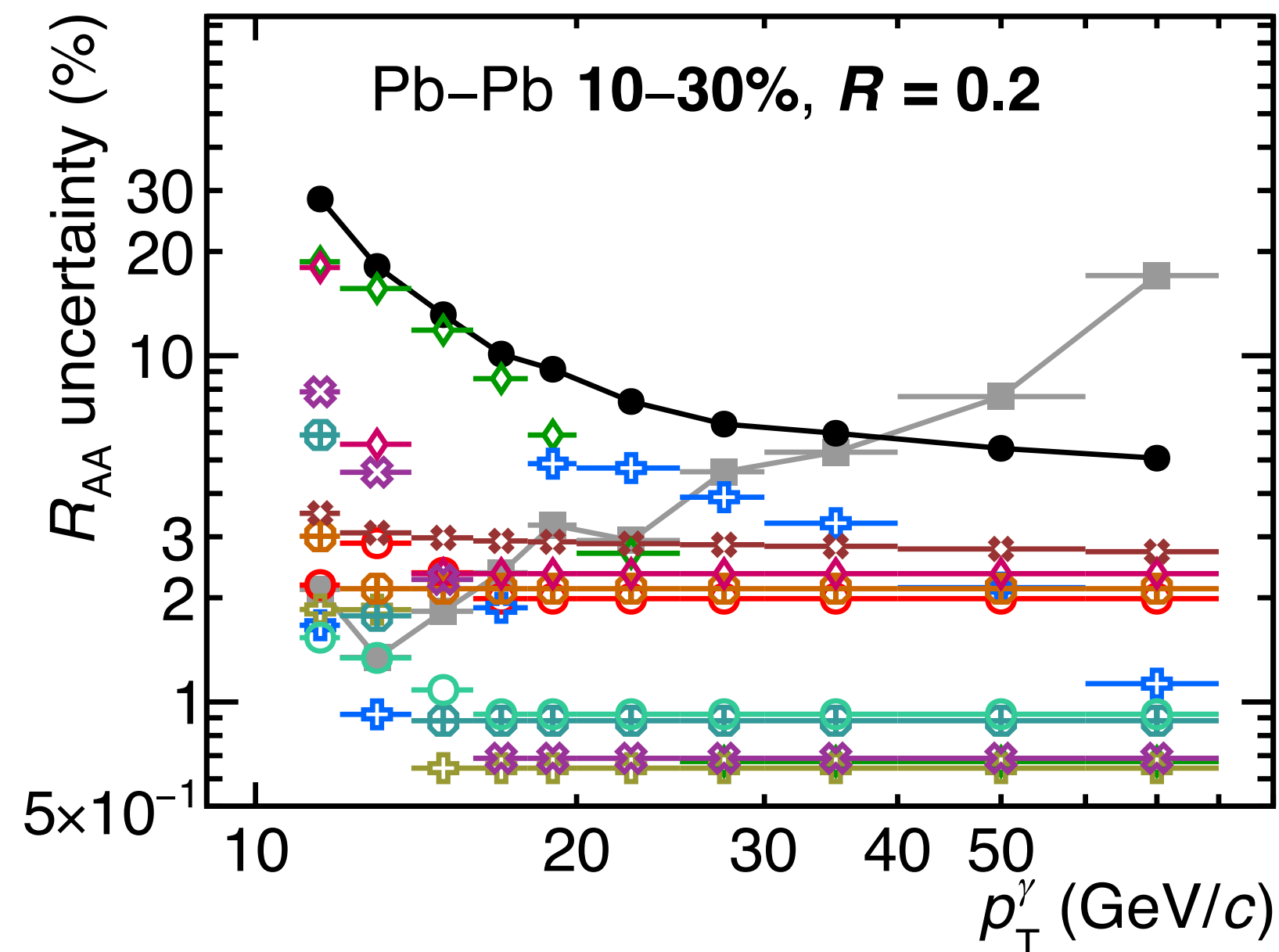
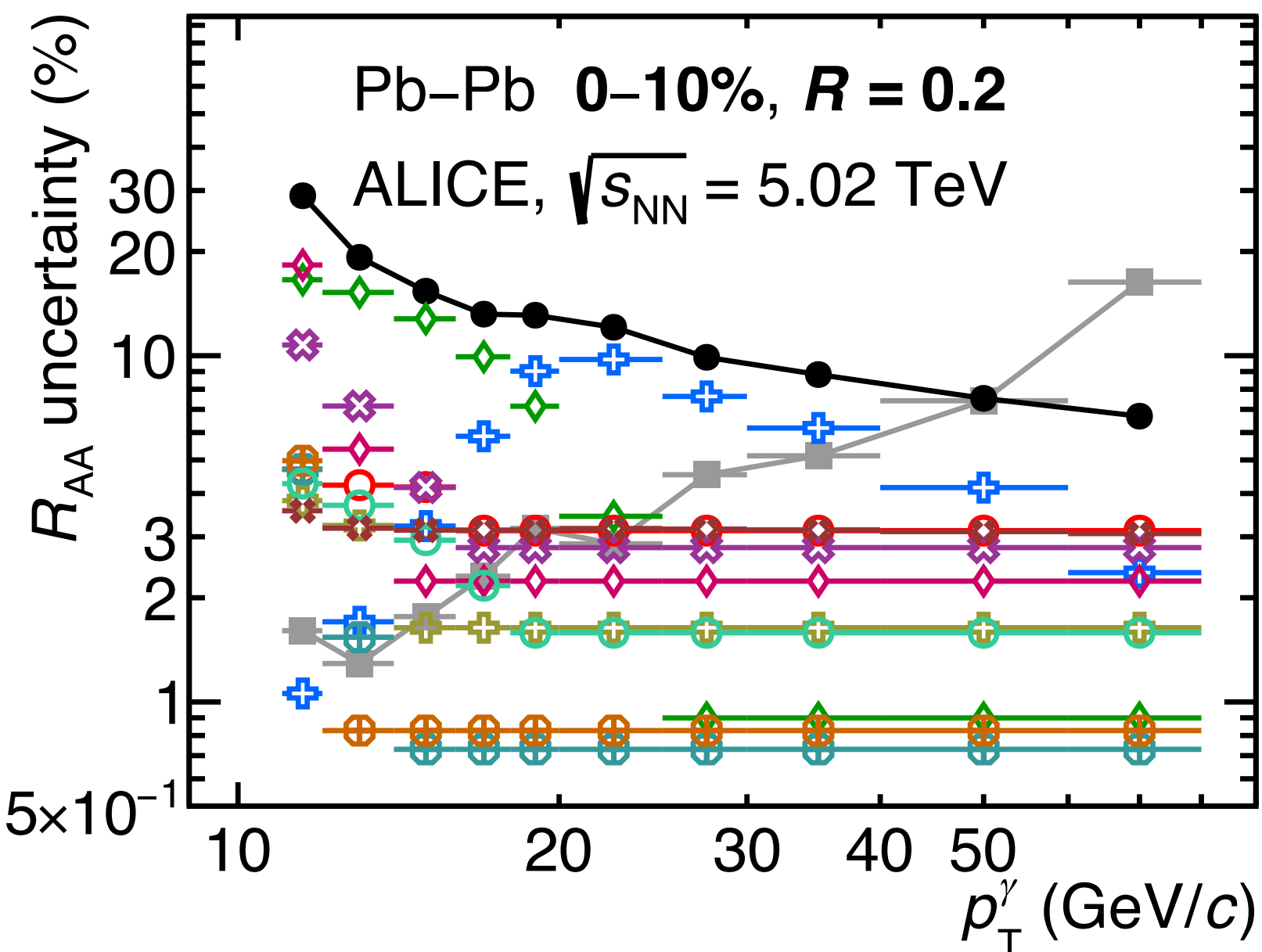


- Total systematic
- Statistical
- Purity
- ⊕ No MC tuning
- ⊕ Spectra shape
- ⊕ UE area
- ⊕ UE gap
- ◇ Sig. $\sigma_{long, 5 \times 5}^2$
- ⊗ F_+
- SM dependence
- ⊕ Other systematic



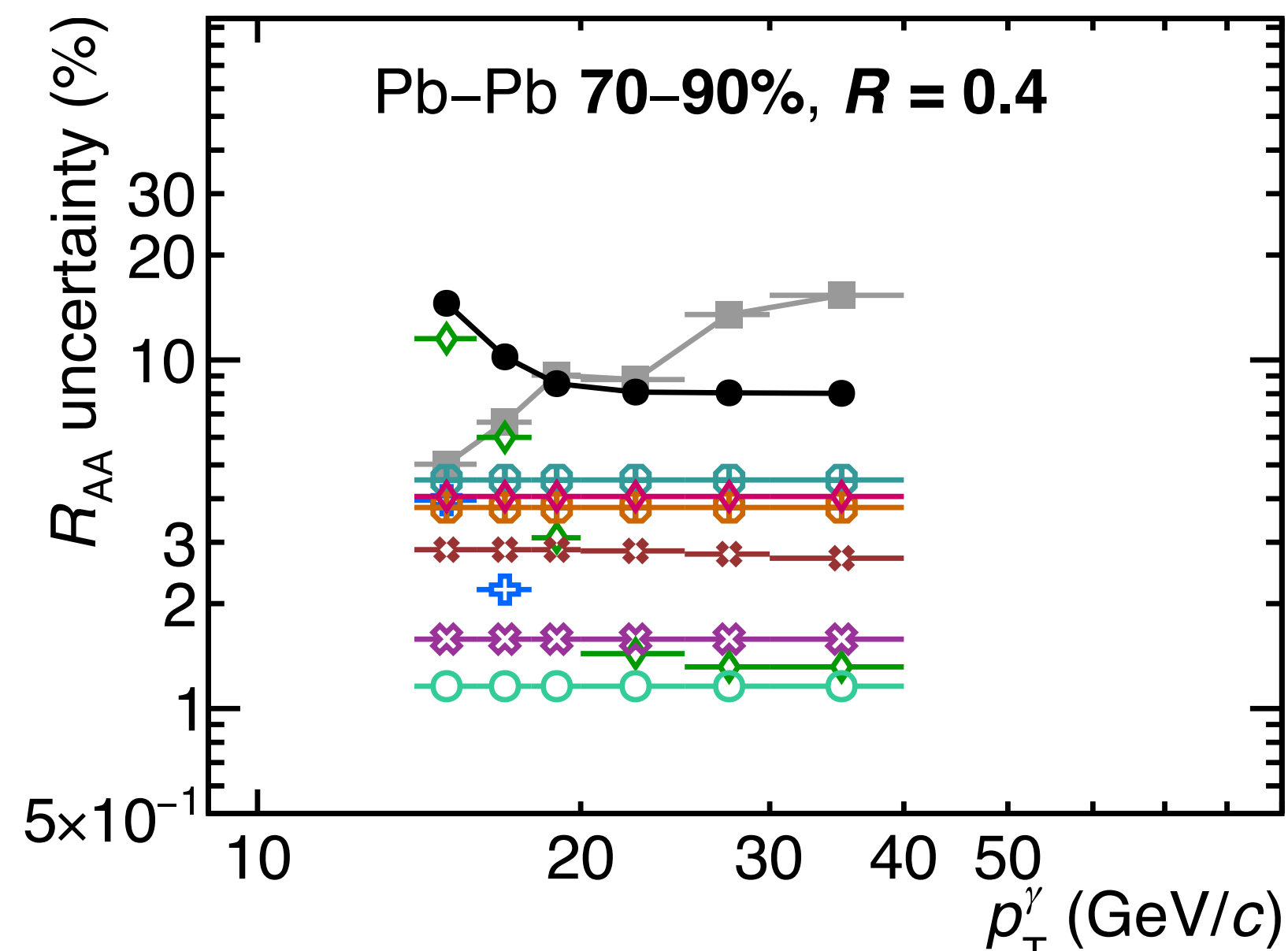
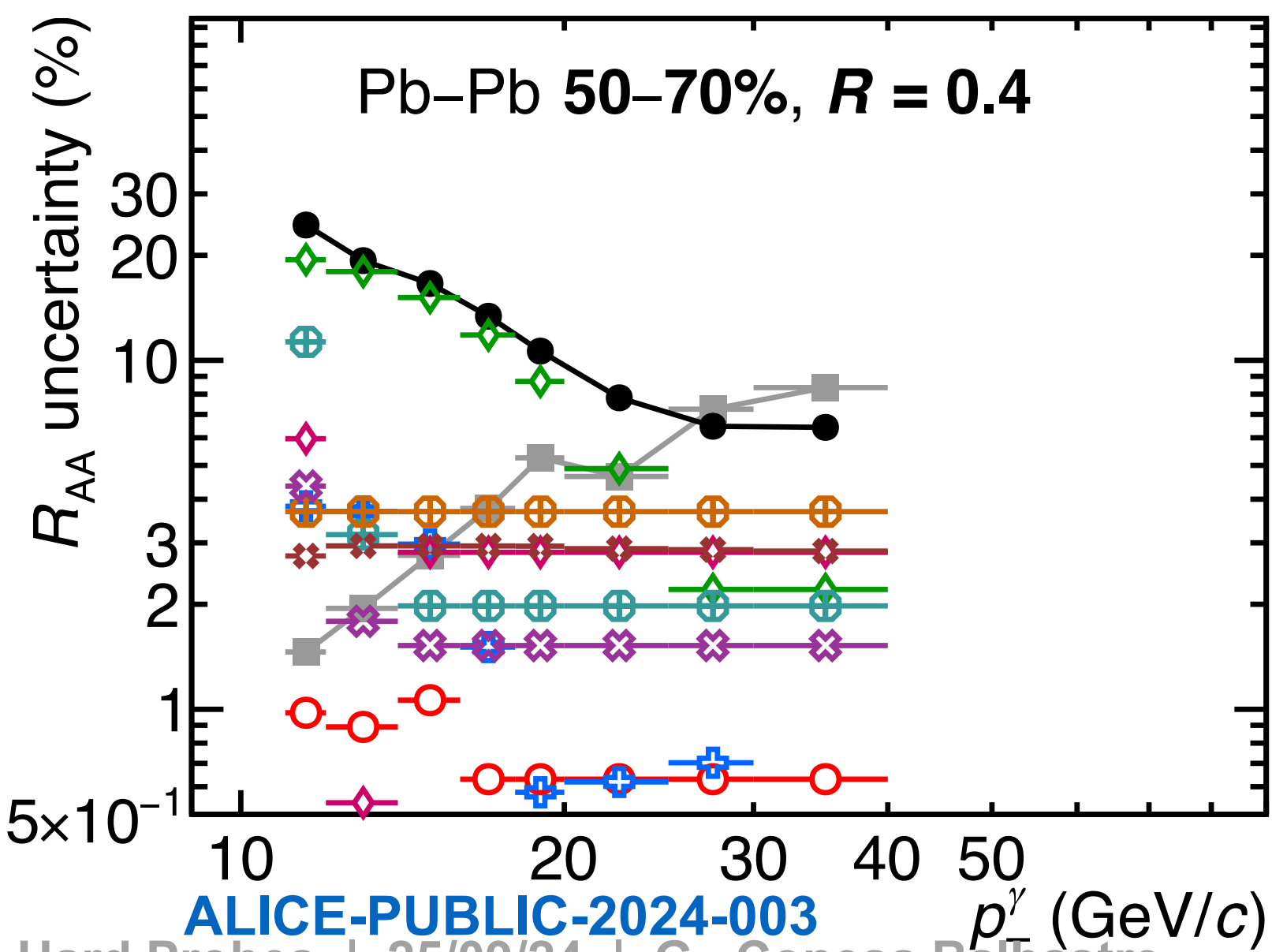
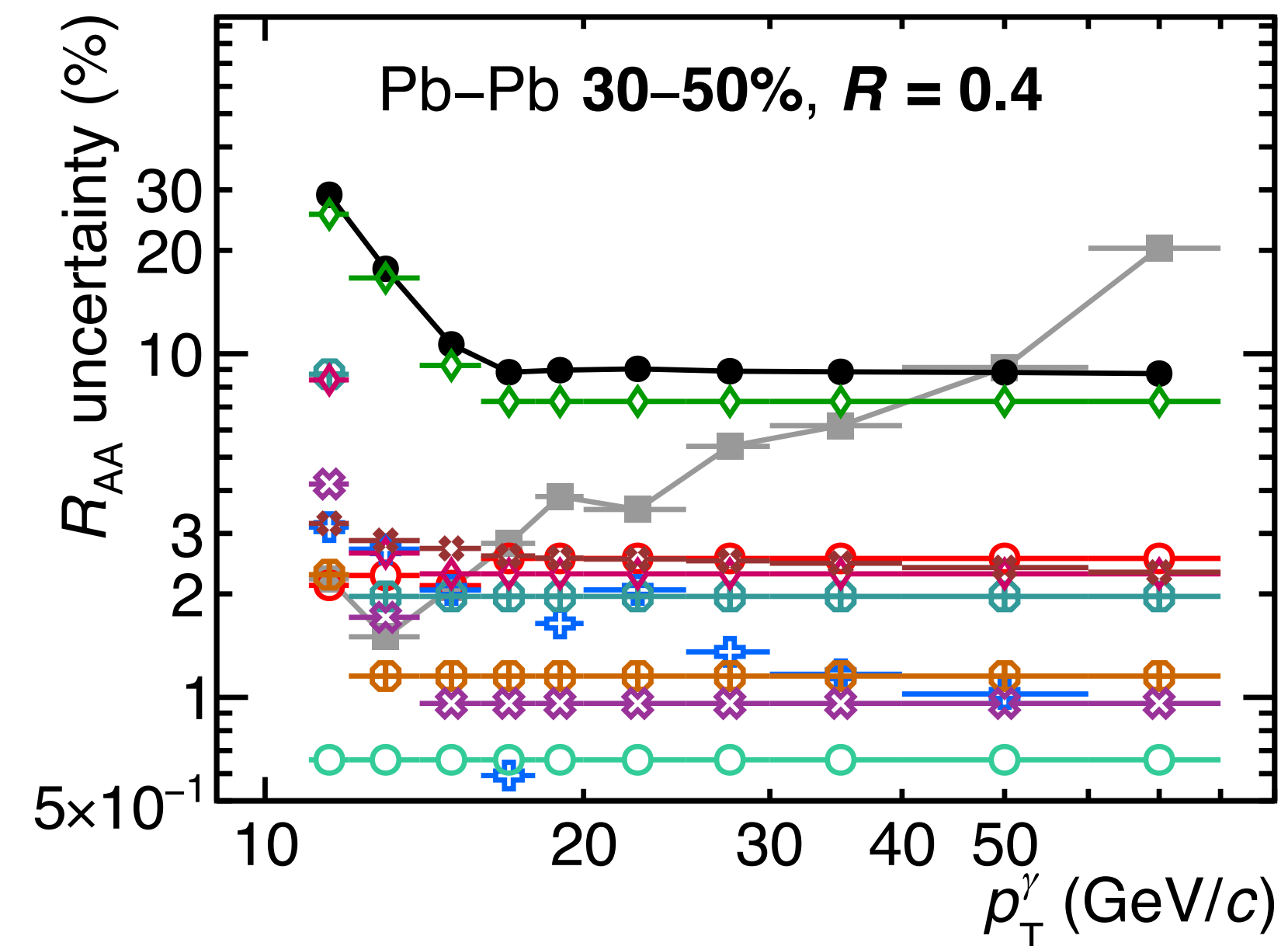
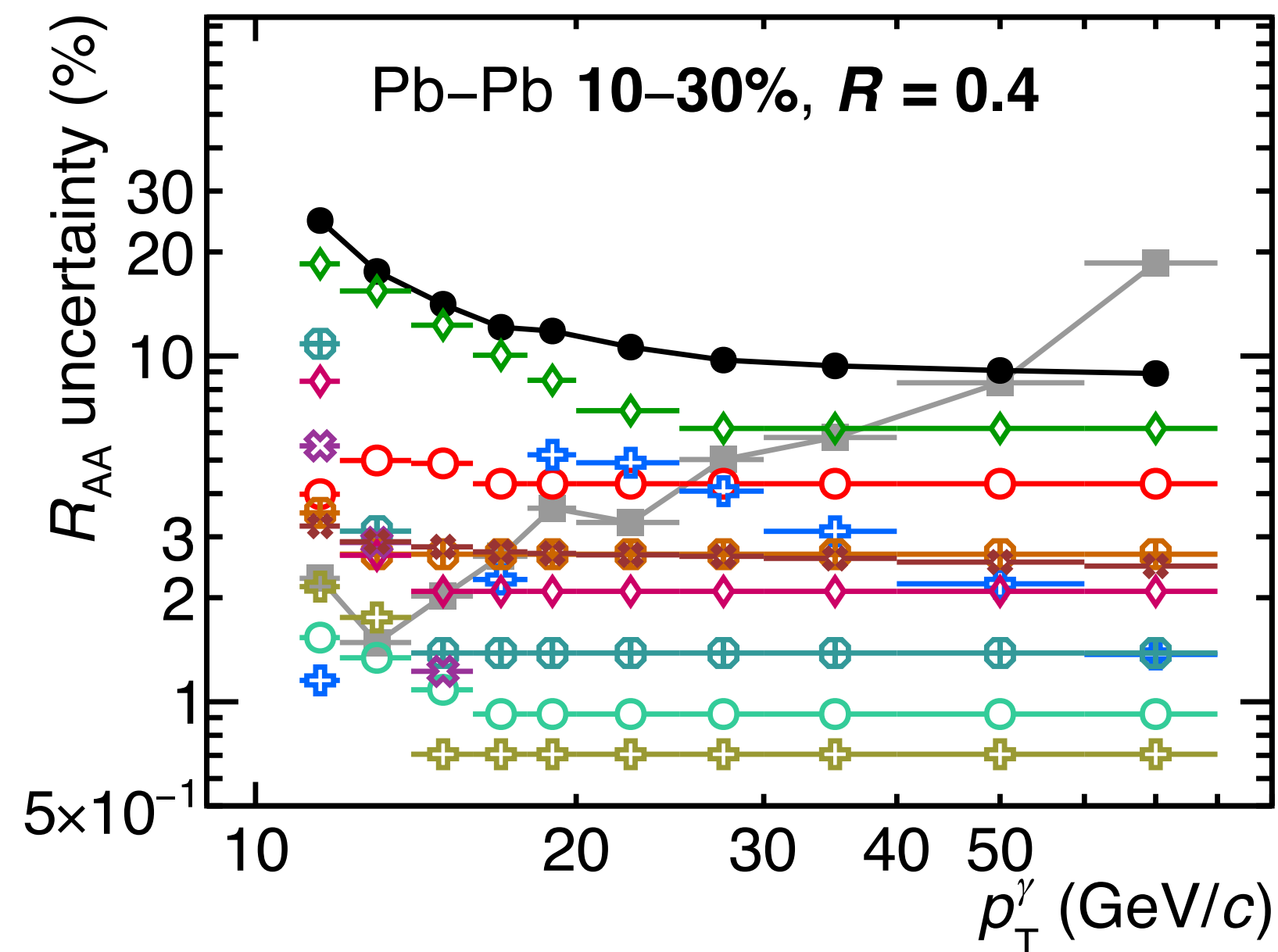
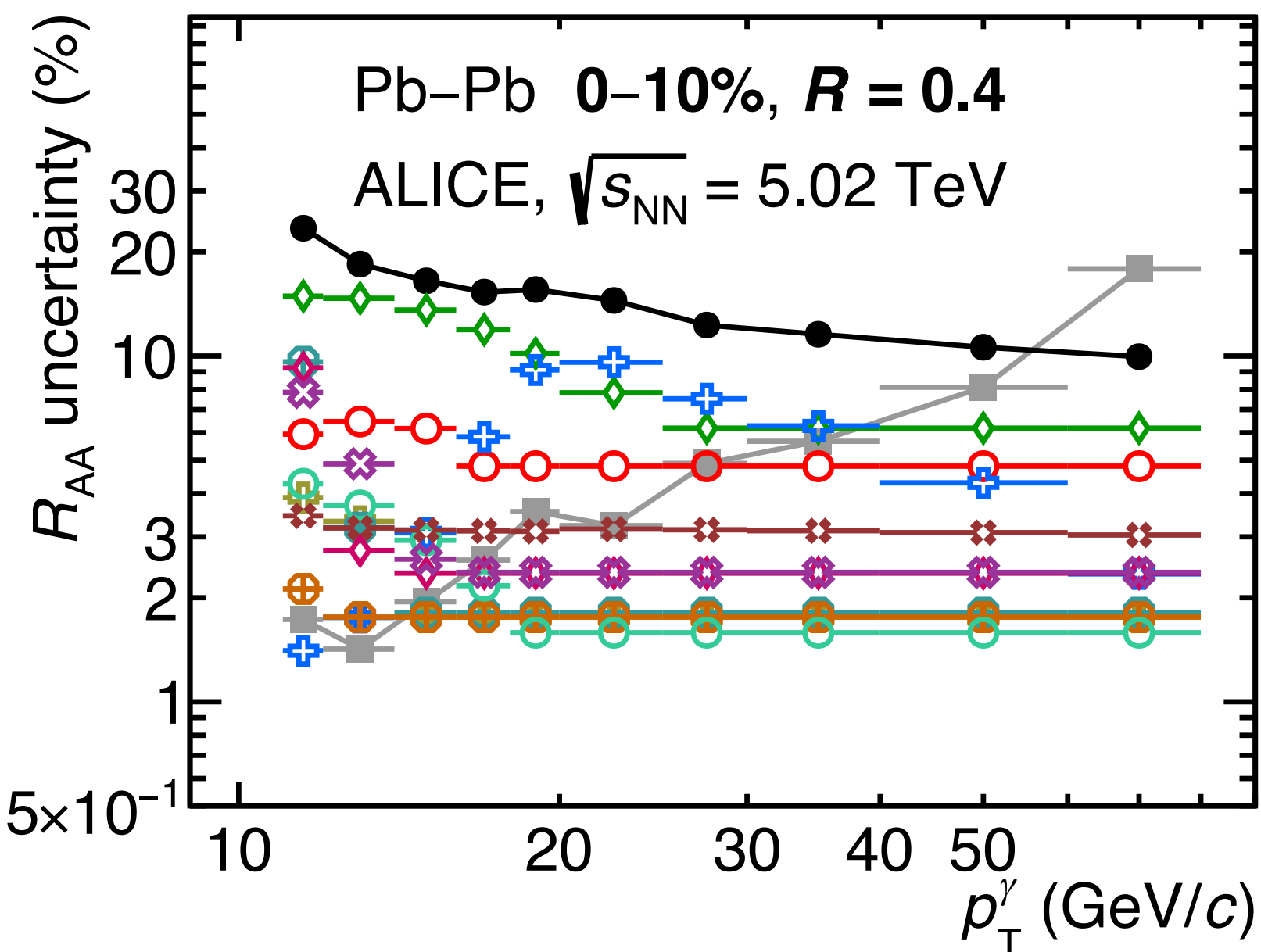
ALICE-PUBLIC-2024-003

R_{AA} uncertainties, $R = 0.2$



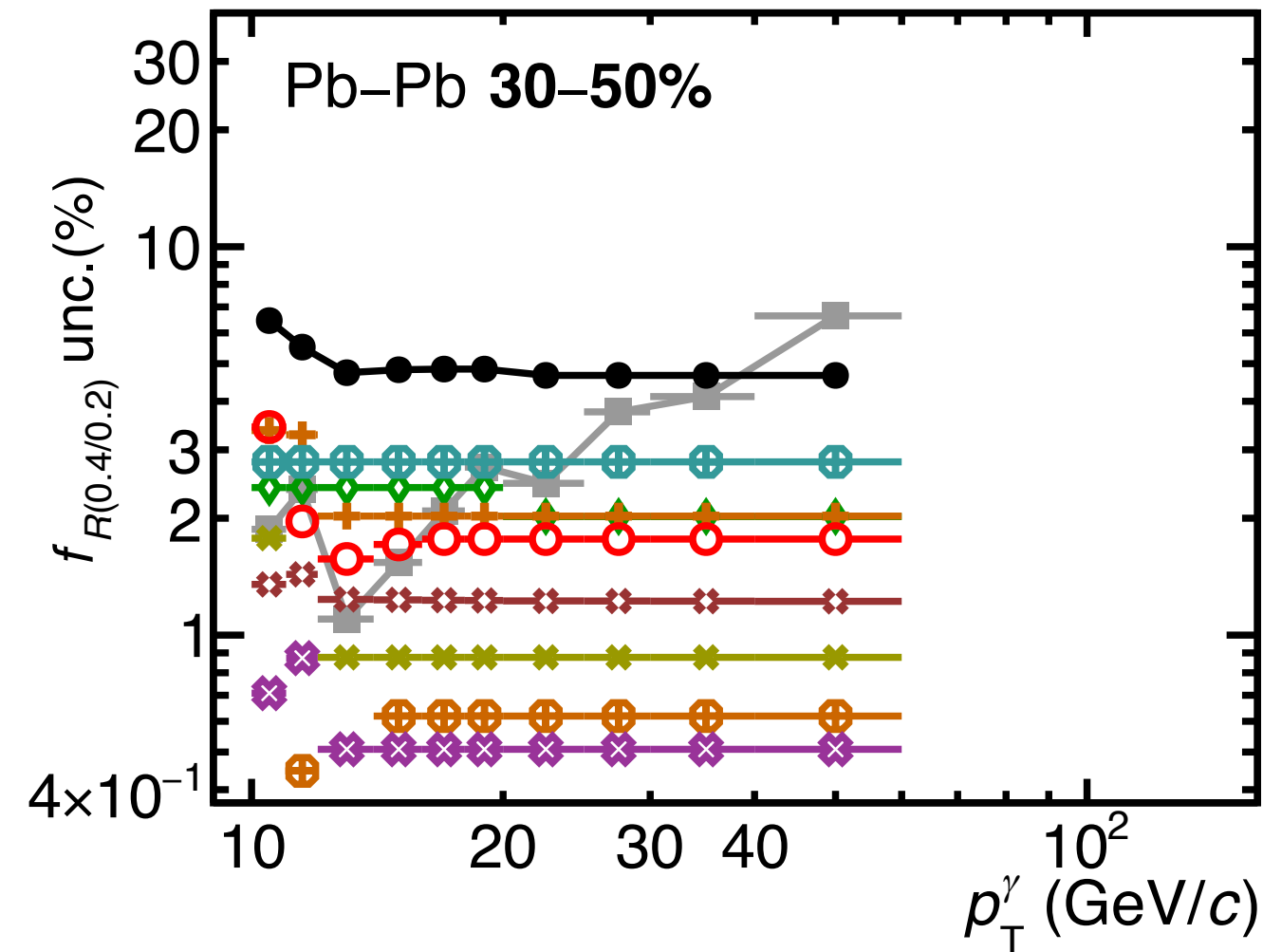
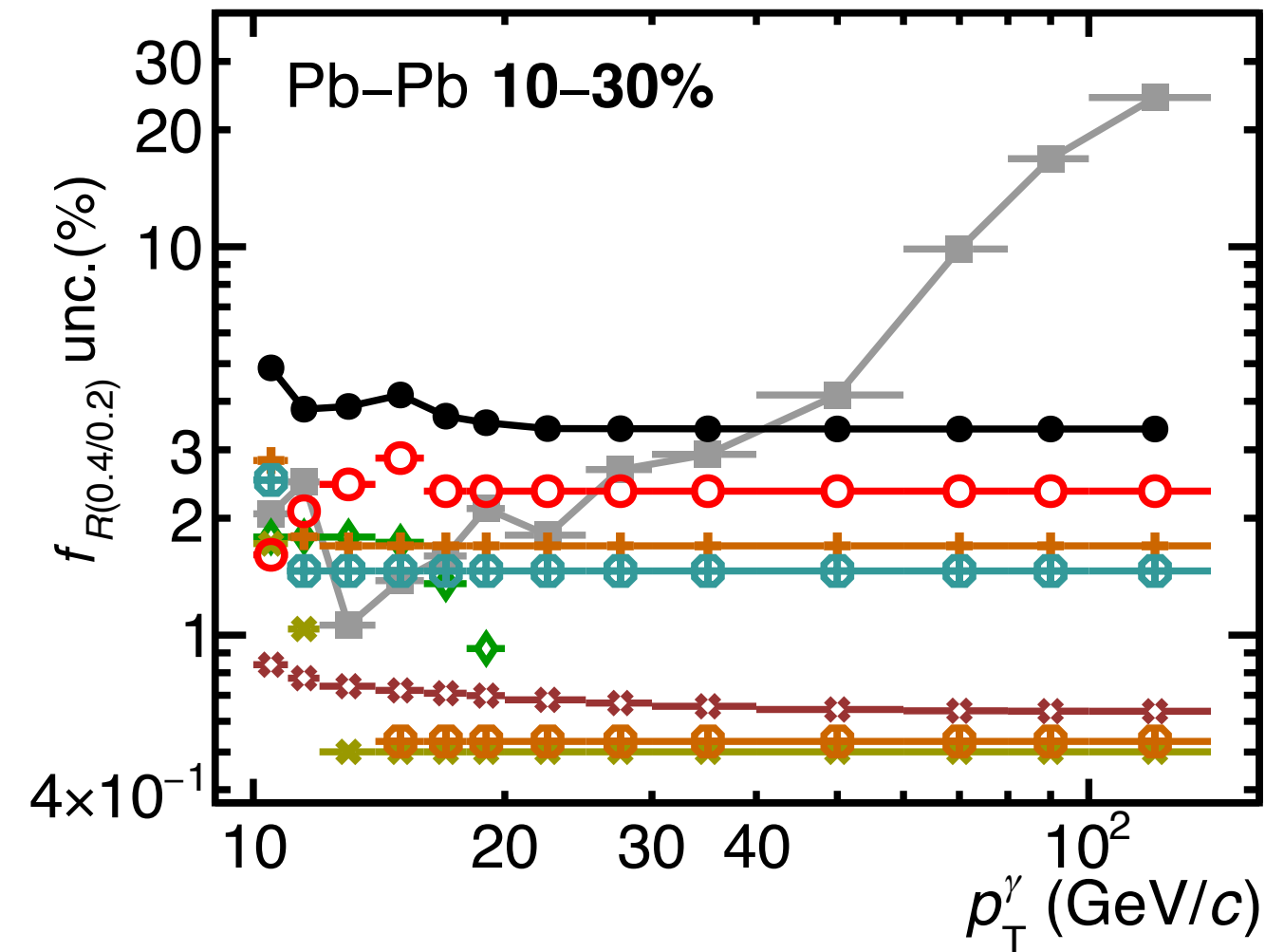
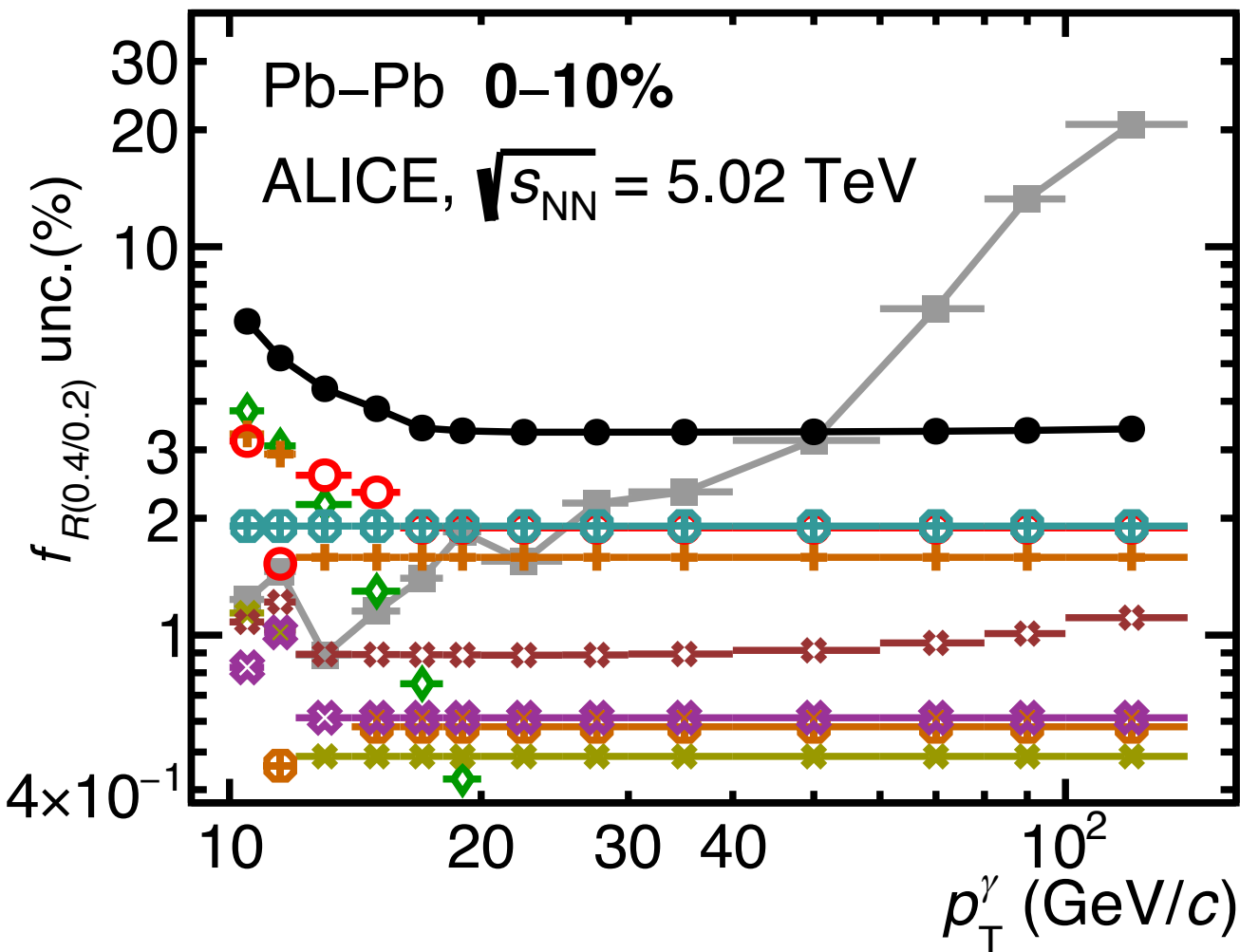
- Total systematic
- Statistical
- ◇ Isolation probability
- MC signal amount
- + No MC tuning
- + Spectra shape
- ⊕ UE area
- ⊕ UE gap
- ◇ Sig. $\sigma_{long, 5 \times 5}^2$
- Time
- ◇ F_+
- ⋄ Other systematic

R_{AA} uncertainties, $R = 0.4$

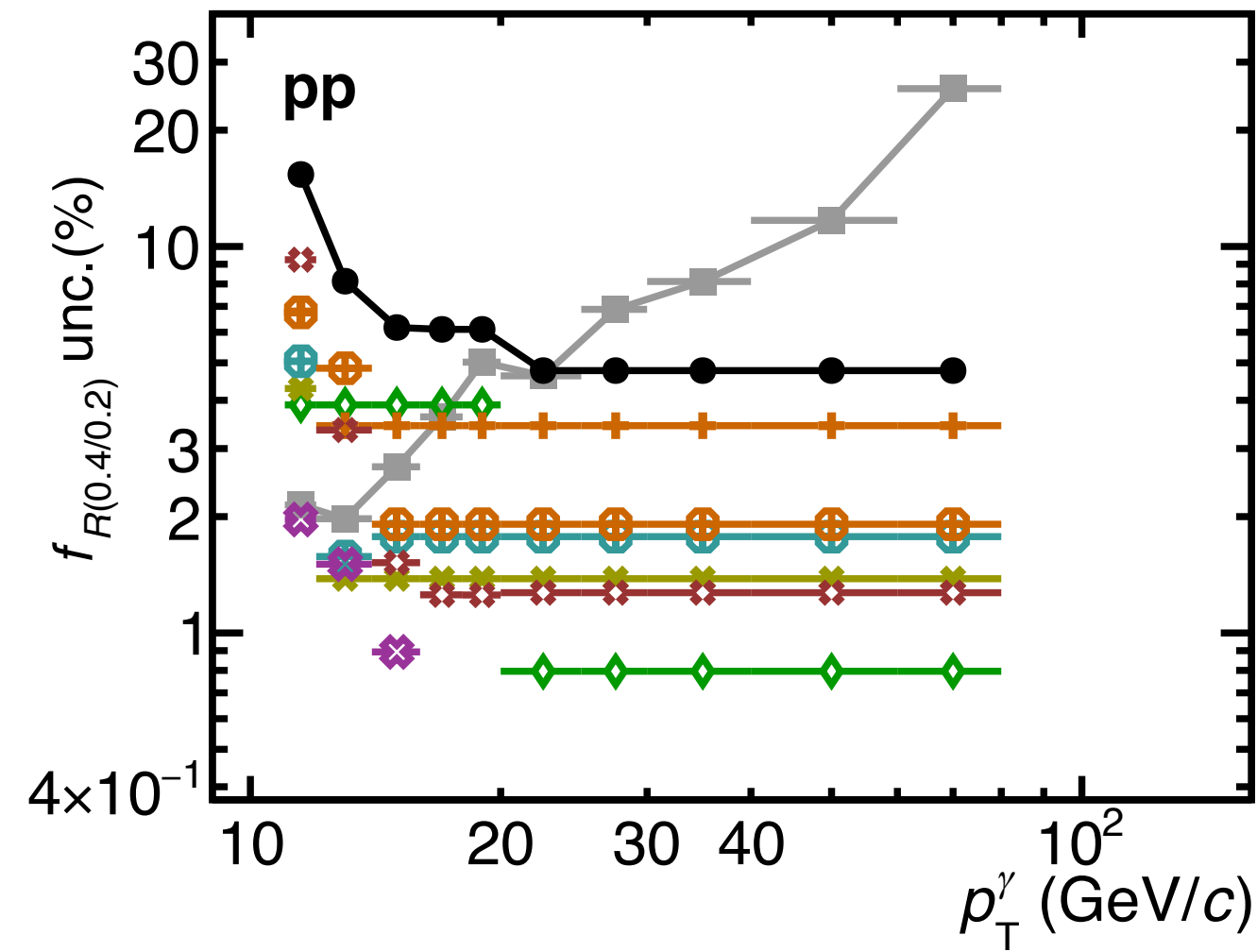
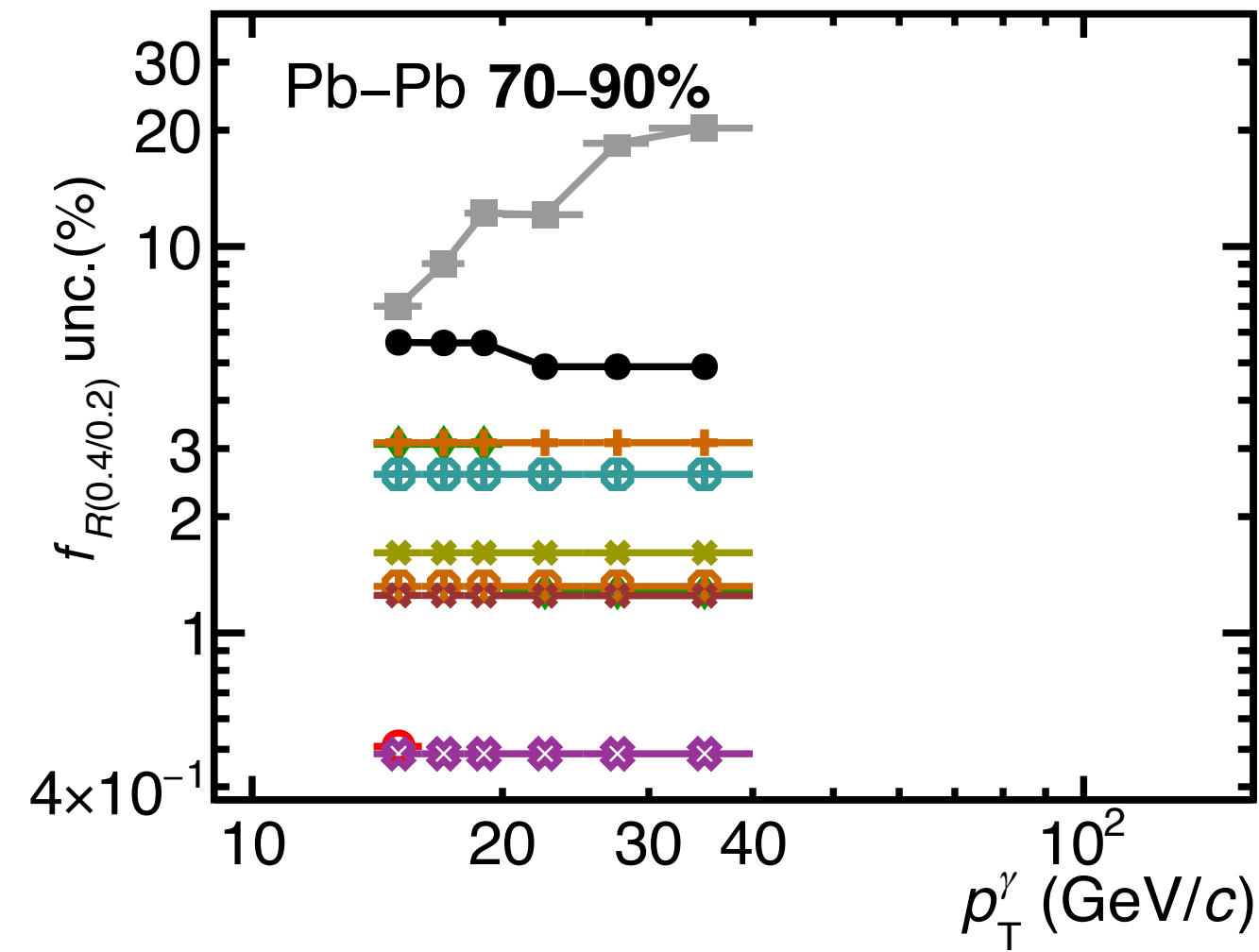
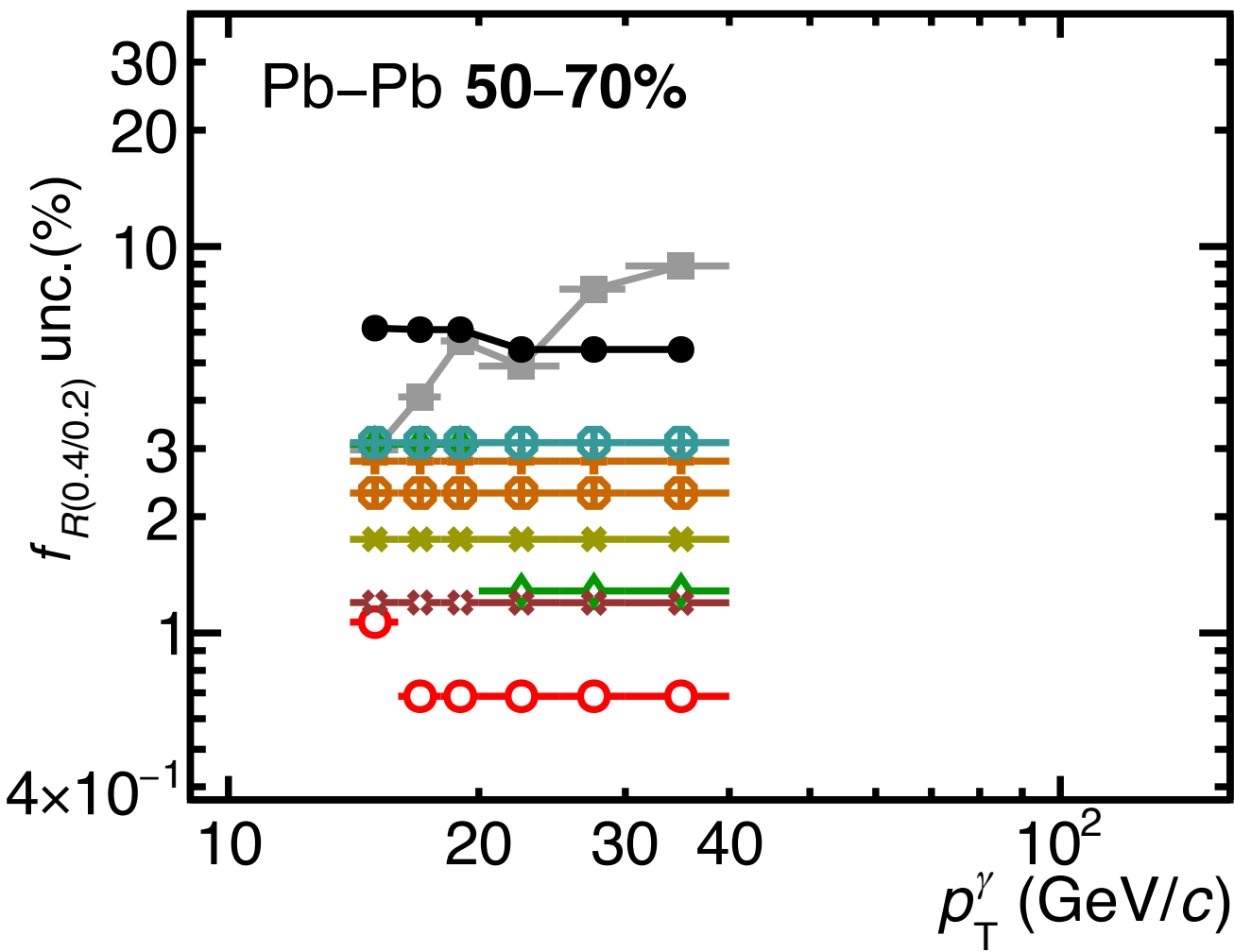


- Total systematic
- Statistical
- ◇ Isolation probability
- MC signal amount
- ⊕ No MC tuning
- ⊕ Spectra shape
- ⊕ UE area
- ⊕ UE gap
- ◇ Sig. $\sigma_{long, 5 \times 5}^2$
- Time
- ⊗ F_+
- ⊗ Other systematic

$R = 0.4$ over $R = 0.2$ ratio uncertainties, pp & Pb-Pb $\sqrt{s_{NN}} = 5.02$ TeV



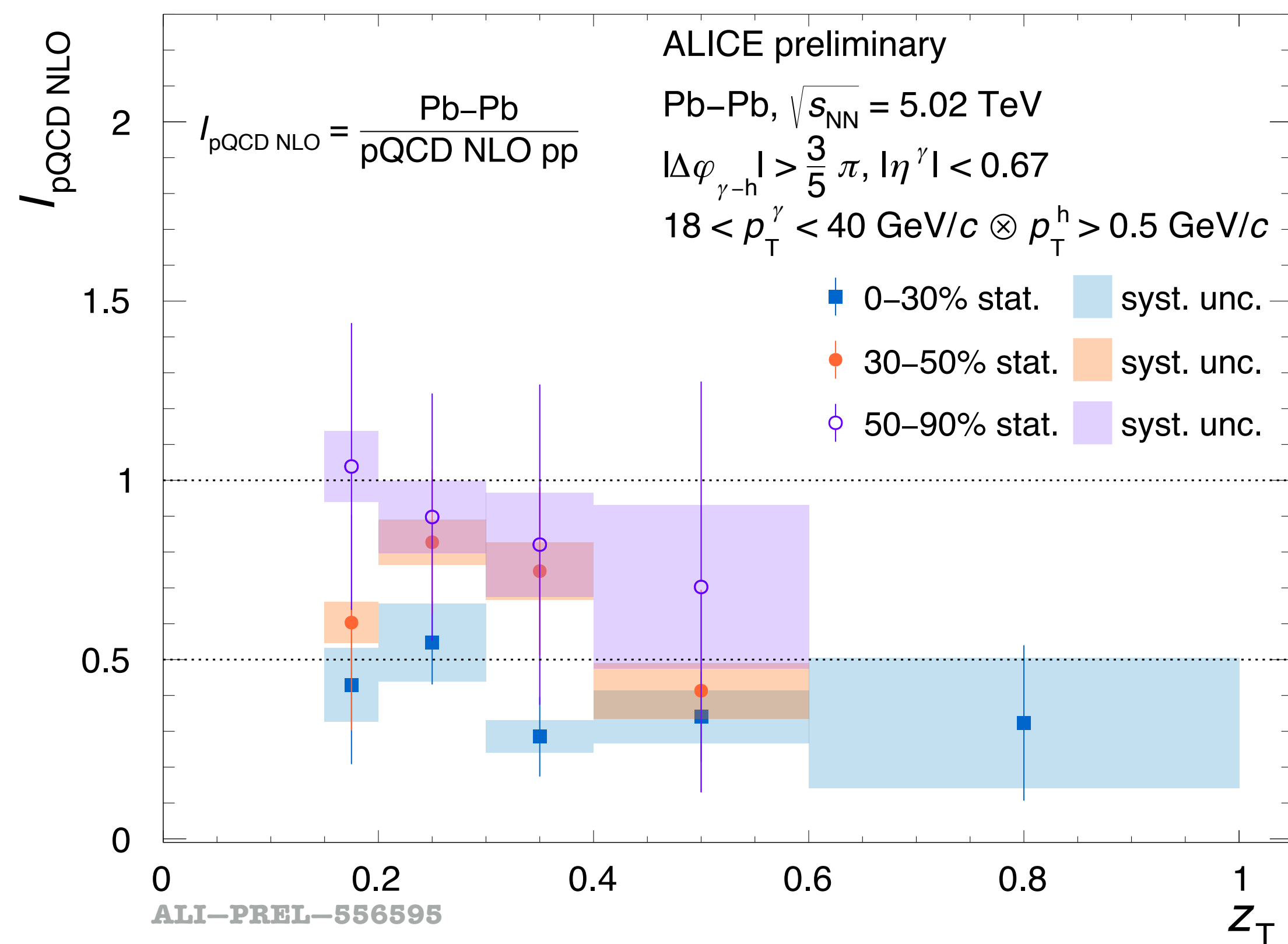
- Total systematic
- Statistical
- ◆ Isolation probability
- + Bkg. $p_T^{iso, ch}$
- × Bkg. $\sigma_{long, 5 \times 5}^2$
- MC signal amount
- UE area
- UE gap
- × F_+
- × Other systematic



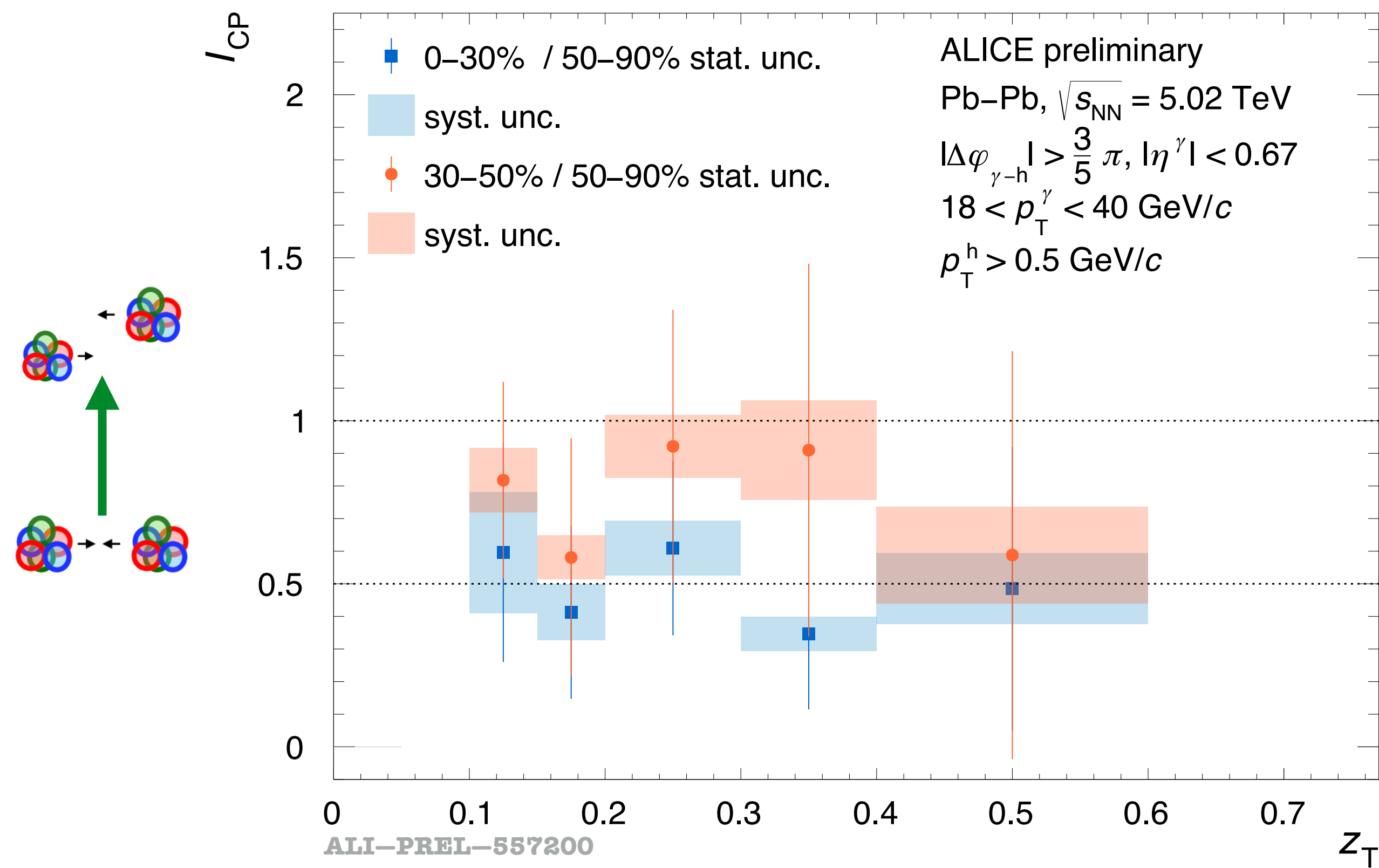
ALICE-PUBLIC-2024-003

Isolated γ -hadron correlations in Pb-Pb: $D(z_T)$

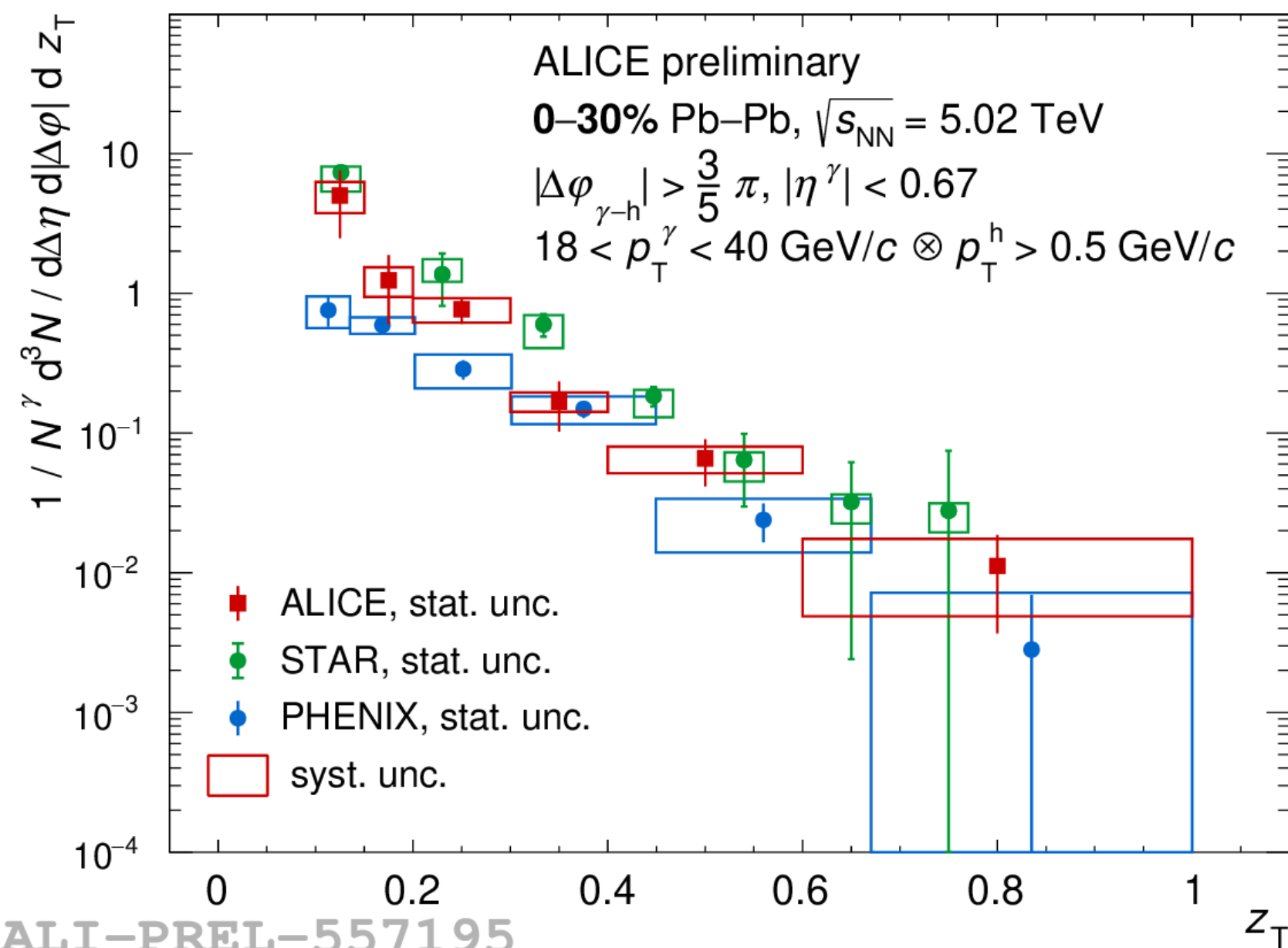
$$I_{\text{pQCD}} = \text{Pb-Pb Data} / \text{pp pQCD}$$



$$I_{\text{CP}} = \text{Pb-Pb (semi) central} / \text{peripheral}$$



Isolated γ -hadron correlations in Pb–Pb: RHIC & LHC



STAR, Phys.Lett.B 760 (2016) 689-696

0–12% Au–Au, $\sqrt{s_{NN}} = 200$ GeV

$|\Delta\phi_{\gamma-h} - \pi| \leq 1.4$

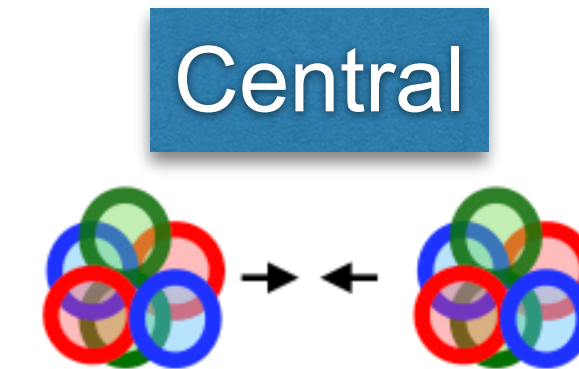
$12 < p_T^\gamma < 20$ GeV/c $\otimes p_T^h > 1.2$ GeV/c

PHENIX, PRL 111, 032301 (2013)

0–40% Au–Au, $\sqrt{s_{NN}} = 200$ GeV

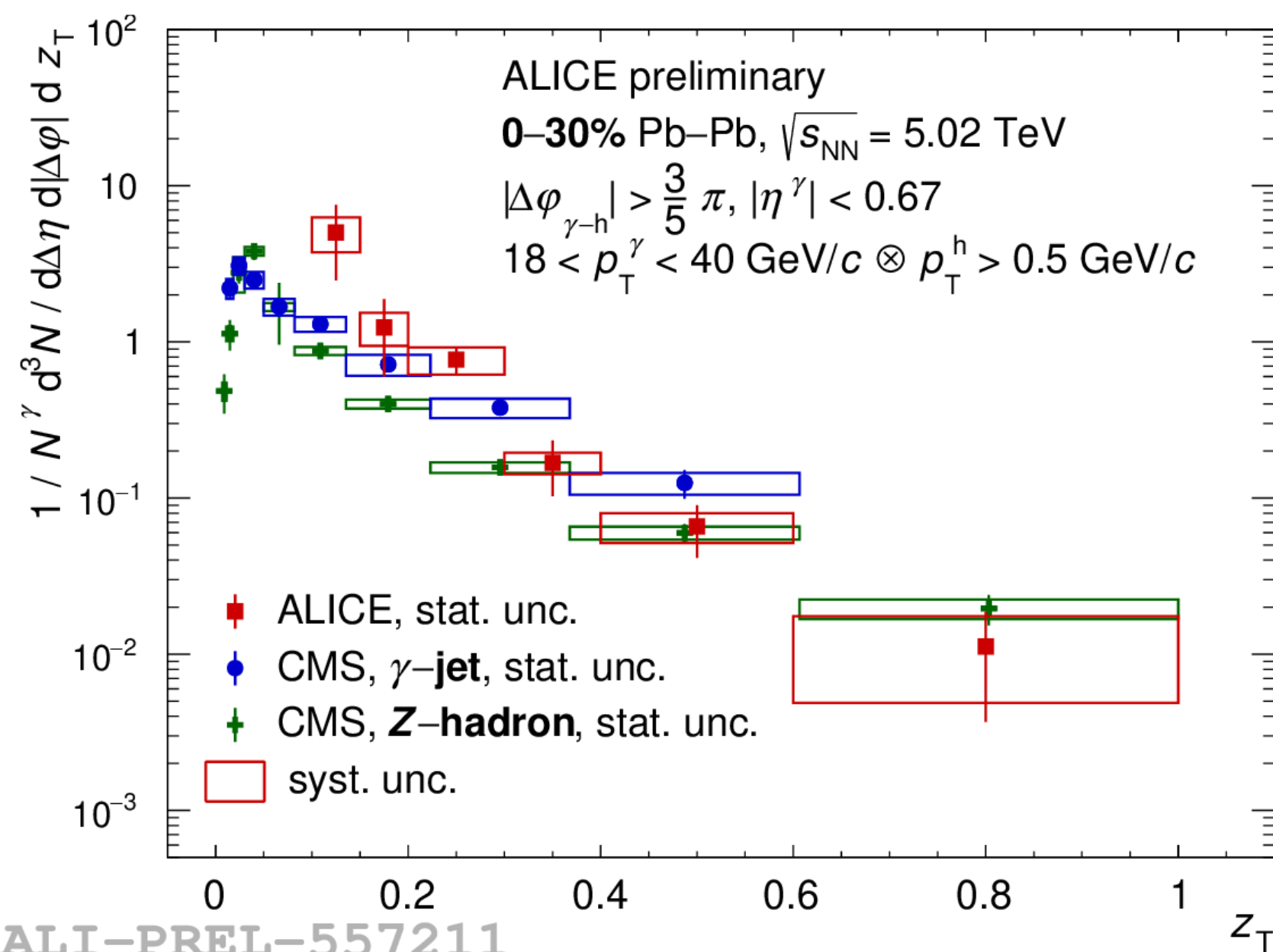
$|\Delta\phi_{\gamma-h} - \pi| < \pi/2$, $|y| < 0.35$

$5 < p_T^\gamma < 9$ GeV/c $\otimes 0.5 < p_T^h < 7$ GeV/c



- Similar behaviour as observed at RHIC and LHC experiments

➔ Note: not completely apple-to-apple comparisons!



CMS, Phys.Rev.Lett. 121 (2018) 24, 242301, 2018

γ -jet, 0–10%

anti- k_T jet R = 0.3, $p_T^{\text{jet}} > 30$ GeV/c, $|\eta^{\text{jet}}| < 1.6$

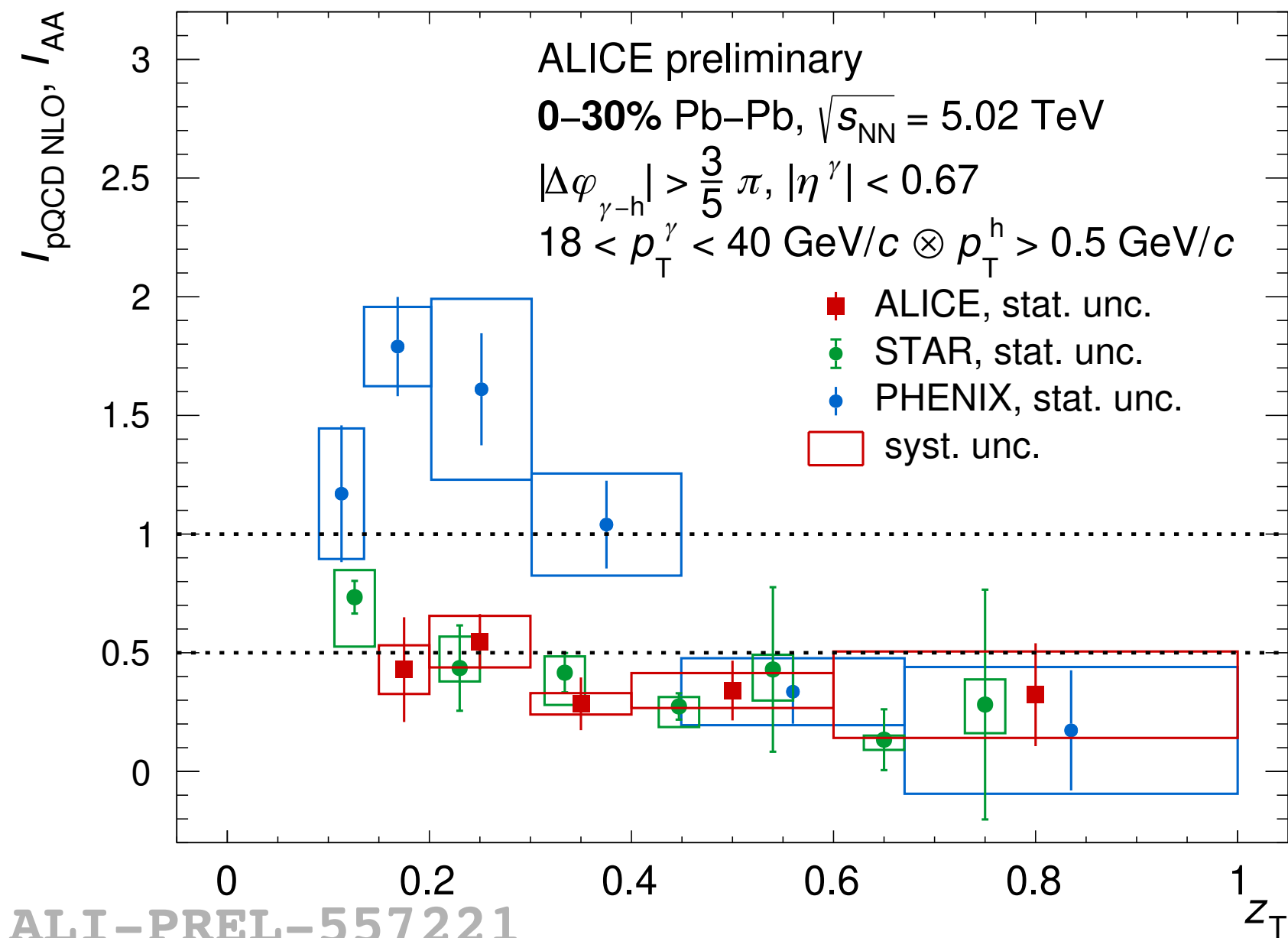
$|\Delta\phi_{\gamma\text{-jet}}| > \frac{7}{8}\pi$, $|\eta^\gamma| < 1.44$, $p_T^\gamma > 60$ GeV/c $\otimes p_T^h > 1$ GeV/c

CMS, Phys.Rev.Lett. 128 (2022) 12, 122301, 2022

Z-hadron, 0–30%

$|\Delta\phi_{Z-h}| > \frac{7}{8}\pi$, $p_T^Z > 30$ GeV/c $\otimes p_T^h > 1$ GeV/c

Isolated γ -hadron correlations in Pb–Pb: RHIC & LHC



STAR, Phys.Lett.B 760 (2016) 689-696

0–12% Au–Au, $\sqrt{s_{NN}} = 200$ GeV

$|\Delta\varphi_{\gamma-h} - \pi| \leq 1.4$

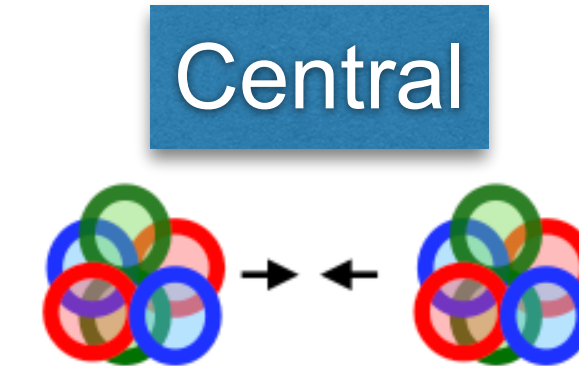
$12 < p_T^\gamma < 20$ GeV/c $\otimes p_T^h > 1.2$ GeV/c

PHENIX, PRL 111, 032301 (2013)

0–40% Au–Au, $\sqrt{s_{NN}} = 200$ GeV

$|\Delta\varphi_{\gamma-h} - \pi| < \pi/2$, $|y| < 0.35$

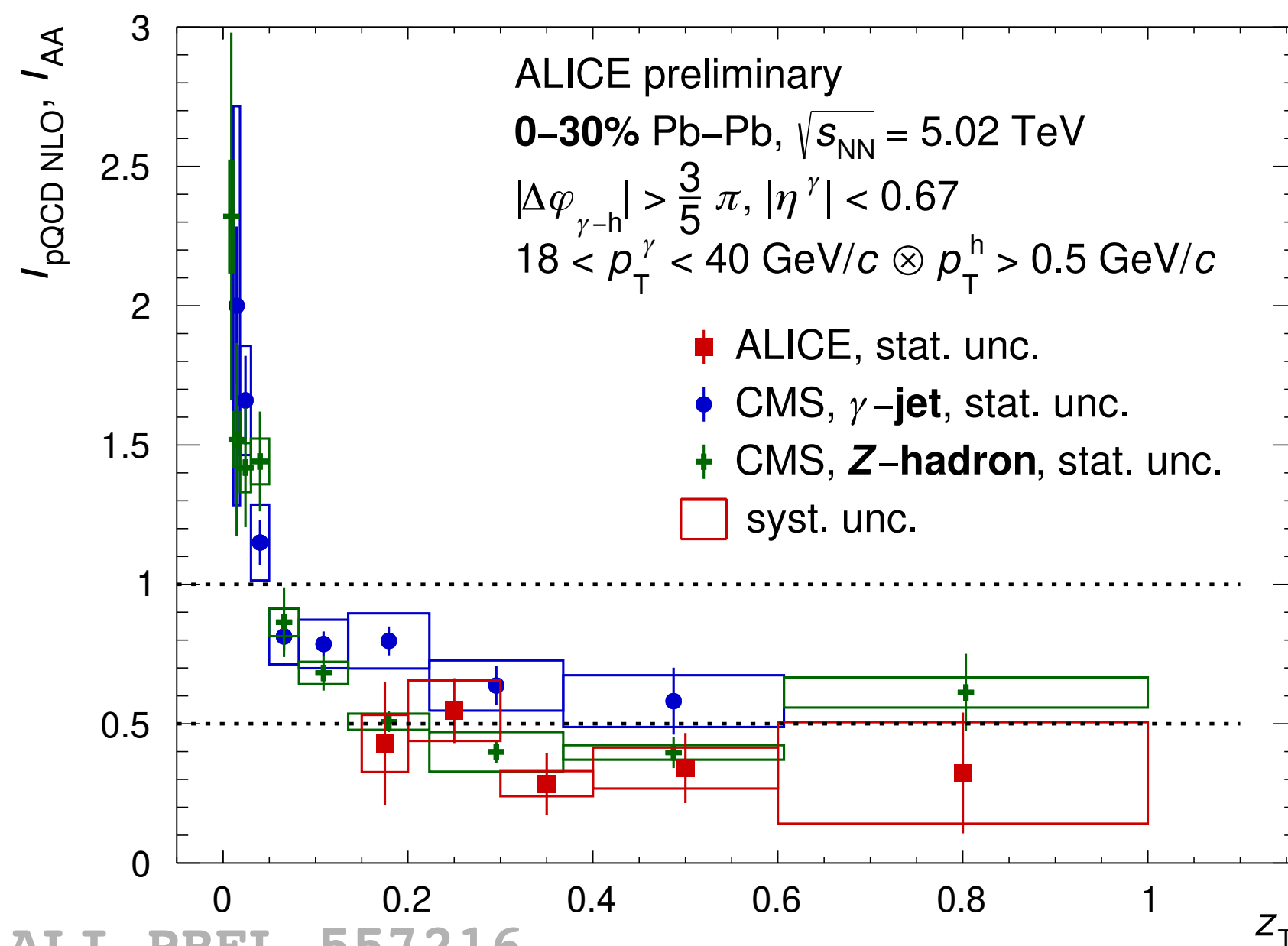
$5 < p_T^\gamma < 9$ GeV/c $\otimes 0.5 < p_T^h < 7$ GeV/c



$$I_{AA}(z_T) = \frac{D(z_T, \text{Pb} - \text{Pb})}{D(z_T, \text{pp})}$$

- Similar behaviour as observed at RHIC and LHC experiments

➔ Note: not completely apple-to-apple comparisons!



CMS, Phys.Rev.Lett. 121 (2018) 242301, 2018

γ -jet, 0–10%

anti- k_T jet R = 0.3, $p_T^{\text{jet}} > 30$ GeV/c, $|\eta^{\text{jet}}| < 1.6$

$|\Delta\varphi_{\gamma\text{-jet}}| > \frac{7}{8}\pi$, $|\eta^\gamma| < 1.44$, $p_T^\gamma > 60$ GeV/c $\otimes p_T^h > 1$ GeV/c

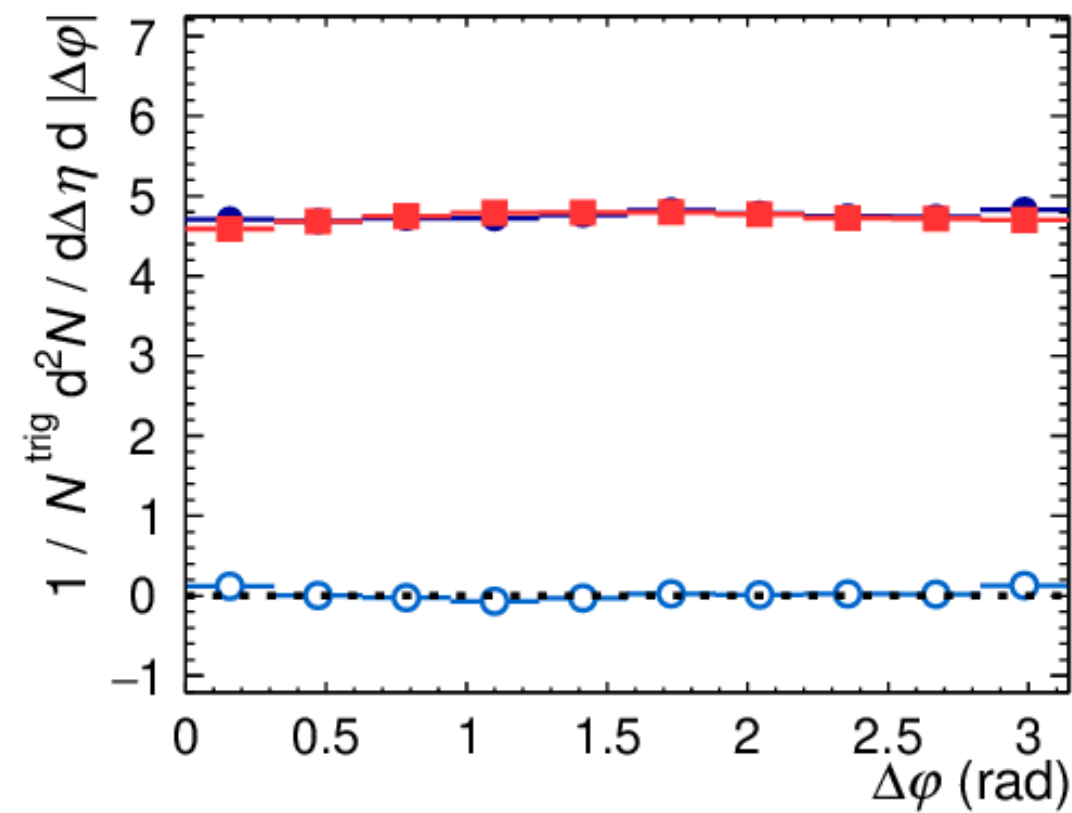
CMS, Phys.Rev.Lett. 128 (2022) 122301, 2022

Z-hadron, 0–30%

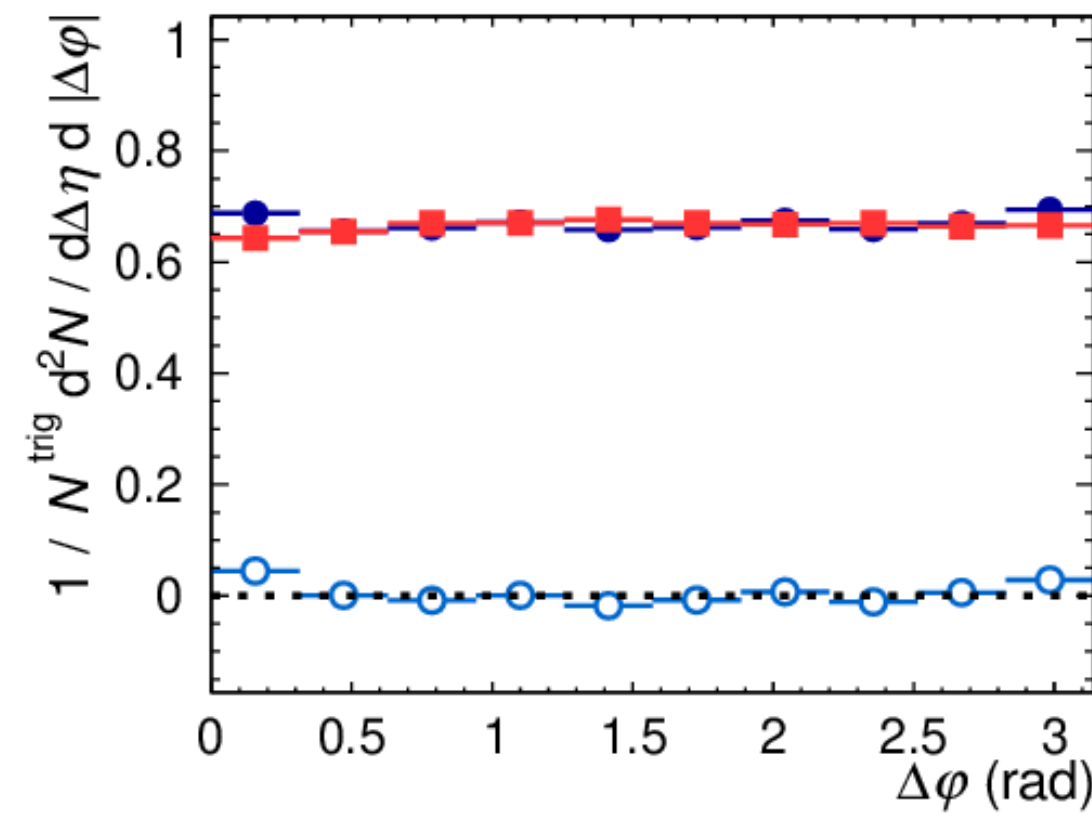
$|\Delta\varphi_{Z-h}| > \frac{7}{8}\pi$, $p_T^Z > 30$ GeV/c $\otimes p_T^h > 1$ GeV/c

Isolated γ -hadron correlations in Pb-Pb: $D(z_T)$

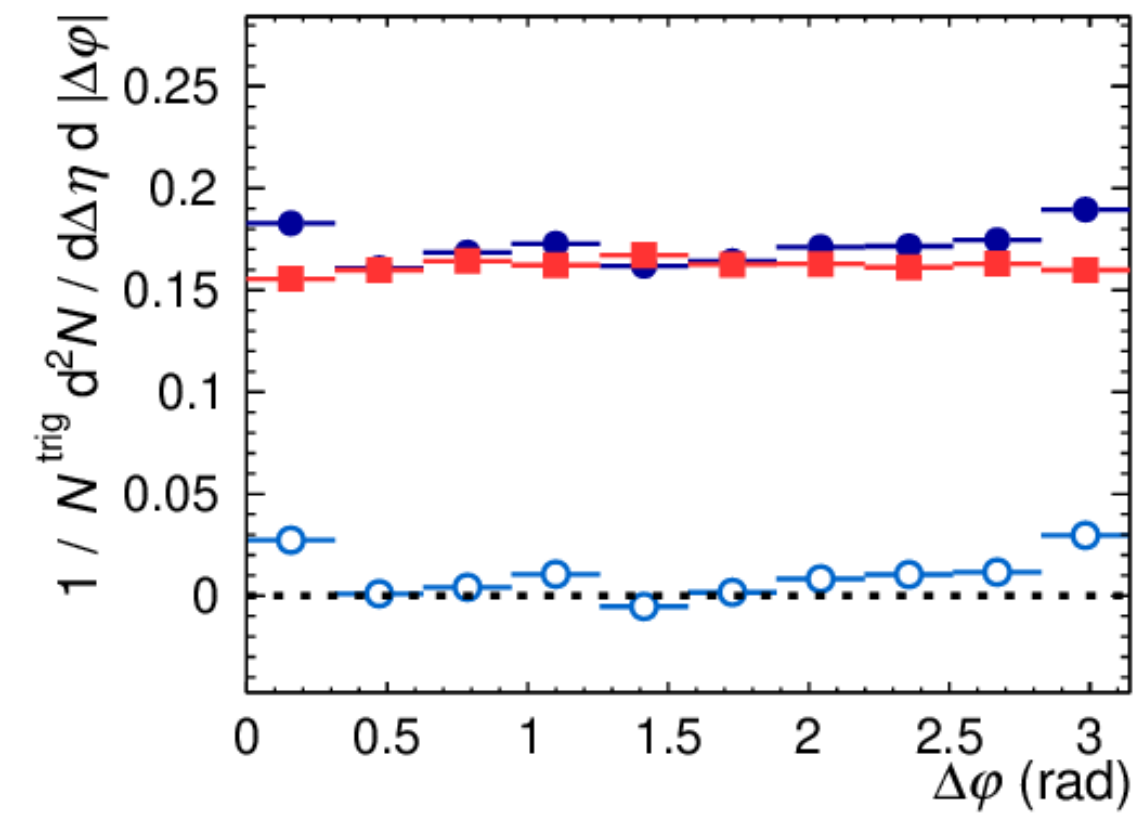
$0.10 < z_T < 0.15$



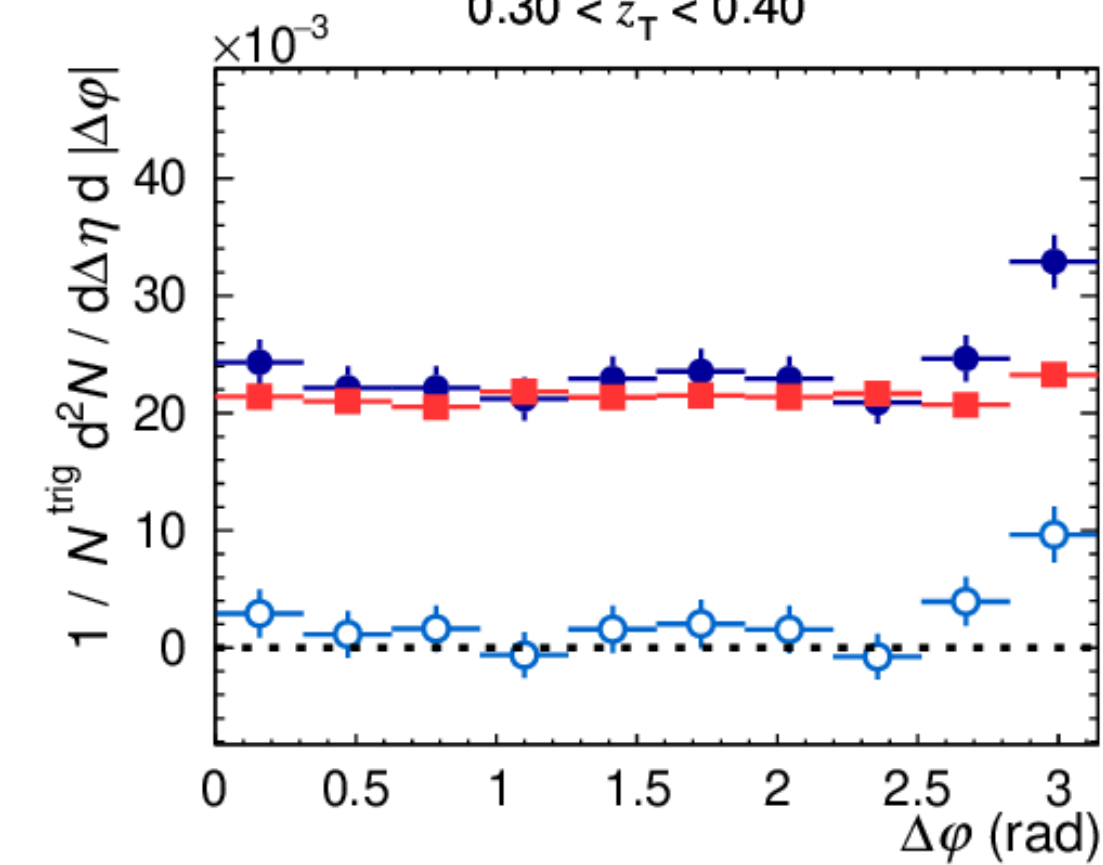
$0.15 < z_T < 0.20$



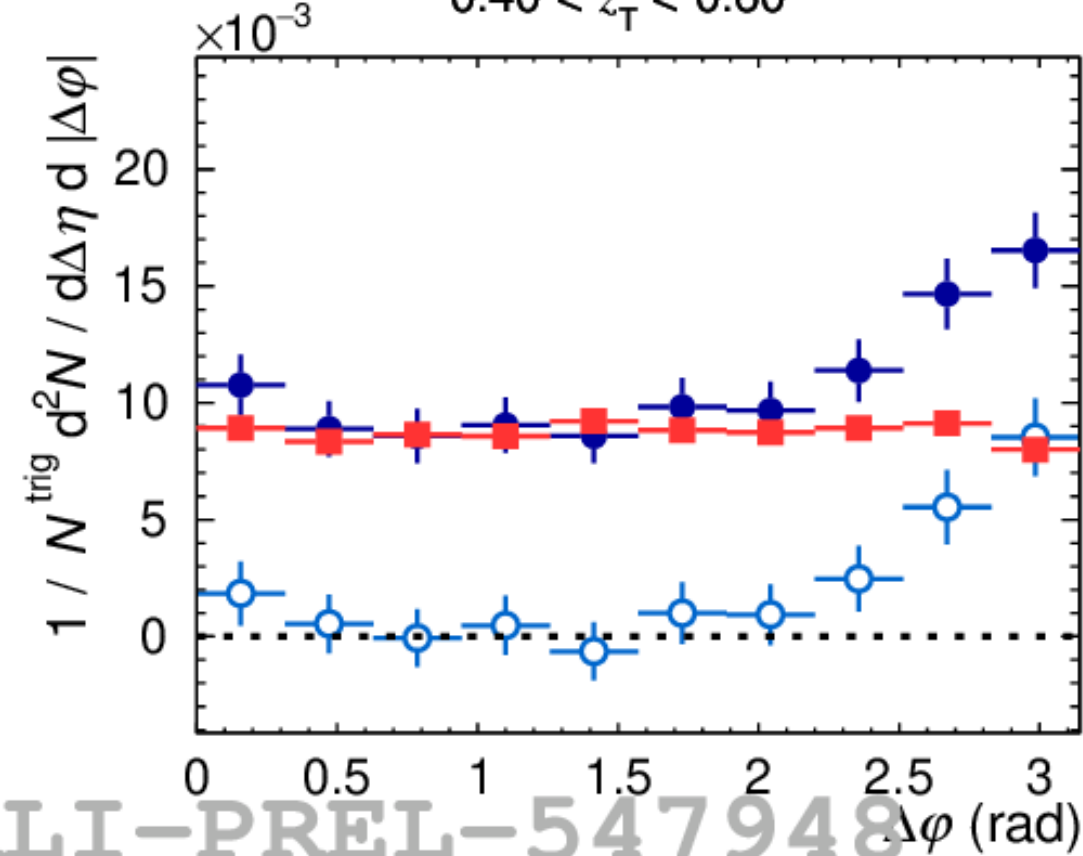
$0.20 < z_T < 0.30$



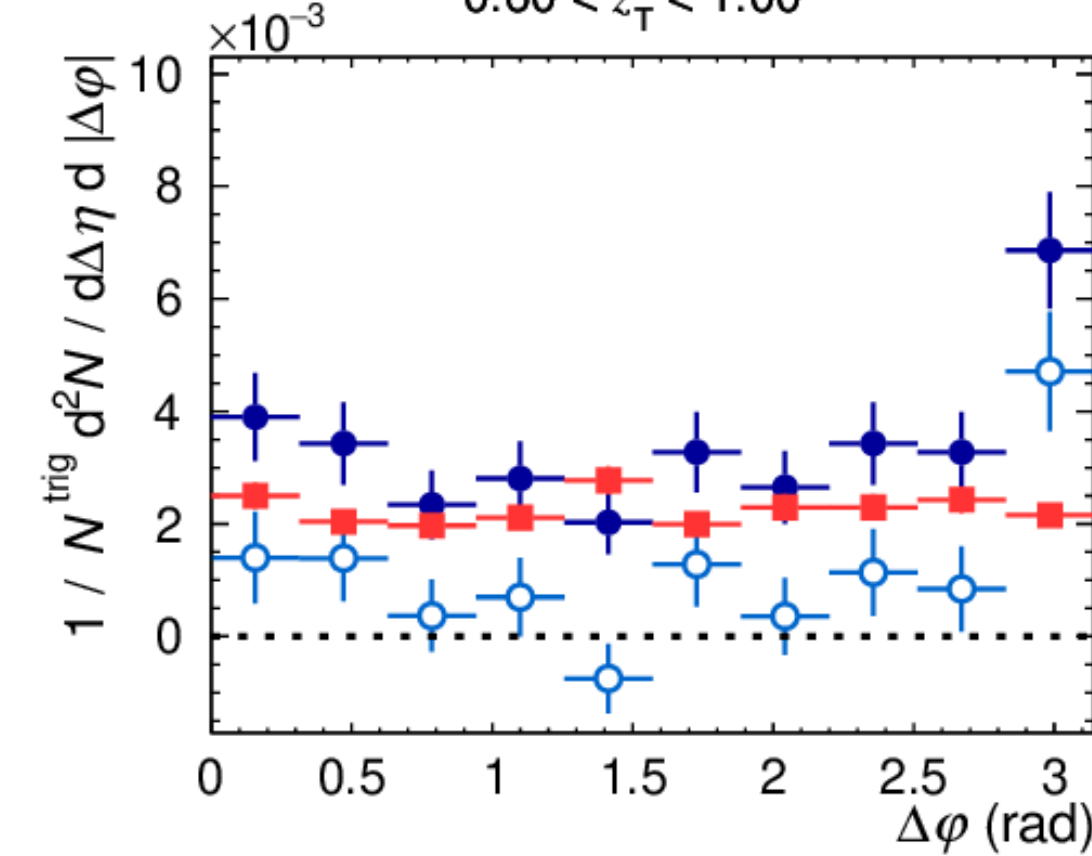
$0.30 < z_T < 0.40$



$0.40 < z_T < 0.60$



$0.60 < z_T < 1.00$



ALICE preliminary

0-10% Pb-Pb, $\sqrt{s_{NN}} = 5.02$ TeV, $|\eta^{trig}| < 0.67$

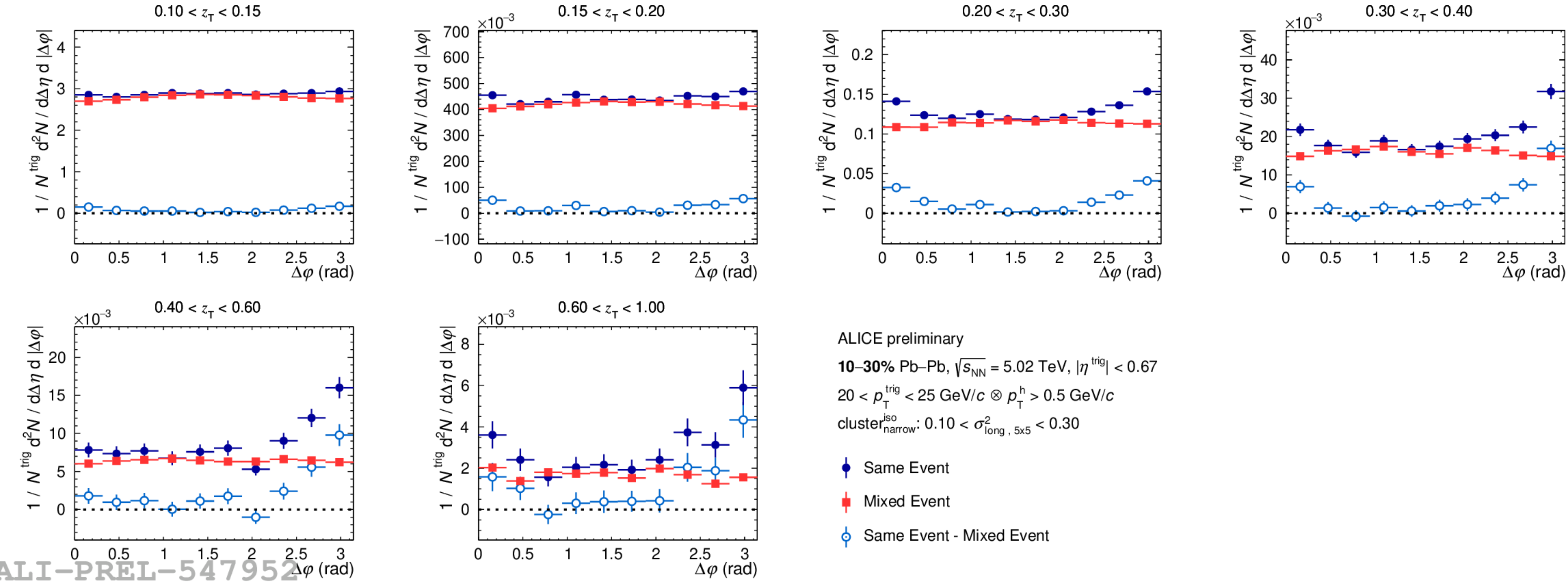
$20 < p_T^{trig} < 25$ GeV/c \otimes $p_T^h > 0.5$ GeV/c

cluster_{narrow}^{iso}: $0.10 < \sigma_{long, 5 \times 5}^2 < 0.30$

- Same Event
- Mixed Event
- Same Event - Mixed Event

ALI-PREL-547948

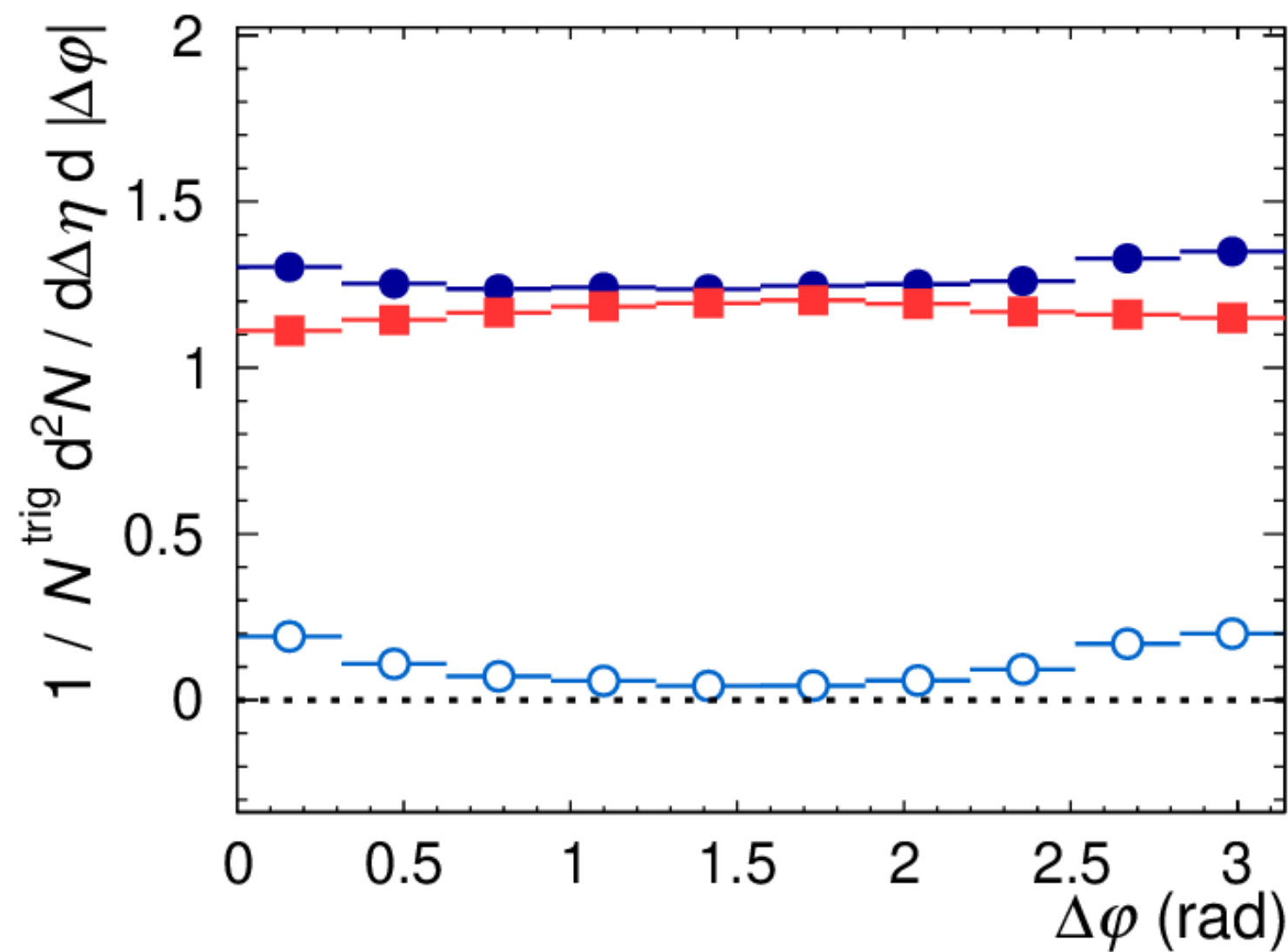
Isolated γ -hadron correlations in Pb-Pb: $D(z_T)$



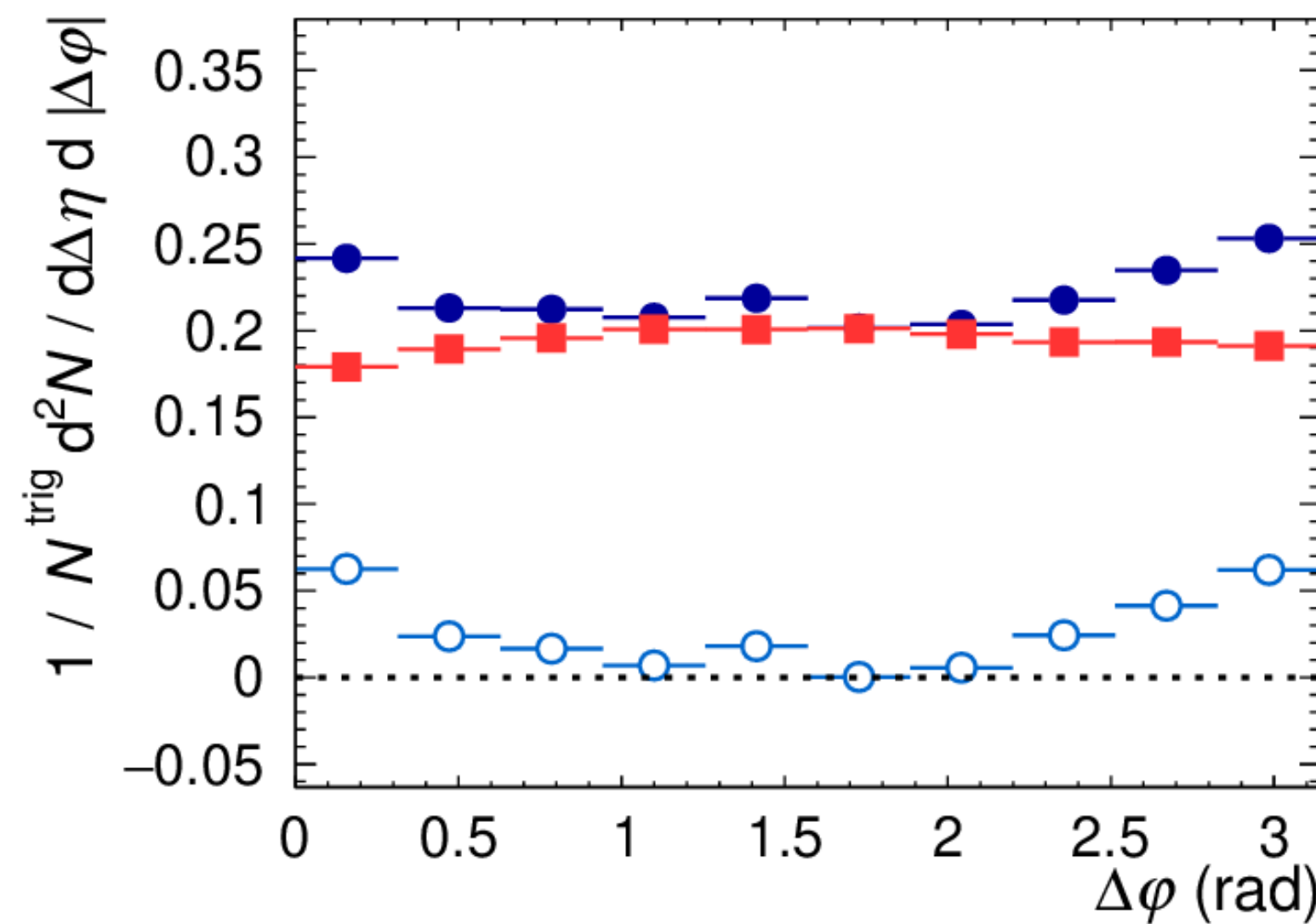
ALI-PREL-547952

Isolated γ -hadron correlations in Pb-Pb: $D(z_T)$

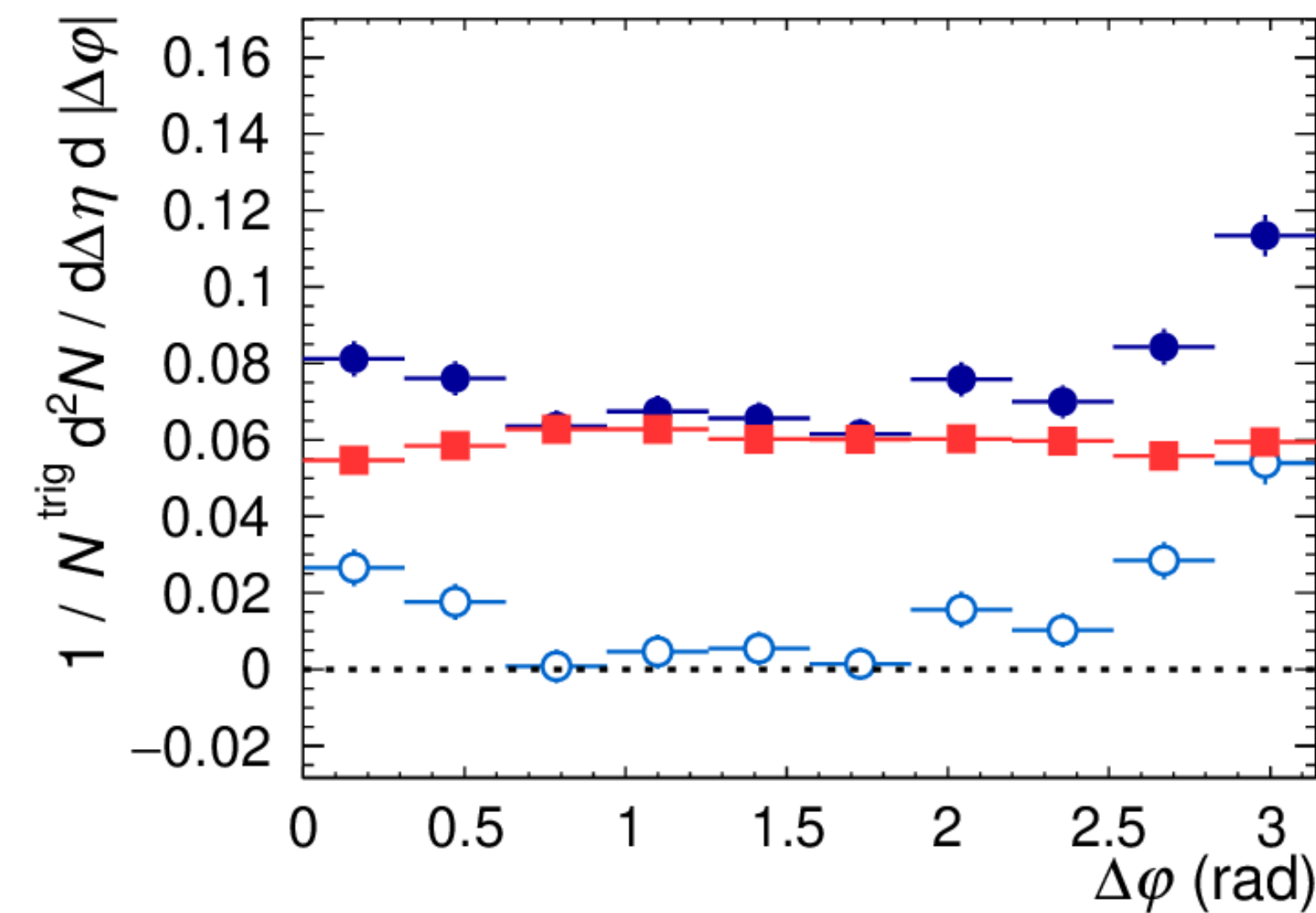
$0.10 < z_T < 0.15$



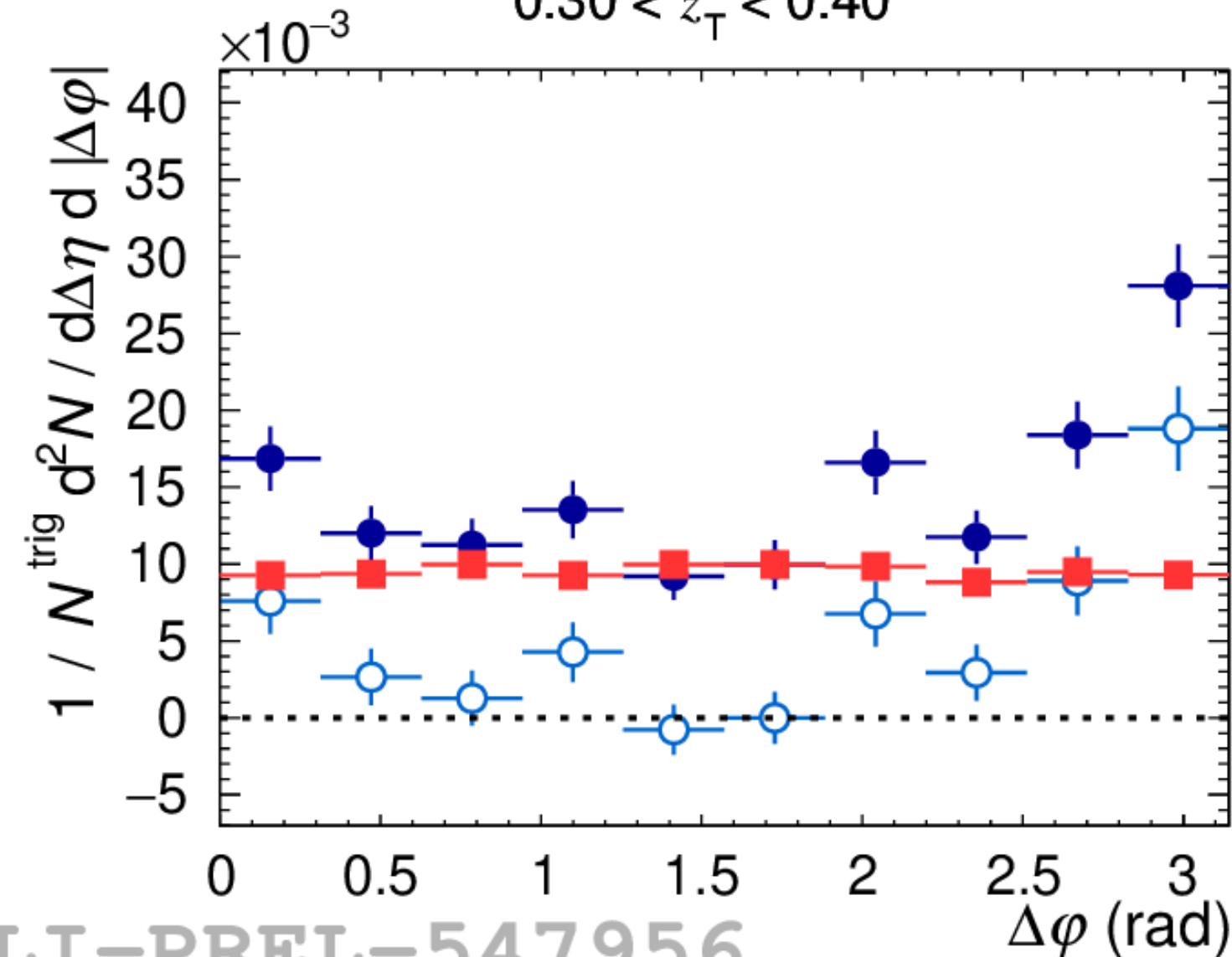
$0.15 < z_T < 0.20$



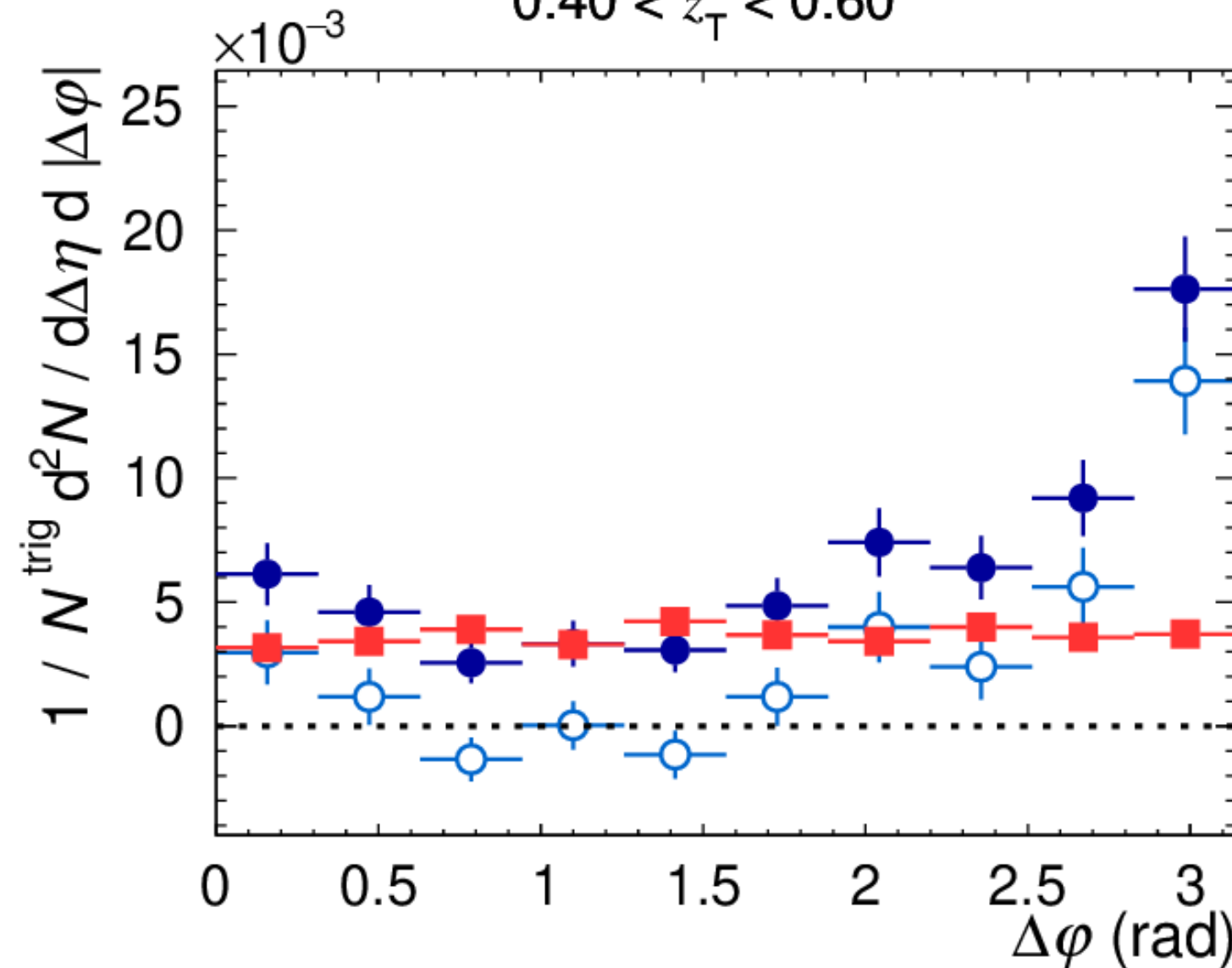
$0.20 < z_T < 0.30$



$0.30 < z_T < 0.40$



$0.40 < z_T < 0.60$



ALICE preliminary

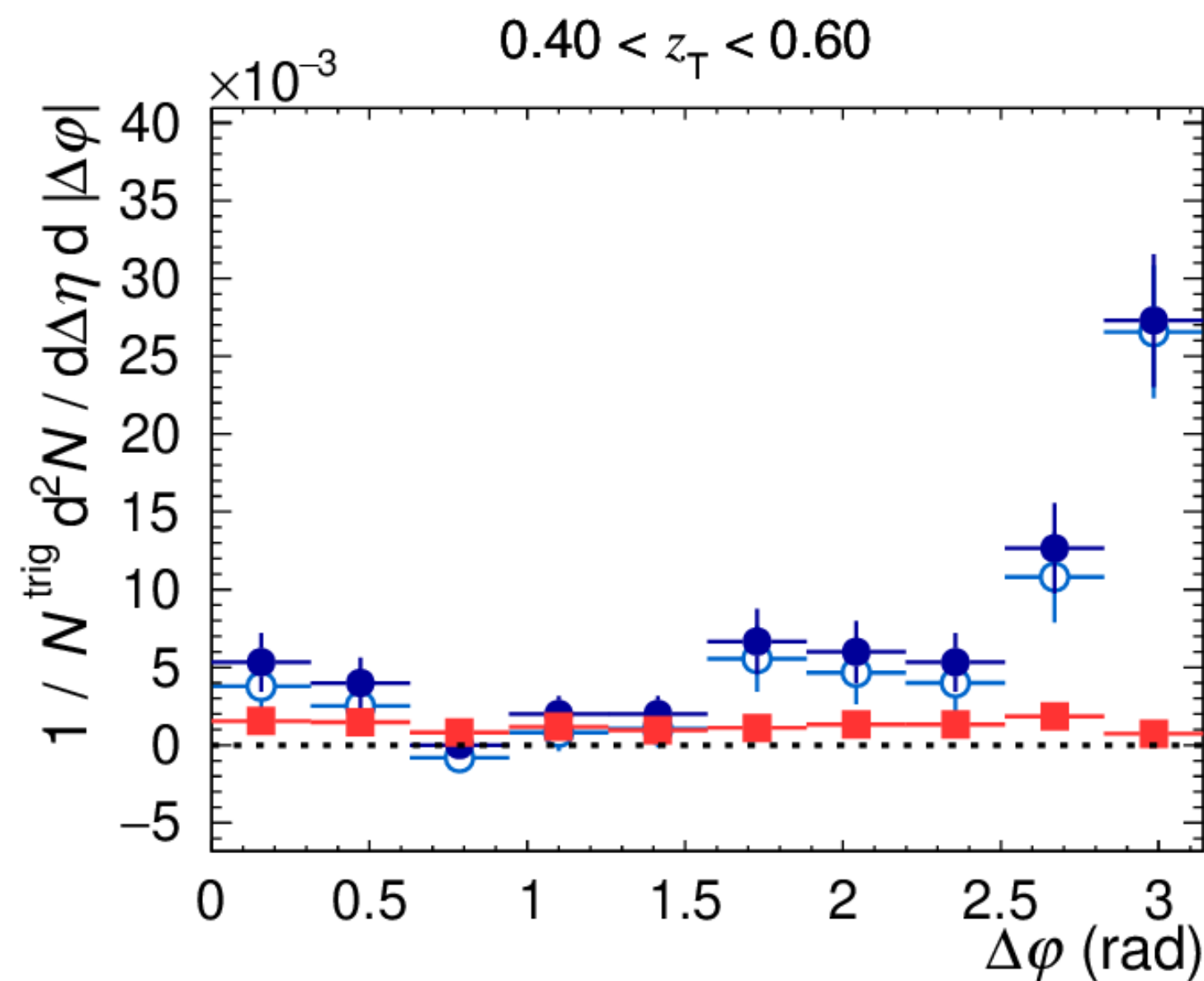
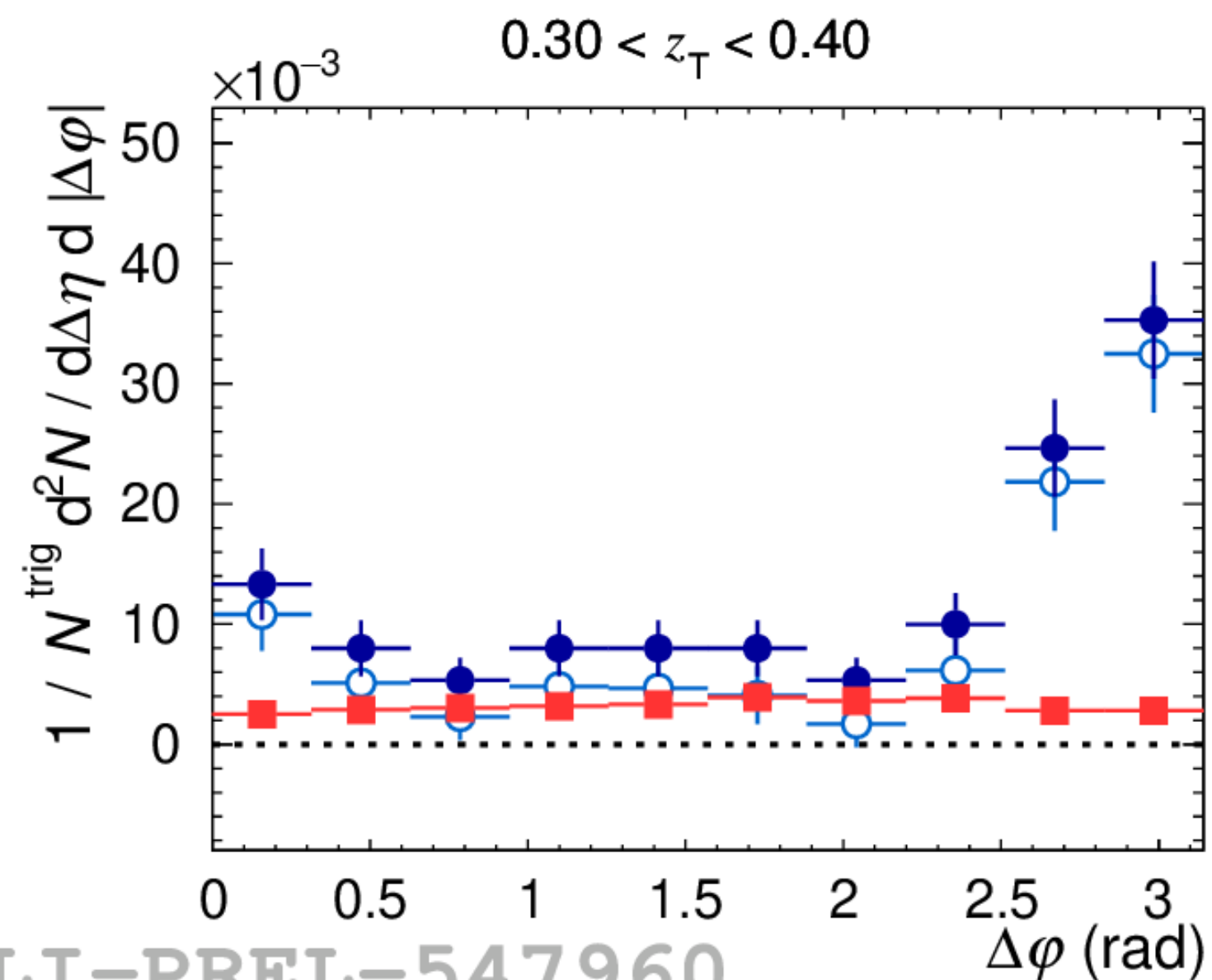
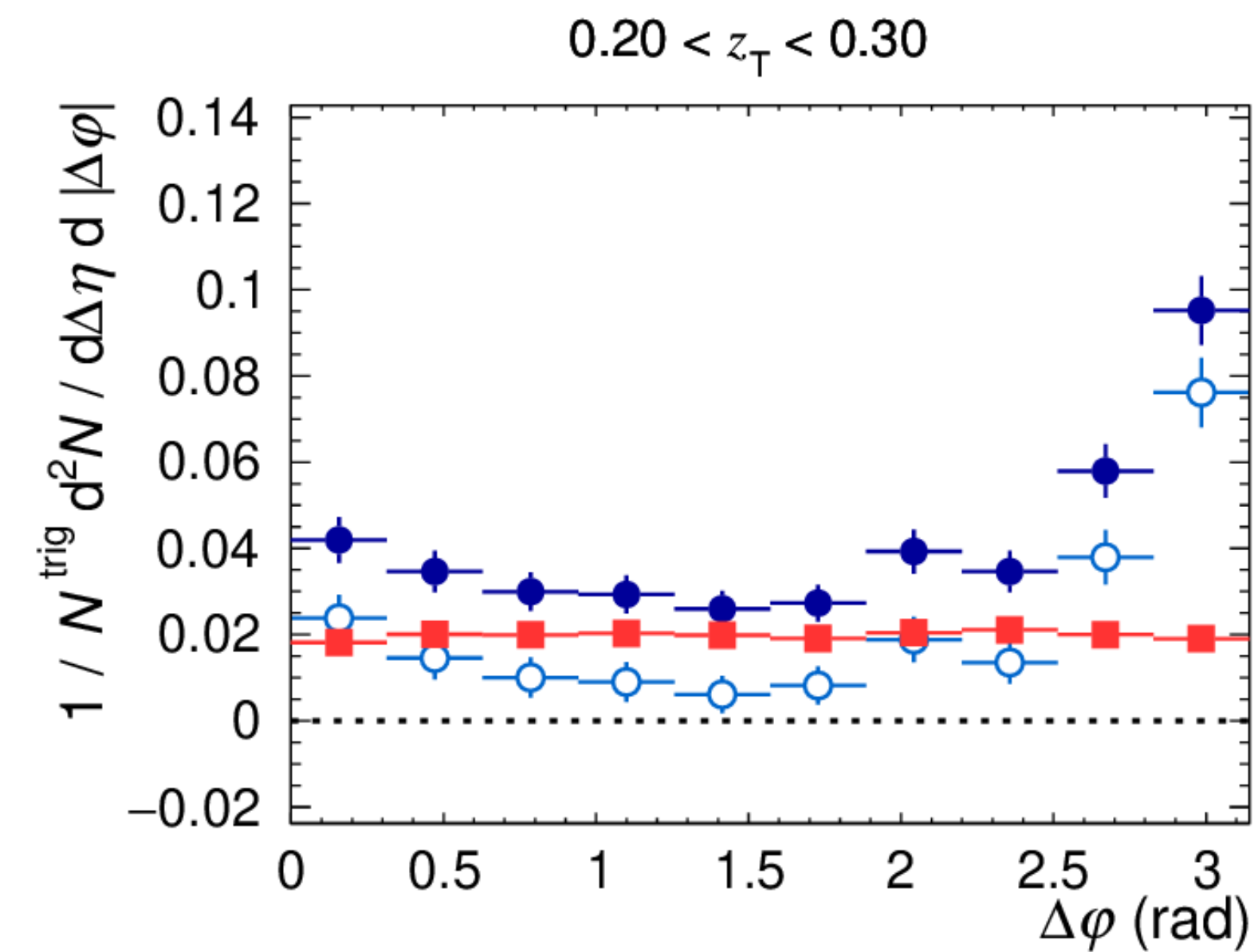
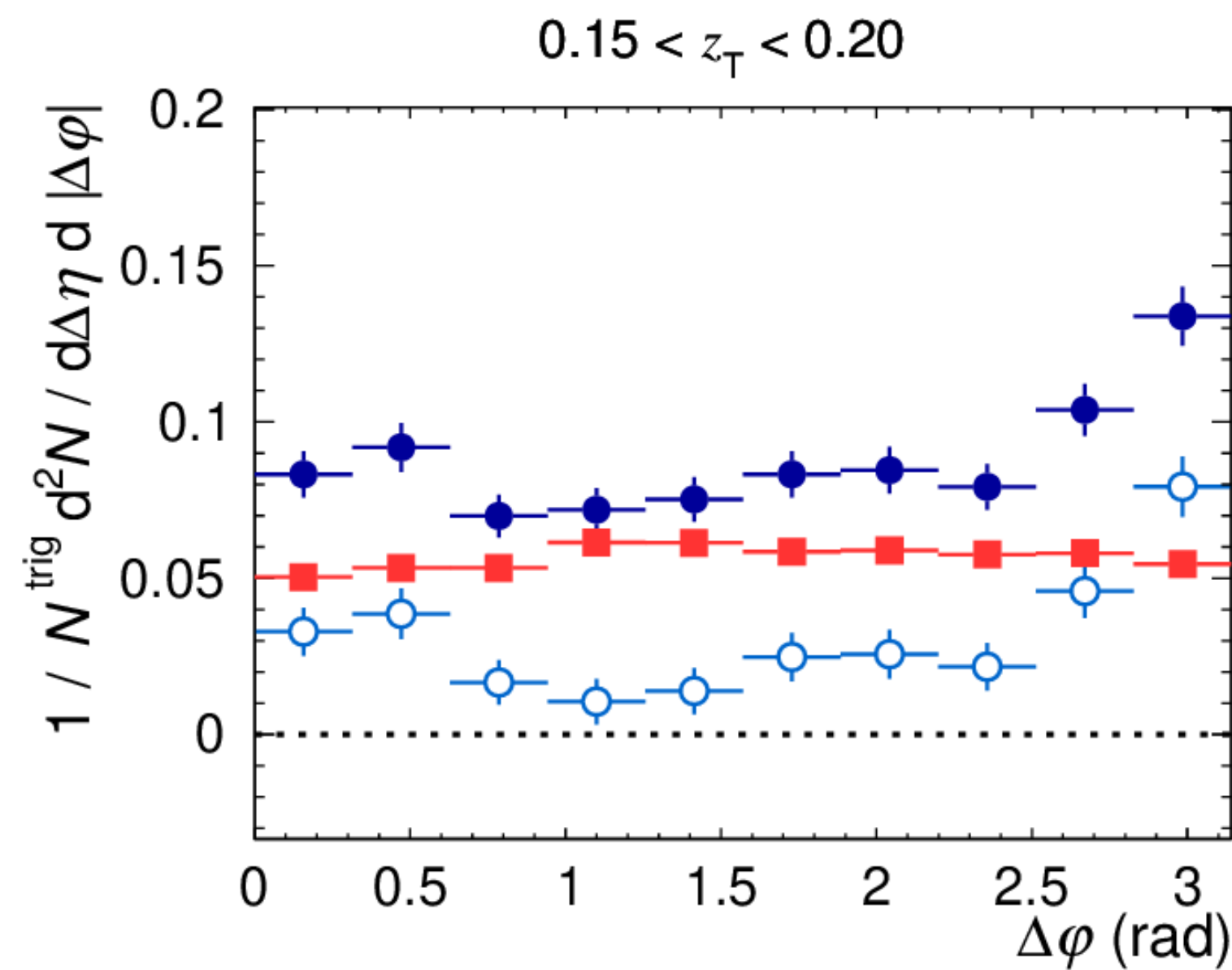
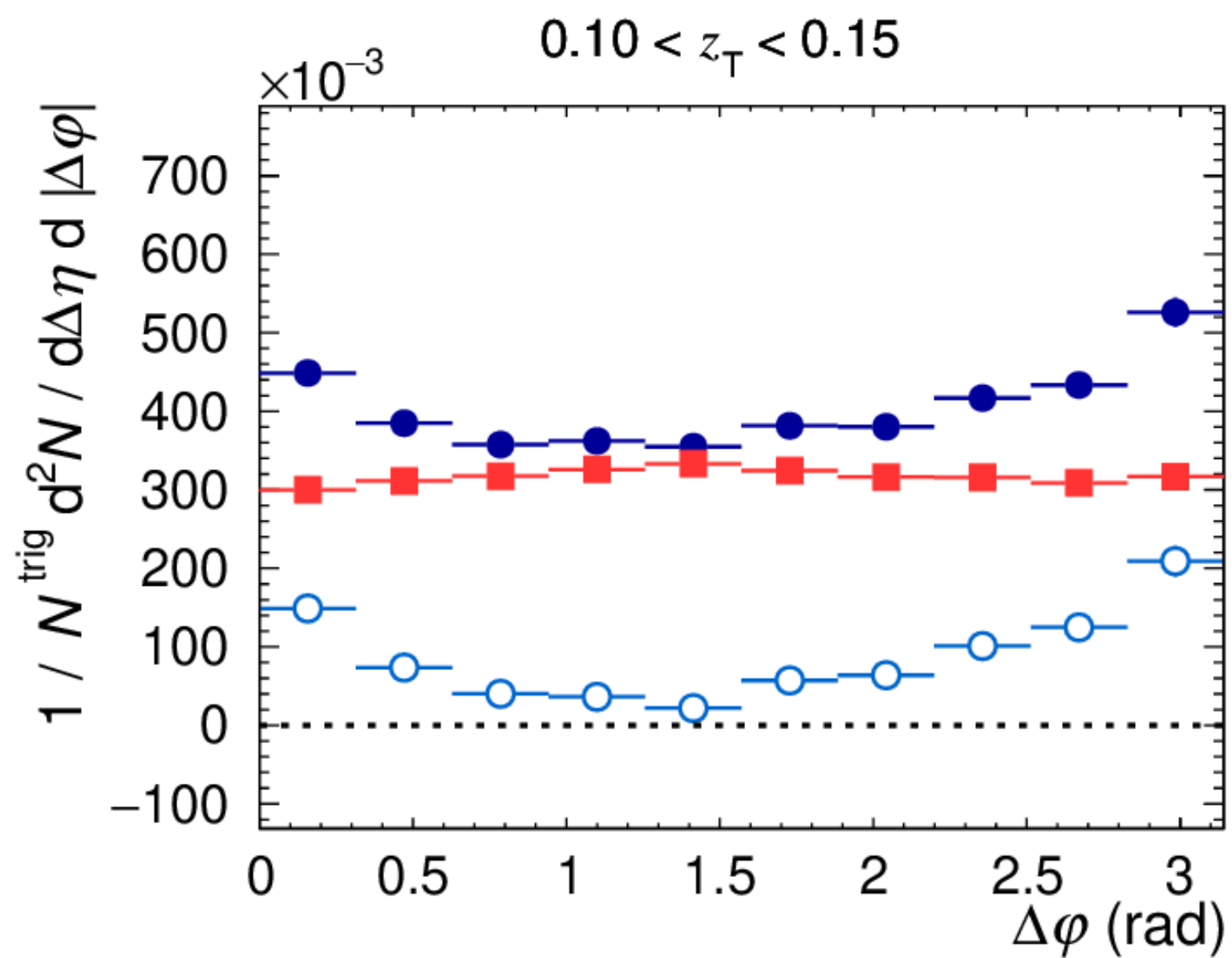
30–50% Pb–Pb, $\sqrt{s_{NN}} = 5.02$ TeV, $|\eta^{trig}| < 0.67$

$20 < p_T^{trig} < 25$ GeV/c \otimes $p_T^h > 0.5$ GeV/c

cluster_{narrow}^{iso}: $0.10 < \sigma_{long, 5 \times 5}^2 < 0.30$

- Same Event
- Mixed Event
- Same Event - Mixed Event

Isolated γ -hadron correlations in Pb-Pb: $D(z_T)$



ALICE preliminary

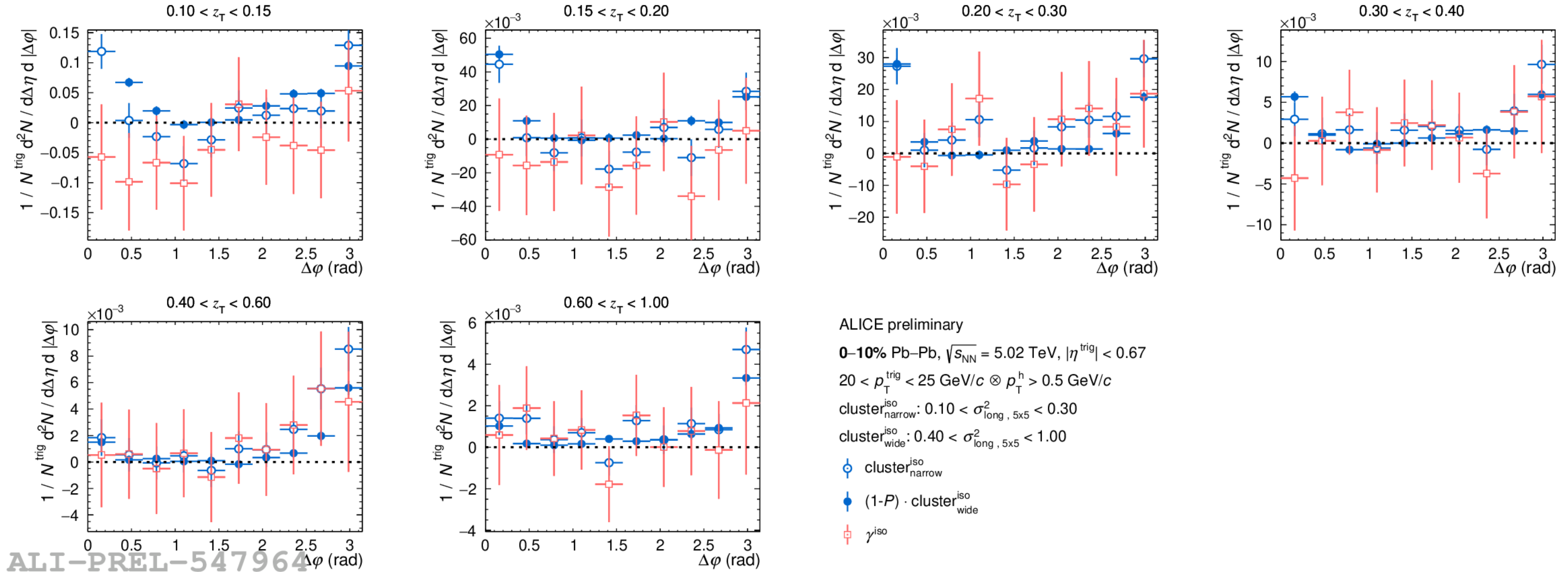
50–90% Pb–Pb, $\sqrt{s_{NN}} = 5.02$ TeV, $|\eta^{trig}| < 0.67$

$20 < p_T^{trig} < 25$ GeV/c \otimes $p_T^h > 0.5$ GeV/c

cluster_{narrow}^{iso}: $0.10 < \sigma_{long, 5 \times 5}^2 < 0.30$

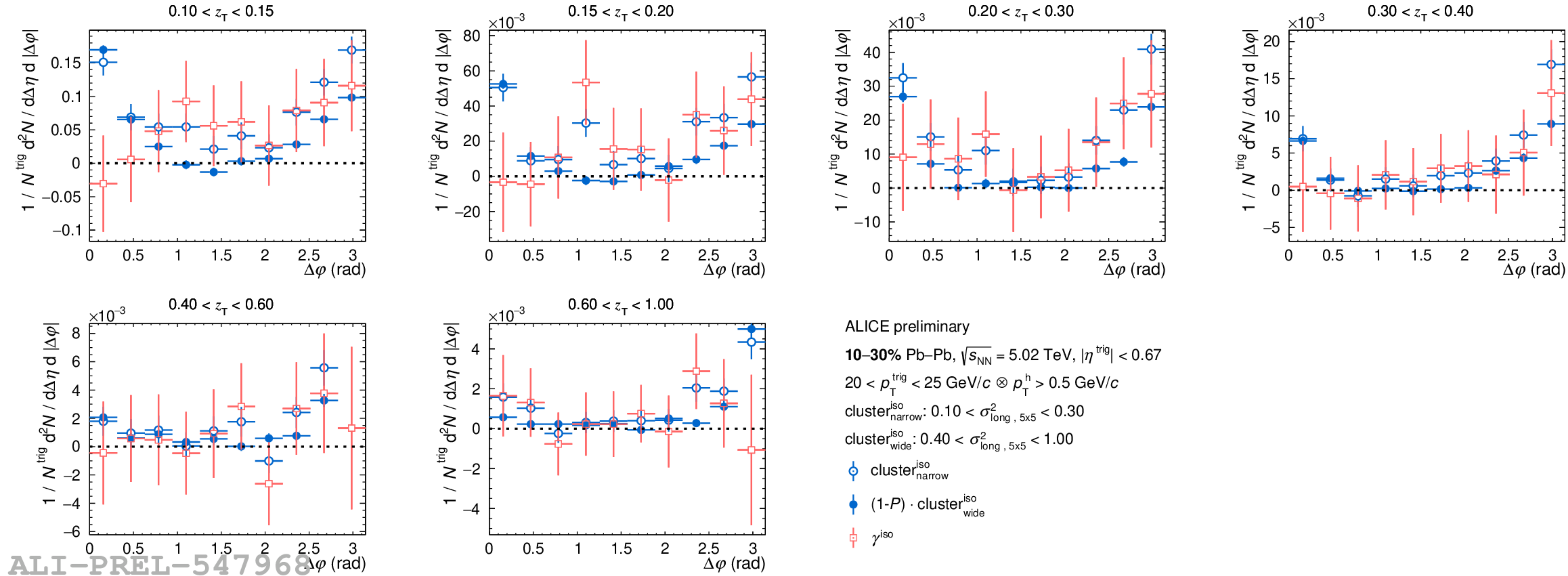
- Same Event
- Mixed Event
- Same Event - Mixed Event

Isolated γ -hadron correlations in Pb-Pb: $D(z_T)$



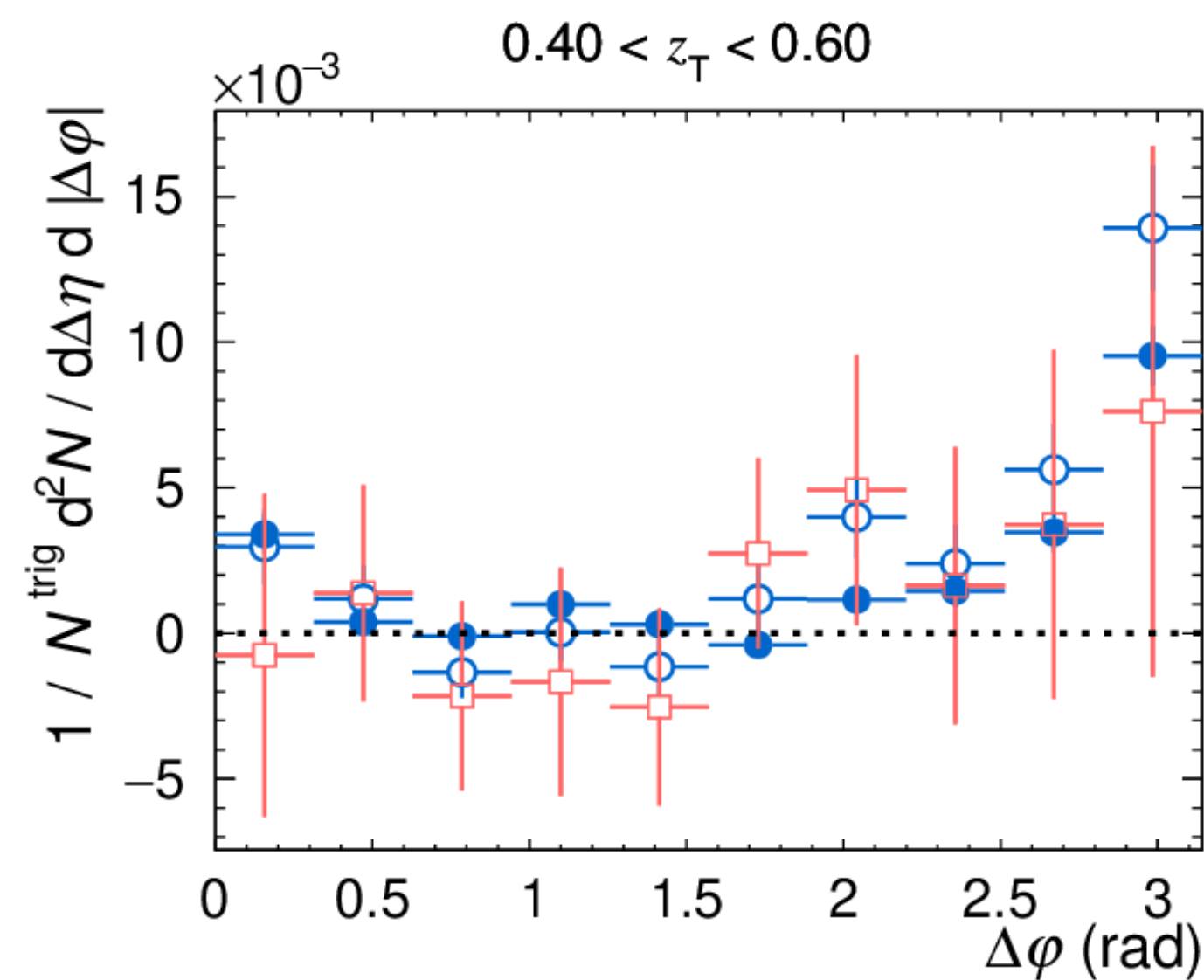
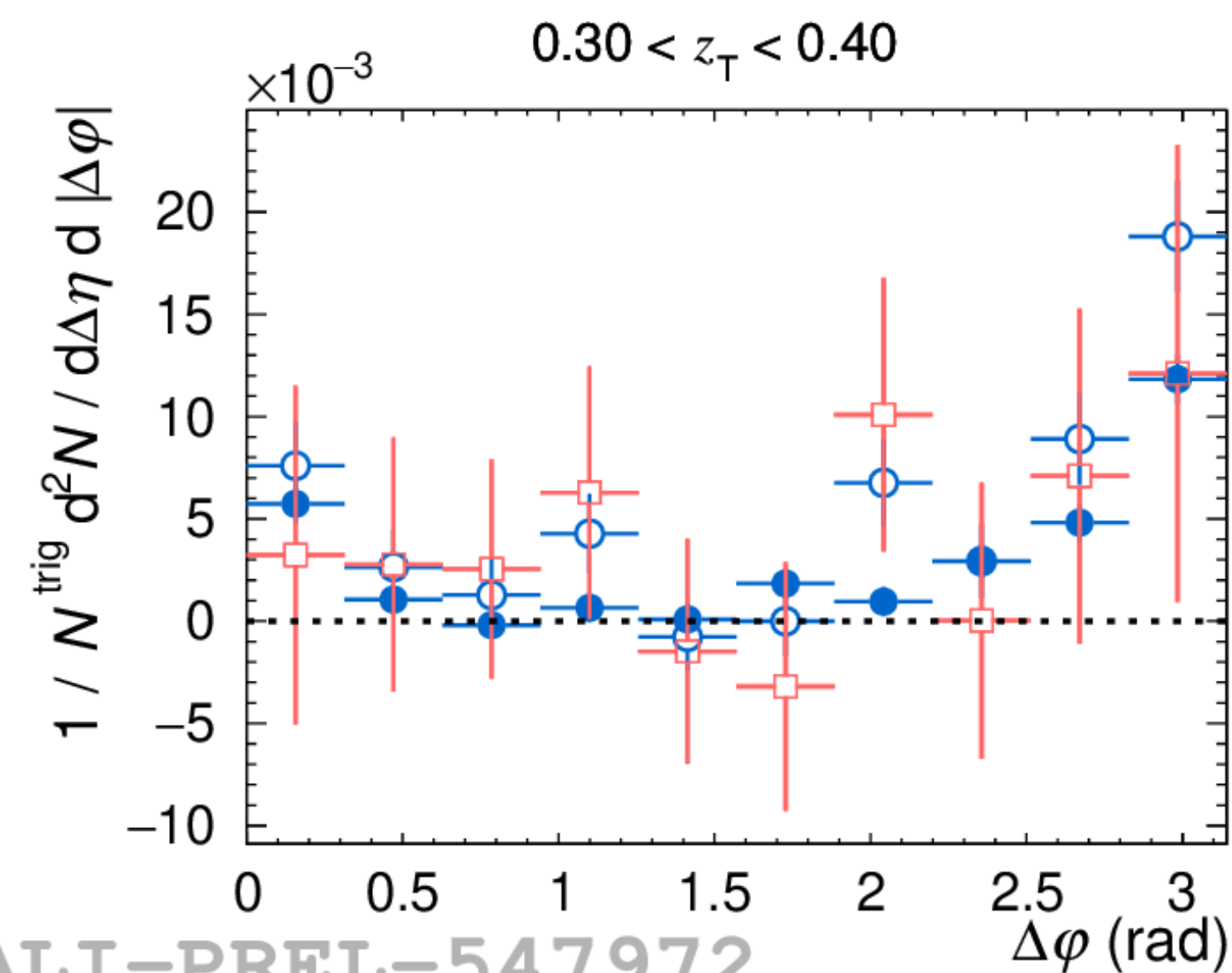
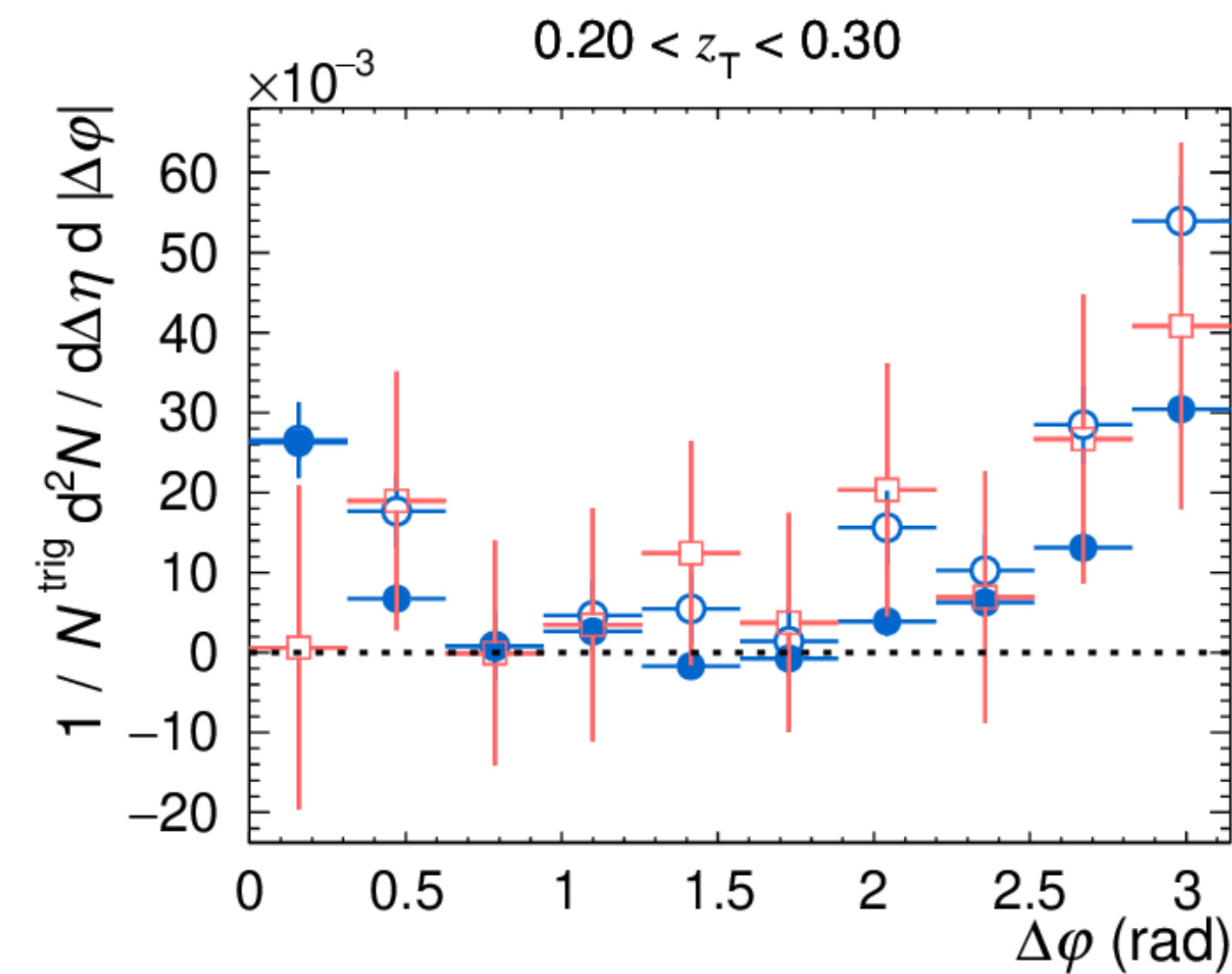
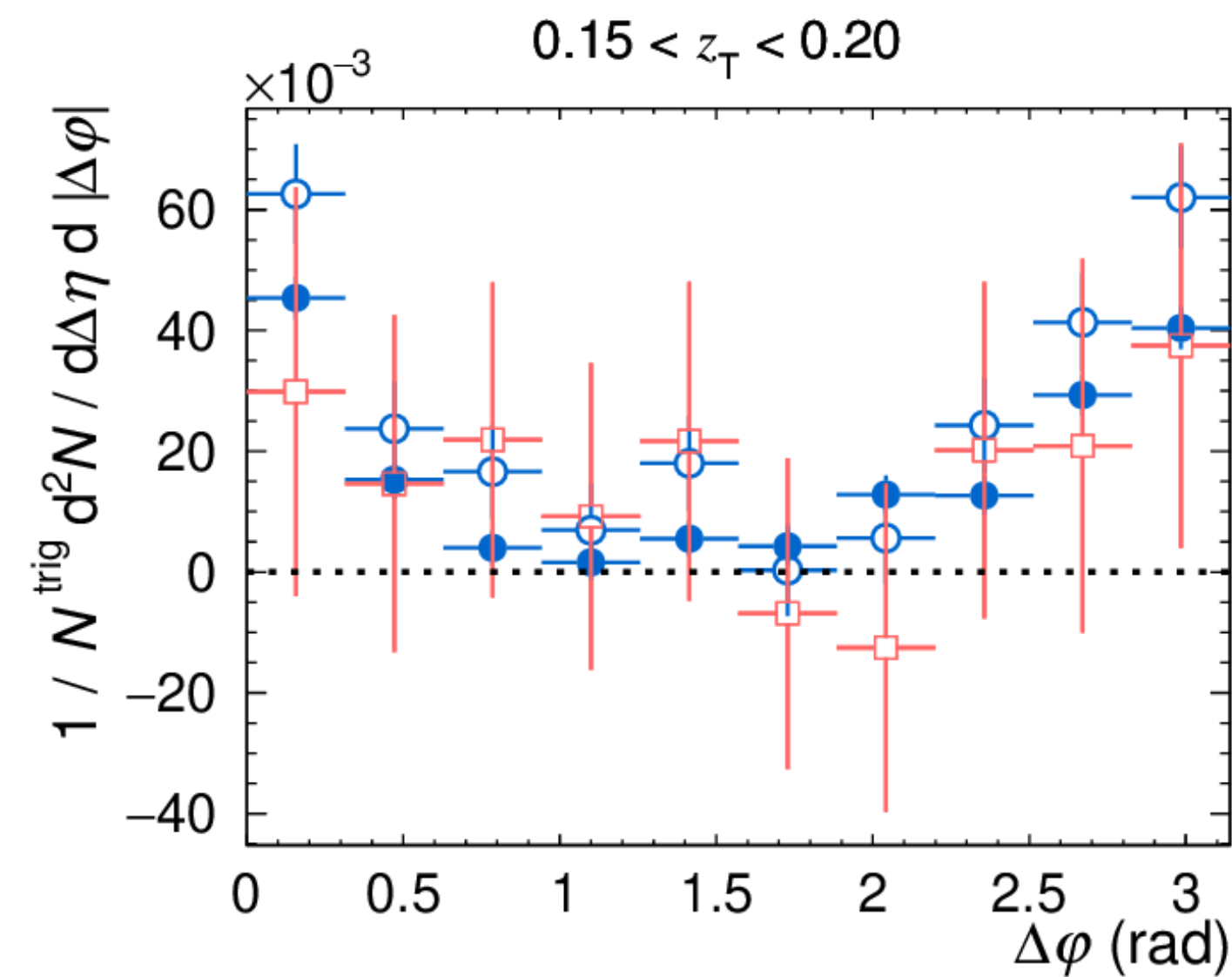
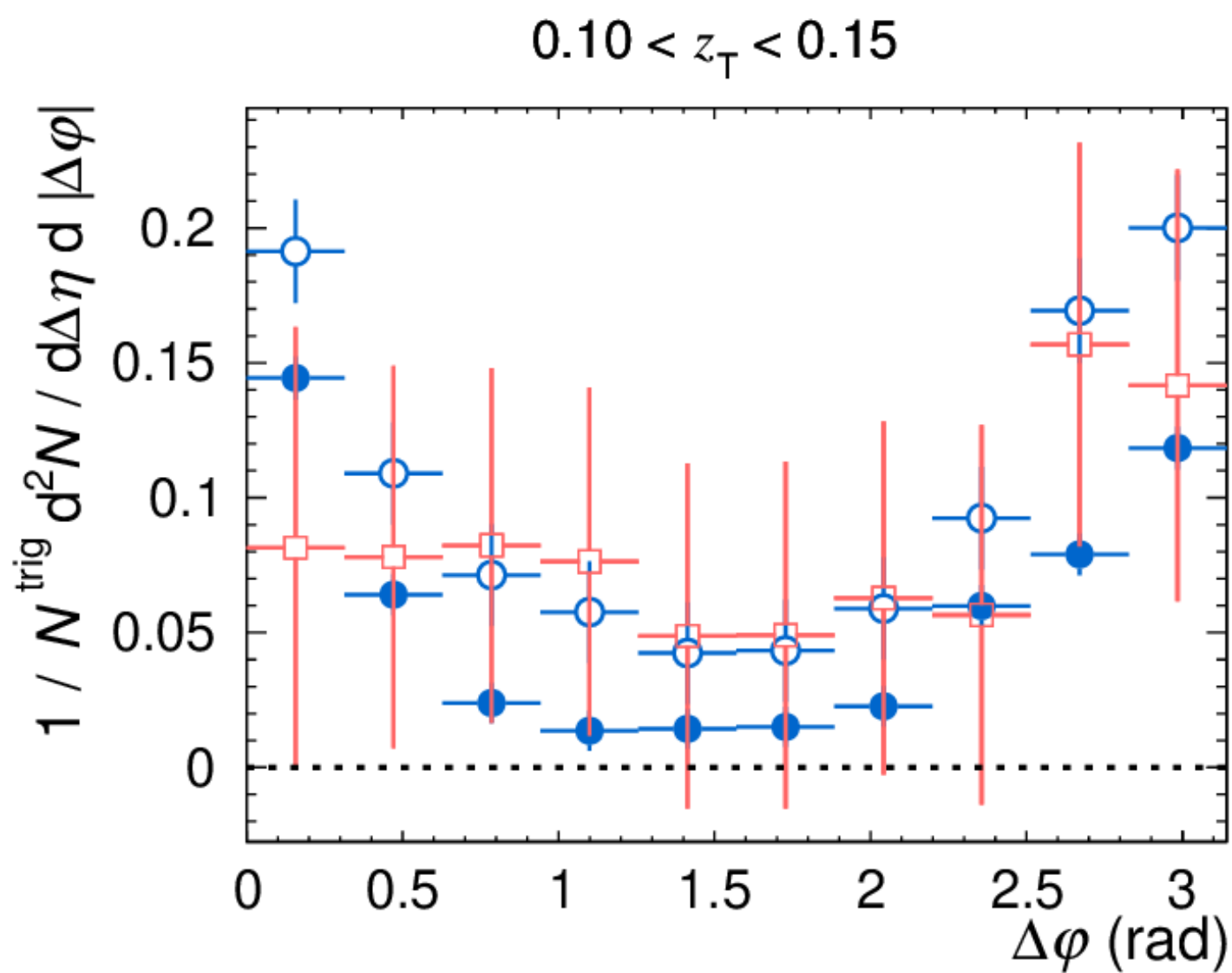
ALI-PREL-547964

Isolated γ -hadron correlations in Pb–Pb: $D(z_T)$



ALI-PREL-547968

Isolated γ -hadron correlations in Pb-Pb: $D(z_T)$



ALICE preliminary

30–50% Pb–Pb, $\sqrt{s_{NN}} = 5.02$ TeV, $|\eta^{trig}| < 0.67$

$20 < p_T^{trig} < 25$ GeV/c $\otimes p_T^h > 0.5$ GeV/c

cluster_{narrow}^{iso}: $0.10 < \sigma_{long, 5 \times 5}^2 < 0.30$

cluster_{wide}^{iso}: $0.40 < \sigma_{long, 5 \times 5}^2 < 1.00$

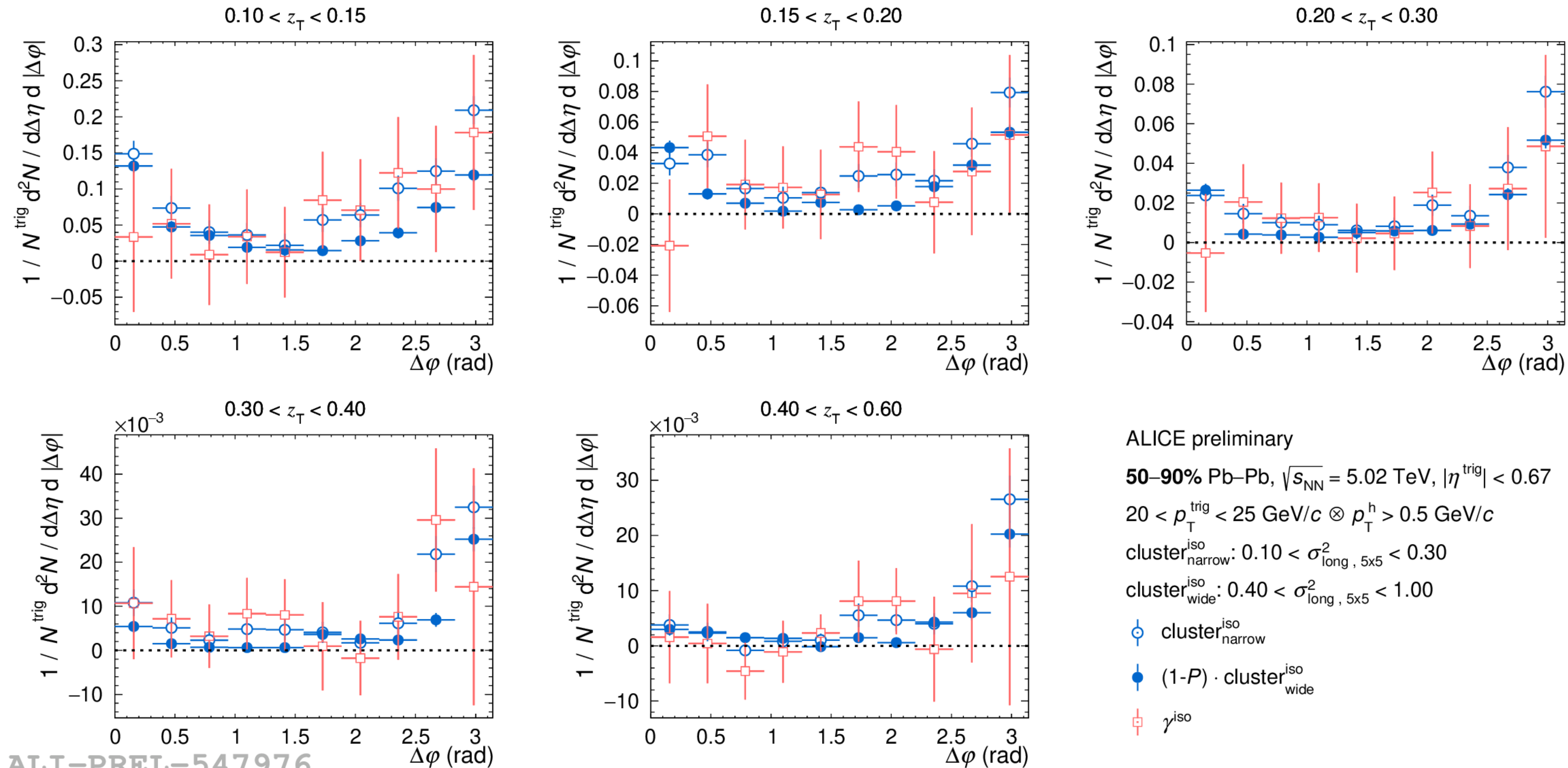
\circ cluster_{narrow}^{iso}

\bullet (1- P) \cdot cluster_{wide}^{iso}

\square γ^{iso}

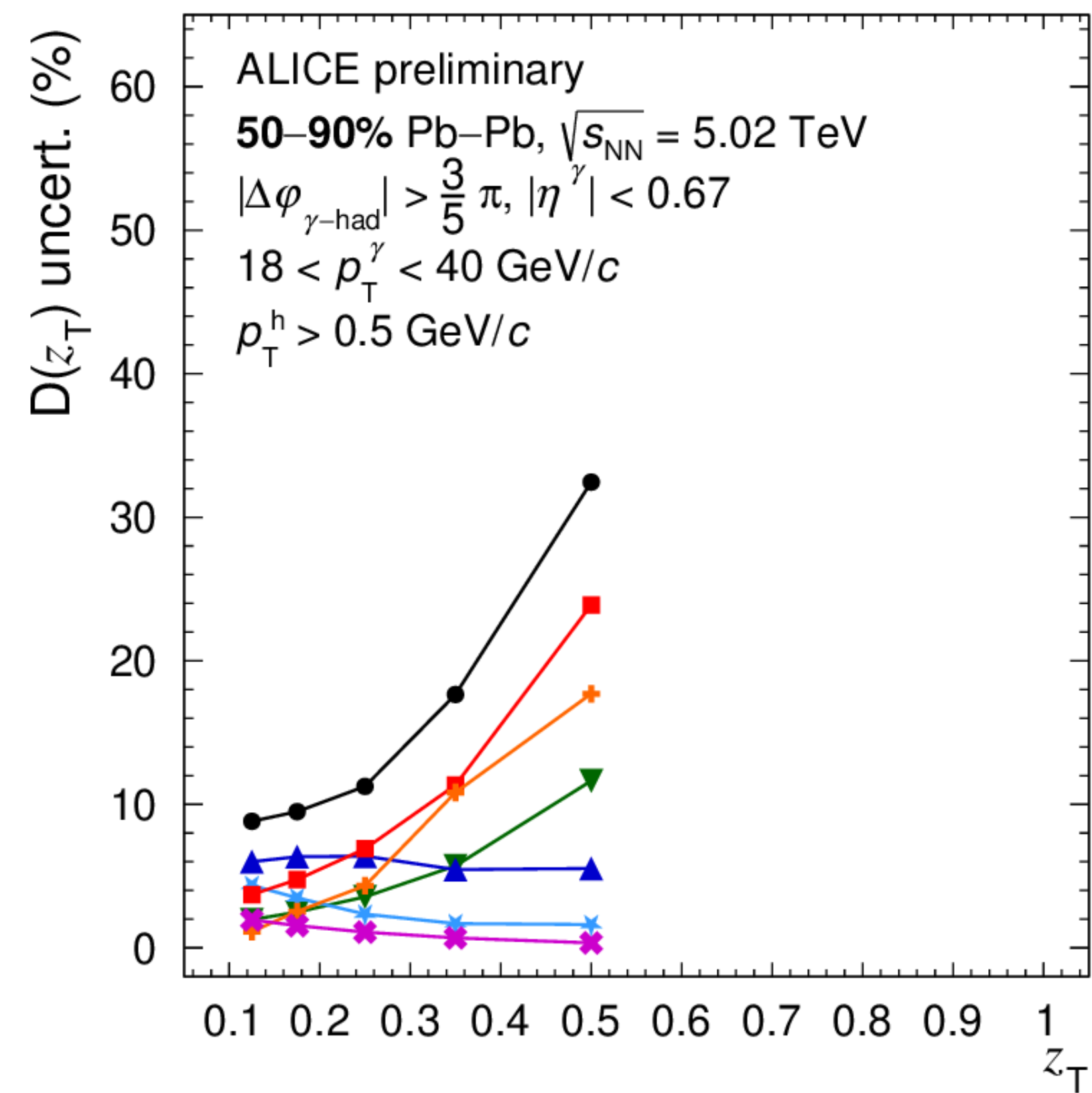
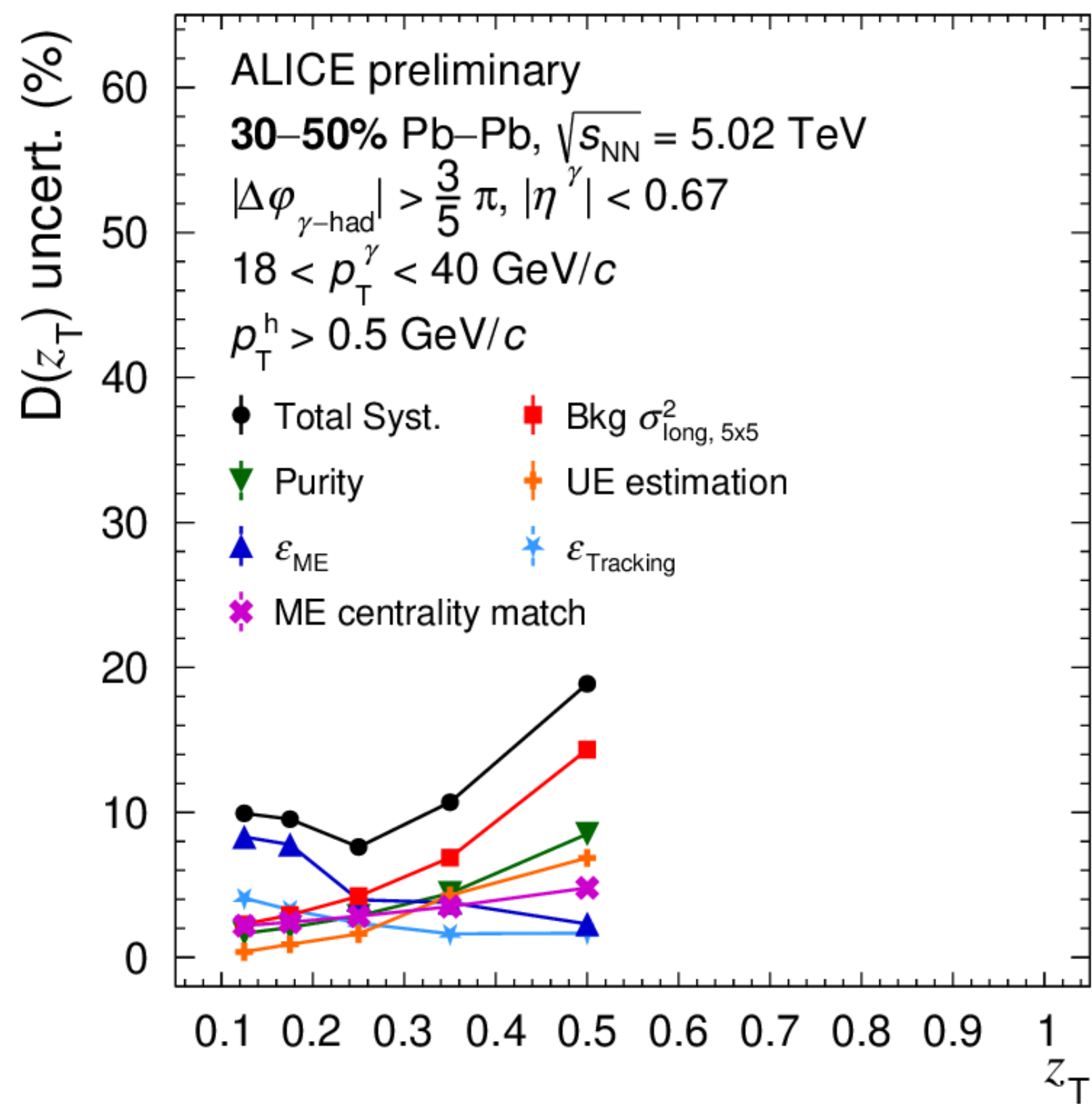
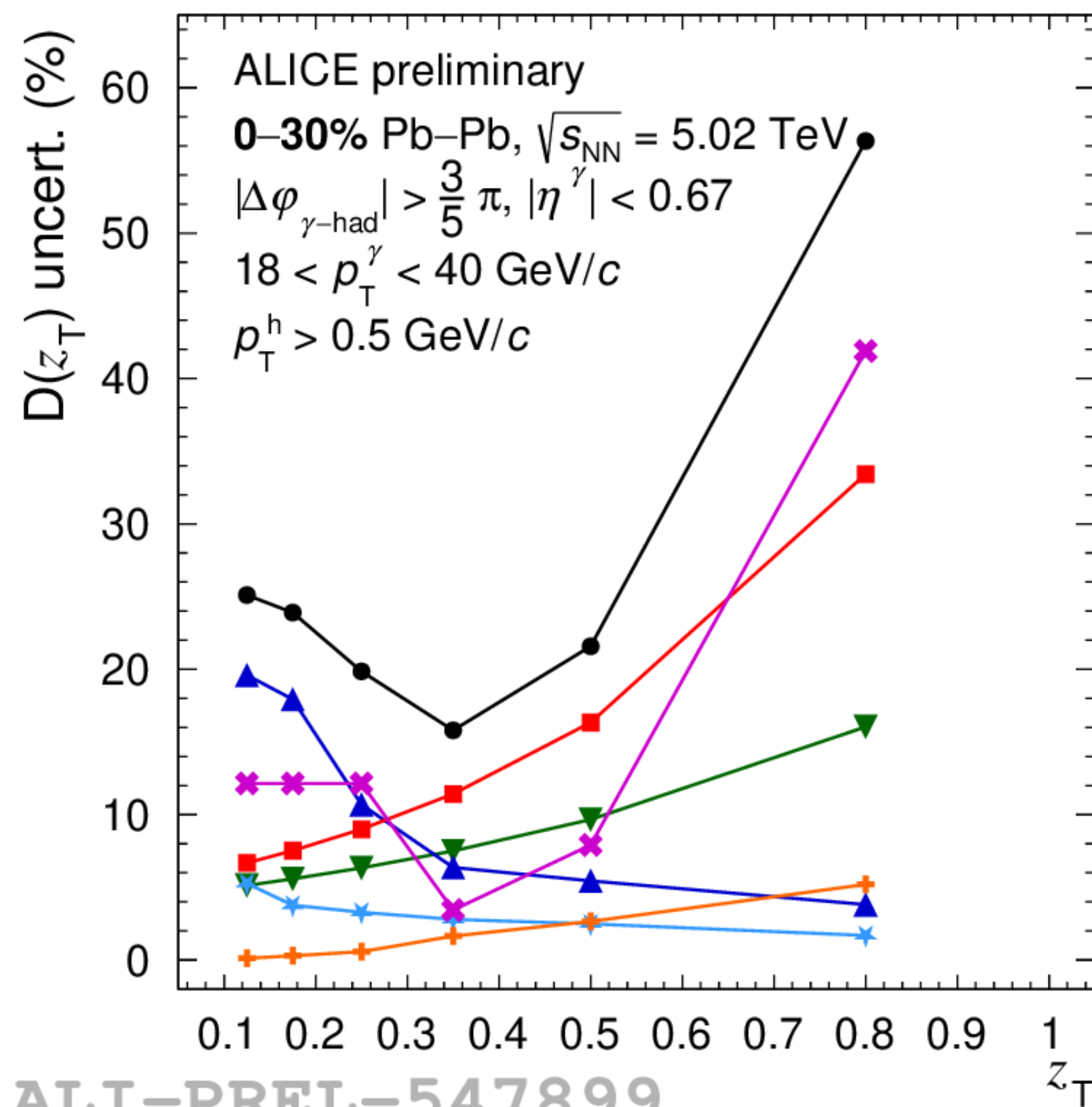
ALI-PREL-547972

Isolated γ -hadron correlations in Pb–Pb: $D(z_T)$

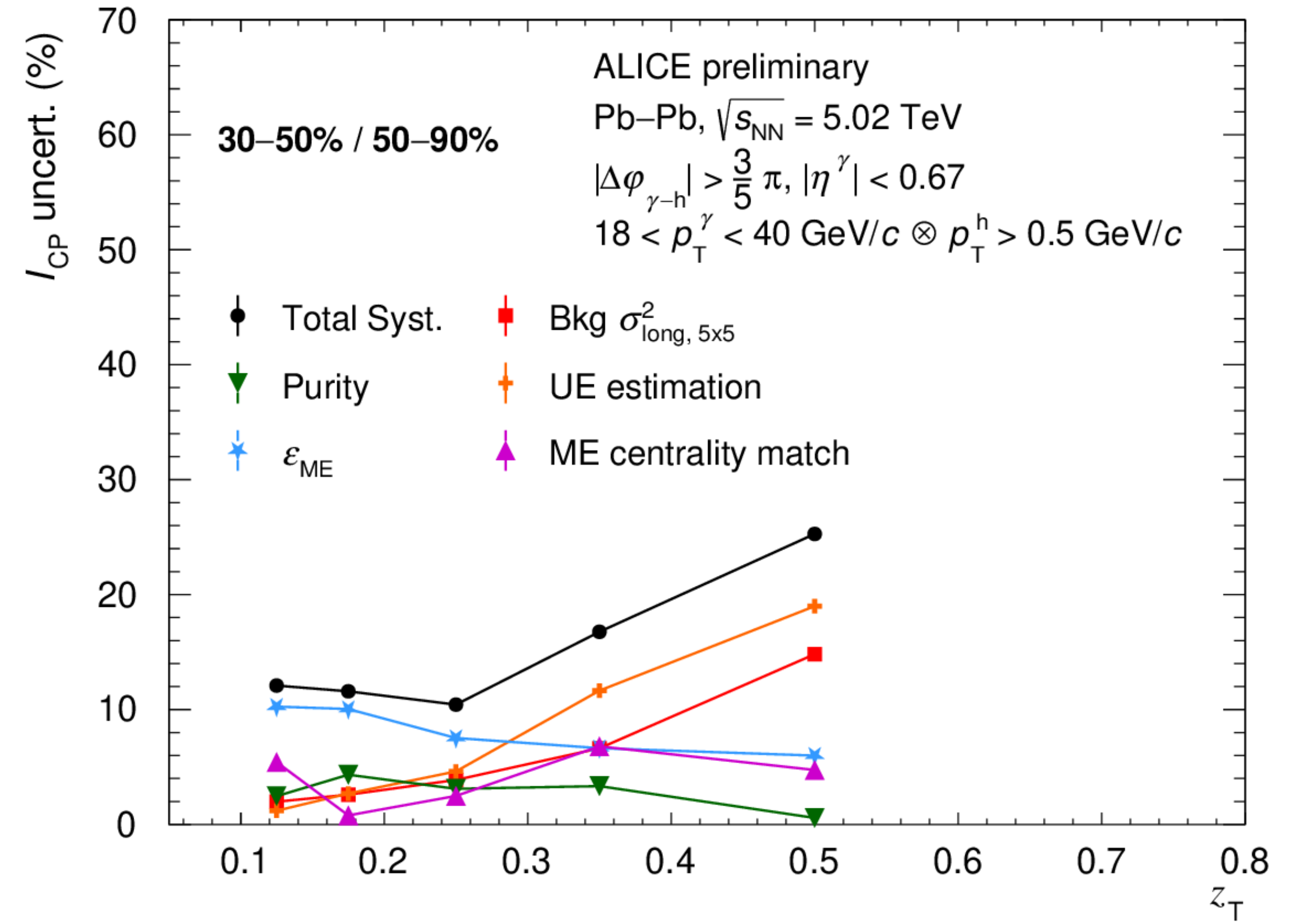
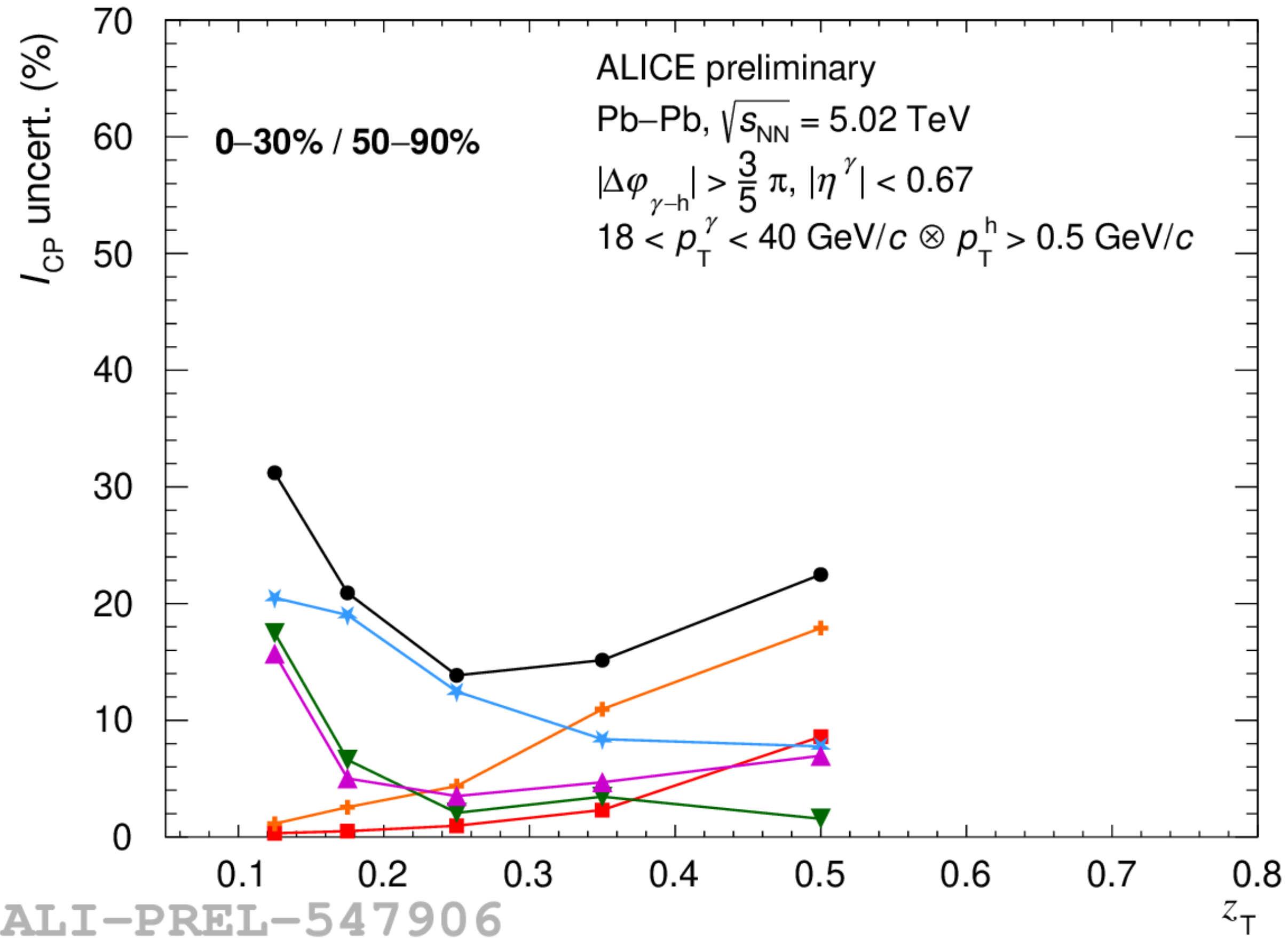


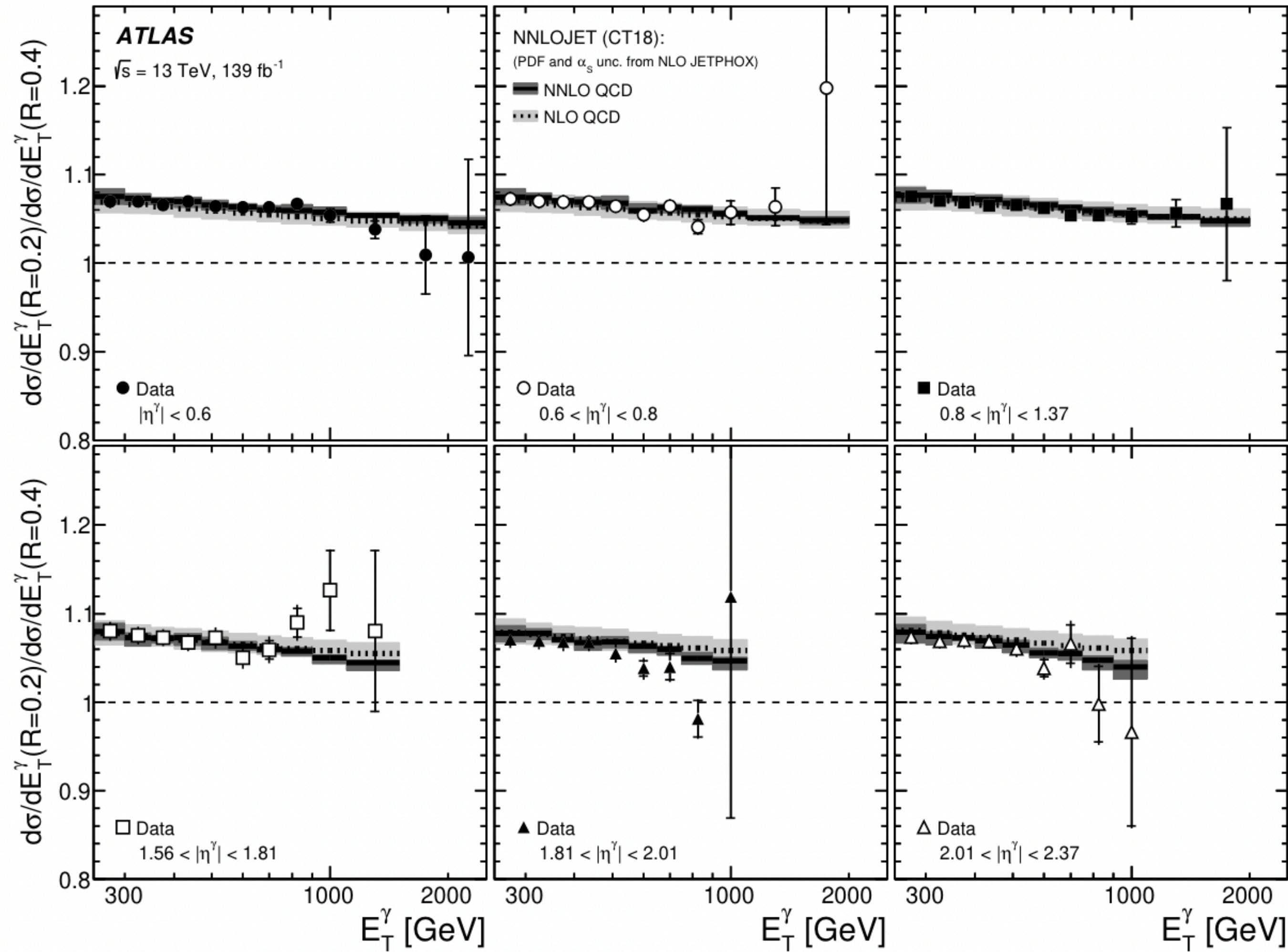
ALI-PREL-547976

Isolated γ -hadron correlation uncertainty: $D(z_T)$



Isolated γ -hadron correlation uncertainty: I_{CP}





[JHEP 07 \(2023\) 86](#)

[arXiv:2302.00510](#)

Figure 21: Measured ratios of the differential cross sections for inclusive isolated-photon production for $R = 0.2$ and $R = 0.4$ as functions of E_T^γ in different η^γ regions. The NLO (dotted lines) and NNLO (solid lines) pQCD predictions from NNLOJET based on the CT18 PDF set are also shown. The inner (outer) error bars represent the statistical uncertainties (statistical and systematic uncertainties added in quadrature) and the shaded bands represent the theoretical uncertainties. For some of the points, the inner and outer error bars are smaller than the marker size and, thus, not visible.